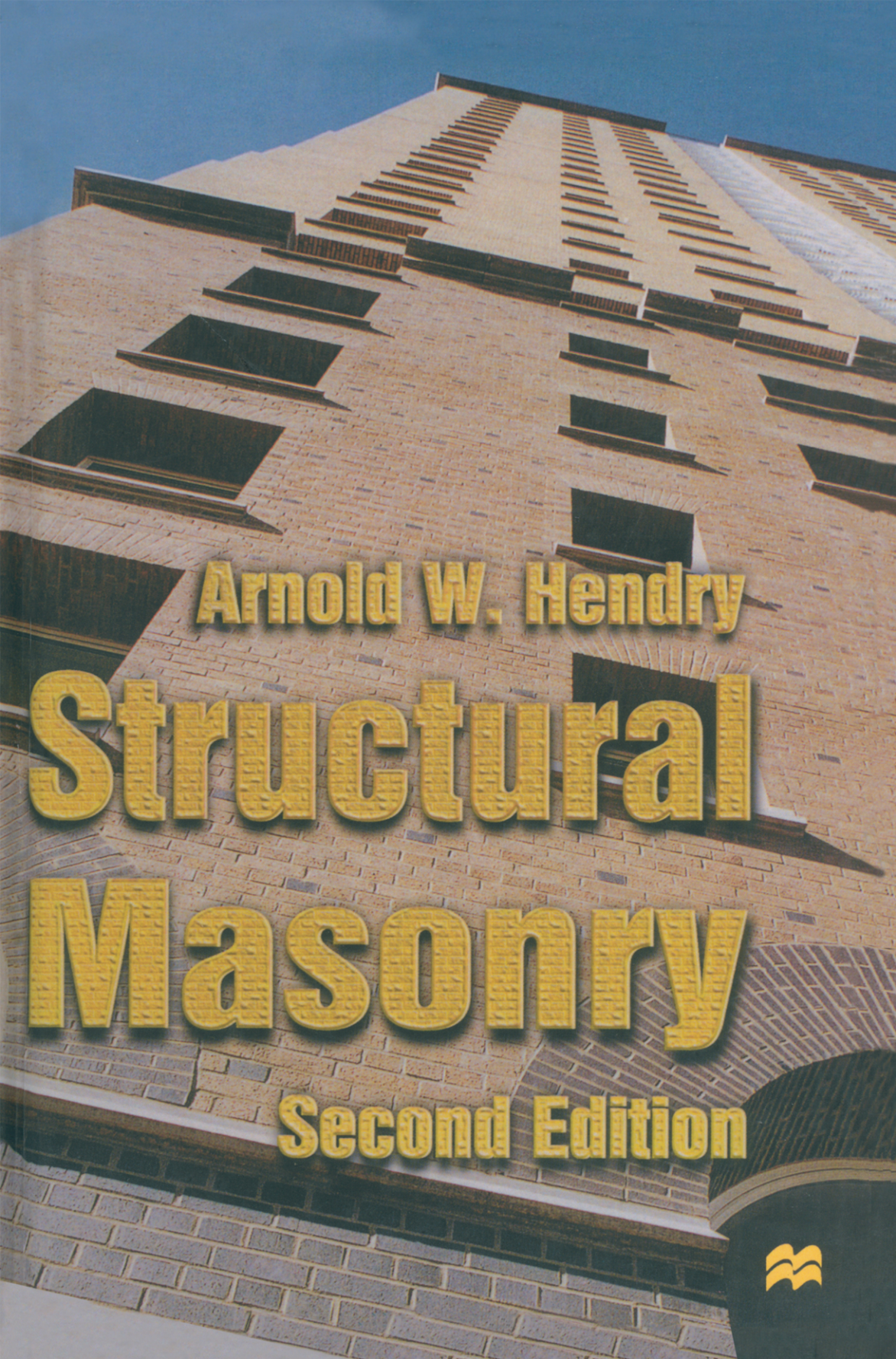
Arnold W. Hendry
Structural Masonry
Second Edition

STRUCTURAL MASONRY

Other titles of interest to Civil Engineers

An Introduction to Engineering Fluid Mechanics
J. A. Fox

Polymer Materials: An Introduction for Technologists and Scientists
Christopher Hall

Reinforced Concrete Design by Computer
R. Hulse and W. H. Mosley

Prestressed Concrete Design by Computer
R. Hulse and W. H. Mosley

Civil Engineering Materials, third edition
edited by N. Jackson

Reinforced Concrete Design, third edition
W. H. Mosley and J. H. Bungey

Microcomputer Applications in Structural Engineering
W. H. Mosley and W. J. Spencer

Strength of Materials, third edition
G. H. Ryder

Surveying for Engineers
J. Uren and W. F. Price

Also by A. W. Hendry

Design of Masonry Structures, 3rd edition (with B. P. Sinha and S. R. Davies)
[published by E. & F. N. Spon, 1997]

Structural Masonry

Arnold W. Hendry
BSc, PhD, DSc, FICE

Emeritus Professor of Civil Engineering,
University of Edinburgh
Past President, The British Masonry Society

Second Edition

Softcover reprint of the hardcover 2nd edition 19

First published 1998 by
MACMILLAN PRESS LTD
Houndmills, Basingstoke, Hampshire RG21 6XS
and London
Companies and representatives throughout the world

ISBN 978-1-349-14829-5 ISBN 978-1-349-14827-1 (eBook)
DOI 10.1007/978-1-349-14827-1

A catalogue record for this book is available from the British Library.

This book is printed on paper suitable for recycling and made from fully managed and sustained forest sources. Logging, pulping and manufacturing processes are expected to conform to the environmental regulations of the country of origin.

CONTENTS

PREFACE TO FIRST EDITION

The first edition of this book, written some ten years ago, was devoted to Structural Brickwork and had the aim of reviewing the principles underlying the use of that form of construction in Structural Engineering. A considerable amount of research data was then available and this has been considerably extended during the past decade. The structural use of blockwork has also been greatly developed over this period and there has been a general drawing together of research interest in both brickwork and blockwork, to the great advantage of both materials. Having regard to this tendency, the contents of the original book have been updated and the coverage extended to include reference to blockwork as well as brickwork. Additional chapters have been added dealing with masonry arches and testing methods, both topics which have become of wide interest in recent years.

Although a large number of references to source material have been included, they by no means encompass the entire literature on Structural Masonry. It is hoped, however, that the text will be an adequate guide to the subject and that it will enable readers who require more detailed information to follow up their particular problem in the literature. Particular attention is drawn to the proceedings of the series of *International Brick and Block Masonry Conferences*, the *Journal* and *Proceedings of the British Masonry Society*, and the *Proceedings of the North American* and the *Canadian Masonry Conferences*. Together these publications form a veritable mine of research and practical information.

This book is addressed not only to research workers and students but also to practising engineers who may require background information to assist them in using structural masonry codes of practice which are becoming increasingly sophisticated as knowledge of the subject increases.

I would again express my indebtedness to the very numerous authors on whose work I have drawn in writing this book. I also wish to offer my sincere thanks to my former research students who have contributed greatly to the subject. Masonry research is not a field which readily attracts large

sums of money and I would therefore express my thanks to the brick industry in Britain, and in particular to the Brick Development Association, for its support over the years. Finally, I am grateful to my colleagues in many countries of the world for their friendship and encouragement in pursuing my work in structural masonry.

Edinburgh, 1989 Arnold W. Hendry

PREFACE TO SECOND EDITION

The content of *Structural Masonry* has been revised to take account of research results which have been published in the decade or so since the first edition was prepared. New sections have been added on movement and durability, and on non-destructive testing.

In recent years structural design in masonry has become increasingly sophisticated and the related codes of practice correspondingly more complex. This is illustrated by the recently published draft European code of practice on the Design of Masonry Structures which in due course will become Eurocode 6. For effective use of this and similar codes, a sound understanding of the underlying principles is essential and it is hoped that this book will be of assistance in this direction. The more general intention of providing a source or guide book to the literature for research workers and others of course remains.

Attention is again directed to the proceedings of the various national and international conferences on masonry which between them now take place more or less annually. The *Journal of the British Masonry Society*, *Masonry International*, and the *Journal of the Masonry Society (USA)* continue to be important sources of information on all aspects of masonry construction.

Edinburgh, 1997 Arnold W. Hendry

1 STRUCTURAL DESIGN OF MASONRY BUILDINGS

1.1 **Introduction**

A large proportion of masonry buildings for residential and other purposes is satisfactorily designed and built in accordance with empirical rules and practices without the need for special structural consideration. However, the limits of this approach cannot be extended much beyond the scale of two-storey houses of very conventional construction without having to use very thick walls, which in turn result in waste of materials and other disadvantages. Indeed for a considerable time this led to the eclipse of masonry as a structural material for larger buildings, and it is only since the 1950s that the application of structural engineering principles to the design of masonry has resulted in the re-adoption of this material for certain classes of multi-storey buildings, and to its use in situations which would have been precluded by reliance on rule-of-thumb procedures.

The economic success of masonry construction has been achieved not only by the rationalisation of structural design, but also because it is possible for the walls which comprise a building structure to perform several functions which in a framed structure have to be provided-for separately. Thus, masonry walls simultaneously provide structure, subdivision of space, thermal and acoustic insulation, as well as fire and weather protection. The material is relatively cheap and durable, can provide infinite flexibility in plan form and can offer an attractive external appearance. Furthermore, masonry buildings can be constructed without heavy capital expenditure on the part of the builder.

To make the best use of these inherent advantages in multi-storey buildings it is necessary to use masonry construction in cases where the accommodation gives rise to moderate or small floor spans and where it is possible to continue the loadbearing walls uninterrupted from foundations to roof. In some buildings where there has been a need for large spans on the first and second floors (for example, in hotels), these floors have been built in framed construction with loadbearing walls above this level. It is likely,

however, that with the development of reinforced masonry this limitation will be removed and that the entire structure will be of masonry.

Types of multi-storey building compatible with the adoption of masonry structures include hotels, hostels, flats and other residential buildings, but engineered masonry is frequently advantageous in low-rise buildings where its use can, for example, reduce wall and column sizes and thus increase the flexibility of the design while retaining the advantages of the material.

A recently developed application of masonry construction is to large single-cell buildings for industrial or leisure purposes where there is a requirement for relatively high outer walls supporting a steel roof structure. For these, cellular or fin walls may be used, with or without prestressing.

1.2 **Wall layout in multi-storey buildings**

The first consideration in the design of a multi-storey masonry building is to determine the plan arrangement of the walls in accordance with the function of the building. From the structural point of view the wall arrangement is important: firstly, as a means of providing lateral strength and rigidity, and secondly, in order to ensure that the building is generally robust in the sense that any local damage to the structure does not result in catastrophic collapse.

Possible wall arrangements are almost unlimited but it may be helpful to distinguish three basic categories

(1) Cellular
(2) Simple or double cross-wall systems
(3) Complex service core structures.

A cellular arrangement is one in which both internal and external walls are loadbearing and in which these walls form a cellular pattern in plan as indicated in figure 1.1.

The second category includes cross-wall structures of various kinds. These may be used either for slab or point blocks: in case of slabs (figure

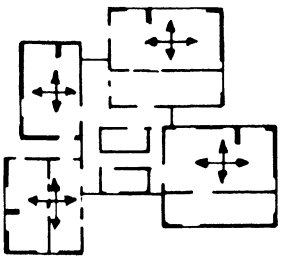

Figure 1.1 Cellular wall layout

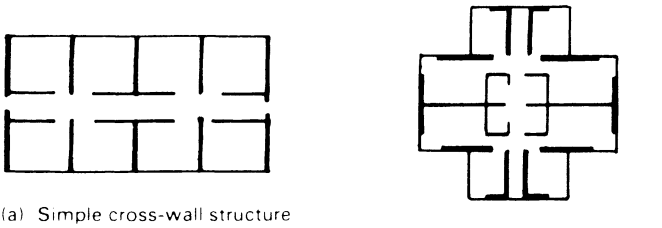

(a) Simple cross-wall structure

(b) Double cross-wall system

Figure 1.2 Cross-wall structure

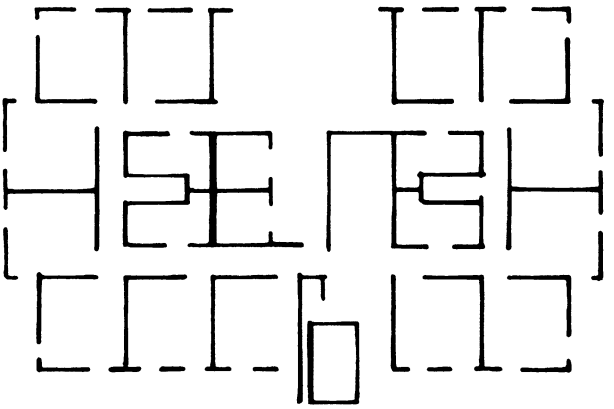

Figure 1.3 Core-wall structure

1.2a) longitudinal stability is frequently achieved by means of internal corridor walls or partition walls. Buildings have been designed in which longitudinal stability depends on a stair-well or lift-shaft somewhere along the length of the structure, but this is unsatisfactory in that failure of one wall could precipitate collapse of a large part of the building; this practice should therefore be avoided even in relatively low-rise buildings.

Point blocks require double cross-wall systems as suggested in figure 1.2b.

In both of the above systems the external walls may be in masonry, curtain wall or indeed any other external walling at the choice of the architect, thus giving considerable freedom of elevational treatment. It will be observed, however, that there is a limit to the depth of a cross-wall building if the rooms are to have effective day-lighting.

The third category is typified in figure 1.3; lateral stability is here provided by a complex service core incorporating lift-shafts, stair-wells, service rooms, toilets, etc., the walls of which, acting together, form a strong tower-

like structure. Surrounding walls or columns need only transmit vertical loading from the floors while the external, perimeter walls can be non-loadbearing.

The arrangement chosen tends to evolve from the site plan and the required sizes and disposition of rooms. It is not particularly critical from the structural point of view, provided that a reasonable balance is allowed between walls orientated in the principal directions of the building so as to permit the development of adequate lateral strength and rigidity against forces applied in these directions.

Very unsymmetrical wall arrangements are, however, to be avoided as these will give rise to torsional effects, which are difficult to calculate and which may produce undesirable stress conditions. Slender piers and cantilevered slabs can be accommodated but will inevitably add to the cost and may give rise to structural problems.

General robustness and stability are not usually difficult to ensure in any type of masonry structure, but the desirability of incorporating returns at the ends of walls and other similar strengthening features will be apparent. Detailed consideration of the means of checking and controlling the effects of local damage is contained in chapter 9.

1.3 **Plain and reinforced masonry**

The essential difference between plain and reinforced masonry is that the former is incapable of resisting significant tensile stresses whereas the latter acts in a manner similar to reinforced concrete, tensile stresses being taken by suitably placed steel.

Most masonry buildings are constructed in plain masonry without reinforcement, but in seismic areas it is essential to use reinforced masonry in order to provide resistance to dynamic forces of considerable magnitude. In northern Europe and Australia, therefore, structures are normally unreinforced whereas in the United States and New Zealand, reinforced brickwork is generally required.

Apart from construction in seismic areas, however, there is a field of application for reinforced brickwork elements in building construction in situations where the use of plain masonry would be impractical. One such case has already been mentioned, namely the possible use of cellular-section, prestressed masonry walls for large single-cell buildings. The potentialities of reinforced and prestressed masonry should therefore be kept in mind at the preliminary design stage of masonry structures.

1.4 **Limit state design of masonry**

The basic aim of structural design is to ensure that a structure should fulfil its intended function throughout its lifetime without excessive deflection,

cracking or collapse, and this aim must of course be met with due regard to economy. The designer is assisted in this task by the availability of a code of practice which is based on accumulated experience and research. Until recently, such codes have sought to ensure the safety and serviceability of masonry structures by specifying permissible stresses for various types and combinations of materials. Structural masonry codes generally give basic compressive stresses for a range of brick–mortar combinations; the basic stress in wall design has then to be adjusted for the slenderness ratio of the element and the eccentricity of the loading. The basic stresses are derived from tests on walls or piers, the ultimate stresses having been divided by an arbitrary factor of safety sufficiently large to avoid cracking at working loads. Thus, to this extent, masonry design has always been related to ultimate strength and to a serviceability limit state.

In recent years a more rational procedure has been evolved for dealing with structural safety and serviceability through consideration of the relevant 'limit states'. A structure, or part of a structure, reaches a limit when it becomes incapable of fulfilling its function or when it no longer satisfies the conditions for which it was designed. Two categories of limit state normally have to be considered, namely, ultimate limit states corresponding to failure or collapse and serviceability limit states at which deflections or cracking become excessive.

The general method of applying the limit states approach to the design of structures is outlined in a publication of the International Organization for Standardization [1] in which the criterion for a satisfactory design is expressed in terms of design loading effects (S^*) and design strengths (R^*), as follows

$$R^* \geqslant S^* \tag{1.1}$$

Design loading effects are determined from the characteristic actions from the relationship

$$S^* = \text{effects of} \left(\gamma_f Q_k\right) \tag{1.2}$$

where γ_f is a multiplier (or partial safety factor) and Q_k is a characteristic load which, if defined in statistical terms, is given by

$$Q_k = Q_m\left(1 + k\delta\right)$$

where Q_m is the value of the most unfavourable load with a 50 per cent probability of its being exceeded once in the expected life of the structure

δ is the coefficient of variation of the distribution of the maximum loading

k is a constant depending on a selected probability of maximum loadings being greater than Q_k.

It is usual to take the characteristic load as that which will have a 5 per cent probability of being exceeded during the lifetime of the structure. In

many situations, however, statistical data are not available and the characteristic loads have to be based on nominal values given in codes of practice or other regulations. The factor γ_f is a function of several partial coefficients:

γ_{f1} which takes account of the possibility of unfavourable deviation of the loads from the characteristic external loads, thus allowing for abnormal or unforeseen actions;

γ_{f2} which takes account of the reduced probability that various loads acting together will all be simultaneously at their characteristic values;

γ_{f3} which is intended to allow for possible modification of the loading effects due to incorrect design assumptions (for example, introduction of simplified support conditions, hinges, neglect of thermal and other effects which are difficult to assess) and constructional discrepancies such as dimensions of cross-section, deviation of columns from the vertical and accidental eccentricities.

Similarly, design strengths of materials, R^*, are defined by

$$R^* = \frac{R_k}{\gamma_m} \tag{1.3}$$

where $R_k = R_m(1 - ks)$ is the characteristic strength of the material

R_m is the arithmetic mean of test results

s is the coefficient of variation

k is a constant depending on the probability of obtaining results less than R_k.

The characteristic strength of a material is usually taken as the 95 per cent confidence limit of the material strength in a relevant test series. The reduction coefficient γ_m is a function of two coefficients:

γ_{m1} which is intended to cover possible reductions in the strength of the materials in the structure as a whole, as compared with the characteristic value deduced from the control test specimen;

γ_{m2} which is intended to cover possible weakness of the structure arising from any cause other than the reduction in the strength of the materials allowed for by coefficient γ_{m1}, including manufacturing tolerances.

Additionally, ISO 2394 allows for the introduction of a further coefficient γ_c which may be applied either to the design values of loadings or material strengths. This coefficient is in turn a function of two partial coefficients:

γ_{c1} which is intended to take account of the nature of the structure and its behaviour, for example, structures or parts of structures in which partial or complete collapse can occur without warning,

where redistribution of internal forces is not possible, or where failure of a single element can lead to overall collapse;

γ_{c2} which is intended to take account of the seriousness of attaining a limit state from other points of view, for example, economic consequences, danger to the community, etc.

Usually γ_c is incorporated into either γ_f or γ_m and therefore does not appear explicitly in design calculations.

The advantage of the limit state approach is that it permits a more detailed and flexible assessment of structural safety and serviceability; the various relevant factors are identified and up to a point can be expressed in numerical terms. Ideally, loadings and strengths should be available in statistical terms but this is seldom possible, so that characteristic values have to be determined on the basis of available evidence. In the case of loads, the evidence generally results from surveys of buildings in service. Characteristic strengths of materials, on the other hand, are derived from laboratory tests, the results of which can sometimes provide a statistical basis for characteristic strength. In the absence of such statistical data, characteristic strengths have to be based on nominal values proved by experience.

1.5 **Derivation of partial safety factors**

In principle, the γ-factors can be derived by probability methods, provided that the necessary statistical information is available. Again, this information is at best incomplete, but consideration of calculated safety factors is valuable in assessing the relative importance of variables, and in reducing the purely arbitrary nature of selecting suitable values for design codes. The following discussion, in simplified terms, may be helpful in appreciating this approach.

Considering the ultimate limit state of a particular structure, we have the condition that for failure to occur

$$R^* - S^* \leqslant 0 \tag{1.4}$$

where

$$R^* = \frac{R_k}{\gamma_m}$$

and

$$S^* = f(\gamma_f Q_k)$$

This situation is illustrated graphically in figure 1.4. In statistical terms, the safety requirement is satisfied by ensuring that the probability of failure is very small, that is

$$P[R^* - S^* \leq 0] = p \tag{1.5}$$

where P is the probability of occurrence of the expression within the brackets and p is the required, small value, of this probability. In practice, this will generally be in the range 10^{-5} to 10^{-6}.

The problem has been examined in terms of a global safety factor, γ, mean values $\overline{R}$ and $\overline{S}$ and their standard variations by Macchi [2] and Beech [3]. On the basis of assumed normal distributions of strength and loading about their mean values, Macchi produced the set of curves shown in figure 1.5 showing the relationship between the safety factor and the coefficient of

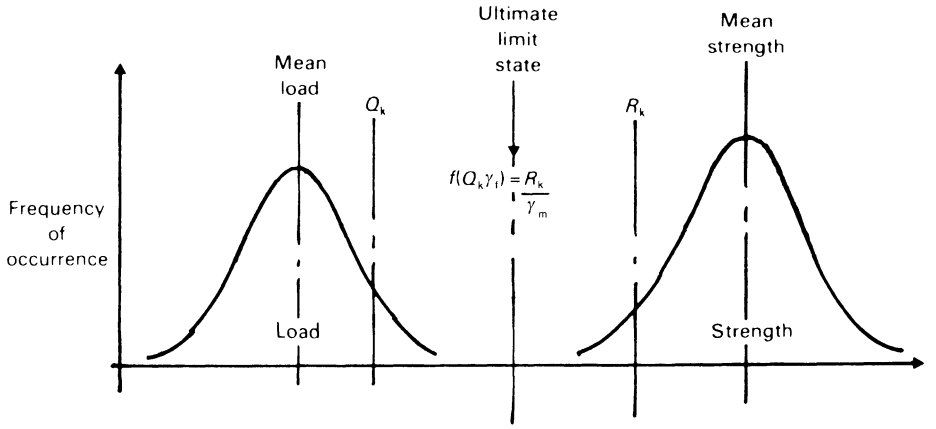

Figure 1.4 Ultimate limit state condition

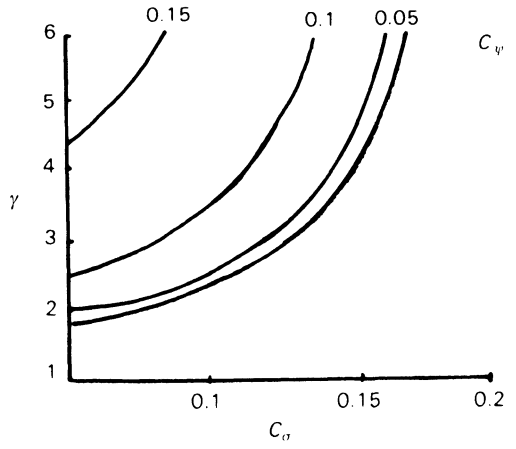

Figure 1.5 Global safety factors for normal distribution (Macchi). Coefficient of variation of area $C_a = 0$, of strength C_σ, of eccentricity C_ψ, of loading $C_s = 0.15$; probability of failure 10^{-6}

variation of the strength of the material, for coefficients of variation of the loads $C_s = 0.15$, of the level of uncertainty of eccentricity and slenderness $C_{\psi} = 0, 0.05, 0.1$ and 0.15, and for probability of failure of 10^{-6}. From these curves it is clear that, other things being equal, the safety factor required to ensure a given probability of failure rises quite rapidly with the coefficient of variation of the strength of the material.

However, Beech has suggested that the assumption of normal distribution is unrealistic in practical terms unless the coefficients of variation are small. He expresses the view that lognormal and truncated normal distributions have greater validity and has shown (figure 1.6) that these result in a much less steep rise in the factor of safety with an increase in the coefficient of variation of material strength.

The investigations outlined above are in terms of a global safety factor whereas in the application of limit state design two or more partial safety factors are used. Assuming homogeneity of units, and introducing the partial safety factors in equation 1.4, at the ultimate limit state

$$\frac{R_k}{\gamma_m} = \gamma_f Q_k \tag{1.6}$$

or

$$\frac{R_k}{\gamma_m \gamma_f} = Q_k \tag{1.7}$$

It would appear from this that the product $\gamma_m \gamma_f$ is equivalent to a global safety factor but, as Beech has pointed out, the probability of failure asso-

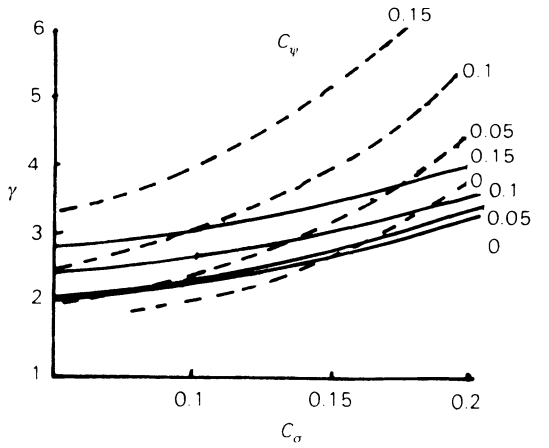

Figure 1.6 Global safety factors for lognormal (full line) and truncated normal (broken line) distributions (Beech). Coefficients of variation and probability of failure as in figure 1.5

ciated with the product of two partial safety factors is generally different from the product of the partial probabilities. Thus if the probabilities of γ_m and γ_f are both 10^{-3} the probability associated with their product is not necessarily 10^{-6}. It has been suggested by Baker [4] that the following approximate relationship holds between the global and partial safety factors

$$\gamma = \gamma_m + \gamma_f - 1$$

provided that the probabilities involved are not much less than 10^{-5} and the coefficients of variation are not greater than 0.4. This formula will result in values of less than the product of the partial safety factors but if truncated normal distribution is applicable, the product is valid.

Beech has derived equations for calculating the partial safety factor γ_m on the basis of lognormal and truncated normal distributions for any combination of variability in material strength and other factors, and on the assumption that the masonry strength σ is related to the unit strength by a power law of the form $\sigma = u^n L$, where u is the compressive strength of the units, n an exponent less than unity and L a reduction factor relating masonry strength to unit strength. The results so obtained are given in table 1.1, from which it will be seen that there is little practical difference between the results obtained using the alternative distributions. The determination of safety factors is by no means an exact science, but considerable progress has been made in establishing a rational framework for their selection and the values calculated by Beech and quoted in table 1.1 are very similar in magnitude to those recommended in the British limit state code for masonry BS 5628: 1978 (table 1.2). Assuming that practical conditions are reasonably reflected by Beech's theoretical model, there is no doubt that satisfactory levels of safety will result from the use of the γ_m values specified in this code. Reassurance on this point comes in any case from a rough comparison of the overall safety factor implicit in the previous permissible stress code (CP 111: 1964, 1970) with the global safety factor resulting from the combination of γ_m and γ_f in the new code.

In the British limit state code for masonry, BS 5628: 1978, the values of γ_f are taken to be the same as those specified for concrete construction. This is a convenience for design engineers, but may not be strictly valid in terms of the ISO definitions of partial safety factors, since γ_f is intended to provide for inaccuracies in design calculations, deviation of columns from the vertical and accidental eccentricities, etc., which may or may not be the same for concrete as for masonry.

In Canada, a similar set of partial safety factors [5] has been adopted and values of γ_m have been derived by comparing strength test results for masonry elements with those computed by proposed code of practice procedures. By this means safety levels similar to those inherent in existing methods have been obtained.

Table 1.1 Values of partial safety factors calculated by Beech

(a) Partial safety factor γ_m from lognormal distribution

Unit strength coefficient of variation	*n*	*Coefficient of variation in masonry strength*	
		0.15	0.22
0.055	1.0	2.25	3.08
	0.8	2.22	3.04
	0.6	2.19	3.01
0.08	1.0	2.37	3.19
	0.8	2.29	3.11
	0.6	2.23	3.05

Assumed probability of failure 10^{-4}.

(b) Partial safety factor γ_m from truncated normal distribution

Unit strength coefficient of variation	*n*	*Coefficient of variation in masonry strength*	
		0.12	0.16
0.05	1.0	2.22	2.77
	0.8	2.15	2.68
	0.6	2.08	2.59
0.07	1.0	2.40	2.98
	0.8	2.28	2.84
	0.6	2.18	2.71

Table 1.2 Values of γ_m recommended in British masonry code BS 5628: Part 1: 1978

	Category of construction control	
	special	*normal*
Category of manufacturing: special	2.5	3.1
Control of structural units: normal	2.8	3.5

Statistical parameters relating to material strength, dimensional properties, mathematical modelling and resistance of brickwork masonry have also been determined by Hu [6] and on the basis of reliability theory used to assess the adequacy of safety factors in the Chinese masonry code. Hu observes that the statistical data on which reliability indices for structural design could be based are not at present available. It is clear from his analysis, however, that equal safety as expressed by the normally used safety factors does not mean equal reliability of masonry strength, owing to differences in the statistical parameters between the various factors involved. Reliability of masonry structures can be increased by reducing the variability of material strengths and by improving the accuracy of mathematical modelling.

1.6 **Analysis of masonry structures**

Limit state design calls for the comparison of the effects of load actions with the strength of the material. This in turn calls for the use of suitable methods of structural analysis to estimate the effects of loads on the structure in terms of forces, bending moments and deformations, and for the use of appropriate methods of calculating the resistance of masonry elements and of establishing deformation limits.

Unreinforced masonry is a brittle material and although its stress–strain relationship is non-linear, it is customary to use elastic analysis to determine the forces at particular sections of a structure. Calculation of resistance is now sometimes based on the assumption of a rectangular internal stress block, neglecting tensile strength. In the past, methods of analysis have been relatively crude, but the construction of taller buildings in masonry and the general need for increased economy in the use of materials have led to the development of more refined methods. Similarly, the resistance of masonry was calculated, in the past, on an entirely empirical basis but is now increasingly supported by analytical studies.

Reinforced and prestressed masonry are designed on the same principles as have been developed for reinforced and prestressed concrete with appropriate adjustments for differences in the material properties.

Methods of analysis and estimation of the strength of masonry elements will be discussed in subsequent chapters of this book.

1.7 **Movement and durability considerations**

In the design of masonry structures careful attention has to be given to certain factors which, although not directly related to structural behaviour, may affect it during the lifetime of the building and are of primary concern in relation to serviceability. These factors include provision for movement, assurance of durability and avoidance of rain penetration.

Building materials such as masonry, concrete and steel possess considerable rigidity but are by no means free from movement under service conditions. Furthermore, their dimensional changes are generally different, so that when they are interconnected quite severe stresses can be set up by one material restraining the movement of another. Restraint of movement of a brittle material can thus result in its fracture and the appearance of a crack. In most cases such cracks are not of structural significance, but are unsightly and may allow water penetration with consequent damage to the fabric of the building and the need for expensive repairs.

Movement in masonry buildings resulting in cracking may arise from the following causes:

Moisture movements in materials
Temperature changes
Strains resulting from applied loads
Foundation movement
Chemical reactions in materials.

Dimensional changes take place in all masonry materials with change in moisture content. This may be irreversible following manufacture – thus kiln dry clay bricks show an initial irreversible expansion for a short time, while concrete and calcium silicate products have an initial shrinkage. Additionally, masonry expands or contracts with change in moisture content at all stages of its existence. Some indication of the magnitude of these moisture movements may be gained from table 1.3.

Temperature movements depend on the coefficient of expansion of the material and the range of temperature experienced by the building element. This in turn depends on a variety of factors and will be greatest for external walls where it will be influenced, among other things, by colour, orientation, thickness, thermal properties and insulation. The temperature range experienced by a heavy external wall in the United Kingdom has been given as

Table 1.3 Moisture and thermal movement indices for masonry materials, concrete and steel

Material	*Reversible moisture movement (%)*	*Irreversible moisture movement (%)*	*Coefficient of thermal expansion/°C*
Clay brickwork	0.02	+0.02–0.07	$5–8 \times 10^{-6}$
Calcium silicate brickwork	0.01–0.05	−0.01–0.04	8–14
Concrete brick- or blockwork	0.02–0.04	−0.02–0.06	6–12
Aerated, autoclaved blockwork	0.02–0.03	−0.05–0.09	8
Dense aggregate concrete	0.02–0.10	−0.03–0.08	10–14
Steel	—	—	12

from −20 to +65°C, and the possible expansion of a clay brick wall of the order of 1 mm per metre.

At the design stage, provision should be made for thermal and moisture movements to take place without the occurrence of unacceptable cracking. This is achieved mainly by selection of suitable materials and careful detailing rather than by methods based on calculation. A considerable amount of information is available regarding the provision of movement joints and correct detailing in relevant codes of practice [7] and other publications [8].

Elastic and creep deformation resulting from load application or self-weight will require to be taken into account where masonry is used as a cladding to a loadbearing structure or to a steel or concrete frame [9].

Foundation movements are a common cause of cracking in masonry walls, particularly in low-rise buildings on certain types of clay soils. Avoidance of damage from this cause depends on adequate attention to foundation design which, however, is beyond the scope of this book.

Clay, concrete and calcium silicate units are relatively resistant in normal conditions of exposure but disruption of masonry can occur as a result of chemical attack on mortar or corrosion of embedded steel. Thus ordinary cement mortars are vulnerable to attack by sulphates originating either in ground water or in clay units which have an unduly high content of soluble sulphate. Avoidance of trouble from these causes lies in the correct selection of materials and the provision of adequate cover for carbon steel components [7].

References

1. *General Principles for the Verification of the Safety of Structures, ISO 2394* (1973).
2. G. Macchi, 'Safety Considerations for a Limit State Design of Masonry', *Proceedings of the Second International Brick Masonry Conference* (Stoke-on-Trent) 1971, eds H. W. H. West and K. H. Speed (British Ceramic Research Association, Stoke-on-Trent, 1971), pp. 229–32.
3. D. G. Beech, 'Some Problems in the Statistical Calculation of Safety Factors', *Proceedings of the Fourth International Brick Masonry Conference* (Brugge) 1976, Paper 4.b.8.
4. A. L. L. Baker, quoted by E. Rosenbleuth and L. Esteva in *Reliability Basis for some Mexican Codes* (American Concrete Institute, Detroit, Mich., 1972), Publication SP-31.
5. C. J. Turkstra, J. Ojinaga and C-T. Shyu, 'Development of a Limit States Masonry Code', *Proceedings of the Third Canadian Masonry Symposium* (Edmonton) 1976, Paper 2.
6. Chiu-Ku Hu, 'Chinese Research on the Reliability of Brick Masonry', *Proceedings of the Seventh International Brick Masonry Conference* (Melbourne), 1985, pp. 1427–35.
7. *BS 5628 Code of Practice for Use of Masonry. Part 3* (British Standards Institution, London, 1985).

8. A. W. Hendry, B. P. Sinha and S. R. Davies, *Design of Masonry Structures* (E. & F. N. Spon, London, 1997), Ch. 13.
9. B. V. Rangan and R. F. Warner (Eds), *Large Concrete Buildings* (Longman, Harlow, 1996), Ch. 8.

2 MASONRY MATERIALS IN COMPRESSION

2.1 **Compressive strength: general**

The strength of masonry in compression, tension and shear has been the subject of systematic investigation over a very considerable period. As masonry structures are primarily stressed in compression, there has naturally been a concentration of interest in the resistance of the material to this type of loading, and many investigations have been carried out with a view to establishing the relationship between available unit types and materials, and a variety of mortar mixes. These tests have formed the basis for the masonry strengths used in structural design codes, and in order to reduce the almost unlimited range of unit and mortar combinations to manageable proportions, tables of basic compressive strength have been evolved in which the principal variables are the unit compressive strength and the mortar mix. The strengths of the component materials are defined by standardised tests, which do not necessarily reproduce the state of stress in the component material in service, but which serve as index values in the selection of design stresses.

2.2 **Factors affecting compressive strength**

Research work has shown that the following factors are of importance in determining the compressive strength of masonry:

Unit characteristics
Strength
Type and geometry
  Solid
  Perforated
  Hollow
  Relative height
Absorption

Mortar characteristics
Strength
  Mix
  Water/cement ratio
  Water retentivity
Relative deformation characteristics
Relative thickness

Masonry
Bond
Direction of stressing
Local stress raisers

Some of these factors, such as the unit characteristics, are determined in the manufacturing process, while others, such as mortar properties, are susceptible to variations in constituent materials, proportioning, mixing and accuracy of construction.

2.2.1 *Indications from standard tests*

A number of important points have been derived from compression tests on masonry and from associated standard materials tests. These include, firstly, the observation that masonry loaded in uniform compression will fail either by the development of tension cracks parallel to the axis of loading or by a kind of shear failure along certain lines of weakness, the mode of failure depending upon whether the mortar is weak or strong relative to the unit. Secondly, it is evident that the strength of masonry is smaller than the nominal strength of the unit in a compression test. On the other hand, the masonry strength may greatly exceed the cube crushing strength of the mortar. Finally, it has been found that the compressive strength of masonry varies roughly as the square root of the unit strength and as the third or fourth root of the mortar cube strength.

From these observations it may be inferred that: (1) the tensile splitting failure, when it takes place, is initiated by the restrained deformation of the mortar in the bed joints; (2) the apparent crushing strength of the unit, when this type of failure occurs, is not a direct measure of the strength of the unit in the masonry, since the mode of failure is different in the two situations; (3) the mortar is able to withstand higher compressive stresses in the bed joint than in a cube because of the restraint on its lateral deformation imposed by the units.

2.2.2 *Effect of properties of bed materials*

While the cube crushing strength of mortar is only weakly related to the masonry strength by a third or fourth root relationship, the properties of the bed material exert a controlling influence on the masonry strength achieved; this has been demonstrated by a number of investigations. Francis *et al.* [1] showed that brickwork prisms consisting of loose bricks, the bedding planes of which had been ground flat, achieved compressive strengths approximately twice as high as those obtained from prisms with normal mortar joints. Astbury and West [2] reported a similar effect in relation to brickwork cubes.

A series of experiments conducted by the Structural Clay Products Research Foundation in the United States [3] examined the effect on the compressive strength of brick couplet specimens in which the jointing materials ranged from 0.8 mm aluminium sheet placed between ground surfaces to a normal cement:lime:sand mortar, and included a dry sand joint contained by adhesive tape. Some of the results of these experiments are summarised in table 2.1.

The effect of bed material on brick prism strength was also investigated by Morsy [4]. In his experiments the bed material in a series of model brick prisms was varied, from rubber at one end to steel at the other, and the results of these experiments, summarised in table 2.2, show that there is an eight-fold change in the prism strength with the substitution of steel for rubber in the bed joints. In the case of rubber jointing material the bricks failed in tension as a result of tensile stresses induced by the deformation of the rubber. Steel in the bed joints, on the other hand, had the effect of restraining lateral deformation of the bricks and this induced a state of triaxial compressive stress in them. Failure in this case was by crushing as in a typical compression test on a brittle material.

Since the deformation properties of the joint material between masonry units is critical, it follows that the higher the ratio of mortar joint thickness to height of masonry wall, the greater will be the tendency for the unit to fail by lateral splitting. This has been demonstrated experimentally by several investigations [1, 5–7], and some of the results obtained are shown in figure 2.1.

Table 2.1 Effect of different joint materials on the compressive strength of brick couplets (Monk [3])

Joint material	*Compressive strength (N/mm^2)*	*Ratio to brick strength*
Aluminium sheet	106	0.96
Mortar ($1:\frac{1}{2}:4\frac{1}{2}$)	44	0.40
Sand	65	0.59
Ground surfaces	98	0.89

Table 2.2 Effect of different joint materials on the compressive strength of three brick stack prisms; one-sixth scale model bricks, faces ground flat; six specimens of each type tested (Morsy [4])

Joint material	*Compressive strength (N/mm^2)*	*Ratio to brick strength*
Steel	56.48	1.4
Plywood	46.39	1.15
Hardboard	43.89	1.09
Polythene	16.99	0.42
Rubber with fibres	11.71	0.29
Soft rubber	6.99	0.17
No joint material	37.20	0.93
Mortar ($1:\frac{1}{4}:3$)	14.0	0.35

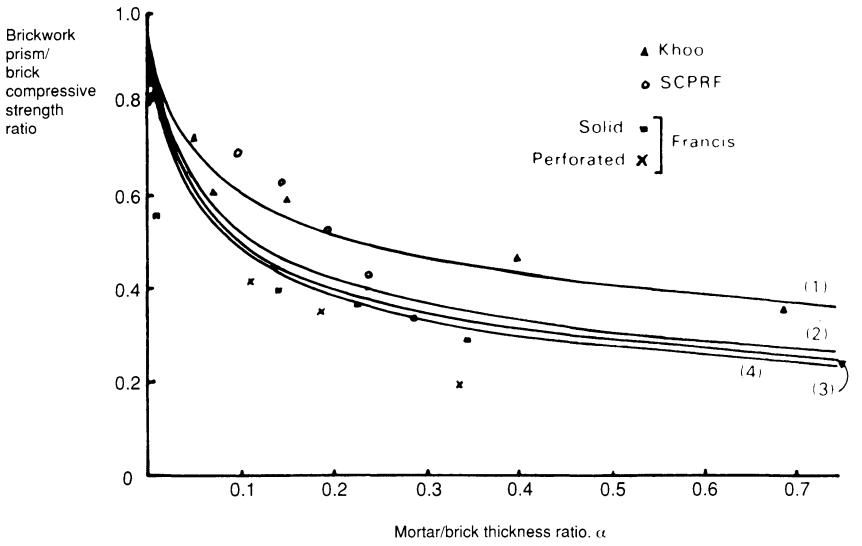

Figure 2.1 Effect of mortar/brick thickness ratio on brickwork compressive strength: comparison with experimental data

An essential difference between brickwork and solid block masonry can be seen from this diagram in that the ratio of joint thickness to unit height in brickwork is typically 0.15 and in blockwork about 0.05 or less. The influence of the mortar joint in relation to the compressive strength of the masonry is thus much less in blockwork and the strength of the masonry more closely approaches that of the unit.

In certain types of concrete blockwork, the mortar strength is similar to, or even greater than, the unit strength. In such a case, the mortar will tend to reduce the lateral strains in the blocks, and a kind of shear failure along certain lines of weakness in the masonry will be observed rather than the vertical tensile cracking typical of brickwork.

2.2.3 *Effect of unit height*

It should be noted also that the apparent strength of units of the material in a conventional compression test decreases with the height of the unit. This follows because the strength of a unit in such a test is influenced by friction between the unit and the platens of the testing machine, which has the effect of reducing the lateral strain in the unit. The platen effect is clearly reduced for a unit of given thickness as its height is increased and thus the apparent compressive strength is reduced. This is illustrated in figure 2.2 which shows the strength of the unit with platen restraint related to its unconfined compressive strength, plotted against the aspect ratio (height/thickness).

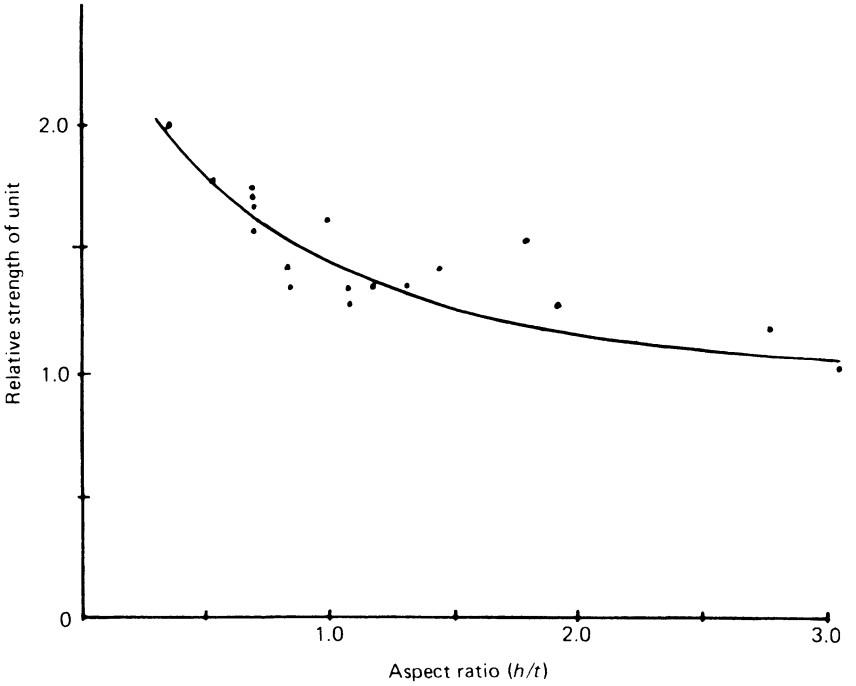

Figure 2.2 Ratio of unit strength with platen restraint to unconfined compressive strength against aspect ratio (after Page)

This diagram is based on results obtained by Page [8] from tests on calcium silicate units.

The combined effect of the joint thickness factor and the apparent unit strength, also related to height, is to give ratios of masonry strengths to unit strength higher than those for brickwork, suggesting that blockwork is 'more efficient' than brickwork. In terms of real material strengths, however, this is illusory and any comparison of brickwork and blockwork strengths must take into account the relative height of the units.

2.2.4 *Masonry with perforated and hollow block units*

A number of investigators have studied the effect of different types of units on compressive strength – an extensive series of tests was undertaken by West *et al.* [9] at the British Ceramic Research Association to examine the compressive strength of brickwork built with a variety of wire-cut bricks having different hole patterns with perforation ratios up to 20 per cent. The results of these tests showed that if the brickwork strength was calculated on the basis of a standard crushing test on the unit, the perforation pattern made little practical difference. In these tests, the perforations were either

circular holes or slots with round ends, but in some tests reported by Monk [3] the units had rectangular slots, and these tests showed reduced compressive strength in prisms. It would seem probable that such slots would introduce stress concentrations, not only in service but also in manufacture, which would be a source of weakness.

Schellbach [10] has examined the strength of various types of highly perforated units and has found that the highest ratio of masonry strength to unit strength was obtained with a perforation ratio of 38–43 per cent. Schellbach's study included examination of stress concentration factors associated with different perforation patterns, and he concluded that these remain within acceptable limits even with rectangular slots, provided that the corners are well rounded.

Hollow block masonry may be built with the cores either unfilled or filled with concrete. In the former case the mortar joint may cover the whole of the bed face of the block (full-bedded) or only the outer shells (face-shell-bedded). These different construction methods result in considerable variations in structural behaviour and this quite clearly results in a more complex situation than for solid units in assessing masonry strength.

It is usual to take the strength of hollow units which are to be laid full-bedded as the maximum test load divided by the gross area of the unit. This value is then used to determine the masonry strength as if the unit were solid.

The stress conditions and mode of failure of shell-bedded hollow block masonry differ considerably from those in solid block masonry. They have been investigated by Shrive [11] who has shown that tensile stresses are developed in the webs of the blocks, which eventually lead to failure. This may be illustrated by reference to figure 2.3 which shows, in simplified form, the stress conditions in a quadrant of the web of a hollow block with face-shell bedding. Compression from the block above is applied at point A setting up compressive stresses along the line BC at mid-depth of the block. For equilibrium, a stress system must result along the line CD with tensile stresses towards the top surface of the block. If the load is applied eccentrically, the location of the tensile stresses causing failure

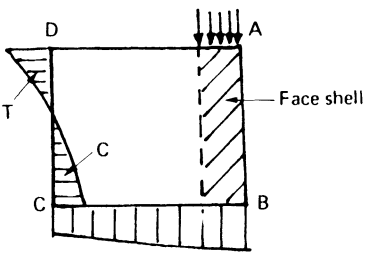

Figure 2.3 Failure of face-shell bedded masonry; quarter section of block (Shrive)

will move in the same direction as the load, but with higher eccentricities the mode of failure will be modified [12]. Shrive has found failure stresses under eccentric loading to be higher than under axial loading, but tests by Drysdale and Hamid on hollow blockwork prisms have not shown this effect [13].

The strength of shell-bedded masonry should be calculated on the basis of the mortared area of the units and if the strength is assessed by prism tests, the specimens should be shell-capped and not loaded over the total area of the unit. Because of the possible strain-gradient effect and the change in mode of failure, tests should be carried out under eccentric as well as axial load conditions.

Hollow blockwork masonry is frequently built with the cores filled with concrete (grout). The compressive strength of this type of masonry is found to be considerably less than the sum of the strengths of the hollow block and concreted core tested separately, even when the materials are of approximately the same nominal strength. This is because there is a difference in the strains in block and fill materials at ultimate load. Thus Hamid and Drysdale [14] have found the strain at ultimate strength of fill material used in their investigations to be about 0.0024 compared with the strains at failure of the block material of 0.0036. This leads to large tensile lateral stresses in the hollow block and failure before it has reached its ultimate strength. The properties of hollow block and core materials have been further investigated by Khalaf *et al.* [15].

2.2.5 *Natural stone masonry*

Although very little new construction is carried out in stone masonry, there is frequently a need to assess the strength of this material in the course of renovation or restoration of old buildings. Very little information is available from laboratory tests on stone masonry other than from a series of tests carried out at Edinburgh University. These tests included two on large piers taken from a building which was being demolished and two series of tests on laboratory built specimens, the results of which are summarised in table 2.3. The masonry strengths from the small pier tests are plotted against stone strengths in figure 2.4.

The relatively low strength of the large pier taken from the building will be understood from figure 2.5 which shows its cross-section. The outer face of the pier was built in ashlar masonry while the inner face was in random rubble. In the test the inner-face masonry failed first, throwing an eccentric load on the ashlar masonry. The laboratory built piers were constructed in coursed rubble and may be considered to give a reasonable indication of the strength of such masonry in good condition.

Stone masonry built from accurately shaped blocks with thin joints would approximate in strength to the stone strength irrespective of the mortar strength.

Table 2.3 Tests on stone masonry piers

Piers removed from building – sandstone

Pier no.	*Cross-sectional* (m^2)	*Stone strength* (N/mm^2)	*Mortar strength* (N/mm^2)	*First crack* (N/mm^2)	*Failure stress* (N/mm^2)
A	1.04	112	0.78	—	2.15
B	0.99	112	0.78	1.21	2.78

Piers built in laboratory
Average size of piers 775 × 410 × 930 ($w \times t \times h$) mm
No. of courses 5
Average stone size 360 × 200 × 160 mm
Joint thickness 20 mm

Pier no.	*Type of stone*	*Crushing strength* (N/mm^2)	*Mortar mix and strength* (N/mm^2)	*Stress at first crack* (N/mm^2)	*Failure stress* (N/mm^2)
First series					
1.1	Whinstone	167.6		6.16	9.86
1.2	Limestone	31.0		3.58	4.88
1.3	Sandstone	38.6	1:2:9	2.77	4.24
1.4	Sandstone	46.8	(2.57)	6.30	6.93
1.5	Granite	130.6		4.94	10.91
1.6	Granite	130.6		5.81	12.32
Second series					
2.1		49	1:2:9	2.77	5.96
2.2		49	1:2:9	3.48	6.38
2.3		49	1:3:12 (1.25)	5.09	7.14
2.4		49	1:3:12 (1.30)	3.96	7.07
2.5		35	1:3:12 (0.95)	2.50	4.09
2.6		35	1:3:12 (1.40)	2.94	4.36
2.7		58	1:2:9 (1.4)	4.37	11.12
2.8		87	1:2:9 (1.18)	3.36	>11.8
2.9		83	1:2:9	4.35	10.14
2.10		83	1:2:9	7.15	10.98
2.11		65	1:2:9 (2.0)	4.95	10.22
2.12		65	1:2:9 (2.1)	5.51	11.16

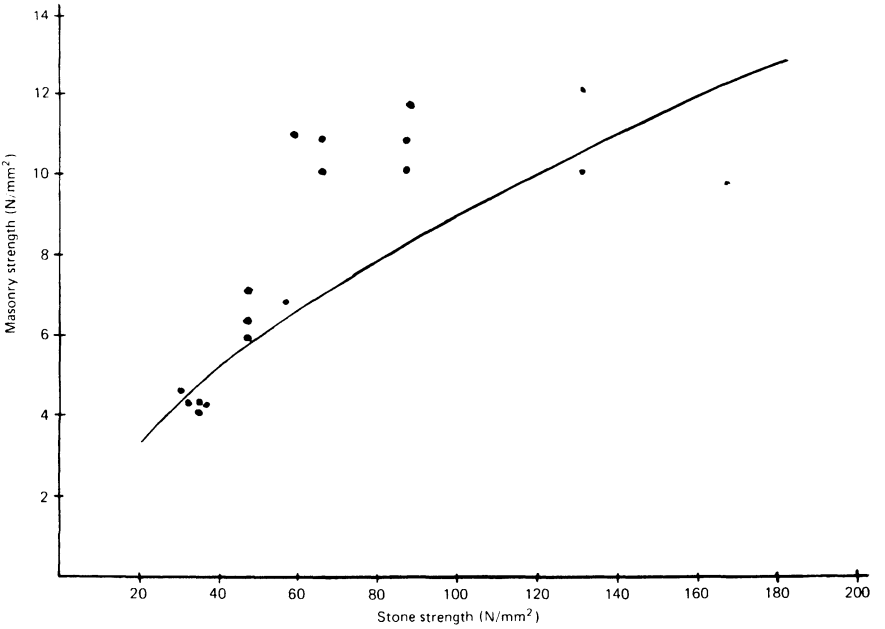

Figure 2.4 Compressive strength of rubble masonry piers in 1:2:9 mortar

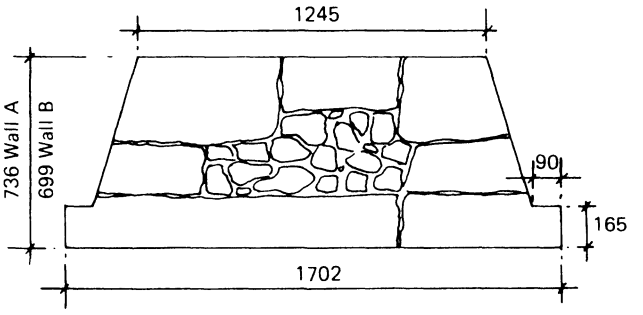

Figure 2.5 Cross-section of piers taken from demolished building

2.2.6 *Effect of brickwork bond, wall type and direction of loading*

In general the effect of various brickwork bonds on basic compressive strength has been shown to be relatively small, but the results of a few tests [16] on walls built in what is sometimes described as stretcher bond, that is, two leaves or wythes of brickwork without headers, suggested that this type of masonry is of lower strength than normally bonded brickwork of the same materials. The comparisons leading to this conclusion were, however, rather limited, but some further work reported by Beard [17] indicated that

the strength of a 219 mm wall, consisting of two 105 mm leaves, was reduced by about 16 per cent when butterfly wire ties giving 40 mm^2/m^2 of wall were used and by about 10 per cent when using special rectangular ties giving 340 mm^2/m^2 of wall. On the other hand, comparative tests by James [18, 19] on 219 mm walls with headers every fourth course, and 219 mm stretcher bond walls with various kinds of ties, showed no significant difference between the two types. Also some model-scale tests in which standard twisted steel ties were simulated, showed no significant reduction in strength, while stretcher bonded walls without ties showed about an 11 per cent reduction. Although the number of tests is rather limited, it would appear that the difference between the strength of stretcher bond walls and normally bonded walls is unlikely to be greater than 10 per cent, with normal spacing of twisted steel ties, and therefore unlikely to be important considering the safety factors currently used in brickwork construction.

Closely related to the stretcher bond wall is the open cavity wall built of two stretcher bond leaves of equal thickness. Tests on cavity walls equally loaded on both leaves [20] indicated that the strength of the wall was about 70 per cent of the strength of two single-leaf walls of the same materials. The probable reasons for this were suggested to be that: (1) it is difficult to ensure that loading is equally applied to the two leaves, (2) it is difficult to construct both leaves of a cavity wall equally well in terms of ensuring that the joints are completely filled, and (3) the strength of the cavity wall will be limited by the strength of the weaker leaf, failure of which will precipitate failure of the whole wall. An investigation conducted by Fisher [21] showed about a 14 per cent reduction in cavity wall strength for walls built of perforated bricks, and no difference for single frog, semi-dry pressed bricks. These tests also indicated that the strength of cavity walls is not greatly affected by tie spacing, even when the cavity wall was loaded only on one leaf. Cavity walls tested by James [18] under axial load were practically equal in strength to two single-leaf walls. The number of tests reported is again rather small and is insufficient to resolve the apparent discrepancy between the various results. It would, however, be reasonable to assume that the brickwork in a 270 mm cavity wall was equal in strength to that of a 229 mm bonded wall of the same height.

It has been found by many investigators [9, 18, 19, 21–23] that, in terms of ultimate compressive stress, walls whose thickness is equal to the width of the bricks used are stronger than bonded walls. Thus a 105 mm thick masonry wall is significantly stronger than a 219 mm bonded masonry wall built with the same materials. This point may be illustrated by reference to the results of comparable tests reported by James [18], Fisher [21] and Bradshaw and Hendry [23]. In each case 105 mm and 219 mm walls built of the same materials were tested, and the load factor for each wall was calculated on the basis of the code of practice in use at the time and place of the tests, with the following results:

	105 mm	*219 mm*
James	10.6	7.2
Fisher	7.4	4.3
	14.9	5.6
Bradshaw and Hendry	7.5	3.6

An extensive series of tests on 105 mm walls built of wire-cut bricks carried out by West *et al.* [9] and the earlier results of Bradshaw and Hendry [23] provide further evidence of the consistently high load factors found experimentally for this type of brickwork. The point also emerged clearly from the statistical analysis by Hendry and Malek, discussed in section 2.3.

In certain situations, brickwork may be stressed in compression in directions other than normal to the bed joint. A number of investigations [24–27] have therefore been carried out to determine the strength of brick masonry in which the brickwork is compressed parallel to the bed joints with the bricks stressed parallel to either their length or thickness. Some of the results reported are summarised in table 2.4. These cover a range of brick types and strengths but do not show any consistent relationship between the perforation pattern and the brick and prism strengths. As would be expected, the strength of the unit tested in a direction other than normal to the bed joint is considerably reduced, but the prism strength does not vary

Table 2.4 Compressive strength of bricks and prisms compressed in different directions (Sinha and Pedreschi)

Brick type	*Brick strength (N/mm^2) tested*		
	On bed	*On edge*	*On end*
14 hole	74.3 (100)	26.2 (35)	10.4 (14)
10 hole	70.2 (100)	29.5 (42)	21.7 (31)
3 hole	82.0 (100)	53.2 (65)	40.2 (49)
5 slots	64.1 (100)	51.8 (81)	13.8 (22)
Brick	*Prism strength (N/mm^2) laid*		
	On bed	*On edge*	*On end*
On end			
14 hole	28.9 (100)	8.5 (29)	14.6 (51)
10 hole	22.0 (100)	15.0 (66)	20.0 (91)
3 hole	37.6 (100)	30.5 (78)	21.8 (56)
5 slots	34.1 (100)	29.0 (85)	13.9 (41)

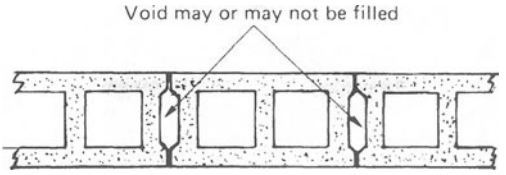

Figure 2.6 Longitudinally stressed hollow concrete blockwork

in the same proportion. Also the ratio of prism strength to brick strength in the various directions is generally quite different. It is not, therefore, a reliable procedure to base an estimate of masonry strength, when the units are stressed in a direction other than normal to the bed joint, on the strength of the unit tested in the relevant direction. It would appear that the only method of determining brickwork strength for a particular type of brick in these circumstances is to carry out a series of tests on appropriately designed specimens.

Grouted hollow blockwork is used for reinforced masonry beams and in this situation the blocks may be stressed in the longitudinal direction. This case has been investigated by Khalaf [28] who points out the important difference in behaviour between flat-ended blocks and those which are of the shape indicated in figure 2.6. With blocks of this type a void is created between abutting units, which may or may not be filled with concrete. If these voids are not filled, the blocks will be loaded through the face-shells. As in the case of filled hollow blockwork loaded normal to the bed face, the strength of specimens loaded longitudinally shows a reduction compared with unfilled blocks. This is again attributable to the difference in strain compatibility between the block and core fill materials. At present there is insufficient information on which to base a general method of determining masonry strength in this direction, and in practice recourse must be made to tests. In this respect, it would appear that tests on appropriately filled single block prisms would give a reasonable estimate of masonry strength.

2.3 **Empirical formulae for the compressive strength of masonry**

There is now available a considerable volume of data from tests on masonry walls carried out in various countries in the world [9, 10, 15–23, 29–54] and covering a wide variety of unit types and strengths. Hendry and Malek [55] have carried out a statistical analysis of several hundred wall tests and have obtained best fit equations for the mean strength of storey height brickwork walls 102.5 mm and 215 mm thick built with solid units in 1:1/4:3 and 1:1:6 cement:lime:sand mortar. The 102.5 mm thick walls were of the same thickness as the units while the 215 mm walls were of bonded brickwork equal in thickness to the length of a brick. The equations obtained were as follows:

Masonry thickness (mm)	*Mean compressive strength of wall (N/mm)*	
102.5	$f = 1.242 f_b^{0.531} f_m^{0.208}$	(2.1)
215.0	$f = 0.334 f_b^{0.778} f_m^{0.234}$	(2.2)

where f_b and f_m are respectively the brick and mortar compressive strengths. These equations are shown in figure 2.7 for four typical mortar strengths and for 102.5 mm thickness.

Making allowance for the slenderness ratio of the 102.5 mm test walls on the basis of a slenderness reduction factor of 0.77, characteristic masonry strengths are given by the same equations but with initial constants of 1.017 and 0.217 for the 102.5 and 215 mm walls respectively. The resulting curves are shown in figures 2.7 and 2.8.

Following earlier work, Rostampour [52] found that the mean compressive strength of blockwork masonry built in 1:1:6 cement:lime: sand mortar is well represented by the equation

$$f_{mw} = 0.9 f_b^{0.67} f_m^{0.33} \tag{2.3}$$

This applies to masonry in which the block strength:mortar strength is greater than 1.7 and the ratio of block height to thickness is around 2.2. Figure 2.9 shows a comparison between this formula and experimental results [52]. Based on a statistical analysis of the results of 925 wall tests in various types of unit and mortar strengths Mann [56] observed a relationship between masonry, unit and mortar strengths $f_{mw} = 0.83 f_b^{0.66} f_m^{0.33}$, which is similar to that found by Rostampour.

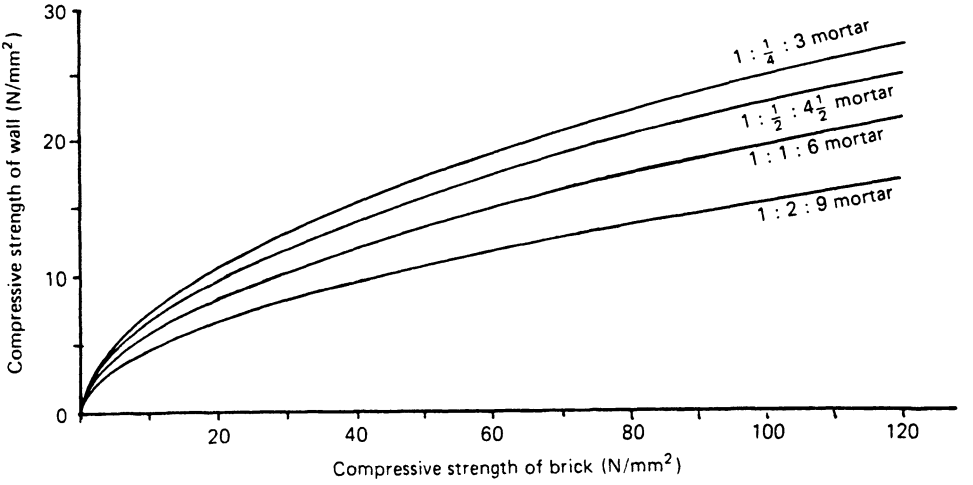

Figure 2.7 Mean compressive strength of walls against brick strength for 102.5 mm thick brickwork in various mortars. Derived by statistical analysis of test results

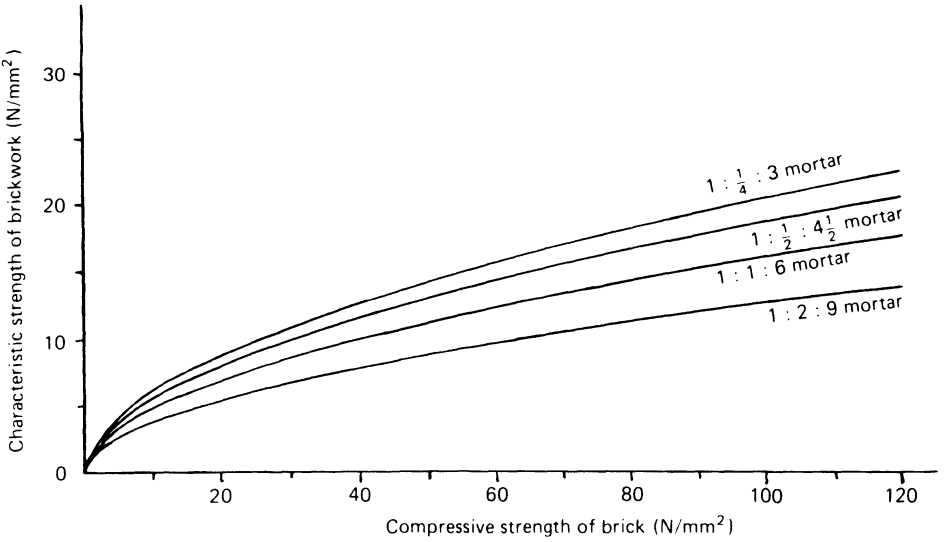

Figure 2.8 Characteristic strength of brickwork in 215mm thick walls built in various mortars. Derived by statistical analysis of test results

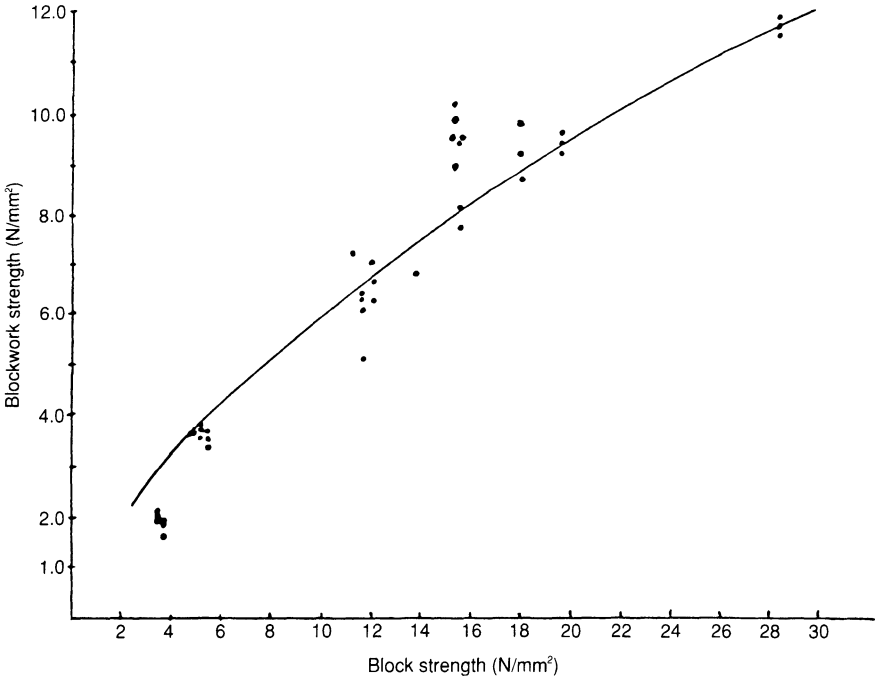

Figure 2.9 Compressive strength of solid concrete blockwork in 1:1:6 mortar

Kirtschig [57] has shown that for different types of mortar the modulus of elasticity rather than the strength is the controlling factor and has accordingly proposed the relationship

$$f_{mw} = 0.97 f_b^{0.43} E_{vmo}^{0.26} \text{ N/mm}^2 \tag{2.4}$$

where E_{vmo} is the elastic modulus of the mortar divided by 1000.

The above formulae apply to rather specific sets of results and attempts have been made to derive equations of a more general nature, applying to both brickwork and blockwork. Thus Render and Phipps [58] have suggested a bi-linear representation of the unit/masonry strength on the basis of collected brick and block masonry wall tests. This relationship varies according to the mortar strength and applies to a unit of height/thickness ratio of 0.65, which is typical of a brick. For other shaped units these authors have derived the unit shape factor, shown in figure 2.10, which will give the equivalent strength of the unit of *h/t* ratio 0.65 to be used in determining the masonry strength from the appropriate unit/masonry strength relationship.

A somewhat similar proposal for calculation of characteristic strength has been adopted in Eurocode 6 [59] using the equation:

$$f_k = K(f_b)^{0.65}(f_m)^{0.25} \tag{2.5}$$

where K is a factor depending on the type of masonry

f_b is the 'normalised' compressive strength of a masonry unit

f_m is the mean compressive strength of mortar.

The recommended values of K vary from 0.6 for walls which are of the same thickness as the units and of the highest category of quality, to 0.4 in the case of walls which have a longitudinal joint in their thickness and are of lower quality units. The normalised unit strength is intended to be the

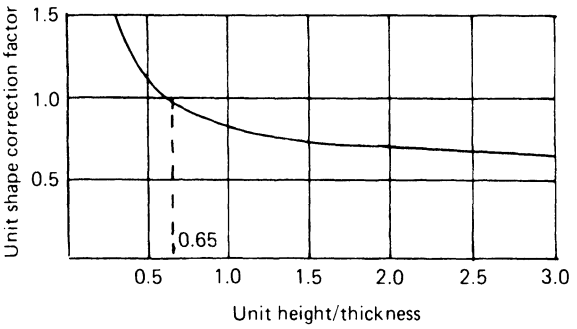

Figure 2.10 Relationship for the conversion of unit strength to equivalent strength of unit with the height-to-thickness ratio of 0.65 (Render and Phipps)

equivalent of a 100 mm cube, introduced to give a single formula for units of different proportions. The Eurocode gives a table of values for a constant δ by which the test strength of the unit should be multiplied to give f_b in the formula. Very similar values are given by the following formula derived by Khalaf and Hendry [60] from test results:

$$\delta = \left(h/\sqrt{A}\right)^{0.37}$$

where h is the height of the unit

A is the loaded area.

Drysdale and Hamid [13] have given the following equation for grout filled hollow block prisms:

$$f'_{mg} = \zeta\left[1 - K(1 - \zeta)\frac{f_{cg}}{f'_{mu}}\right]f'_{mu} + (1 - \zeta)f_{cg} \qquad (2.6)$$

where

ζ = core area ratio

f_{cg} = compressive strength of the grout material

f'_{mu} = compressive strength of the block material

K = a stress adjustment factor = $1.08 + 0.21/n$ where $n = E_{block}/E_{grout}$.

This relationship shows good agreement with experimental results over a range of grout strengths up to 50 N/mm^2, as may be seen from figure 2.11.

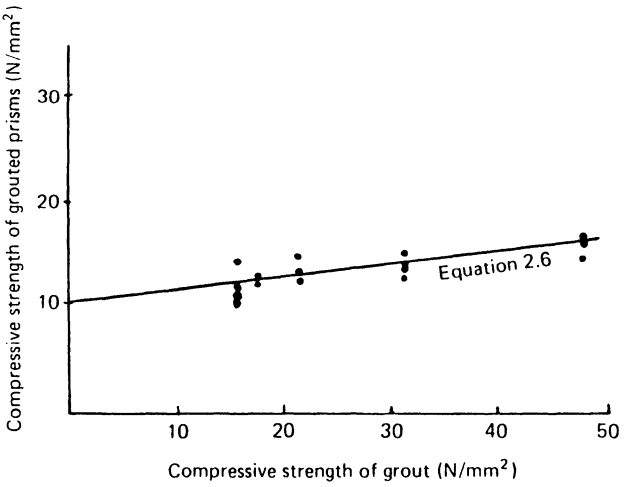

Figure 2.11 Grouted prism strength against grout strength (block strength 16 N/mm^2, ζ = 0.62, K = 1.15) (Drysdale and Hamid)

2.4 **Effects of certain construction details**

2.4.1 *Concentrated loads on masonry*

It has been known for many years that the contact stress between a beam-bearing and a supporting masonry wall may considerably exceed the uniaxial strength of the material. The effect is allowed for in various design codes and has been the subject of considerable investigation in recent years [61–76].

Experimental and analytical studies of the problem have been reviewed by Page and Hendry [75]. This review showed that the following factors influence the enhancement of strength in the region beneath a concentrated load:

1. the ratio of the loaded area to the length of the wall
2. the position of the load along the wall
3. whether the load extends across the full width of the wall or is limited to part of the width (that is, strip or patch loading)
4. whether the load is applied through a rigid or a flexible plate
5. the type and strength of the masonry materials
6. the length-to-height ratio of the wall and its thickness
7. the presence of compressive loading from above
8. the presence of a spreader beam or padstone
9. the application of multiple loads.

In view of the large number of such factors and with differences in testing procedures and interpretation it is not surprising to find that experimental results show considerable variation. One of the most critical factors influencing evaluation of test results is the definition of the uniaxial compressive strength of masonry. Ideally, the increased bearing strength should be related to the strength of a storey height wall, with sufficient tests being performed to establish mean and characteristic values of material strength under both uniform and concentrated loading. This has seldom been achieved in reported test programmes and in most cases the results are based on the mean of only a few tests. Collected results of tests on brickwork built of solid units are shown in figure 2.12 in which the enhancement factor is plotted on a base of loaded-area ratio for loads applied at the centre and at the end of a wall of limited length. These parameters are the most important and lower bound curves are shown for the two loading cases, the equations for which are shown.

As may be observed, the enhancement factor rises sharply for values of the loaded-area ratio less than about 0.15 and is greater for the centrally loaded case. The enhancement factor for loaded-area ratio greater than 0.3 is very small. Tests show that the relationship defined for strip loading also applies with reasonable accuracy to patch loading.

Most tests have been carried out on small specimens of roughly square aspect ratio. In these cases the loaded-area ratio has been calculated on the

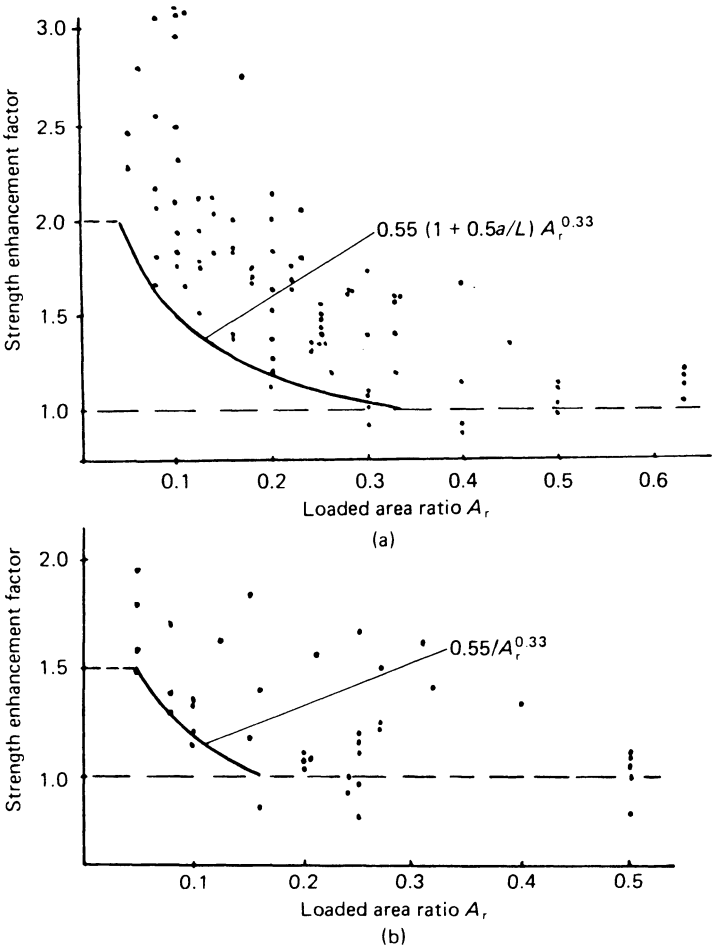

Figure 2.12 Concentrated load enhancement factors: (a) central load; (b) end load

basis of the full plan area of the specimen, but in practice it is obvious that a limited length of wall has to be taken as the effective length in defining the loaded-area ratio.

Page and Hendry [75] have suggested that for a central strip load the effective length may be taken as the actual length but not greater than $(b + 1.2h)$, where b is the length of the loaded area and h is the height of the wall. This is based on the concept that the spread of load will be contained within a 45° line from the edge of the loaded area and that the vertical compressive stress will be relatively uniform at 0.6 of the wall height from the top.

Applying this definition of effective length to a wall 2.5m in height carrying a beam 150mm in width would mean that the length of wall to be

considered, assuming central loading, would be 3.15 m, giving a loaded-area ratio of 0.048. With an end load the effective length would be 1.05 m and the loaded-area ratio 0.14. Comparing the enhancement factors from figure 2.12 will show that the end loading case gives a considerably smaller increase in strength than the centrally loaded case.

The effect of compressive loading from above must in principle be to reduce the failure stress under a concentrated load. Experiments reported by Hendry [76] indicate that the effect may be neglected for compressive stresses from above up to 30 per cent of the compressive strength of the masonry using the enhancement factors given above.

There is little or no experimental evidence as to the effect of spreader beams or pad stones, in the absence of which it would seem reasonable to assume a dispersion of the concentrated load through the beam at 60° or 45° and then to evaluate the strength enhancement by the method described above. Similarly, there is an absence of data on the effect of multiple loads on a wall. In this case it would seem logical to calculate the effective length for each load and to terminate it where it overlaps with adjacent loads.

The above discussion applies only to masonry built in solid units. It has been found [63] that there is no strength enhancement for concentrated loads applied at the end of a wall built in perforated units. Investigation of concentrated loads on hollow block masonry by Page *et al.* [74] shows that in this case the mode of failure is by splitting of the webs of the blocks rather than by vertical cracking.

2.4.2 *Chases in masonry*

In practical building construction the need to accommodate electrical wiring conduit, switch boxes and other fittings frequently leads to the cutting of chases and holes in brickwork; if the walls are slender this may lead to an appreciable reduction in wall strength. Tests by Prasan *et al.* [22] indicated

Table 2.5 Decrease in strength with chasing

Wall type	*Percentage decrease in strength*		
	178 mm walls	*102.5 mm walls*	*215 mm walls*
A	11.2*	16.9*	23.8*
B	6.7	1.1*	—
C	1.2	14.7	—
D	20.1	4.0	6.4
E	—	13.1*	13.3*
F	9.5	7.7*	28.5*

*Based on one result only: in other tests mean of three walls.

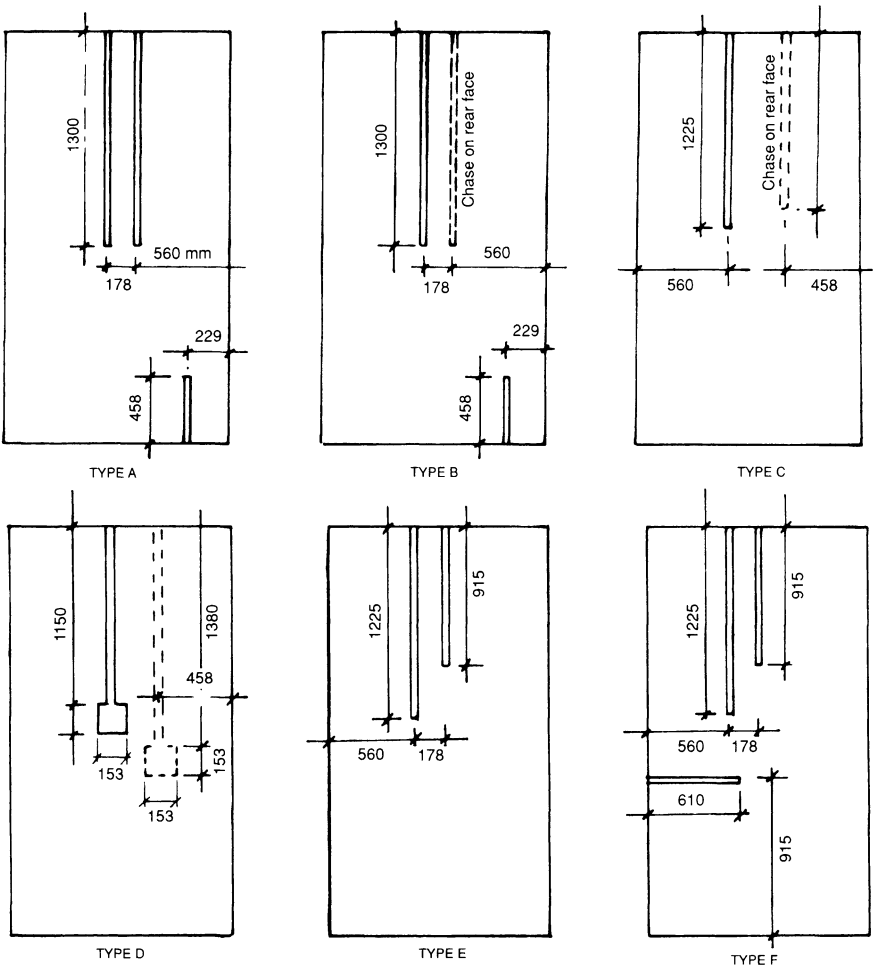

Figure 2.13 Effect of chases on compressive strength; patterns of chases tests by Fisher

that vertical chases 19 mm wide by 12 mm deep in a 105 mm wall had little effect on strength. In a more extensive investigation, Fisher [46] tested walls of 102.5 mm, 178 mm and 215 mm thickness with 38 mm wide by 25 mm deep chases cut in the patterns shown in figure 2.13. The decrease in strength as compared with corresponding walls without chases may be seen in table 2.5.

Kirtschig and Metje [77] have reported an extensive series of tests on the effect on the compressive strength of walls built in perforated clay brick masonry vertical and horizontal chases. The type of masonry used in this investigation was quite different from that in Fisher's work and the size of the chases much larger. Nevertheless, the maximum reduction of strength

was of the order of 25 per cent in both cases. Kirtschig and Metje conclude that the reduction in strength may be considered to be in proportion to the reduction of the cross-sectional area up to a limit of 25 per cent, and suggest various other limitations on the size and location of chases or recesses.

In general, it would seem prudent to limit the cutting of chases and the like in highly stressed walls, and where they are essential they should preferably be formed during construction of the wall or at least with special tools. Horizontal and diagonal chases should be avoided unless specifically allowed for in the structural design of the wall.

2.5 **The effect of workmanship factors on compressive strength**

In common with other construction materials and techniques, the strength of masonry is affected by site workmanship. To some degree this has been exaggerated, and has led to the adoption of very large safety factors in design codes that do not take into account the factors involved, and thus the possibility of achieving near laboratory strengths by appropriate control measures. It is therefore essential to identify the workmanship factors that are significant in relation to strength and serviceability, and from there to devise the necessary specification clauses and site control measures. It should be made quite clear that we are not concerned here with gross errors or omissions – such as the use of the wrong bricks or mortar materials, or with defective materials – but with the identification of various defects in site work and an assessment of their effect on the performance of masonry. The most obvious workmanship factors are as follows:

Incorrect proportioning and mixing of mortar
Incorrect adjustment of suction rate of bricks
Incorrect jointing procedures
Disturbance of units after laying
Failure to build walls 'plumb and true to line and level'
Unfavourable curing conditions.

Practically all available information of a quantitative nature on the effect of these factors relates to brickwork, and the following discussion will be in terms of this type of masonry. However, some of the effects will apply equally to blockwork.

2.5.1 *Incorrect proportioning and mixing of mortar*

The effect of mortar strength on the compressive strength of brickwork has been referred to in previous sections of this chapter. Generally, the mortar strength, as defined by cube crushing strength, is not a very critical factor in masonry strength; for example, with bricks of crushing strength 35 N/mm^2, a halving of the mortar cube strength from 14 N/mm^2 to 7 N/mm^2 may be expected to reduce the compressive strength of the brickwork from about

16 N/mm^2 to 14 N/mm^2. This corresponds roughly to a change in mortar mix from 1:3 cement to sand to 1:4$\frac{1}{2}$ or, say, 30 per cent too little cement in the mix. A similar reduction in mortar strength could, of course, be brought about by an excess of water – moving from a water:cement ratio of about 0.6 to one of about 0.8 in a typical case. McIntosh [78] has stated that "the cement content of a 1:1:6 mix composed of cement gauged with ready-mixed lime:sand for mortar, could vary from about 13$\frac{1}{2}$ to 19% of the weight of dry lime plus dry sand; the corresponding range in water:cement ratio required to produce mortar of standard consistency was from about 1.6 to 1.1 resulting in a change of 7 day strength from 2.9 to 6.5 N/mm^2. Greater differences might be expected if all the materials are batched separately on site." Thus it is clear that while a 2:1 variation in the strength of site-produced mortar to the same nominal specification is possible, the effect on masonry compressive strength is proportionately much less, at any rate when the units are of low to medium strength. In the case of high-strength units, however, the effect of variation of mortar strength is likely to be more significant.

2.5.2 *Incorrect adjustment of suction rate*

In order to achieve optimum brickwork strength it has long been realised that the suction rate of bricks should be controlled to prevent excessive removal of water from the mortar. It seems possible that the water absorbed by the bricks leaves cavities in the mortar, which fill with air and result in a weakened material on setting. On the other hand, brickwork built with saturated bricks develops poor adhesion between bricks and mortar, and is of course susceptible to frost damage and other troubles. Some specifications recommend a limiting suction rate, or alternatively the use of a high retentivity mortar to control the extraction of water from the mortar. In so far as water extraction affects the final strength of mortar, one would not expect it to result in a serious weakening of brickwork in compression. However, Haller [29] has demonstrated that, in certain circumstances, suction rate has a considerable effect on brickwork strength because de-watered mortar tends to form a rounded joint during building owing to a loss of 'elasticity'. It would appear, for example, that with eccentric loading an increase in the suction rate from 2 kg/m^2/min to 4 kg/m^2/min could halve the compressive strength of a slender masonry wall.

It is clear, therefore, that suction rate is a factor to be taken very seriously, especially in the case of slender walls built in relatively low-strength bricks. If the bricks being used have a high initial rate of absorption, it is clearly essential to adjust this by wetting them before laying.

2.5.3 *Incorrect jointing procedures*

A variety of defects can arise from incomplete filling of joints and some evidence is available on the structural effects of these defects. The effect of

incomplete filling of perpend joints has been investigated by the British Ceramic Research Association [79] and by the Building Development Laboratories of Australia [80]. A total of thirty walls were tested at BCRA with unfilled vertical joints, using two types of brick and mortar with the results shown in table 2.6. Statistical examination of the results showed that there was no significant difference between corresponding sets of walls with joints filled and unfilled. The Australian tests (table 2.7) also showed that unfilled vertical joints had no significant effect on the strength of walls. There are theoretical reasons for expecting that this would be the case, but careless filling of vertical joints may be indicative of poor workmanship in other respects, and would certainly reduce non-structural performance in terms of sound insulation and resistance to rain penetration to a serious extent.

Incomplete filling of bed joints is, from the structural point of view, much more serious and has been investigated by the Structural Clay Products Institute in the United States [81] and by the Building Research Laboratories in Australia [80]. In the SCPI tests, the results of which are summarised in table 2.8, the 'uninspected' workmanship included unfilled vertical joints, as well as deeply furrowed bed joints, and resulted in a reduction of strength of about 33 per cent. As it is known that unfilled vertical joints do not affect strength significantly, it may be assumed that most of this reduction arose from the furrowed bed joints. The Australian tests (table 2.7) show a reduction of similar magnitude from this cause.

This third factor in brickwork jointing is that of thickness, which has already been discussed in section 2.2.2. This has been investigated by the Building Research Laboratories in Australia and at the Universities of Edinburgh [20] and Melbourne [1], and elsewhere [3]. It is difficult to compare the results of all these investigations, but it has been shown beyond doubt that excessively thick bed joints, say 16–19 mm, may be expected to reduce the strength of brickwork by something of the order of 30 per cent, as compared with normal 10 mm thick joints. This is of the same order of magnitude as the reduction caused by deep furrowing, but excessively thick joints are at least easily seen.

Another laying defect arises from the practice of spreading too long a bed of mortar – only sufficient mortar should be spread as will permit bricks to be set in plastic mortar. There is, however, no quantitative data on the effect of this defect on brickwork strength.

2.5.4 *Disturbance of bricks after laying*

Any disturbance of bricks after they have been placed will result in the bond between bricks and mortar being broken, with possible adverse effects on strength and resistance to moisture penetration. This commonly happens at corners, when the bricklayer attempts to correct plumbing errors by hammering bricks into a true plumb position, but there is no

Table 2.6 Effect of unfilled perpend joints on strength of brick walls (tests carried out by the British Ceramic Research Association)

Mean brick strength (MN/m^2) and water absorption	*Mortar*	*Mean mortar cube strength (MN/m^2)*	*Wall thickness (mm) and bond*	*Cross-joints filled or unfilled*	*Wall strength (MN/m^2)*
92	1 : $\frac{1}{4}$: 3	19.30	102.5 (4$\frac{1}{2}$ in.)	Filled	18.40
7.9%		15.30	Stretcher		21.16
		19.65			20.89
		18.13			20.15
		16.89		Unfilled	20.75
		16.27			13.99
		20.54			23.37
		17.92			19.37
92	1 : $\frac{1}{4}$: 3	15.65	215 (9 in.)	Filled	23.64
7.9%		22.27	English		16.75
		19.03			24.06
		18.96			21.44
		20.54		Unfilled	17.99
		19.30			19.37
		18.34			16.41
		19.37			17.92
92	1 : $\frac{1}{4}$: 3	15.72	215 (9 in.)	Filled	18.27
7.9%		17.03	Flemish		23.85
		15.10			16.89
		15.92			19.65
92	1 : $\frac{1}{4}$: 3	16.68	275 (11 in.)	Filled	21.37
7.9%		13.85	Cavity		21.09
		13.37			19.92
		14.61			20.75
46	1 : $\frac{1}{4}$: 3	13.79	102.5 (4$\frac{1}{2}$ in.)	Filled	15.65
14.5%		16.27	Stretcher		16.68
		17.51			13.72
		15.85			15.30
		15.44		Unfilled	13.79
		18.05			12.75
		10.41			10.75
		14.61			12.41
46	1 : 1 : 6	5.94	102.5 (4$\frac{1}{2}$ in.)	Filled	10.48
14.5%		4.27	Stretcher		9.72
		4.37			9.44
		4.86			9.85
		5.37		Unfilled	8.27
		4.88			10.20
		4.56			7.30
		4.96			8.61

quantitative data available on the effect of disturbance on the strength of brickwork. It is, however, related to the effect noted by Haller [29], whereby bricks with high initial rate of absorption tend to result in lowered strength of slender walls.

Table 2.7 Summary of wall and specimen strengths and their relationship to the 'no faults' wall and specimen strengths (from investigation of the effect of workmanship and curing conditions on the strength of brickwork, Building Development Laboratories Pty Ltd, Melbourne)

Wall type	*Wall strength* (MN/m^2)	f_m *prisms* (MN/m^2)	*Bond piers* (MN/m^2)	*Strength relationship to no faults specimens*		
				Walls	f_m *prisms*	*Bond piers*
No faults	21.2	18.1	0.524			
	21.5	18.9	0.613			
Average	21.4	18.5	0.565	1.00	1.00	1.00
Outside curing	19.0	15.0	0.310			
	20.8	18.6	0.351			
Average	19.9	16.8	0.330	0.93	0.91	0.59
Furrowed bed	16.1	15.0	0.841			
	16.1	14.3	0.792			
Average	16.1	14.6	0.813	0.76	0.79	1.44
No perpends	21.9	19.2	0.717			
	21.7	21.9	0.579			
Average	21.8	20.5	0.648	1.02	1.11	1.15
10 mm bed joints	16.6	14.1	0.448			
	15.2	14.8	0.482			
Average	15.9	14.4	0.468	0.75	0.78	0.83
12 mm bow	19.8	19.0	0.620			
	17.5	18.8	0.565			
Average	18.6	18.9	0.592	0.87	1.02	1.05
All faults	8.27	6.75	0.158			
	8.20	8.13	0.186			
Average	8.27	7.44	0.172	0.39	0.40	0.30

2.5.5 *Failure to build wall 'plumb and true to line and level'*

This type of defect can give rise to eccentric loading in a wall under compression and thus to reduced strength; information on this is available from tests carried out at the University of Edinburgh [23] and at the Building Development Laboratories in Australia. A summary of the Edinburgh results is shown in table 2.9. In these tests 105 mm brickwork walls were tested in compression between reinforced concrete slabs to give realistic end conditions. Two-storey height walls were tested with the applied load 20 mm eccentric with respect to the axis of the wall, and two walls were built 20 mm off-plumb. Comparing the strength of the walls with eccentrically applied loads with corresponding axially loaded walls indicates a reduction in strength of the order of 15 per cent; the reduction for those built off-plumb is similar. In the Australian tests (table 2.7) similar walls were built

Table 2.8 Effect of workmanship on the compressive strength of non-reinforced brick walls* (from Gross *et al.* [81])

Wall thickness and type	*Mortar type*	*h/t*	*Workmanship†*	*Average ultimate stress (N/mm^2)*	*Relative effect of workmanship*
90 mm (3.6 in.) single wythe‡	M	22.7	I	18.4	1.00
			U	12.2	0.66
	N	22.7	I	10.8	1.00
			U	6.84	0.63
200 mm (8.0 in.) multi wythe (metal-tied)‡	M	20.5	I	16.0	1.00
			U	11.0	0.68
	S	20.5	I	12.2	1.00
			U	7.92	0.65
	N	20.5	I	8.82	1.00
			U	6.02	0.68

* Data from unpublished SCPI tests. Walls were tested with hinged ends; eccentricity at top = $t/6$ and eccentricity at bottom = 0. Walls tested at age of 14 days. Metal-tied walls contained one 4.8 mm (3/16 in.) steel tie for each 0.25 m^2 (2.7 ft^2) of wall area.
† I = Inspected; U = Uninspected.
‡ Brick compressive strength = 81 N/mm^2 (11 760 p.s.i.).

Table 2.9 Results of 105 mm wall tests with eccentric loading

Wall no.	*Brick strength (N/mm^2)*	*Mortar strength (N/mm^2)*	*Brickwork strength (N/mm^2)*	*Loading*	*Remarks*
2–7	42.9	12.3	14.9	Axial	Av. of 6 walls
10–11	42.9	5.96	12.7	20 mm eccentric	Av. of 2 walls
12–13	42.9	5.03	12.6	20 mm off-plumb	Av. of 2 walls

with a 12 mm bow resulting in a 13 per cent strength reduction as compared with a truly plumb wall.

A survey of ten buildings in England carried out by the Building Research Establishment [82] showed that the following levels of accuracy were attained in brickwork construction

Wall plumb over a storey height ±13 mm
Vertical alignment between top and bottom of walls of successive storeys ±20 mm.

These figures are similar in magnitude to those used in the tests referred to in the previous paragraph, which therefore give a reasonable indication of the maximum probable reduction in strength arising from lack of plumb and vertical alignment.

2.5.6 *Failure to protect work from the weather*

Newly completed brickwork can be adversely affected by exposure to unfavourable weather conditions such as curing under very hot conditions, frost and rain damage, and some information is available on the effect of the first two of these conditions. The Building Development Laboratories in Australia reported [80] a series of tests on walls that were built in temperatures between 78°F and 100°F and cured in the sun for five to six days. These walls showed about a 10 per cent reduction in strength as compared with walls cured in the shade under polythene.

At the other end of the climatic scale, tests have been carried out in Norway and Finland to examine the effect on brickwork properties of laying and curing at low temperatures [83]. Masonry piers of 1 m height were built in various mortars at room temperature and in cold rooms at temperatures down to −15°C; curing of the piers built at low temperatures was carried out at −15°C and the results showed, perhaps surprisingly, no deterioration in strength as between the walls built at room temperature and those in the cold conditions (table 2.10). On the other hand, the liability of masonry built under freezing conditions to develop undesirable deformations is pointed out, and one would suspect that this could give rise to indirect reduction of strength as a result of bowing, or lack of plumb. No information is available about the effects of damage by rain.

2.5.7 *Overall effects of workmanship on brickwork strength*

In the foregoing sections the separate effects of a number of workmanship factors have been discussed. In any particular case, these defects will be present in varying degrees and the overall strength of the brickwork will reflect their combined effect. Various efforts have been made to assess the overall effect of workmanship on the strength of brickwork, the most systematic being the programme carried out by the Building Development Laboratories in Australia already referred to [80], in which controlled defects were introduced separately and in combination. As may be seen in table 2.7, the combined effect of outside curing, deep bed furrowing, unfilled perpends, 16 mm bed joints and 12 mm bow was to reduce the wall strength from 21.4 N/mm^2 to 8.3 N/mm^2, that is, a 61 per cent reduction. This is generally consistent with experiments at the US National Bureau of Standards where unsupervised site brickwork was from 55 to 62 per cent of the strength of supervised brickwork. (A further study of the relative strength of supervised and unsupervised brickwork will be found in reference 84.)

The Australian report makes the following assessment of the relative importance of the various defects in terms of the probable reduction in strength of a wall built under laboratory conditions:

Table 2.10 Compression tests on piers at low temperatures

Pier no.	*Laid in mortar type**	*Brick**	*Breaking strength (N/mm^2)*	*Cracking load / Breaking load*
Mortar 1, KC 50/50/610				
1	S	t	9.88	0.57
2				0.53
3	S	v	14.2	0.79
4				0.73
5	K_2	t	10.3	0.59
6				0.56
7	K_2	v	13.5	0.65
8				0.72
9	K_1	t	11.1	0.64
10				0.63
11	K_1	v	13.6	0.70
12				0.73
Mortar 2, KC 35/65/520				
13	S	t	11.1	0.55
14				0.62
15	S	v	19.1	0.87
16				0.91
17	K_2	t	12.3	0.63
18				0.60
19	K_2	v	18.0	0.77
20				0.87
21	K_1	t	11.7	0.57
22				0.63
23	K_1	v	15.5	0.79
24				0.70
25	K_1	vv	15.4	0.81
26				0.69
Mortar 3, KC 20/80/440				
27	S	t	12.9	0.72
28				0.70
29	S	v	21.3	0.89
30				0.90
31	K_2	t	13.9	0.78
32				0.62
33	K_2	v	21.9	0.87
34				0.72
35	K_1	t	13.8	0.64
36				0.85
37	K_1	v	21.6	0.82
38				0.90

* S = laboratory; K_1 = room at −15°C; K_2 = room at +6–7°C during laying then reduced slowly to −15°C; vv = warm, wet brick; v = wet brick; t = dry brick.

Outside curing (warm conditions)	10 per cent
Furrowed bed	25 per cent
16 mm thick bed joints	25 per cent
Perpend joints unfilled	Nil
12 mm bow	15 per cent

It was concluded that these effects are not interactive and that the separate factors are additive.

2.6 The deformation properties of masonry in compression

2.6.1 E-*values for short-term loading*

Knowledge of the stress–strain relationship for brickwork in compression is frequently required in structural design, and numerous measurements have been made on small specimens and on walls and piers to establish the nature of the stress–strain curve and the value of Young's modulus.

The stress–strain relationship for brickwork loaded in compression to failure has been determined for four brick types by Powell and Hodgkinson [85]. The results of these tests are summarised in table 2.11 and figure 2.14a.

Powell and Hodgkinson were able, by using a suitable load control technique, to determine the stress–strain relationship past the maximum compressive stress to failure. There was some variation of results between specimens of the same materials, but reasonable consistency was obtained, and the curves in figure 2.14a are average values for three tests in each case.

Table 2.11 Stress–strain relationship for brickwork (mortar $1:\frac{1}{4}:3$, mean compressive strength 15.24 N/mm^2)

Brick type	*Brick compressive strength (N/mm^2)*	*Brickwork compressive strength (N/mm^2)*	*Elastic modulus*	
			tangent (N/mm^2)*	*secant† (N/mm^2)*
A – 16 hole perforated	69.6	19.93	18230	11900
B – Class A, blue engineering	71.7	27.65	17370	12930
C – Fletton	25.5	9.33	4960	3740
D – Double frogged stiff plastic	45.3	20.10	16830	11610

* Initial tangent modulus.

† Secant modulus at 2/3 of maximum stress.

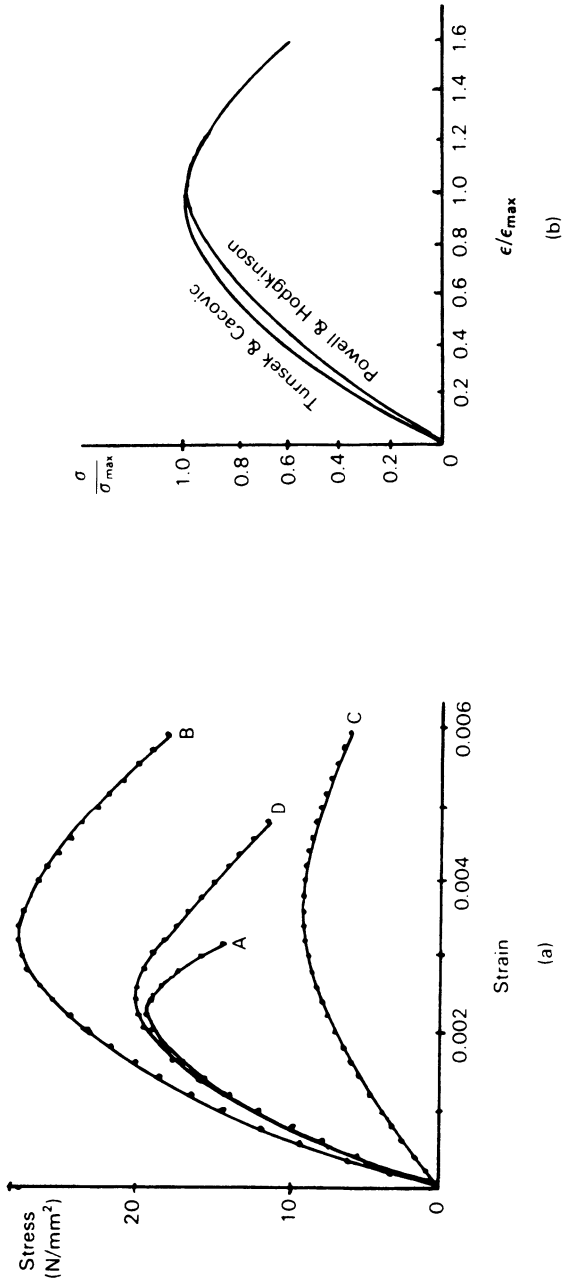

Figure 2.14 Stress–strain curves for brickwork in compression: (a) four types of brick in $1:\frac{1}{4}:3$ mortar (Powell and Hodgkinson); (b) dimensionless stress–strain curves

By plotting these stress–strain curves on a dimensionless basis (figure 2.14b), it is found that the curves for the four types of brick are, for practical purposes, of the same form, which in turn is in good agreement with that reported by Turnsek and Čačović [35]. The relationship is closely represented by the parabola

$$\frac{\sigma}{\sigma'} = 2\left(\frac{\varepsilon}{\varepsilon'}\right) - \left(\frac{\varepsilon}{\varepsilon'}\right)^2$$

where σ' and ε' are respectively, the stress and the strain at the maximum point of the curve. The initial tangent modulus is given by

$$E = 2\sigma'/\varepsilon' \tag{2.7}$$

and the secant modulus at $0.75\sigma'$ is three-quarters of this value. Sinha and Pedreschi [24] have found a cubic parabola relationship from tests on reinforced brickwork beams while Ameny *et al.* [86] have developed a method for calculating the elastic modulus of masonry from the characteristics of unit and mortar.

A number of authors [87, 88] have related the modulus or elasticity of masonry to its compressive strength on an empirical basis. This has resulted in values of E between 400 and 1000 times the masonry crushing strength (f_m). Schubert [89], on the basis of a statistical analysis of test results for several types of masonry, gives a similar range of values and also the formula $E = 2116\sqrt{f_m}$. Sinha and Pedreschi [24] have proposed the expression $E = 1180 f_m^{0.83}$ for brick masonry. Based on a particular test method, Knutsson and Nielsen [90] have suggested the use of a secant modulus between 0.05 and 0.35 of the compressive stress which is close to that at $0.4f$, as used in the design of concrete and wood structures. A value equal to 1.2 times this is suggested for use in the design of compression elements by the Ritter method (see section 5.5, page 109). They report a series of tests on brickwork specimens and confirm the general validity of the parabolic relationship.

The difference between the initial tangent modulus and the secant modulus at two-thirds to three-quarters of the maximum compressive strength is indicative of the non-linearity of the stress–strain curve. A number of investigators have noted an apparent increase in the tangent modulus for brickwork with an increase in stress at low stress levels. This effect is mentioned by Sahlin [88] in relation to lime and other relatively weak mortars, but it has also been observed in high strength brickwork by others [91]. The reason for an initial increase in the elastic modulus is not altogether clear, but it is almost certainly connected with deformations in the mortar bed, possibly resulting from uneven bedding. Strain measurements in walls are, in fact, usually found to be very variable both in terms of the point or line of measurement and the general stress level.

2.6.2 *Creep strains in masonry*

The E-values discussed in the preceding section are the result of short-term measurements. Under long-term loading, creep strains will occur and may be of importance in practice, especially where there is the possibility of differential movements between different materials. An example of such a situation is where a wall consists of an outer leaf of clay brickwork and an inner leaf of concrete blockwork; differential movements are possible in this case as a result of shrinkage or expansion of the two kinds of masonry as well as from thermal effects and creep. Creep is also an important factor in prestressed masonry construction.

Lenczner *et al.* [91–101] have investigated creep in a variety of brick and block masonry walls and piers. As a result of this work, they have given the following equations for the ratio of the total strain (that is, the sum of the creep strain and the initial strain) to the initial strain:

$$\text{For walls: } R_w = 5.46 - 0.33\sqrt{f_b} \tag{2.8}$$

$$\text{For piers: } R_p = 2.73 - 0.14\sqrt{f_b} \tag{2.9}$$

where f_b is the crushing strength of the brick.
These equations apply to brickwork built in $1:\frac{1}{4}:3$ or $1:1:6$ mortar.

Warren and Lenczner [102] have developed a method of predicting the creep strains in a building, through and subsequent to its construction based on an adaptation of Ross's equation [103]:

$$\varepsilon_{ct} = \frac{t}{a + bt} \quad \text{or} \quad \frac{1}{\varepsilon_{ct}} = \frac{a}{t} + b \tag{2.10}$$

where t = time in days, ε_{ct} = creep strain, and a and b are constants.

Putting $t = \infty$ in the Ross equation gives

$$\varepsilon_{ct} = 1/b = \varepsilon_{cmax} \tag{2.11}$$

and if $C_c = \varepsilon_{cmax}/\varepsilon_i$, where ε_{cmax} = maximum creep strain and ε_i = instantaneous strain, we have

$$\varepsilon_{cmax} = C_c\varepsilon_i = 1/b \tag{2.12}$$

Also $\varepsilon_i = \sigma/E_b$ where σ = applied stress and E_b = elastic modulus of brickwork, so that

$$b = \left(E_b/C_c\right)\sigma \tag{2.13}$$

Analysis of experimental work has established that

$$a\sigma = 3.8\ln\left(b\sigma\right) + 18.21 \tag{2.14}$$

and that

$$C_c = 7.35 - 0.62\sqrt{f_b} \tag{2.15}$$

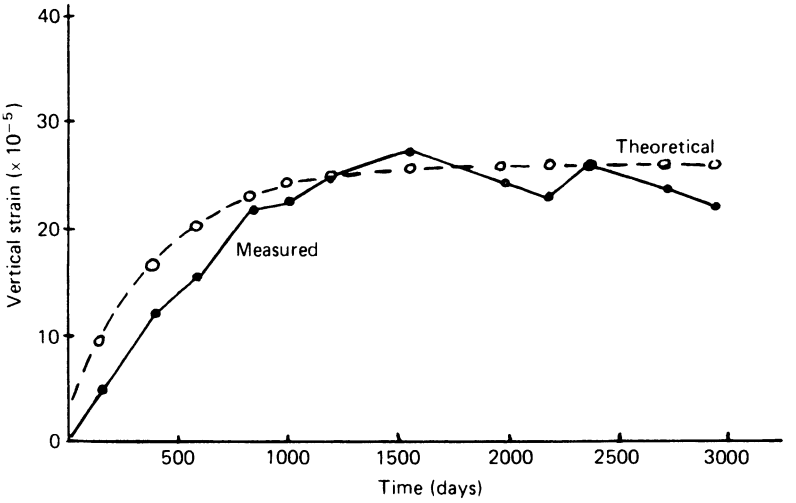

Figure 2.15 Comparison of measured and theoretical strains in a brick masonry wall in a building (Lenczner)

Using these relationships the creep strains can be calculated on an incremental basis to find the development of strain in the walls of a building with time. Lenczner [104] has been able to compare the results of such a calculation with measurements taken in a ten-storey apartment building over a period of 3000 days with the results shown in figure 2.15.

Shrive and England [105] have also put forward an incremental method of calculating creep and shrinkage movements in masonry, and have confirmed that such movements may be several times the initial deformation. In addition, they have developed the concept of an effective modulus E' for calculating overall strains by defining

$$E' = \frac{\sigma}{\varepsilon_i + \varepsilon_c + \varepsilon_s} \tag{2.16}$$

where ε_i = elastic strain, ε_c = creep strain and ε_s = shrinkage strain. Since the short-term elastic strain $\varepsilon_i = f/E$ and since there is a linear relationship between creep strain in mortar and stress within the working range, the expression for the effective modulus can be written as

$$E' = \frac{E}{1 + Ec + \dfrac{E}{f}\varepsilon_s} \tag{2.17}$$

where c is the creep strain per unit stress, which can be determined from creep tests at constant stress.

Table 2.12 Proposed design values for creep (Shrive)

Type of masonry unit	*Design value*
Fired clay	0.7
Calcium silicate	1.5
Autoclaved aerated concrete	1.5
Concrete	1.5
Lightweight concrete	2.0

In brickwork, most of the creep strain takes place in the mortar, but in concrete blockwork the units also develop creep strains of the same order. It is therefore to be expected that this type of masonry will show larger ratios of initial-to-final strains. Shrive [106] has quoted proposed design values for the ratio of maximum creep strain to initial elastic strain for various types of masonry, as shown in table 2.12, which are in accord with test results reported by Schubert [107].

References

1. A. J. Francis, C. B. Horman and L. E. Jerems, 'The Effect of Joint Thickness and other Factors on the Compressive Strength of Brickwork', *Proceedings of the Second International Brick Masonry Conference* (Stoke-on Trent) 1971, eds H. W. H. West and K. H. Speed (British Ceramic Research Association, Stoke-on-Trent, 1971), pp. 31–7.
2. N. F. Astbury and H. W. H. West, 'Tests on Storey Height Brickwork Panels and Development of Site Control Test for Brickwork', in *Designing, Engineering and Constructing with Masonry Products*, ed. F. B. Johnson (Gulf, Houston, Tex., 1969), pp. 216–20.
3. C. B. Monk, 'A Historical Survey and Analysis of the Compressive Strength of Brick Masonry', *Research Report No. 12* (Structural Clay Products Research Foundation, Geneva, Ill. 1967).
4. E. H. Morsy, 'An Investigation of Mortar Properties Influencing Brickwork Strength', PhD Thesis (University of Edinburgh, 1968).
5. C. L. Khoo, 'A Failure Criterion for Brickwork in Axial Compression', PhD Thesis (University of Edinburgh, 1972).
6. *Small Scale Specimen Testing Program* (Structural Clay Products Research Foundation, Geneva, Ill., 1964).
7. J. Y. Houston and C. T. Grimm, 'Effect of Brick Height on Masonry Compressive Strength', *J. Mater. ASTM*, **7** (1972) 388–97.
8. A. W. Page, 'A Study of the Influence of Brick Size on the Compressive Strength of Calcium Silicate Masonry, *Engineering Bulletin CE 13* (University of Newcastle, NSW, 1984).
9. H. W. H. West, H. R. Hodgkinson, D. G. Beech and S. T. E. Davenport, 'The

Performance of Walls Built of Wirecut Bricks with and without Perforations', Parts i and ii, *Proc. Br. Ceram. Soc.*, **17** (1970) 1–39.

10. G. Schellbach, 'The Influence of Perforation on the Load-bearing Capacity of Hollow Brick Masonry Structures', *Proceedings of the Second International Brick Masonry Conference* (Stoke-on-Trent) 1971, eds H. W. H. West and K. H. Speed (British Ceramic Research Association, Stoke-on-Trent, 1971), pp. 50–5.
11. N. G. Shrive, 'The Failure Mechanism of Face-shell Bedded (Ungrouted and Unreinforced) Masonry', *Int. J. Masonry Construction*, **2** (3) (1982) 115–28.
12. M. Hatzinikolas, J. Longworth and J. Warwaruk, 'Failure Modes of Eccentrically Loaded Concrete Block Masonry Walls', *ACI Journal*, **77** (1980) 258–63.
13. R. A. Drysdale and A. A. Hamid, 'Capacity of Concrete Block Masonry Prisms under Eccentric Compressive Loading', *ACI Journal*, **80** (1983) 102–8.
14. A. A. Hamid and R. A. Drysdale, 'Suggested Failure Criteria for Grouted Concrete Masonry under Axial Compression', *ACI Journal*, **76** (2) (1979) 1047–61.
15. F. M. Khalaf, A. W. Hendry and D. R. Fairbairn, 'Mechanical Properties of Materials used in Blockwork Construction', *Magazine of Concrete Construction*, **44** (158) (1992) 1–14.
16. 'Loading Tests on Brick Walls Built in Stretcher Bond', *Res. Note Clay Prod. Tech. Bur. (Lond.)*, **1** (1968).
17. R. Beard, 'The Compressive Strength of some Grouted Cavity Walls', *Proc. Br. Ceram. Soc.*, **21** (1973) 113–40.
18. J. A. James, 'Investigation of the Behaviour of Single Leaf, 9″ and 11″ Cavity Storey Height Walls under Axial Load', *Report W/3/A* (Building Development Laboratories, Morley, W. Australia, 1972).
19. J. A. James, 'Investigation of the Behaviour of Storey Height Single Leaf Walls, 9″ Walls and 11″ Cavity Walls under Eccentric Compressive Load', *Report W/4/A* (Building Development Laboratories, Morley, W. Australia, 1973).
20. A. W. Hendry, R. E. Bradshaw and D. J. Rutherford, 'Tests on Cavity Walls and the Effect of Concentrated Loads and Joint Thickness on the Strength of Brickwork', *Res. Note Clay Prod. Tech. Bur. (Lond.)*, **1** (1968).
21. K. Fisher, 'The Effect of Wall Ties on the Compressive Strength of Cavity Walls', *Proceedings of the Second International Brick Masonry Conference* (Stoke-on-Trent) 1971, eds H. W. H. West and K. H. Speed (British Ceramic Research Association, Stoke-on-Trent, 1971), pp. 177–85.
22. S. Prasan, A. W. Hendry and R. E. Bradshaw, 'Crushing Tests on Storey Height Walls $4\frac{1}{2}$″ Thick', *Proc. Br. Ceram. Soc.*, **4** (1965) 67–81.
23. R. E. Bradshaw and A. W. Hendry, 'Further Crushing Tests on Storey Height Walls $4\frac{1}{2}$″ Thick', *Proc. Br. Ceram. Soc.*, **11** (1968) 25–54.
24. B. P. Sinha and R. Pedreschi, 'Compressive Strength and Some Elastic Properties of Brickwork', *Int. J. Masonry Construction*, **3** (1) (1983).
25. D. Lenczner and D. Foster, 'Strength and Deformation of Brickwork Prisms in Three Directions', *Proceedings of the Fifth International Brick Masonry Conference* (Washington) 1977, pp. 49–55.
26. H. R. Hodgkinson and S. Davies, 'The Stress Strain Relationships of Brickwork when Stressed in Directions other than Normal to the Bed Face',

Proceedings of the Sixth International Brick Masonry Conference (Rome) 1982, pp. 290–6.

27. B. P. Sinha and R. C. de Vekey, 'A Study of the Compressive Strength in Three Orthogonal Directions of Brickwork Prisms Built with Perforated Bricks', *Masonry International*, **3** (3) (1990) 105–10.
28. F. M. Khalaf, 'The Performance of Concrete Blocks Loaded Parallel to the Bed Face', *Masonry International*, **2** (1) (1988) 20–4.
29. P. Haller, 'Load Capacity of Brickwork', in *Designing, Engineering and Constructing with Masonry Products*, ed. F. B. Johnson (Gulf, Houston, Tex., 1969), pp. 129–49.
30. 'Compressive and Transverse and Racking Strength Tests in Four-inch Brick Walls', *Research Report No. 9* (Structural Clay Products Research Foundation, Geneva, Ill., 1965).
31. 'Compressive and Transverse Strength Tests of Eight-inch Brick Walls', *Research Report No. 10* (Structural Clay Products Research Foundation, Geneva, Ill., 1966).
32. 'Compressive and Transverse Tests of Five-inch Brick Walls', *Research Report No. 8* (Structural Clay Products Research Foundation, Geneva, Ill., 1965).
33. W. Albrecht and H. Schneider, 'Der Einfluss der Saugfähigkeit der Mauerziegel auf die Tragfähigkeit von Mauerwerk', *Berichte aus der Bauforschung*, Heft 46 (Wilhelm Ernst, Berlin, 1966).
34. H. Motteu, 'Research on Load-bearing Masonry in Belgium since 1963', in *Designing, Engineering and Constructing with Masonry Products*, ed. F. B. Johnson (Gulf, Houston, Tex., 1969), pp. 171–84.
35. V. Turnsek and F. Čačović, 'Some Experimental Results on the Strength of Brick Masonry Walls', *Proceedings of the Second International Brick Masonry Conference* (Stoke-on-Trent) 1971, eds H. W. H. West and K. H. Speed (British Ceramic Research Association, London, 1971), pp. 149–56.
36. S. Sahlin, *Structural Masonry* (Prentice-Hall, Englewood Cliffs, N. J., 1971), pp. 36–8.
37. T. Grimm, 'Strength and Related Properties of Brick Masonry', *J. Struct. Div. Am. Soc. Civ. Engrs*, **107** (1975) 217–32.
38. L. G. Simms, 'The Strength of Walls Built in the Laboratory with some Types of Clay Bricks and Blocks', *Proc. Br. Ceram. Soc.*, **4** (1965) 81–92.
39. J. Y. Houston and C. T. Grimm, 'Effect of Brick Height on Masonry Compressive Strength, *J. Mater. ASTM*, **7** (1972) 388–92.
40. H. W. H. West, H. R. Hodgkinson, D. G. Beech and S. T. E. Davenport, 'The Comparative Strength of Walls Built of Standard and Modular Bricks', *Proceedings of the Second International Brick Masonry Conference* (Stoke-on-Trent) 1971, eds H. W. H. West and K. H. Speed (British Ceramic Research Association, Stoke-on-Trent, 1971), pp. 172–6.
41. P. Szabo, 'The Effect of Brick Size on the Load Bearing Capacity and Shear Strength of Masonry Construction, *Proceedings of the Third International Brick Masonry Conference* (Essen) 1973, eds L. Foertig and K. Gobel (Bundesverband der Deutschen Ziegelindustrie, Bonn, 1975), pp. 124–6.
42. A. Ilantzis, 'Mechanical Strength of Walls of Hollow Bricks and Hollow Blocks of Light and Heavy Aggregate under Axial and Eccentric Load', *Proceedings of the Third International Brick Masonry Conference* (Essen)

1973, eds L. Foertig and K. Gobel (Bundesverband der Deutschen Ziegelindustrie, Bonn, 1975), pp. 115–19.

43. A. Huizer and M, Ward, 'The Effect of Brick Type on the Compressive Strength of Masonry, *Proceedings of the Fourth International Brick Masonry Conference* (Brugge) 1976, Paper 4.a.2.
44. W. Albrecht and H. Schneider, 'Der Einfluss des Mauerverbandes von 30 cm dicken Hochlochziegel werden auf deren Tragfähigkeit', *Berichte aus der Bauforschung*, Heft 46 (Wilhelm Ernst, Berlin, 1966).
45. R. E. Bradshaw and A. W. Hendry, 'Preliminary Crushing Tests on Storey Height Cavity Walls', in *Designing, Engineering and Constructing with Masonry Products*, ed. F. B. Johnson (Gulf, Houston, Tex., 1969), pp. 101–9.
46. K. Fisher, 'The Effect of Chasing on the Compressive Strength of Brickwork', *Proceedings of the Third International Brick Masonry Conference* (Essen) 1973, eds L. Foertig and K. Gobel (Bundesverband der Deutschen Ziegelindustrie, Bonn, 1975), pp. 106–14.
47. K. Fisher, 'The Effect of Low-strength Bricks in High-strength Brickwork', *Proc. Br. Ceram. Soc.*, **21** (1973) 79–98.
48. A. W. Hendry and C. K. Murthy, 'Comparative Tests on $\frac{1}{3}$ and $\frac{1}{6}$ Scale Model Brickwork Piers and Walls', *Proc. Br. Ceram. Soc.*, **4** (1965) 46–66.
49. H. Motteu, Y. Collet, M. Lejeune and M. Dzulyinsky, 'Etude des Maçonneries Portantes', *Compte Rendu Recherche 2* (Brussels, 1970).
50. F. Y. Yokel and R. D. Dikkers, 'Strength of Load-Bearing Masonry Walls', *J. Struct Div., ASCE* (1971).
51. J. B. Read and S. W. Clements, 'The Strength of Concrete Block Walls Phase II: Under Uniaxial Loading', *Technical Report 42.473* (Cement and Concrete Association, London, 1972).
52. M. Rostampour, 'Aspects of the Design of Multistorey Buildings in Lightweight Concrete Blockwork', PhD Thesis (University of Edinburgh, 1973).
53. W. B. Cranston and J. J. Roberts, The Structural Behaviour of Concrete Masonry – Reinforced and Unreinforced', *Struct. Engr.*, **54** (11) (1976), 423–36.
54. M. Hatzinikolas, J. Longworth and J. Warwaruk, 'Concrete Masonry Walls', *Structural Engineering Report No. 70* (University of Alberta, 1978).
55. A. W. Hendry and M. H. Malek, 'Characteristic Compressive Strength of Brickwork from Collected Test Results', *Masonry International*, **7** (1986) 15–24.
56. W. Mann, 'Statistical Evaluation of Tests on Masonry by Potential Functions', *Proceedings of the Sixth International Brick Masonry Conference* (Rome) 1982, pp. 86–98.
57. K. Kirtschig, 'On the Failure Mechanism of Masonry Subject to Compression', *Proceedings of the Seventh International Brick Masonry Conference* (Melbourne) 1985, pp. 625–9.
58. S. Render and M. Phipps, 'The Effect of Unit Aspect Ratio on the Axial Compressive Strength of Masonry', *Masonry International*, **8** (1986) 28–28.
59. *Eurocode 6, Design of Masonry Structures, Part 1-1: General rules for buildings. Rules for reinforced and unreinforced masonry.* ENV 1996-1-1 (CEN, 1995).
60. F. M. Khalaf and A. W. Hendry, 'Masonry Unit Shape Factors from Test Results', *Proc. Br. Masonry Soc.*, **6** (1994) 136–9.

61. Department of Scientific and Industrial Research, 'Brick Piers and Some Slender Brick Walls under Uniform and Concentrated Loading', *Structural Aspects of Housing, Interim Report No. 15* (Building Research Station, December 1956).
62. A. W. Hendry, R. E. Bradshaw and D. J. Rutherford, 'Tests on Cavity Walls and the Effects of Concentrated Loads and Joint Thickness on the Strength of Brickwork', *CPTB Research Note*, **1** (2) (1968).
63. K. Kirtschig and D. Kasten, 'Partial Surface Load of Masonry', *Proceedings of the Fifth International Brick Masonry Conference* (Washington) 1979, pp. 391–7.
64. V. Lind, 'Edge Strength of Masonry', *Ziegelindustrie International*, **3** (1985) 199–204.
65. W. Mann and M. Pfiefer, 'Investigations on the Stresses in Masonry Walls Subjected to Concentrated Loads', *Proceedings of the Seventh International Brick Masonry Conference* (Melbourne) 1985, pp. 735–46.
66. S. Ali and A. W. Page, 'An Elastic Analysis of Concentrated Loads on Brickwork', *Masonry International*, **6** (1985) 9–21.
67. S. Ali, A. W. Page and P. W. Kleeman, 'Non-linear Finite Element Model for Concrete Masonry with Particular Reference to Concentrated Loads', *Proceedings of the Fourth Canadian Masonry Symposium*, June 1986, pp. 137–48.
68. S. Ali and A. W. Page, 'Non-linear Finite Element Analysis of Masonry Subjected to Concentrated Loads', *Proc. Inst. C. E. Part 2*, **83** (1987) 815–32.
69. A. W. Page and A. Ali, 'The Behaviour of Solid Masonry Walls Subjected to Concentrated Load', *Proceedings of the Fourth North American Masonry Conference* (Los Angeles) 1987, Paper 14.
70. M. H. Malek and A. W. Hendry, 'Compressive Strength of Brickwork Masonry under Concentrated Loading', *Br. Masonry Soc. Proc.*, **2** (1988) 56–60.
71. S. K. Arora, 'Performance of Masonry Walls Under Concentrated Load', *Br. Masonry Soc. Proc.*, **2** (1983) 50–5.
72. S. Ali, 'Concentrated Loads on Solid Masonry', PhD Thesis (University of Newcastle, Australia, 1987).
73. T. Dia-Xin, 'Testing and Analysis of the Bearing Strength of Brick Masonry', *Proceedings of the Seventh International Brick Masonry Conference* (Melbourne) 1985, pp. 747–55.
74. A. W. Page, N. G. Shrive and E. L. Jessop, 'Concentrated Loads on Hollow Masonry – A Pilot Study', *Masonry International*, **1** (2) (1987) 58–61.
75. A. W. Page and A. W. Hendry, 'Design Rules for Concentrated Loads on Masonry', *Structural Engineer*, **66** (1987) 273–81.
76. A. W. Hendry, 'Concentrated Loading on Brick Masonry with Precompresion', *Proceedings of the Eighth Brick and Block Masonry Conference* (Dublin) 1988, pp. 458–66.
77. K. Kirtschig and W. R. Metje, 'Influence of Chases and Recesses on the Strength of Masonry', *Proc. Br. Masonry Soc.*, **2** (1988) 61–3.
78. J. D. McIntosh, 'Specifying the Quality of Bedding Mortars', *Proc. Br. Ceram. Soc.*, **17** (1970) 65–82.
79. 'Investigation of the Effect on Brickwork of not Filling Vertical Mortar

Joints', Internal Report (British Ceramic Research Association, Stoke-on-Trent, 1972).
80. J. A. James, 'Investigation of the Effect of Workmanship and Curing Conditions on the Strength of Brickwork', *Proceedings of the Third International Brick Masonry Conference* (Essen) 1973, eds L. Foertig and K. Gobel (Bundesverband der Deutschen Ziegelindustrie, Bonn, 1975), pp. 192–201.
81. J. G. Gross, R. D. Dikkers and J. C. Grogan *Recommended Practice for Engineered Brick Masonry* (Structural Clay Products Institute, McLean, Va., 1969).
82. R. M. Milner and R. P. Thorogood, 'Accuracy of Load Bearing Brick Construction and its Structural Implications', *Proc. Br. Ceram. Soc.*, **21** (1973) 231–42.
83. S. D. Svendsen and A. Waldum, 'Some Remarks on Winter Masonry', *Technical Translation 1456* (National Research Council of Canada, Ottawa, 1971).
84. I. C. McDowall, T. N. McNeilly and W. G. Ryan, 'The Strength of Brick Walls and Wallettes', *Special Report No. 1* (Building Development Research Institute, Melbourne, 1966).
85. B. Powell and H. R. Hodgkinson, 'The Determination of Stress/Strain Relationship of Brickwork', *Proceedings of the Fourth International Brick Masonry Conference* (Brugge) 1976, Paper 2.a.5.
86. P. Ameny, R. E. Loov and N. G. Shrive, 'Prediction of Elastic Behaviour of Masonry', *Int. J. Masonry Constr.*, **3** (1) (1983).
87. J. M. Plowman, 'The Modulus of Elasticity of Brickwork', *Proc. Br. Ceram. Soc.*, **4** (1965) 37–44.
88. S. Sahlin, *Structural Masonry* (Prentice-Hall, Englewood Cliffs, N.J., 1971), pp. 59–61.
89. P. Schubert, 'Modulus of Elasticity of Masonry', *Proceedings of the Fifth International Brick Masonry Conference* (Washington) 1982, pp. 139–44.
90. H. H. Knutsson and J. Nielsen, 'On the Modulus of Elasticity for Masonry', *Masonry International*, **9** (2) (1995) 57–61.
91. D. Lenczner, Creep in Brickwork with and without Damp Proof Course, *Proc. Br. Ceram. Soc.*, **21** (1973) 39–50.
92. D. Lenczner, 'Creep in Concrete Blockwork Piers', *Struct. Engr.*, **52** (3) (1974) 97–101.
93. K. Wyatt, D. Lenczner and J. Salahuddin, 'The Analysis of Creep Data for Brickwork', *Proc. Br. Ceram. Soc.*, **24** (1975).
94. D. Lenczner, K. Wyatt and J. Salahuddin, 'Effects of Stress on Creep in Brickwork Piers', *Proc. Br. Ceram. Soc.*, **24** (1975).
95. D. Lenczner and J. Salahuddin, 'Creep and Moisture Movements in Brickwork Walls', *Proceedings of the Fourth International Brick Masonry Conference* (Brugge) 1976, Paper 2.a.4.
96. D. Lenczner and J. Salahuddin, 'Creep and Moisture Movements in Masonry Piers and Walls', *Proceedings of the First Canadian Masonry Symposium*, 1976, eds E. L. Jessop and M. A. Ward, pp. 72–86.
97. D. Lenczner, 'Creep and Moisture Movements in Brickwork and Blockwork', *Proceedings of the International Conference on Performance of Buildings* (Glasgow) 1976.
98. D. Lenczner, 'The Effect of Strength and Geometry on the Elastic and Creep

Properties of Masonry Members', *Proceedings of the North American Masonry Conference* (Boulder) 1978, Paper 23.

99. D. Lenczner, 'Creep in Brickwork and Blockwork in Cavity Walls and Piers', *Proc. Br. Ceram. Soc.*, **27** (1978).
100. D. Lenczner, 'Design of Brick Masonry for Elastic and Creep Movements', *Proceedings of the Second Canadian Masonry Symposium* (Ottawa) 1980, pp. 53–66.
101. D. Lenczner, 'Brickwork: a Guide to Creep', *Int. J. Masonry Constr.*, **1** (4) (1981) 127–33.
102. D. Warren and D. Lenczner, 'A Creep–Time Function for Single Leaf Brickwork Walls', *Int. J. Masonry Constr.*, **2** (1) (1981) 13–20.
103. A. D. Ross, Concrete Creep Data', *Struct. Engr.*, **12** (8) (1937).
104. D. Lenczner, 'In-situ Measurement of Creep Movement in a Brick Masonry Tower Block', *Masonry International*, **8** (1986) 17–20.
105. N. G. Shrive and G. L. England, 'Elastic, Creep and Shrinkage Behaviour of Masonry', *Int. J. Masonry Constr.*, **1** (3) (1981) 103–9.
106. N. G. Shrive, 'Effects of Time Dependent Movements in Composite and Post-tensioned Masonry', *Masonry International*, **2** (1) (1988) 25–9.
107. P. Schubert, 'Deformation of Masonry due to Shrinkage and Creep', *Proceedings of the Fifth International Brick Masonry Conference*, 1982, eds J. Wintz and A. Yorkdale, pp. 132–8.

3 COMPRESSION FAILURE THEORIES

3.1 **Failure theories: general**

Consideration of qualitative evidence and empirical relationships as discussed in chapter 2, while extremely valuable and indeed providing the basis for structural design codes, does not provide a detailed insight into the behaviour of masonry. A number of investigators have therefore attempted to derive theories of failure based on the fundamental properties of the component materials. The earliest of these would appear to be due to Haller [1], published in 1959. Haller's formula, however, can give masonry strengths exceeding that of the masonry unit and is thus not generally valid.

As pointed out in chapter 2, it has been observed that the failure of masonry in compression is related to the interaction of the unit and mortar joint as a result of their differing deformation characteristics. Two approaches have been adopted as the basis of failure theories: the first assumes elastic behaviour and the second relates the behaviour of the unit and joint materials under the action of bi- or tri-axial stress.

3.2 **Failure theories based on elastic analysis**

This approach has been developed by Francis *et al.* [2] and Totaro [3].

The formulae proposed by the former were derived by considering a brick–mortar prism subjected to an axial compressive stress σ_y, as shown in figure 3.1a. The lateral stresses induced in a central brick and in the adjacent mortar beds are indicated in figure 3.1b, and the extensional strains in the brick in the x and z directions are

$$e_{xb} = \frac{1}{E_b}\left[\sigma_{xb} + \nu_b\left(\sigma_y - \sigma_{zb}\right)\right] \tag{3.1}$$

$$e_{zb} = \frac{1}{E_b}\left[\sigma_{zb} + \nu_b\left(\sigma_y - \sigma_{xb}\right)\right] \tag{3.2}$$

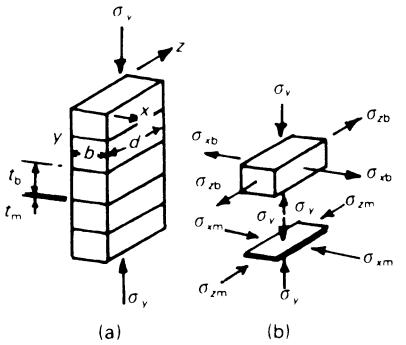

Figure 3.1 Stresses in brick–mortar composite

and similarly in the mortar joints

$$e_{xm} = \frac{1}{E_m}\left[-\sigma_{xm} + \nu_m\left(\sigma_y - \sigma_{zm}\right)\right] \tag{3.3}$$

$$e_{zm} = \frac{1}{E_m}\left[-\sigma_{zm} + \nu_m\left(\sigma_y - \sigma_{xm}\right)\right] \tag{3.4}$$

where E_b and E_m are the elastic moduli of the brick and mortar respectively, and ν_b and ν_m the corresponding Poisson's ratios. For equilibrium, the total lateral tensile force in the brick is equal to the total lateral compressive force in the mortar; hence

$$\sigma_{xm} = \alpha\sigma_{xb} \tag{3.5}$$

and

$$\sigma_{zm} = \alpha\sigma_{zb} \tag{3.6}$$

where α is the ratio of the height of the brick to the thickness of the mortar bed. As the lateral strains in the bricks and mortar are the same, equating equations 3.1 and 3.3, 3.2 and 3.4, and using equations 3.5 and 3.6 gives

$$\sigma_{xb} = \sigma_{zb} = \frac{\sigma_y\left(\beta\nu_m - \nu_b\right)}{1 + \alpha\beta - \nu_b - \alpha\beta\nu_m} \tag{3.7}$$

where $\beta = E_b/E_m$.

Assuming a linear relationship between ultimate longitudinal compressive stress and lateral tensile stress, as shown in figure 3.2, gives the relationship

$$\sigma_{xb} = \frac{1}{\phi}\left(\sigma'_{ult} - \sigma_{ult}\right) \tag{3.8}$$

where $\phi = \sigma'_{ult}/\sigma'_t$. Substituting for σ_{xb} in equation 3.7 and neglecting $(1 - \nu_b)$ gives

$$\frac{\sigma_{ult}}{\sigma'_{ult}} = \frac{1}{1 + \dfrac{\phi(\beta\nu_m - \nu_b)}{\alpha\beta(1 - \nu_m)}} \tag{3.9}$$

Comparison with experimental results using joint thickness as a variable (figure 3.3), shows that this formula gives a fair representation of the actual behaviour of a set of specimens tested by its originators. Discrepancies between theory and experiment were thought to arise from approximations in estimating the true values of the parameter ϕ and Poisson's ratio.

Although this theory shows moderate agreement with experimental results, it has to be said that it is at best qualitative since the materials are not elastic and consequently the parameters are far from constant throughout the loading range. Shrive and Jessop [4] have questioned the validity of the approach on the basis that the lateral tensile stresses developed by differences in E and Poisson's ratio are insufficient to account for the masonry strengths found experimentally. They consider that failure results from the development of pre-existing flaws in the structure of the material. Such development may be initiated by the lateral tensile stresses, although these are not in themselves the primary cause of failure.

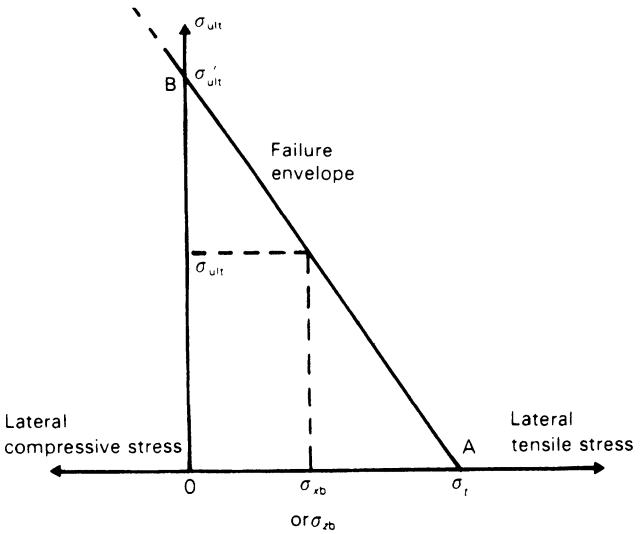

Figure 3.2 Failure envelope for brick material in biaxial compression–tension assumed by Francis *et al.*

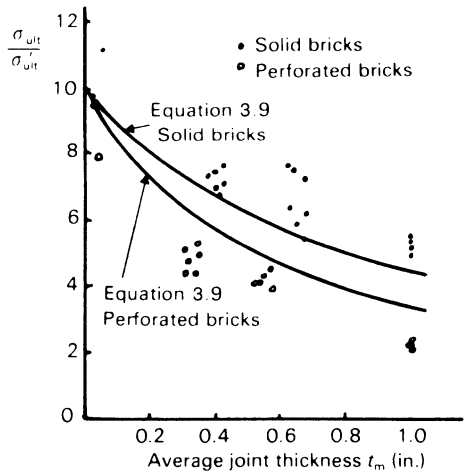

Figure 3.3 Effect of joint thickness on brickwork compressive strength

3.3 Failure theories based on the strength of brick and mortar under multi-axial stress

An alternative approach to the definition of brickwork strength was proposed by Hilsdorf [5], based on an assumed linear relationship between lateral biaxial tensile strength and local compressive stress equal to the mean external compressive stress multiplied by a 'non-uniformity' factor U. Referring to figure 3.4, line A is the failure criterion envelope, and when

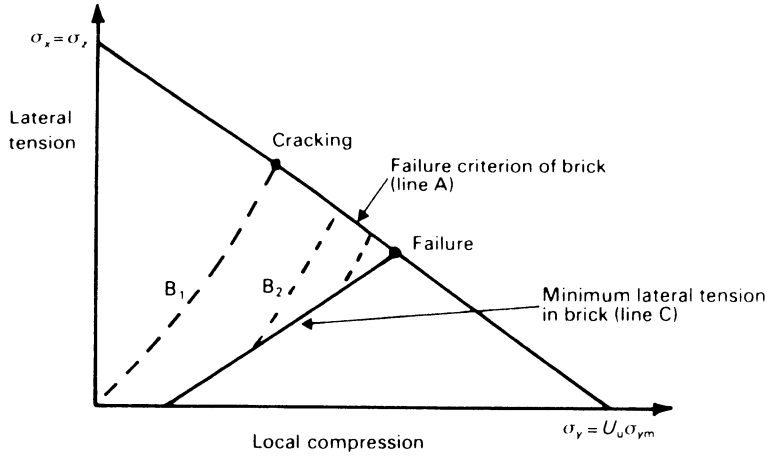

Figure 3.4 Hilsdorf's failure theory

external compression is applied to the brickwork, the internal tensile stresses induced follow some line such as B_1. When this line intersects the failure criterion envelope, a local crack is developed in the brickwork. Further local cracks will appear on subsequent increase of load, but general failure will not take place until the brick can no longer provide the biaxial restraint necessary to prevent failure of the mortar, or alternatively, when the state of stress developed in the brick exceeds its resistance to the combination of stresses developed. This will occur when the line defining the triaxial strength of the mortar line C in figure 3.4, intersects the failure line for the brick.

Hilsdorf assumed that the triaxial strength of mortar could be represented by the equation (obtained originally for concrete)

$$f'_1 = f'_c + 4.1\sigma_2 \tag{3.10}$$

where f'_1 is the compressive strength of a laterally confined cylinder
f'_c is the uniaxial compressive strength of a cylinder
σ_2 is the lateral confinement stress of a cylinder.

$$\sigma_{xj} = \frac{1}{4.1}(\sigma_y - f'_j) \tag{3.11}$$

in which σ_{xj} is the lateral compressive stress in the mortar joint
σ_y is the local stress in the y direction
f'_j is the uniaxial compressive strength of mortar.

Taking into account the equilibrium of lateral forces in bricks and mortar, the equation of line C in figure 3.4 is then

$$\sigma_x = \frac{j}{4.1b}(\sigma_y - f'_j) \tag{3.12}$$

where b is the height of the brick, and j the mortar bed thickness. Line A is expressed by

$$\sigma_x = \sigma_z = f'_{bt}\left(1 - \frac{\sigma_y}{f'_b}\right) \tag{3.13}$$

in which f'_{bt} is the strength of the brick under biaxial tension and f'_b is the uniaxial compressive strength of brick.

The magnitude of the local stress at failure, that is the intersection of lines A and C, is therefore given by

$$\sigma_y = f'_b\left(\frac{f'_{bt} + \alpha f'_j}{f'_{bt} + \alpha f'_b}\right) \tag{3.14}$$

where $\alpha = j/4.1b$.

The average masonry stress at failure is then

$$\sigma_{ym} = \frac{\sigma_y}{U_u} \tag{3.15}$$

where U_u is a coefficient of non-uniformity, which Hilsdorf established experimentally for various brick–mortar combinations. This varies according to the brickwork strength, but for cement mortar it has been shown to have a value of around 1.3 in the medium strength range.

This approach was developed by Khoo and Hendry [6, 7], who investigated the behaviour of brick material under a state of biaxial compression–tension, and of mortar under a state of triaxial compression; these characteristics had to be assumed by Hilsdorf in the absence of direct experimental data. They established that the biaxial compression–tension strength envelope for brick can be represented by the relationship

$$\left(\frac{c}{c_0}\right) = 1 - \left(\frac{t}{t_0}\right)^{0.546} \tag{3.16}$$

This curve is shown in figure 3.5, and was based on the results of tests on a large number of specimens of bricks ranging in crushing strength from 31.63 N/mm^2 to 92.66 N/mm^2. It will be noted that comparing the concave shape of this curve with the linear relationship assumed by Hilsdorf, the compressive strength of brick is severely reduced by the presence of an orthogonal tensile stress.

The effect on the compressive strength of mortar of a confining pressure was investigated by Khoo and Hendry for $1:\frac{1}{4}:3$ and $1:1:6$ mortars using a triaxial test cell [8]. The increase in strength so found was less than that

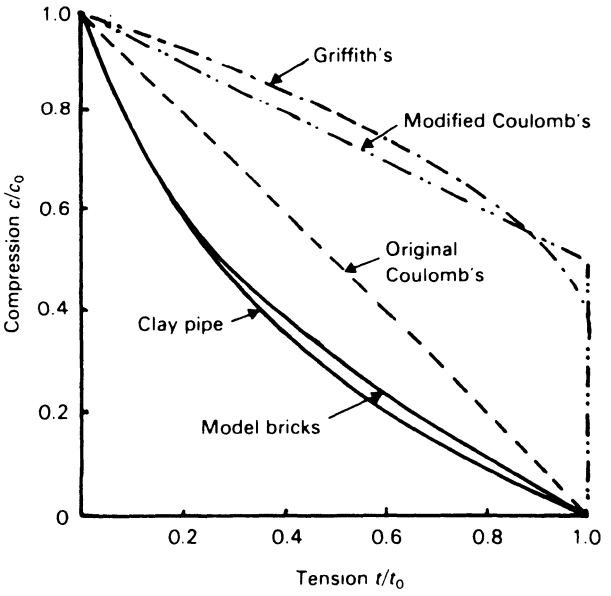

Figure 3.5 Biaxial compression–tension failure envelopes

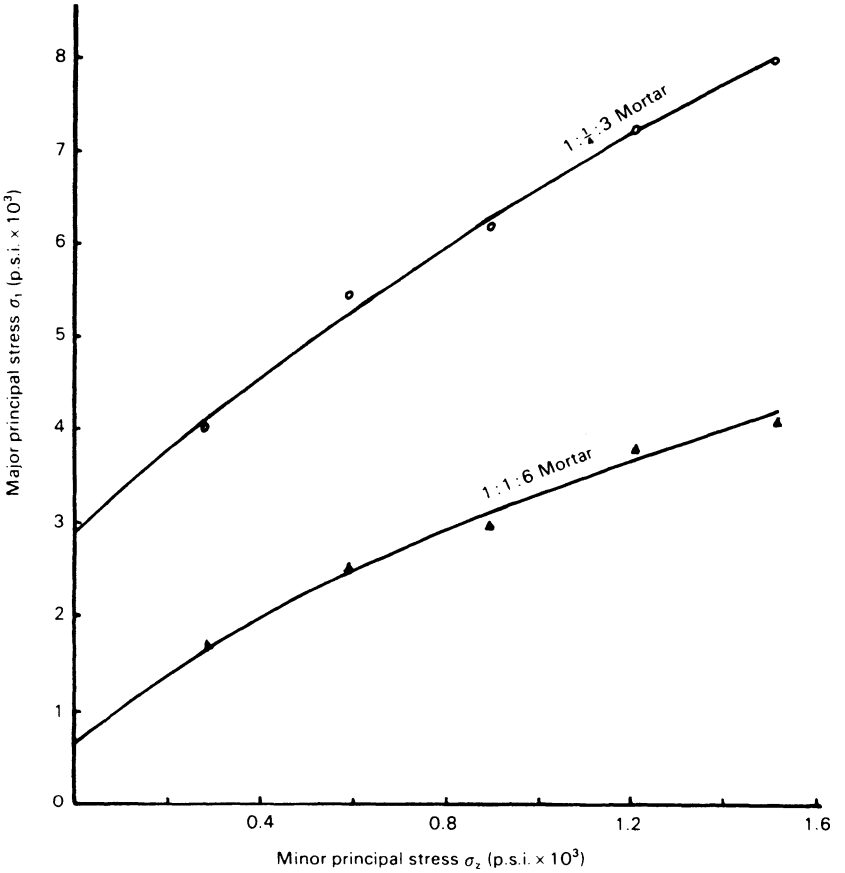

Figure 3.6 Principal stress relationship for mortars in triaxial compression

found for concrete [9–11] and is shown in figure 3.6. The principal stress relationship is non-linear and may be defined by the expression

$$\frac{\sigma_1}{\sigma_0} = 1 + 2.91\left(\frac{\sigma_z}{\sigma_0}\right)^{0.805} \tag{3.17}$$

where σ_1 is the major principal stress
σ_z is the minor principal stress
σ_0 is the uniaxial compressive strength.

On the basis of these studies a failure theory for brickwork has been developed [7, 8]. Thus in figure 3.7, which shows an assumed failure envelope for brick in biaxial compression–tension in a brickwork prism, any state of stress to the right of the envelope curve denotes failure. As the vertical compression acting on the brickwork prism increases, the state of

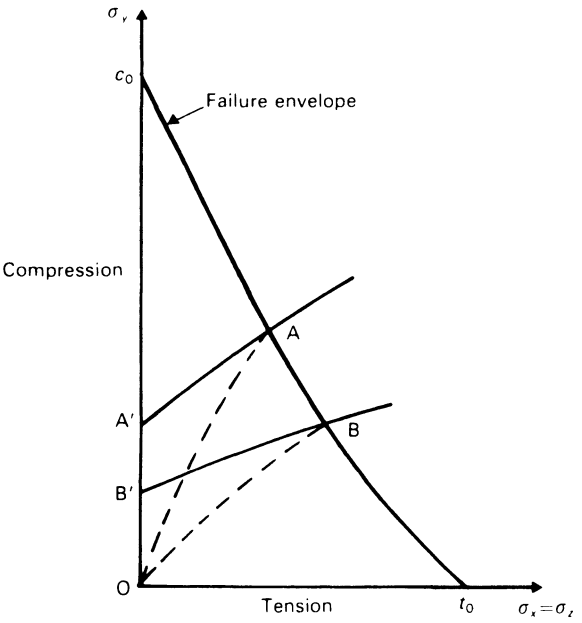

Figure 3.7 Failure envelope for brick in biaxial compression–tension

stress in the brick element proceeds along the dashed line OA. Failure occurs within the brick element when the line OA intersects the failure envelope at A, and hence the compressive strength of the brickwork prism is given by the ordinate of this point. The stress path taken by the line OA depends on the properties of the mortar joint under triaxial compression. For a weaker mortar, whose lateral strain is greater under load, the stress path would travel along the lower line OB, and in this case the point B would define the compressive strength of the brickwork prism.

It is not, however, necessary to determine the stress paths OA and OB: the failure point for a given brick–mortar combination can be located graphically by superimposing on the brick failure envelope a curve derived from the triaxial compressive strength relationship for the mortar, which defines the tensile stress induced in the brick. Such curves have been established by Khoo taking the lateral tensile strain in brick material at failure as approximately 225×10^{-6}. Relating this value to the stress–strain curves for mortar obtained from triaxial tests, as shown in figure 3.8, a relationship between axial and lateral compressive stresses in the mortar is obtained. Introducing the ratio, α, between the mortar joint thickness and the depth of the brick then gives the lateral tensile stress in the brick material, assuming that these stresses are uniformly distributed on vertical sections through the mortar and brick. The resulting axial compression–lateral

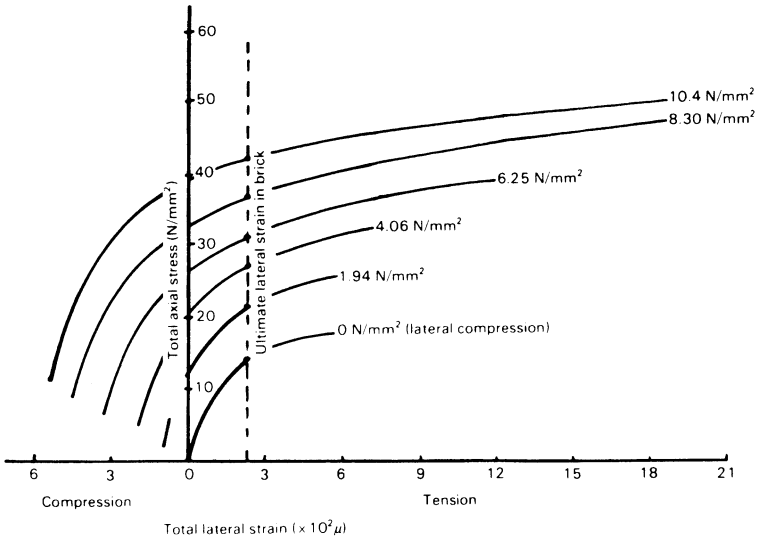

Figure 3.8 Axial stress–lateral strain relationship for $1:\frac{1}{4}:3$ mortar

tensile stress curves can now be plotted on the same axes as the biaxial failure envelope for the brick material, as indicated in figure 3.9, the intersection of the two curves defining failure of the particular brick–mortar combination.

Comparison of brickwork prism strengths calculated by the above theory shows reasonable agreement with experimental results. Such a comparison with the results obtained in a series of tests conducted by the Structural Clay Products Research Foundation [12] in the United States is shown in figure 3.10. The influence of joint thickness on compressive strength has been examined experimentally, and as may be seen from figure 3.11 the theory gives a reasonable representation of this effect.

A further development of the above approach is due to Atkinson *et al.* [13] who have determined experimentally the influence of high confining pressures on Young's modulus and Poisson's ratio of various mortar mixes. An expression has been obtained giving the increment of brick stress per increment of compressive stress, and this has been used in conjunction with the experimental values of E and ν to calculate the strength of stack prisms. Comparison with tests on the latter indicated that the calculated strengths were some 30 per cent lower than the failure strengths, suggesting that the theory was predicting a cracking rather than an ultimate stress.

Ohler [14] has reviewed earlier work on brick/mortar strength and has developed an expression for masonry strength using a tri-linear representation of the biaxial failure curve for brick material based on available

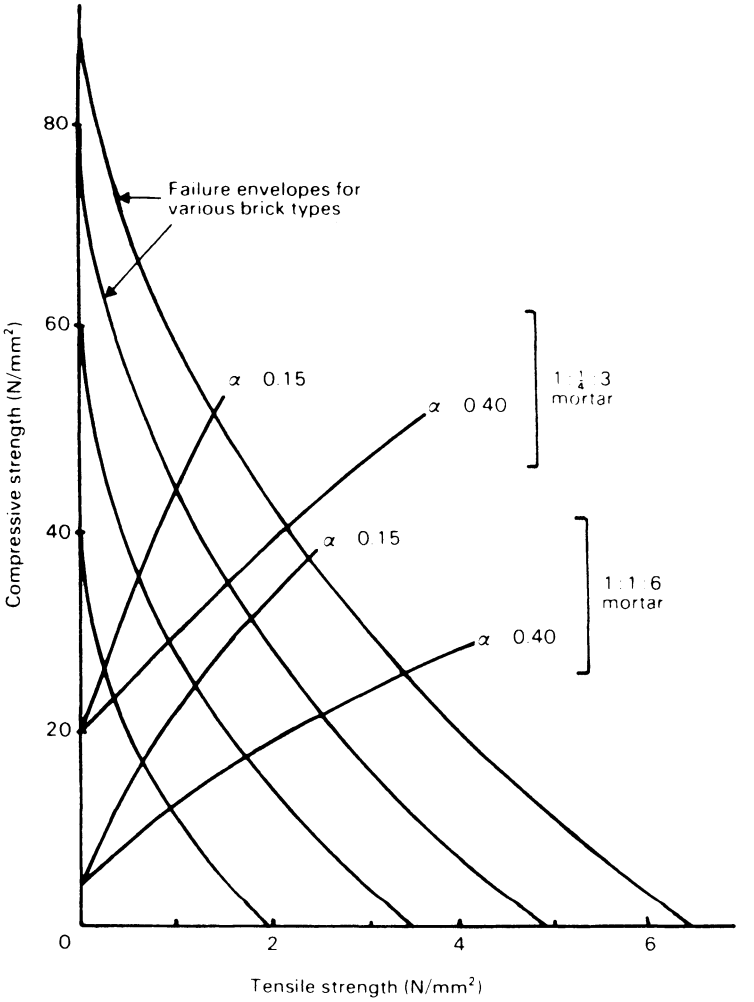

Figure 3.9 Graphical solution for brickwork prism compressive strength

experimental data. Ohler's equation shows good agreement with experimental results and is as follows:

$$\sigma_y = \sigma_{yom} + \frac{s\sigma_{yos} - \sigma_{yom}}{1 + \dfrac{th_m\,\sigma_{yos}}{mh_s\,\sigma_{xos}}} \tag{3.18}$$

where σ_y = compressive stress at failure of masonry
σ_{yom} = uniaxial compressive strength of mortar
σ_{yos} = uniaxial compressive strength of unit

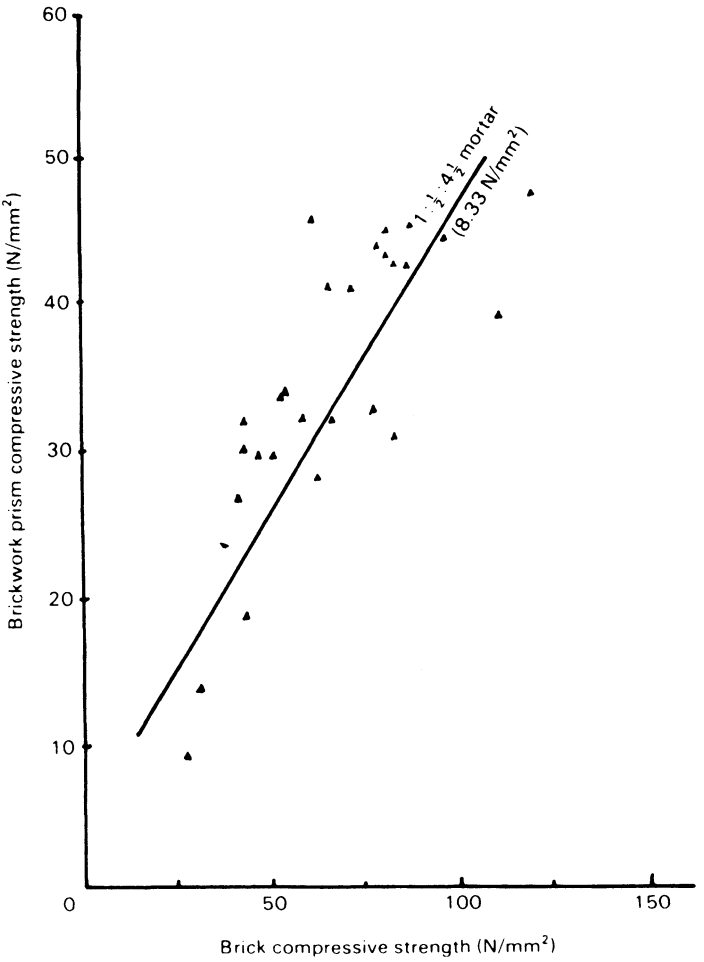

Figure 3.10 Brickwork prism compressive strength (SCPRF National Testing Program)

σ_{xos} = uniaxial tensile strength of unit
h_s, h_m = height of unit and thickness of mortar joint, respectively
m = slope of mortar failure envelope
s, t = parameters defining the unit failure envelope.

Relevant values of s and t are shown in figure 3.12 and are selected according to the zone in which the mortar failure line intersects the brick failure curve. Ohler gives the following values for m:

Mortar compressive strength (σ_{yom}):	31.6	21.4	15.4	6.4 N/mm²
m:	5.3	3.6	2.4	2.1

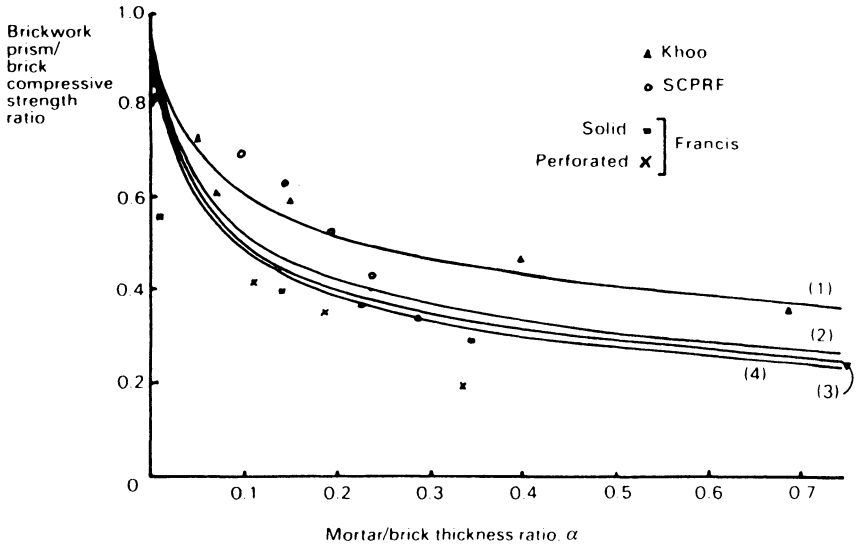

Figure 3.11 Effect of mortar/brick thickness ratio on brickwork compressive strength: comparison with experimental data

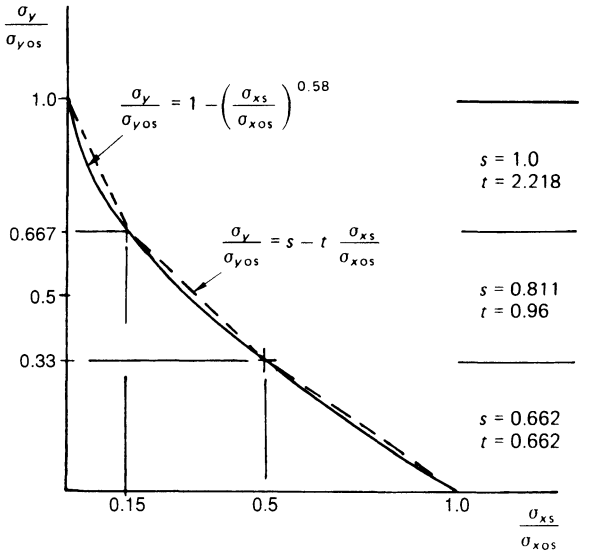

Figure 3.12 Tri-linear representation of brick strength under biaxial compression–tension (Ohler)

It should be noted that the theories discussed above relate to the strength of prisms, which is not in general the same as that of brick masonry in a wall. This is because the apparent compressive strength of a prism is affected by platen restraint and depends on the proportions of the specimen – for this reason, the strength of a prism may be as much as 30–40 per cent higher than the strength of the same material in a wall. The strength of masonry in which there is a joint parallel to the face of the brickwork may be substantially lower than that of a prism. Finally, it should be noted that the failure theory applies to the case where the strength of the brick exceeds that of the mortar, otherwise the deformation properties of the materials will be such that the brick element will no longer be subjected to bilateral tension as envisaged in the theory.

Hollow block masonry clearly requires separate consideration, so Hamid and Drysdale [15] have developed equations defining failure criteria for this case using the principles of the Hilsdorf theory. Two situations have been identified: the first is when the fill material has a lower strain level at maximum stress than that of the block so that its unconfined compressive strength is reached first, resulting in tensile stresses being set up in the unit. The second is when the block material reaches its maximum compressive stress at a lower strain than the fill material, in which case failure of the composite will be controlled by that of the block or by the strength of the core in uniaxial compression.

Hamid and Drysdale's analysis results in the following equations:

$$\text{Case 1: } f'_{mg} = \frac{4.1\sigma_{tb} + 1.14\alpha\sigma_{cm} + \beta\sigma_{ca}}{4.1\sigma_{tb} + 1.14\alpha + \dfrac{c\beta}{n}\sigma_{cb}} \times \frac{\sigma_{cb}}{n\gamma k} \tag{3.19}$$

$$\text{Case 2: } f'_{mg} = \frac{3.6\sigma_{tb} + \alpha\sigma_{cm}}{3.6\sigma_{tb} + \alpha\sigma_{cb}} \times \frac{\sigma_{cb}}{n\gamma k} \tag{3.20}$$

where f'_{mg} = the average compressive strength of the composite
σ_{tb} = the tensile strength of the block material
σ_{cm} = compressive strength of the mortar material
σ_{cb} = compressive strength of the block material
α = t_m/t_b = thickness of mortar joint/height of block
n = E_{blcok}/E_{grout}
η = $A_{block}/(A_{block} + A_{grout})$
γ = $1/(1 + (n - 1)\,\zeta)$
β = $\sqrt{(1 - 3)/(1 - \sqrt{(1 - \zeta)})}$
K = a stress adjustment factor
= $1.08 + 0.21/n$
c = ratio of maximum to minimum grout areas (where core is tapered).

These formulae give an indication of the number of variables which influence the strength of filled hollow block masonry. Note that inspection of equations 3.19 and 3.20 shows the mortar strength to be of minor significance, as has been found in tests on hollow blockwork.

References

1. P. Haller, 'The Physics of the Fired Brick: Part One Strength Properties', *Libr. Commun. Bldg Res. Stn.*, **929** (1960) (trans. G. L. Cairns).
2. A. J. Francis, C. B. Horman and L. E. Jerrems, 'The Effect of Joint Thickness and other Factors on the Compressive Strength of Brickwork', *Proceedings of the Second International Brick Masonry Conference* (Stoke-on-Trent) 1971, eds H. W. H. West and K. H. Speed (British Ceramic Research Association, Stoke-on-Trent 1971), pp. 31–7.
3. N. Totaro, 'A Hybrid Elastic Theory for Evaluation of Compressive Strength fo Brick Masonry', *Proceedings of the Tenth International Brick and Block Masonry Conference* (Calgary) 1994, pp. 1443–51.
4. N. G. Shrive and E. L. Jessop, 'An Examination of the Failure Mechanism of Masonry Piers, Prisms and Walls Subjected to Compression', *Proc. Br. Ceram. Soc.*, **30** (1982) 110–17.
5. H. K. Hilsdorf, 'An Investigation into the Failure Mechanism of Brick Masonry Loaded in Axial Compression', in *Designing, Engineering and Constructing with Masonry Products*, ed. F. B. Johnson (Gulf, Houston, Tex., 1969), pp. 34–41.
6. C. L. Khoo and A. W. Hendry, 'A Failure Criterion for Brickwork in Axial Compression', *Proceedings of the Third International Brick Masonry Conference* (Essen) 1973, eds L. Foertig and K. Gobel (Bundesverband der Deutschen Ziegelindustrie, Bonn, 1975), pp. 139–45.
7. C. L. Khoo and A. W. Hendry, 'Strength Tests on Brick and Mortar under Complex Stresses for the Development of a Failure Criterion for Brickwork in Compression', *Proc. Br. Ceram. Soc.*, **21** (1973) 57–66.
8. C. L. Khoo, 'A Failure Criterion for Brickwork in Axial Compression', PhD Thesis (University of Edinburgh, 1972).
9. G. G. Balmer, 'Shearing Strength of Concrete under High Triaxial Stress, Computation of Mohr's Stress Envelope as a Curve', *Report No. 5P23* (Bureau of Reclamation, Denver, Colo., 1949).
10. T. N. W. Akroyd, 'Concrete under Triaxial Stress', *Mag. Concr. Res.*, **13** (1961) 111.
11. N. J. Gardner, 'Triaxial Behavior of Concrete', *J. Am. Concr. Inst.*, **66** (1969) 136.
12. 'Small Scale Specimen Testing', *National Testing Program* (Structural Clay Products Research Foundation, Geneva, Ill., 1964).
13. R. H. Atkinson, J. L. Noland and D. P. Abrams, 'A Deformation Theory for Stack Bonded Masonry Prisms in Compression', *Proceedings of the Seventh International Brick Masonry Conference* (Melbourne) 1982, pp. 565–76.
14. A. Ohler, 'Zur Berechnung der Druckfestigeit von Mauerwerk unter

Berucksichtigung der mehrachsigen Spannungszustande in Stein und Mörtel', *Bautechnik*, **5** (1986).

15. A. A. Hamid and R. G. Drysdale, 'Suggested Failure Criteria for Grouted Concrete Masonry under Axial Compression', *ACI Journal*, **80** (1983) 102–8.

4 MASONRY IN TENSION, SHEAR AND BIAXIAL STRESS

4.1 **Bond strength between mortar and masonry units**

4.1.1 *Nature of bond*

The resistance of masonry to tensile or shear stresses is dependent on the bond between mortar and masonry units. The mechanism of bond between unit and mortar is incompletely understood but is known to be influenced by a large number of factors. These have been set out by Groot [1] in the matrix form shown in figure 4.1. It will be clear from this that the problem of masonry bond is extremely complex and most investigations so far have been of a phenomenological nature, applying to specific combinations of materials. However, some more fundamental work has been reported in which the physical and chemical nature of the brick/mortar interface has been studied. Experiments by Grandet [2] on the interaction between brick material and cement paste have shown that this is critically affected by the formation of a micro-layer of ettringite ($3CaSO_4$. Al_2O_3. 3CaO. $31H_2O$) at the clay–cement interface, and by the respective mean diameters of the pores of the brick and of the micro-crystals of the ettringite. It is necessary for the pore size of the brick material to be greater than 0.05 mm for a mechanical bond to be formed, and also for the cement to be properly hydrated behind the ettringite layer, despite the withdrawal of some of the water by suction from the brick. If the brick is dry, and has a high suction rate, there will be a partially hydrated zone in the cement paste, to a depth of several millimetres, and possessing poor mechanical strength. The movement of water between the brick and the mortar, and the resulting effects on the development of the mechanical bond between these components, was shown to be considerably affected by their specific surfaces and capillary dimensions. Grandet concluded that it is possible on the basis of these observations to obtain some indication of the likely behaviour of cement mortars, which would, however, also be influenced by such other parameters as the compaction of the mortar, its cement content and water reten-

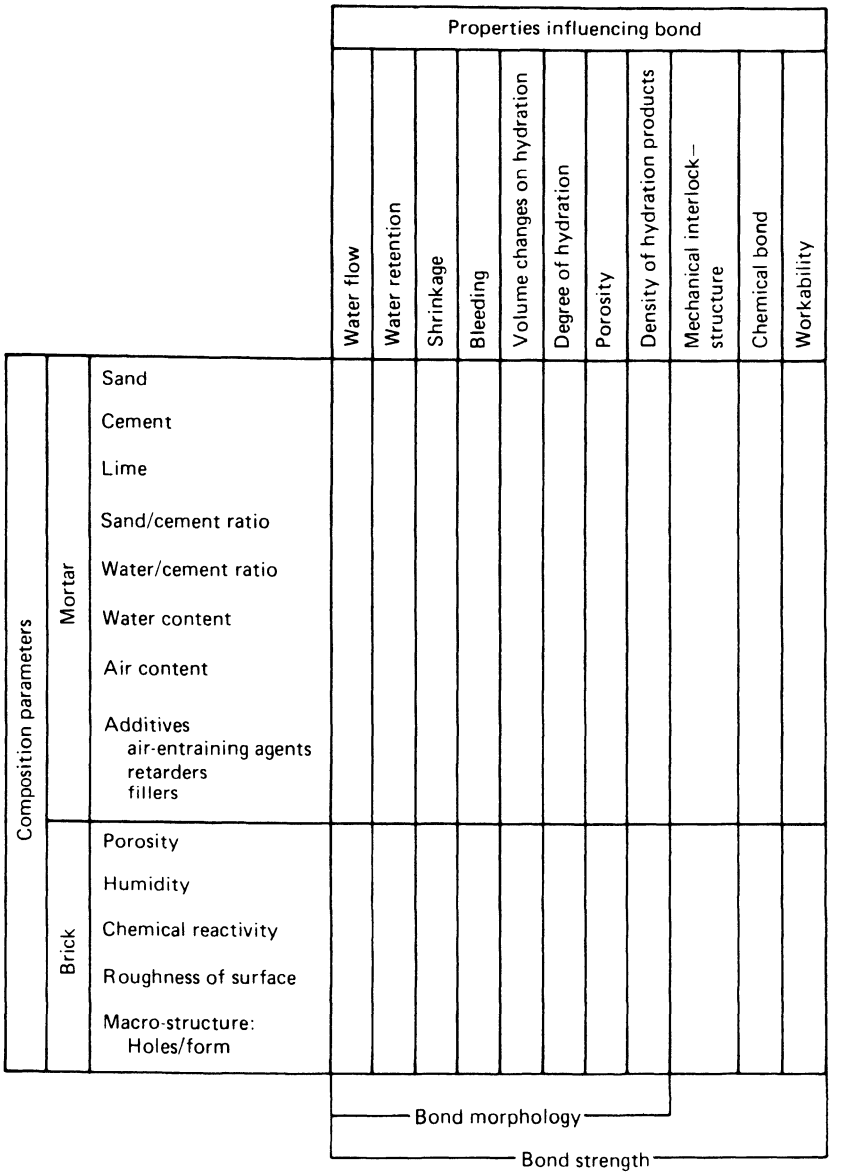

Figure 4.1 Composition parameters of mortar and brick, and their relation with properties influencing bond in masonry (Groot)

tivity. The effects of water movement on bond between various combinations of mortar and unit have been studied by Groot [3] who concluded that a primary cause of poor bond in clay masonry is the presence of an unduly high proportion of fine material at the mortar/brick interface. In the case of

calcium silicate bricks, poor bond results from the presence of too many fine pores in the bricks.

Further work on the nature of the brick/mortar bond based on the scanning electron microscope and microprobe has been reported by Lawrence and Cao [4], including studies of both cement and cement–lime pastes. Lawrence and Cao concluded that the bond was mechanical in nature, and that bond strength seems to develop from the interlocking of hydration products growing on the surface and in the pores of the brick material. The nature of these products was fine fibrous calcium silicate hydrate with some ettringite and calcium hydroxide crystals in a dual layered system. The presence of lime appeared to have beneficial effects in reducing microcracking at the interface and in producing a more continuous structure of hydration products on the brick surface. Lawrence and Cao's work also drew attention to the importance of brick suction and the matching of sand grading to the suction and pore characteristics of the brick.

The investigations described above indicate that the brick/mortar bond is mechanical in nature. This is confirmed by Binda and Baronio [5] for modern cement mortars and clay bricks, but their work has shown that with other materials there may be chemical bonding as well.

4.1.2 *Tensile bond strength: test results*

The effect of a number of variables affecting tensile bond strength has been investigated experimentally. The results have shown that the moisture content of the units at the time of laying is of importance in determining the tensile bond strength. Sinha [6] carried out direct tensile tests on 1/6th scale brick couplets at various moisture contents at the time of laying, between oven-dry and fully saturated, with the results shown in figure 4.2. The extreme variability of tensile bond strength is immediately apparent and although there is no clear relationship between moisture content and tensile bond strength, it will be noted that only very low values were found as the bricks reached their saturation moisture content.

Anderson and Held [7] have reported the results of tests on crossed brick couplets for three types of brick, which again show that the moisture content at the time of laying influences the bond strength: however, the effect depends on the type of brick and on the sand grading, as may be seen from figure 4.3. In general, the higher the fines content of the sand the lower the bond strength. In the Anderson and Held tests, clay bricks showed lower bond strengths with increasing moisture content, but the reverse held for calcium silicate bricks.

Schubert [8] has suggested that where the tensile stress parallel to the bed joints exceeds the tensile strength of the unit, the masonry tensile strength is approximately one-half of the unit tensile strength. Where failure takes place through the mortar joints, the masonry tensile strength can be estimated on the basis of the shear strength and bond overlap between

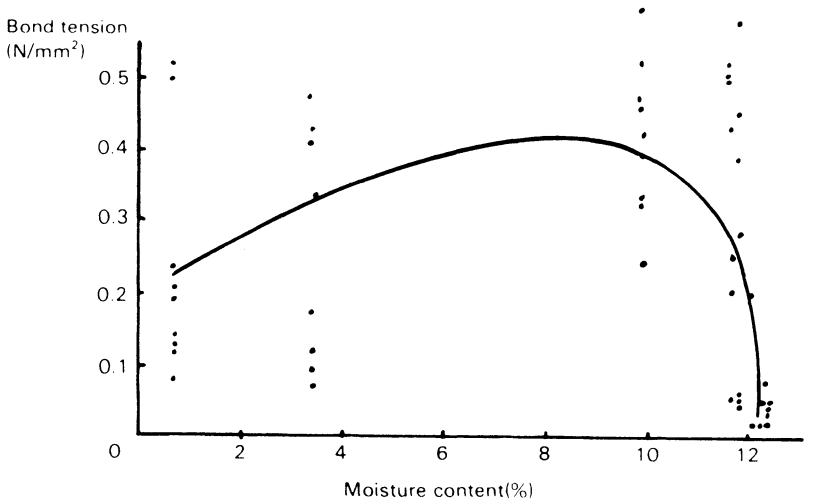

Figure 4.2 Relationship between moisture content of brick and bond tension of brick masonry couplets (Sinha). Brick strength 29.84 N/mm^2. Water absorption (5-hour boiling) 13.75 per cent

units. Individual results are, however, subject to the numerous variables involved and therefore very uncertain.

4.2 **Flexural tensile strength**

Flexural tensile strength, as defined by the modulus of rupture, is of greater practical importance than direct tensile strength and has been investigated in some detail in relation to the resistance of wall panels to wind loads [9–19]. The flexural strength of brickwork is, of course, different for bending in a plane at right angles to the bed joints, than for bending in a plane parallel to this direction, being several times greater in the latter case. The ratio is not constant but varies with the strength achieved. Thus in figure 4.4, values from a number of sources of the two moduli of rupture are plotted against each other, and in figure 4.5 their ratio is plotted against that for bending across the bed joints. These plots reveal the great variability of flexural strength, but a definite trend can be distinguished in the value of the orthogonal strength ratio, which decreases markedly with increase in the flexural strength across the bed joints.

Many investigators have attempted to establish a relationship between material properties and flexural tensile strength. Thus West [14] has shown correlations of flexural strength with suction rate and with water absorption, for thirty-three different bricks and two mortar mixes. In no cases are the correlations very close but, in statistical terms, it was possible to find a

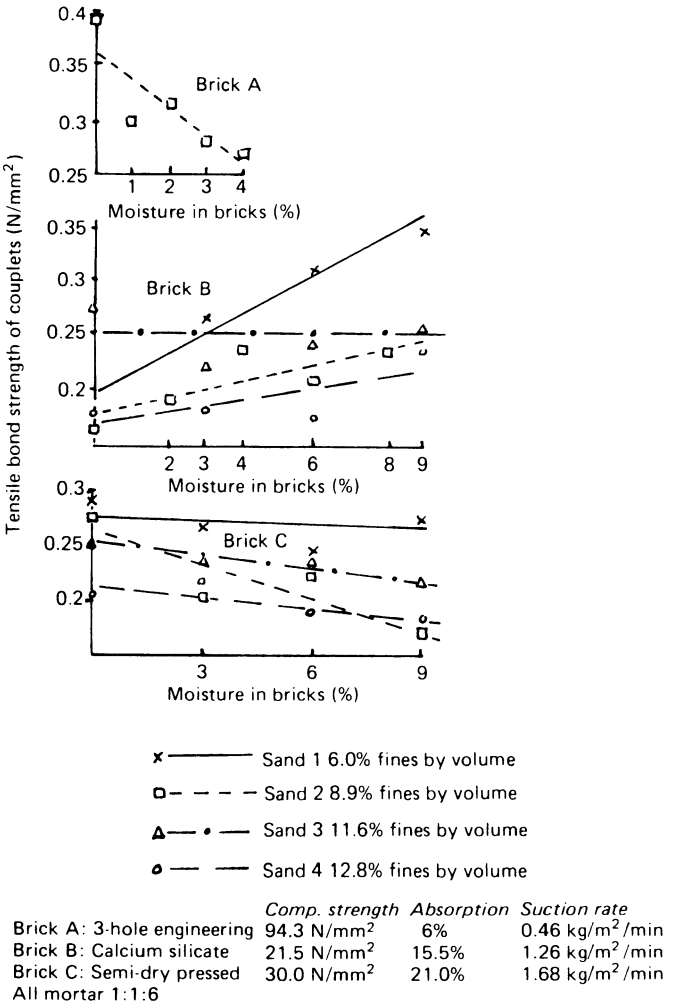

	Comp. strength	Absorption	Suction rate
Brick A: 3-hole engineering	94.3 N/mm²	6%	0.46 kg/m²/min
Brick B: Calcium silicate	21.5 N/mm²	15.5%	1.26 kg/m²/min
Brick C: Semi-dry pressed	30.0 N/mm²	21.0%	1.68 kg/m²/min

All mortar 1:1:6

Figure 4.3 Tensile bond strength of couplets against moisture content of bricks

relationship between flexural tensile strength and water absorption, and this is illustrated in figure 4.6. West's results indicated that for flexure parallel to the bed joints there was not a great difference in strength between 1:$\frac{1}{4}$:3 and 1:1:6 mortars, although a difference was noticeable in the orthogonal direction. James [15] has reported a similar result, as may be seen from table 4.1.

Anderson [18] and Sise *et al.* [19] have reported extensive investigations using specimens of different unit types and mortar mixes, with the aim of assessing the effect of various factors on flexural bond strength in stack bond prisms. Anderson concluded that as well as moisture content of the

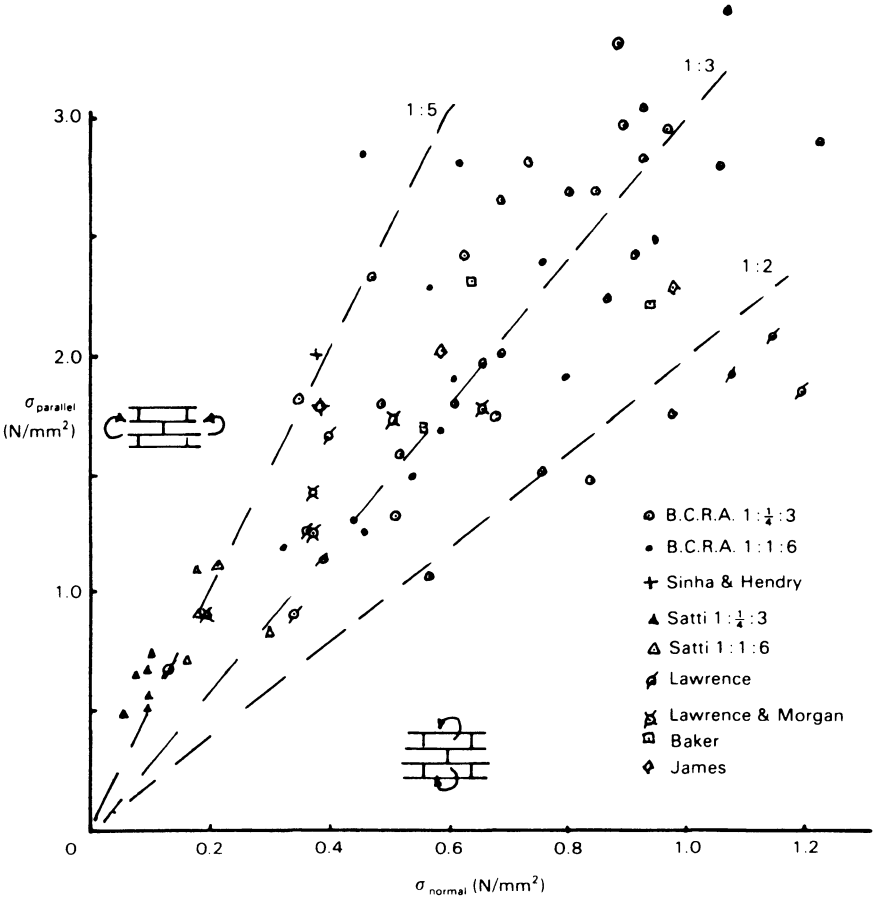

Figure 4.4 Moduli of rupture of brickwork in orthogonal directions

Table 4.1 Flexural tensile strengths of small specimens

Mortar	*Statistic*	*Flexural strengths (N/mm²)*		
		Normal to bed joint Stack prism	*Parallel to bed joint*	
			3-course specimen	*4-course specimen*
1:2:9	Mean	0.39	2.08	1.78
	C of V %	23.3	20.6	26.1
1:1:6	Mean	0.594	2.40	2.03
	C of V %	22.9	15.5	18.5
1:¼:3	Mean	0.984	2.74	2.29
	C of V %	25.4	18.0	16.5

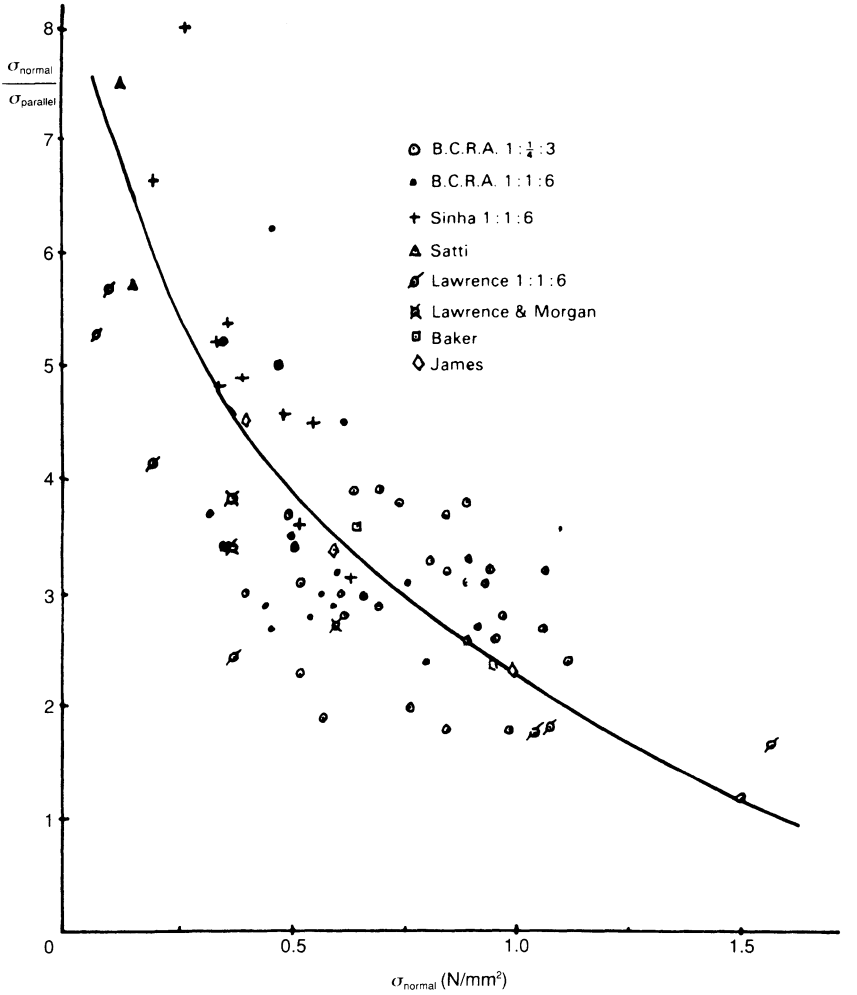

Figure 4.5 Ratio of moduli in orthogonal directions

units, the method of preparing the specimens had a significant effect, as did mortar consistency and surface texture. Sise *et al.* found that mortar joint thickness was the single most important factor affecting flexural bond strength – the thinner the joint the higher the strength, an effect also noted by Schubert [8].

Mann [20] has developed formulae for calculating the flexural strength of masonry where failure results either from rupture of the units or from failure of the bond. Subject to the great variability inherent in this property, these formulae show reasonable agreement with test results.

Values are given in the British Standard Code of Practice for flexural tensile strengths, but it has been pointed out that such strengths are

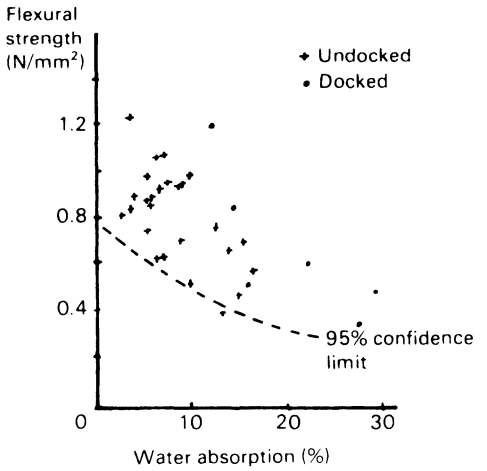

Figure 4.6 Flexural tensile strength of brickwork related to water absorption. Specimens tested in flexure parallel to bed joints; mortar mix 1:$\frac{1}{4}$:3 (West)

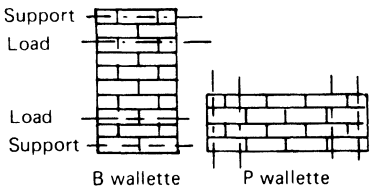

Figure 4.7 Specimens used in flexural strength test according to BS 5628

dependent on the form of the test specimens from which they were derived and on the method of preparation and test [18, 21, 22]. Fried *et al.* have derived the set of conversion factors shown in table 4.2 which give the strength of the wallette type of specimen on which the British Standard is based (figure 4.7) from the results of tests on prisms and individual joints, as proposed by Baker. The form of Baker's test is shown in figure 4.8, a development of which is the bond wrench device [23], illustrated in figure 4.9.

4.3 The strength of masonry in shear

Masonry walls are frequently subjected to racking shear in addition to compressive loads. Consequently, investigations of the shear strength of masonry have been undertaken in a number of countries, both on small and large-scale specimens.

The results of a series of tests on storey-height shear walls, reported by Hendry and Sinha [24, 25] are summarised in figure 4.10. These tests were

Table 4.2 Recommended conversion factors to obtain wallette strengths from the strengths of piers (p); joints (j) and modulus of rupture of unit (M)

Type of wallette (figure 4.7)	*Factors*		
	Blockwork		*Brickwork*
	4-high	*5-high*	
B	0.80p	0.82p	0.90p
B	0.77j	0.82j	0.69j
P	0.35 (j + M)		0.35 (j + M)

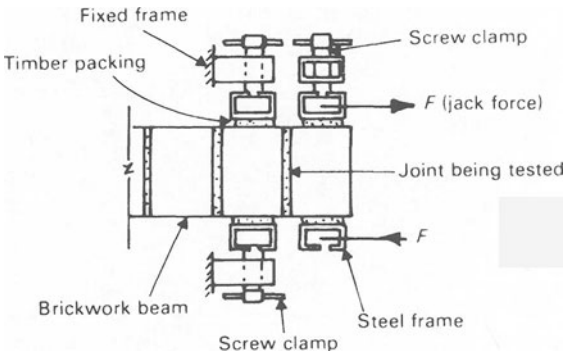

Figure 4.8 Arrangement for multiple flexural tensile tests on brickwork specimen (Baker)

carried out on full-scale and on model structures built of wire-cut bricks in $1:\frac{1}{4}:3$ lime mortar.

The shear strength of this type of brickwork was found to be

$$\tau = 0.3 + 0.5f_n \text{ N/mm}^2 \tag{4.1}$$

where f_n is the precompression; this relationship was found to hold up to values of $f_n = 2\text{N/mm}^2$.

This is a Mohr–Coulomb type of equation and has been used by a number of investigators in interpreting the results of shear tests. A wide range of values of the cohesion (τ_o) and the internal friction term (μ) have been reported depending on the properties of the materials used and on the form of the test specimens and loading arrangements. Some of the results are shown in table 4.3.

As shown by Sinha [6], the initial mode of joint failure represented by the Mohr–Coulomb equation is at a certain point replaced by cracking through

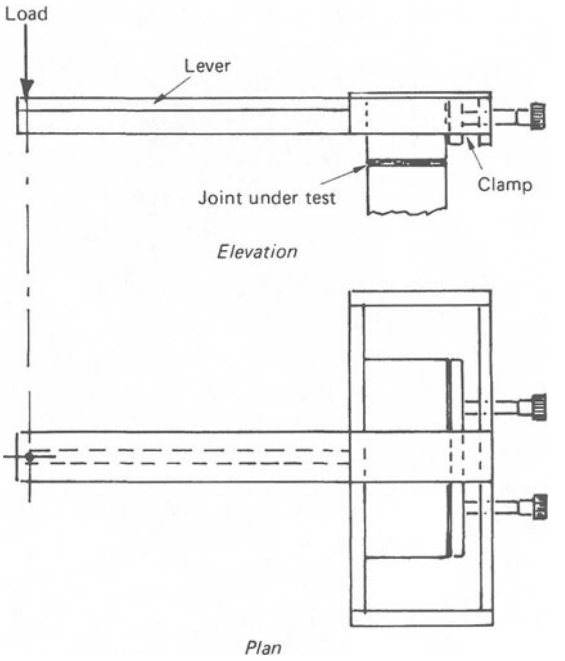

Figure 4.9 Bond wrench test

Table 4.3 Variation of shear strength with precompression, $\tau = \tau_0 + \mu f_n$

Source	*Type of*	*Mortar mix*	τ_0	μ
Hendry and Sinha [24, 25]	Extruded clay	1:0.25:3	0.3	0.5
Chinwah [26]	Extruded clay	1:0.25:3	0.25	0.34
Pieper and Trautsch [27]	Calcium silicate	1:2:8	0.2	0.84
		1:0:4	0.7	1.04
Schneider [28]	Calcium silicate	1:1:6	0.14	0.3
Schneider and Schnell [29]	Lightweight concrete	1:1:6	0.21	0.21
Hamid and Drysdale [30]	Extruded clay	1:0.25:2.81	0.56	0.91 (av.)
		1:0.5:4.0		
		1:1.25:6.75		
Mann and Muller [31]	Solid clay	1:3	0.4	0.3
		1:0:4	0.35	0.37
	Perf. clay	1:3	0.23	0.38
		1:0:4	0.35	0.37
	Calcium silicate	1:3	0.25	0.18
		1:0:4	0.4	0.35
	Aerated conc.	1:0:4	0.35	0.13
		1:3	0.2	0.2

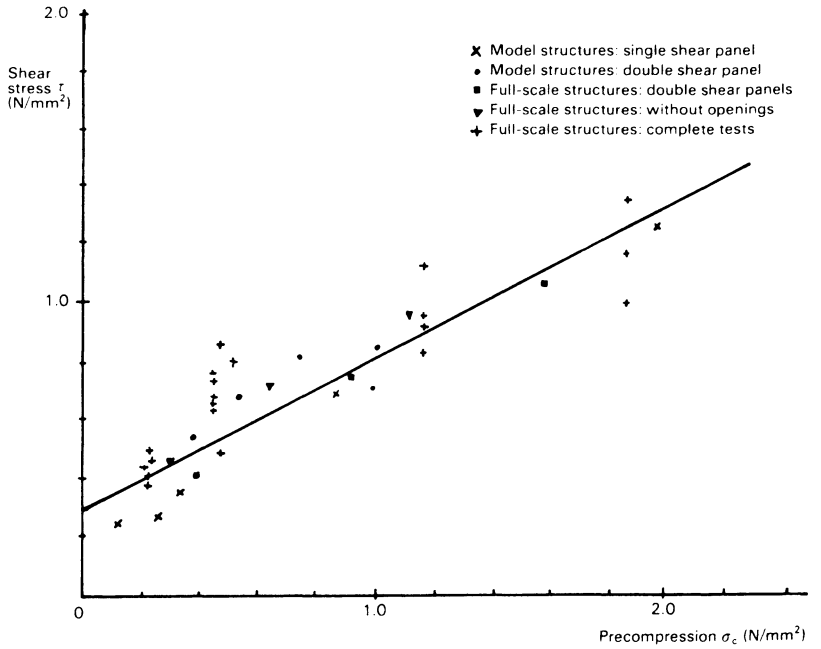

Figure 4.10 Shear strength against precompression: results of full-scale, model and small specimen tests

the units. Mann and Muller [31] have developed a failure theory for the shear strength of masonry based on consideration of the equilibrium and strength of a unit within a wall, and have given the following expression for the shear strength where failure is by the cracking mode:

$$0.45 f_{RZ} \sqrt{\left(1 + f_n / f_{RZ}\right)}$$

where f_{RZ} is the tensile strength of the unit and f_n is the normal stress. A value of $0.033 f_b$ is given for the tensile strength of solid or near-solid units, and $0.025 f_b$ for highly perforated units (such as German *Hohlblocksteine*) where f_b is the compressive strength of the unit.

For very high compressive stress, there will be a further failure mode corresponding to crushing failure of the masonry. The entire failure envelope according to Mann and Muller's theory is thus as indicated in figure 4.11.

Dialer [32] has developed the approach of Mann and Muller to take account of the reduced strength of the mortar in the head joints of brick masonry, giving the following formulae corresponding to shear failure of the bed joints, tensile failure of the units and compressive failure of the masonry, and corresponding to the three modes indicated in figure 4.11:

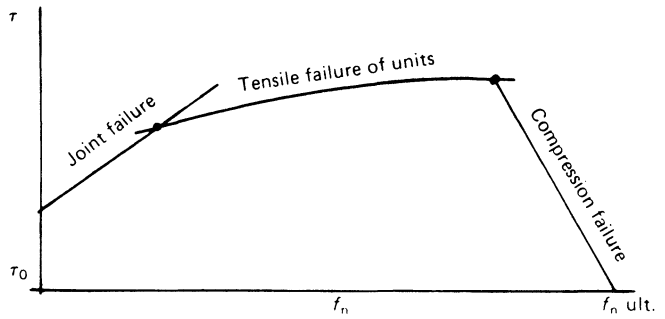

Figure 4.11 Failure modes of masonry in shear with vertical compression

$$\tau_{yx} = \frac{c_{yx} - \mu_{yx}\sigma_y + \nu\mu_{yx}\left(c_{xy} - X\mu_{xy}\sigma_y\right)}{\left(1 + \nu\mu_{yx}\right)} \tag{4.2}$$

$$\tau_{yx} = \frac{1}{2}\left(c_{xy} - X\mu_{xy}\sigma_y\right) + \frac{\beta_{t,b}}{2.3}\sqrt{\left(1 - \sigma_y\frac{\left(1 + X\right)}{\beta_{t,b}} + \frac{X\sigma_y^2}{\beta_{t,b}^2}\right)} \tag{4.3}$$

$$\tau_{yx} = c_{xy} + \omega\beta_{panel} + \sigma_y\left(\omega - X\mu_{xy}\right) \tag{4.4}$$

where τ_{yx} = average shear stress on bed face
c_{yx}, c_{xy} = cohesion on bed and head faces respectively
ν = 2× ratio of length/height of unit
ω = $1/\nu$
μ_{yx}, μ_{xy} = coefficient of friction on bed and end faces respectively
X = ratio of horizontal/vertical stresses on masonry
σ_y = average vertical stress
$\beta_{t,b}$ = tensile strength of unit
β_{panel} = compressive strength of masonry.

4.4 **Masonry under biaxial stress**

A more fundamental approach to the study of shear strength is based on consideration of the strength of masonry under biaxial stress, taking into account the direction of the applied stresses relative to the bed joint of the masonry. Samarasinghe [33] and Page [34] have established failure surfaces for brickwork stressed in orthogonal tension–compression by the application of normal stresses to small specimens of brickwork in which the bed joint was inclined at various angles to the axes of the applied stresses. Figure 4.12 shows in non-dimensional form a representation of the failure surface in terms of the applied stresses and the relative bed-joint angle derived from results reported by Page.

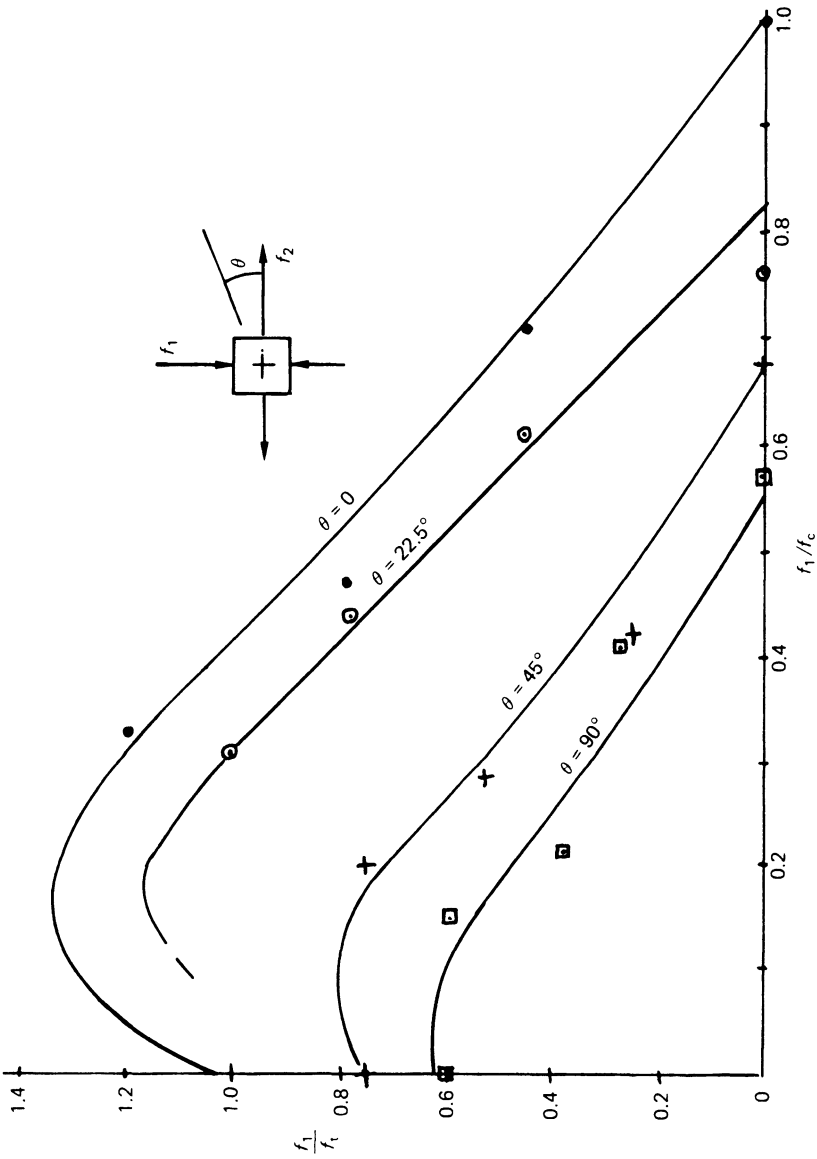

Figure 4.12 Biaxial compression–tension failure relationship, for brick masonry

Ganz *et al.* [35] have produced a set of equations in which the strength of masonry is defined by three parameters, f_{mx} and f_{my}, respectively the uniaxial compressive strengths for loads applied normal and parallel to the bed joints, and tan ϕ the coefficient of friction in the bed joints. The tensile strength of the masonry and cohesion in the bed joints are neglected. On these assumptions the following equations give limiting stress conditions:

For tensile failure:

$$\tau_{xy}^2 - \sigma_x + \sigma_y = 0 \tag{4.5}$$

For compressive failure of the units (first condition):

$$\tau_{xy}^2 - \left(\sigma_x + f_{mx}\right) \cdot \left(\sigma_y + f_{my}\right) = 0 \tag{4.6}$$

For compressive failure of the units (second condition):

$$\tau_{xy}^2 + \sigma_y \cdot \left(\sigma_y + f_{my}\right) = 0 \tag{4.7}$$

For sliding of the horizontal joints:

$$\tau_{xy}^2 - \left(\sigma_x \cdot \tan\phi\right)^2 = 0 \tag{4.8}$$

where σ_x = applied stress normal to bed joints (compression negative)
σ_y = applied stress parallel to bed joints (compression negative)
τ_{xy} = shear stress.

The tests on which the above relationships were determined were on brickwork built from solid units. Hegemeir *et al.* [36] have carried out biaxial stress tests on large specimens of hollow concrete block masonry. The results of these tests showed that for this type of masonry the failure envelope for a panel stressed in the compression–tension quadrant, with the compressive stress normal to the bed joints, could be represented by a straight line, as shown in figure 4.13. It was also found that the panel tensile strength varied only slightly with the angle between the stress axes and the bed joint. This made it possible to obtain the failure envelope for shear stress against normal bed joint stress indicated in figure 4.14, the normal stress parallel to the bed joint being zero. Bernardini *et al.* [37] have obtained a similar relationship for hollow clay unit masonry.

Using the failure surface it is possible to determine the point at which initial cracking of an element takes place, provided that an appropriate stress analysis can be carried out. For this purpose an elastic analysis would probably be sufficiently accurate but a finite element computation would be required to follow the development of the crack pattern through to failure.

Determination of brickwork strength under biaxial stressing requires specialised equipment and has not often been undertaken. Other investigators have proposed failure criteria using a combination of uniaxial and

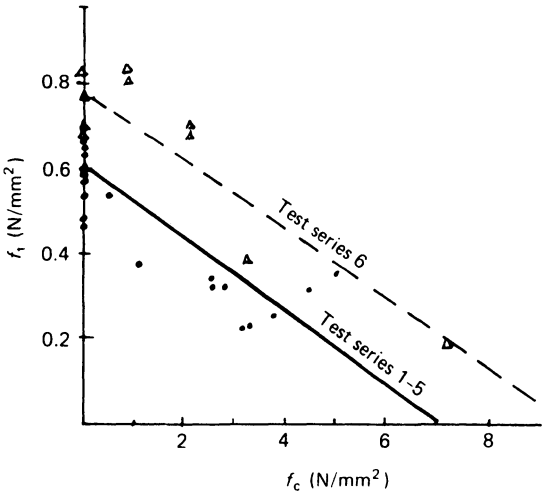

Figure 4.13 Biaxial compression–tension failure stress relationship for concrete block masonry (Hegemeir *et al.*)

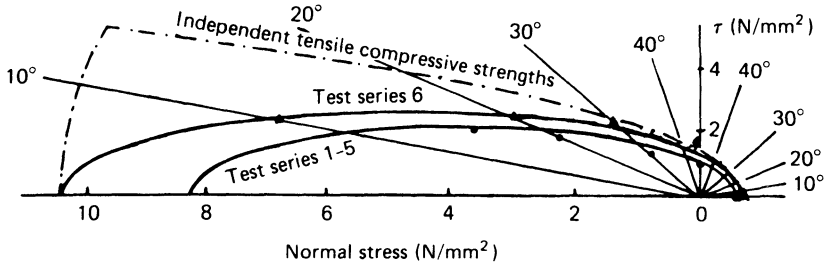

Figure 4.14 Failure envelope for concrete block masonry with zero normal stress on head joint (Hegemeir *et al.*)

splitting tests. Hamid and Drysdale [38, 39] have adapted the theory of single plane of weakness from rock mechanics to predict failure due to shear along the mortar joints, and the maximum stress theory, modified to take into account the strength variation normal and parallel to the bed joints, to predict failure by splitting. These authors take the Mohr–Coulomb equation for failure along a single plane of weakness, in this case the interface between unit and mortar as:

$$\tau = C + f_n \tan\phi \tag{4.9}$$

where τ is the shear stress on the joint at failure, C the cohesion, f_n the compressive stress normal to the joint and ϕ the angle of internal friction.

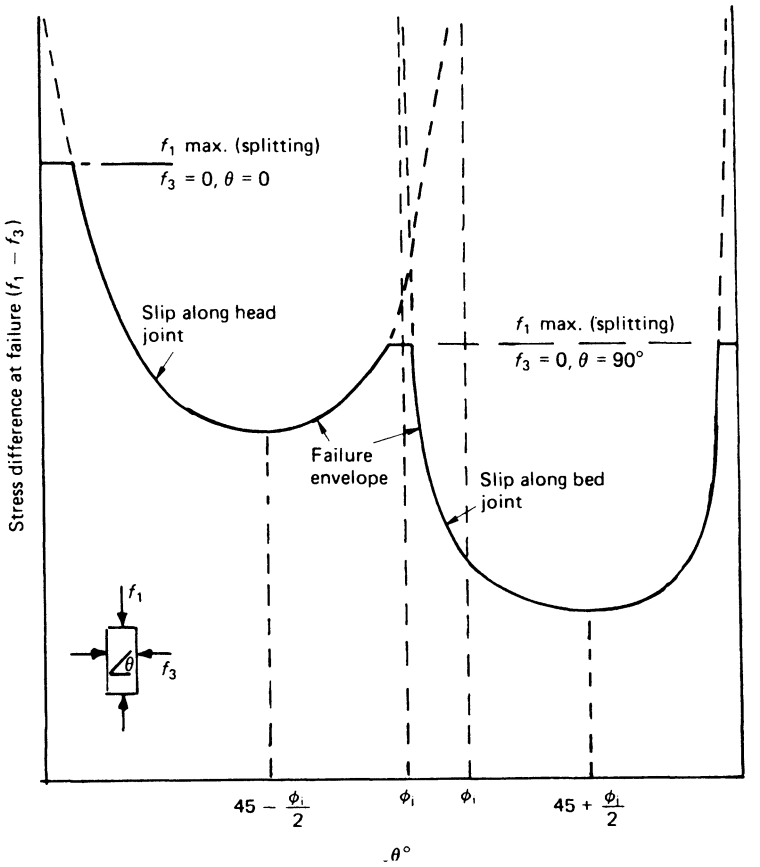

Figure 4.15 Failure envelopes for biaxially stressed masonry (Hamid and Drysdale)

Using the usual equations relating the normal and shear stresses to the applied principal stresses f_1 and f_3 results in the following equation for bed joint failure:

$$f_1 - f_3 = \frac{2\left(C_j + f_3 \tan \phi_j\right)}{\left(1 - \tan \phi_j \cot \theta\right) \sin 2\theta} \tag{4.10}$$

where θ is the angle between the direction of f_3 and the bed joint. A similar equation is obtained for failure of the head joint by substituting C_i and ϕ_i for the corresponding terms in equation (4.10). These equations are shown in figure 4.15 with the addition of horizontal lines defining the intervention of splitting failure of the units. The theory has shown reasonable agreement with the results of tests on specimens subjected to uniaxial compression in which the bed-joint angle varied between 15° and 75°.

4.5 Shear modulus of masonry

The shear modulus of brickwork G was calculated from deflection measurements made on full-scale, storey-height panels tested by Sinha and Hendry [24]. For the type of brickwork tested (31 N/mm^2 bricks set in $1:\frac{1}{4}:3$ mortar) the value of G was in the region of 1500–2000 N/mm^2. The value increased appreciably with precompression and, reflecting the non-linear characteristics of the material, decreased with increase in shear stress. For approximate calculation, G might be taken as

$$E/2(1+\nu) \tag{4.11}$$

where ν is Poisson's ratio. For clay brickwork Atkinson and Noland [40] have found an average initial value in compression tests of 0.17, increasing rapidly when the applied compression exceeds 0.8 of ultimate. Hegemeir *et al.* [36] have reported values of Poisson's ratio for blockwork masonry of 0.18 when loaded normal to the bed joint, decreasing to 0.12 when loaded parallel to this direction. This is an indication of the orthotropy of masonry which has been discussed by Naguib and Suter [41] in relation to numerical modelling, although no experimental data appear to be available.

References

1. C. J. W. P. Groot, 'Bond in Masonry', *Proceedings of the First International Conference on Structural Engineering Analysis and Modelling* (University of Science and Technology, Kumasi, Ghana, 1987).
2. B. Grandet, 'Physico-Chemical Mechanisms of the Bond between Clay and Cement', *Proceedings of the Third International Brick Masonry Conference* (Essen) 1973, eds L. Foertig and K. Gobel (Bundesverband der Deutschen Ziegelindustrie, Bonn, 1975), pp. 217–21.
3. C. Groot, 'Effects of Water on Mortar–Brick Bond', Thesis (Technical Univ. Delft, 1993).
4. S. Lawrence and H. T. Cao, 'An Experimental Study of the Interface between Brick and Mortar', *Proceedings of the Fourth North American Masonry Conference* (Los Angeles) 1987, pp. 48.1–14.
5. L. Binda and G. Baronio, 'Survey of Brick/Binder Adhesion in "Powdered Brick" Mortars and Plasters', *Masonry International*, **2** (2) (1988).
6. B. P. Sinha, 'Model Studies Related to Load Bearing Brickwork', PhD Thesis (University of Edinburgh, 1967).
7. C. Anderson and L. C. Held, 'The Effect of Sand Grading on Mortar Properties and the Tensile Bond of Brickwork Specimens', *Proc. Br. Masonry Soc.*, **1** (1986) 1–6.
8. P. Schubert, 'Tensile and Flexural Strength of Masonry – Influences, Test Methods, Test Results', *Proceedings of the Tenth International Brick and Block Masonry Conference* (Calgary) 1994, pp. 895–907.
9. S. J. Lawrence and T. W. Morgan, 'Strength and Stiffness of Brickwork in Lateral Bending', *Proc. Br. Ceram. Soc.*, **24** (1975) 79–90.

10. S. J. Lawrence, 'Flexural Strength of Brickwork Normal to and Parallel to the Bed Joints', *J. Aust. Ceram. Soc.*, **II** (1975) 5–6.
11. B. P. Sinha and A. W. Hendry, 'Tensile Strength of Brickwork Specimens', *Proc. Br. Ceram. Soc.*, **24** (1975) 91–100.
12. A. W. Hendry, 'The Lateral Strength of Unreinforced Brickwork', *Struct. Engr.*, **57** (1973) 43–50.
13. L. R. Baker, 'Brickwork Panels Subjected to Face Wind Loads', M. Eng. Sci. Thesis (University of Melbourne, 1972).
14. H. W. H. West, 'The Flexural Strength of Clay Masonry determined from Wallette Specimens', *Proceedings of the Fourth International Brick Masonry Conference* (Brugge) 1976, Paper 4.a.6.
15. J. A. James, 'An Investigation of the Lateral Load Resistance of Walls of Unreinforced Brickwork without Precompression Built in Clay Bricks', *Report W/Lat/1* (Building Development Laboratories, Morley, W. Australia).
16. L. R. Baker, 'Variability Aspects of the Flexural Strength of Brickwork', *Proceedings of the Fourth International Brick Masonry Conference* (Brugge) 1976, Paper 2.b.4.
17. L. R. Baker, 'The Flexural Action of Masonry Structures under Lateral Load', PhD Thesis (Deakin University, 1981).
18. C. Anderson, 'Tensile Bond Tests with Concrete Blocks', *Int. J. Masonry Construction*, **1** (4) (1981) 134–48.
19. A. Sise, N. G. Shrive and E. L. Jessop, 'Flexural Bond Strength of Masonry Stack Prisms', *Proc. Br. Masonry Soc.*, **2** (1988) 103–7.
20. W. Mann, 'Tensile and Flexural Strength of Masonry', *Proceedings of the Ninth International Brick/Block Masonry Conference* (Berlin) 1991, pp. 1292–301.
21. C. Anderson, 'Some Observations on Masonry Wallette Testing', *Int. J. Masonry Construction*, **2** (4) (1982) 146–54.
22. A. Fried, C. Anderson and D. Gairns, 'A Comparative Study of Experimental Techniques for Determining the Flexural Resistance of Masonry', *Proc. Br. Masonry Soc.*, **2** (1988) 98–102.
23. R. H. Brown and B. D. Palm, 'Flexural Strength of Brick Masonry using the Bond Wrench', *Proceedings of the Second North American Masonry Conference* (University of Maryland) 1982, Paper 1.
24. B. P. Sinha and A. W. Hendry, 'Racking Tests on Storey-Height Shear Wall Structures with Openings Subjected to Pre-compression', in *Designing, Engineering and Constructing with Masonry Products*, ed. F. B. Johnson (Gulf, Houston, Tex., 1969), pp. 192–9.
25. A. W. Hendry and B. P. Sinha, 'Shear Tests on Full Scale Single Storey Brickwork Structures Subjected to Precompression', *Civ. Engng Publ. Wks Rev.*, **66** (1971) 1339–44.
26. J. C. G. Chinwah, 'Shear Resistance of Brick Walls', PhD Thesis (University of London, 1972).
27. K. Pieper and W. Trautsch, 'Shear Tests on Walls', *Proceedings of the Second International Brick Masonry Conference* (Stoke-on-Trent) 1971, eds H. W. H. West and K. H. Speed (British Ceramic Research Association, Stoke-on-Trent, 1971), pp. 140–3.
28. H. Schneider, 'Tests on Shear Resistance of Masonry', *Proceedings of the Fourth International Brick Masonry Conference* (Brugge) 1976, Paper 4.b.12.

29. H. Schneider and W. Schnell, 'Tests on the Shear Strength of Brickwork', *Betonwerk & Fertigteil-Technik*, **44** (1978) 303–9, 369–75.
30. A. A. Hamid and R. C. Drysdale, 'The Shear Behaviour of Brickwork Bed Joints', *Proc. Br. Ceram. Soc.*, **30** (1982) 101–9.
31. W. Mann and H. Muller, 'Failure of Shear-Stressed Masonry – An Enlarged Theory, Tests and Application to Shear Walls', *Proc. Br. Ceram. Soc.*, **30** (1982) 223–35.
32. C. Dialer, 'Some Remarks on the Strength and Deformation Behaviour of Shear Stressed Masonry Panels under Static Monotone Loading', *Proceedings of the Ninth International Brick/Block Masonry Conference* (Berlin) 1991, pp. 277–82.
33. W. Samarasinghe, 'In Plane Strength of Brickwork', PhD Thesis (University of Edinburth, 1980).
34. A. W. Page, 'An Experimental Investigation of the Biaxial Strength of Brick Masonry', *Proceedings of the Sixth International Brick Masonry Conference* (Rome) 1982, pp. 3–15.
35. H. R. Ganz, R. Guggisberg, J. Schwarz and B. Thurlimann, 'Contributions to the Design of Masonry Walls', Institut für Baustatik und Konstruktion ETH Zurich, *Bericht Nr. 168* (Berkhauser Verlag, Basel, Boston, 1989).
36. G. A. Hegemeir, R. O. Nunn and S. K. Arya, 'Behaviour of Concrete Masonry under Biaxial Stress', *Proceedings of the First North American Masonry Conference* (Boulder) 1976, pp. 1/1–24.
37. A. Bernardini, C. Modena and U. Vescovi, 'An Anisotropic Biaxial Failure Criterion for Hollow Clay Brick Masonry', *Int. J. Masonry Construction*, **2** (4) (1982) 165–71.
38. A. A. Hamid and R. G. Drysdale, 'Proposed Failure Criteria for Concrete Block Masonry under Biaxial Stresses', *Proc. ASCE J. Struct. Div.*, **107** (2) (1981) 1675–87.
39. A. A. Hamid and R.G. Drysdale, 'Proposed Failure Criteria for Brick Masonry under Combined Stresses', *Proceedings of the Second North American Masonry Conference* (Maryland) 1982, pp. 9.1–11.
40. R. H. Atkinson and J. L. Noland, 'A Proposed Failure Theory for Brick Masonry in Compression', *Proceedings of the Third Canadian Masonry Conference* (Edmonton) 1983, pp. 5.1–17.
41. E. M. F. Naguib and G. Suter, 'Effect of Brick Stiffness Orthotropy on the Lateral Stresses in Stack-Bonded Masonry Prisms', *Proceedings of the Fourth North American Masonry Conference* (Los Angeles) 1987, pp. 18.2–11.

5 THE STRENGTH OF MASONRY COMPRESSION ELEMENTS

5.1 **Factors affecting the compressive strength of walls and piers**

The discussion of the compressive strength of masonry in chapter 2 related to short piers or columns, axially loaded. The strength of a wall of a given type will be influenced by the eccentricity of loading and the slenderness ratio, which in turn depend on the geometry of the building, the relative stiffnesses of the walls and floors, the nature of the joints between them and the distribution of the loads. The calculation of the strength of masonry compression elements is further complicated by the low tensile strength of the material, which may crack under certain loading conditions, leading to variations in effective sectional properties.

Structural design is currently based on the results of tests on walls and piers of various slenderness ratios and eccentricities, and with idealised end conditions. The designer has then to make allowance for the actual end conditions by estimating the effective height of the wall or column and the eccentricity of loading on it, generally on the basis of conventional rules or judgement. Covered by large safety factors, these rather crude methods have given satisfactory results, but more rational design methods are clearly desirable and will be discussed in this and the following chapter.

5.2 **Empirical studies of the strength of walls and piers**

With the object of providing design data for structural codes of practice, generally in the form of reduction coefficients on the basic masonry compressive strength to allow for slenderness and eccentricity, tests have been carried out in many countries over a long period of time. As mentioned in section 5.1, these tests have achieved their purpose and have resulted in a fairly reliable knowledge of the effect of the primary factors affecting the strength of simple walls and piers [1].

The literature on the subject shows that a large number of tests have been carried out on axially loaded walls of varying slenderness ratio. Some

of the results, from references 2–8, are plotted in figure 5.1; these show a considerable scatter which appears to increase with slenderness ratio. The reason for the scatter is, presumably, that in testing walls it is difficult to avoid small unintentional eccentricities, the effect of which increases with slenderness. There are fewer available results for walls tested with eccentric loading, but some have been plotted in figure 5.1. In the case of these results the scatter is rather less, no doubt because small experimental deviations from a finite eccentricity are of less importance than they are in the case of nominally axial loading.

It is found from wall tests that up to slenderness ratios (that is, ratio of height to thickness) approaching 30, which is a practical limit, failure under axial load is usually limited by the strength of the material rather than by buckling. The walls fail in this case by the development of vertical cracks or diagonal cracking, as shown in figure 5.2.

Under eccentric load a slender wall may show considerable lateral deflection (figure 5.3) before failure, which takes place by catastrophic collapse (figure 5.4).

These tests have been carried out either with hinged end conditions or 'flat ends', the latter meaning that the walls have been tested between the rigid platens of the testing machine. There have inevitably been differences in the test conditions and in the interpretation of the results, as reflected in the reduction factors used in the various national codes.

5.3 **Theoretical studies of the strength of compression elements**

Although the strength of hinged-end compression elements is satisfactorily described by test results, this is not really a sufficient basis for the design of walls in an actual structure. Such walls are never hinged, and for a given load condition their strength is critically influenced by the stiffness of contiguous walls and floor slabs. In conventional design calculations, the real condition in the structure is related to the hinged-end situation by 'guesstimation' of an equivalent height of the member and of the eccentricity of the loading. To progress beyond this empirical method of design, it is necessary to examine theoretically the mechanics of brittle material columns.

5.3.1 ***Differential equation for brittle columns***

Theories for the elastic buckling of brittle columns were first developed by Royen [9] and by Angervo [10]; the latter's theory was based on the solution of the differential equation for a column without tensile strength. A similar solution by Chapman and Slatford [11] considered pinned and fixed-end columns, with an initial deformation that increased linearly from the ends to mid-height, and an initially straight pinned-end column with eccentric loading. Restricting attention to the last case, it will be

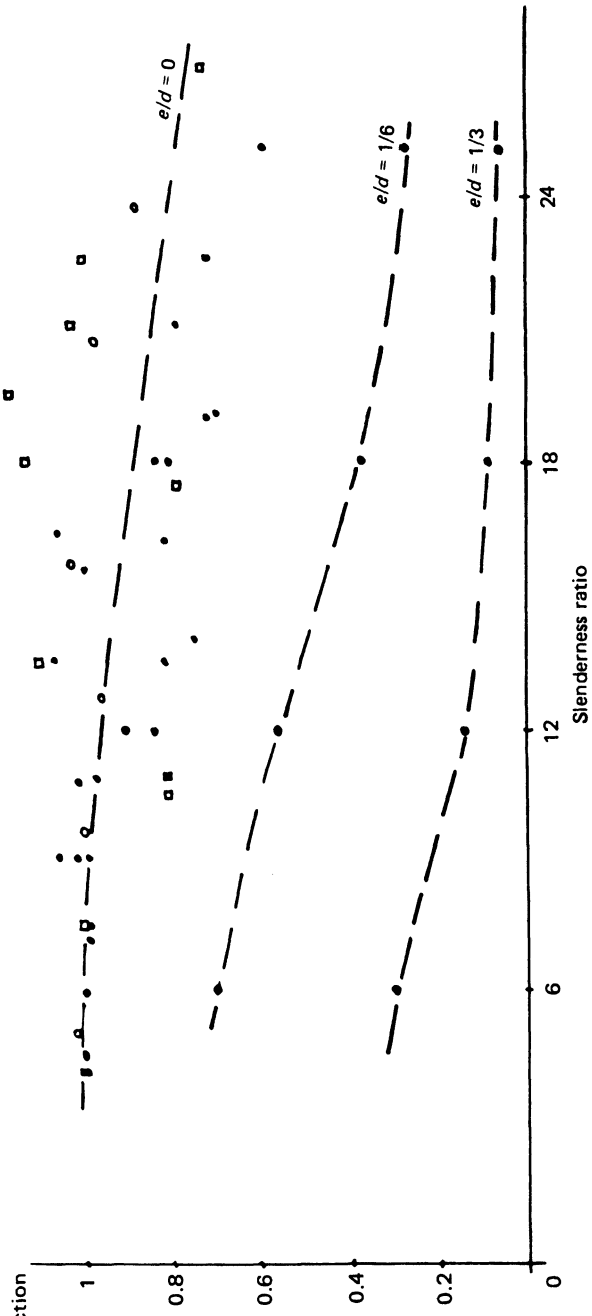

Figure 5.1 Reduction factor against slenderness ratio at various eccentricities

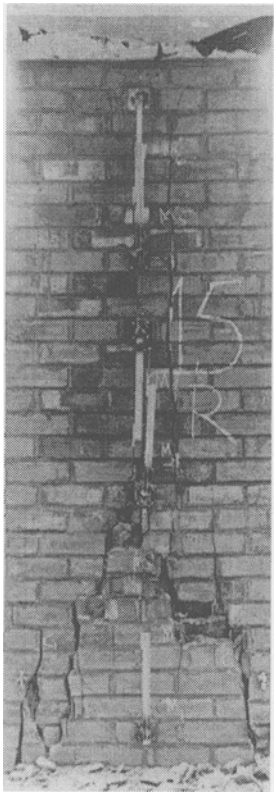

Figure 5.2 Failure of brick masonry wall in compression by vertical splitting and inclined shear cracking

observed that if an eccentric load is applied within the middle third of the section, tension in the material will be produced only when lateral deflection of the column causes the line of thrust to move out of the middle third. As indicated in figure 5.5a, a cracked zone will extend over part of the height of the column and the effective section will be reduced. (If the eccentric load is applied outside the middle third of the section, the cracked zone will extend over the whole height of the column.) The stress distributions at various sections of the column will be as shown, and are assumed to be linear. Failure of the column will take place when the cracked zone reaches the line of thrust; at the moment of collapse, a hinge forms at the mid-height of the column, and the line of thrust passes through it as shown in figure 5.5b. Following the solution proposed by Chapman and Slatford it is necessary to consider two differential equations: one for the uncracked parts of the column, and the other for the cracked length. Thus, for the uncracked part

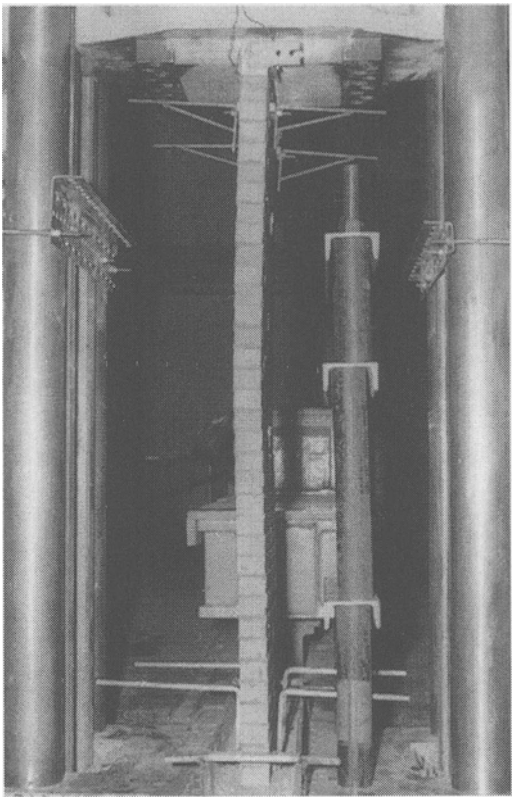

Figure 5.3 Incipient buckling of a slender wall at 75 per cent of ultimate load

$$EI\frac{\mathrm{d}^2y}{\mathrm{d}x^2} + P(e_\mathrm{p} + y) = 0 \tag{5.1}$$

where the symbols have the meaning shown in figure 5.5a, E is Young's modulus and I the second moment of area. The reduced depth of a section within the cracked part is

$$d' = 3\left(\frac{d}{2} - y - e_\mathrm{p}\right)$$

and the corresponding moment of inertia is

$$I\left(\frac{d'}{d}\right)^3$$

The eccentricity of the line of thrust with respect to the cracked section is

$$e' = \left(\frac{d'}{6}\right)$$

Figure 5.4 Collapse of wall shown in figure 5.3 at ultimate load

Therefore, the differential equation at any cracked section is

$$EI\left(\frac{d'}{d}\right)^3 \frac{\mathrm{d}^2y}{\mathrm{d}x^2} + Pe' = 0$$

or

$$EI\frac{\mathrm{d}^2y}{\mathrm{d}x^2} + \frac{Pd^3}{54\left[\left(d/2\right) - y - e_\mathrm{p}\right]^2} = 0 \qquad (5.2)$$

Substituting $z = [(d/2) - y - e_\mathrm{p}]$, $\mathrm{d}^2z/\mathrm{d}x^2 = -\mathrm{d}^2y/\mathrm{d}x^2$, equations 5.1 and 5.2 become respectively

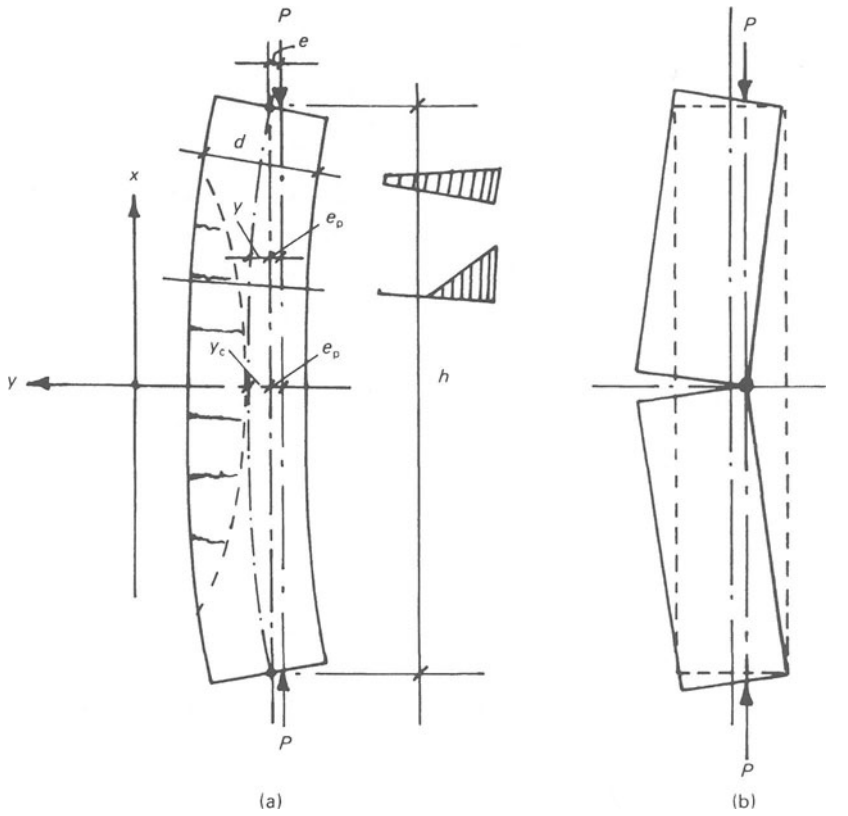

Figure 5.5 Eccentrically loaded pinned-end column of brittle material

$$EI\frac{\mathrm{d}^2z}{\mathrm{d}x^2} - P\left(\frac{d}{2} - z\right) = 0 \tag{5.3}$$

and

$$EI\frac{\mathrm{d}^2z}{\mathrm{d}x^2} - \frac{Pd^3}{54z^2} = 0 \tag{5.4}$$

The general solutions of equations 5.3 and 5.4 are, respectively,

$$z = A\cos\mu x + B\sin\mu x + \frac{d}{2}$$

and

$$f\left(\frac{F}{C}z\right) = \left(\frac{F}{C}\frac{d}{3}\right)^{\frac{3}{2}}\mu x + G$$

in which $\mu = \sqrt{(P/EI)}$ and A, B, C, F and G are constants determined by the end conditions and the conditions at the common sections between the cracked and uncracked parts of the column. Evaluation of these constants leads to the following equation

$$\alpha = \frac{\mu h}{2} = \left(\frac{d}{3z_c}\right)^{-\frac{3}{2}} f\left(\frac{d}{3z_c}\right) + \sin^{-1}\left(\frac{4d}{3z_c} - 3\right)^{-\frac{1}{2}} - \sin^{-1}\frac{6e_p}{d}\left(\frac{4d}{3z_c} - 3\right)^{-\frac{1}{2}} \tag{5.5}$$

The maximum value of P occurs when $d\alpha/dz_c = 0$, and then z_c/d and e_p/d satisfy the equation

$$\left(\frac{d}{3z_c}\right)^{-\frac{5}{2}}\left[3\left(\frac{d}{3z_c} - 1\right)^{\frac{1}{2}}\left(\frac{d}{3z_c}\right)^{\frac{3}{2}} - \frac{3}{2}f\left(\frac{d}{3z_c}\right)\left(\frac{4d}{3z_c} - 3\right)\right.$$
$$\left. +2\left[\left(\frac{d}{6e_p}\right)^2\left(\frac{4d}{3z_c} - 3\right)^{-\frac{1}{2}} - 1\right]\right] = 0 \tag{5.6}$$

Using the above equations, Chapman and Slatford were able to obtain, in dimensionless terms, the load–deflection curves for eccentrically loaded brittle columns reproduced in figure 5.6. In this diagram the load on the column is expressed as a fraction of the Euler load. The broken lines indicate the behaviour of an elastic column with tensile resistance; compared with such a member the load–deflection curve for a brittle column reaches a maximum. The theoretical collapse occurs when the sum of the central deflection and the initial eccentricity becomes equal to half the depth of the section. The vertical chain broken line indicates the onset of cracking, which of course is exceeded as soon as any load is applied with an eccentricity greater than $d/6$.

A second diagram from the Chapman and Slatford analysis, figure 5.7, shows the buckling load of the column as a fraction of the Euler load, plotted against the eccentricity ratio, emphasising the critical importance of eccentricity as a factor influencing the strength of brickwork elements in compression. From this diagram and on the assumption, based on experimental evidence, that axially loaded walls having a slenderness ratio (height/thickness) exceeding about 25 fail by buckling, it is possible to derive a set of reduction factors for slenderness and eccentricity. This has been done, with the results shown in figure 5.8. The curves to the right of the diagram indicate buckling failures as derived from figure 5.7, taking the Euler critical load at a slenderness ratio of 25 as unity and equating it to the compression failure stress for a short column. The reduction factors for short columns with various degrees of eccentricity have been calculated by

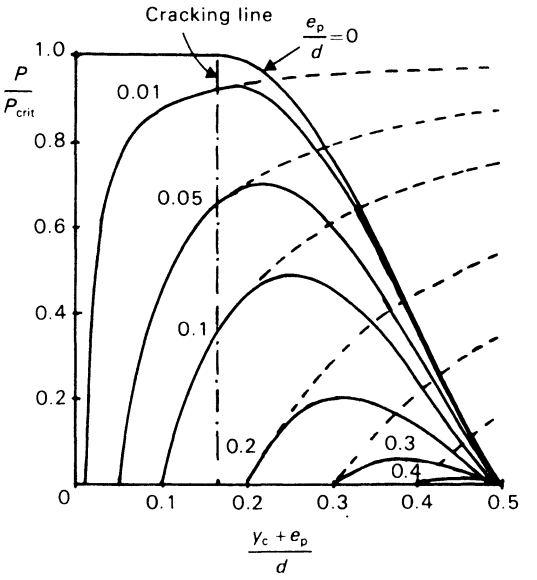

Figure 5.6 Load–deflection curves for column with eccentric load: broken lines refer to wholly elastic columns (Chapman and Slatford)

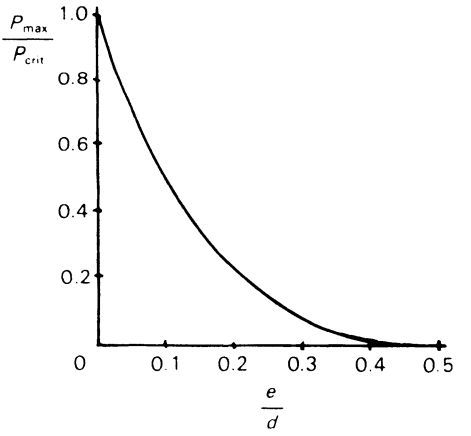

Figure 5.7 Maximum load for column with load eccentricity (Chapman and Slatford)

considering the combined bending and axial stresses, and finding the reduced load necessary to produce unit maximum stress in the material. Although very approximate, these curves serve to illustrate the behaviour of masonry elements in compression and generally correspond with experimental results.

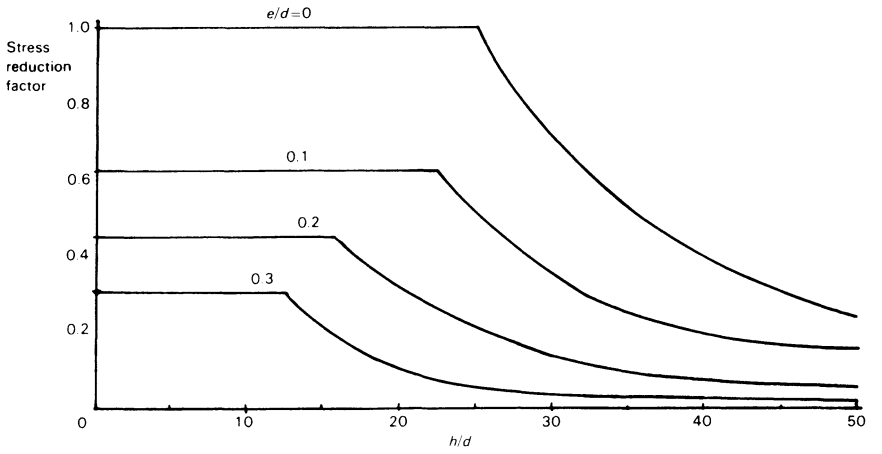

Figure 5.8 Stress reduction factors for pinned-end brickwork compression elements with various eccentricities of loading (Chapman and Slatford)

Angervo's solution to the differential equation for a pinned-end brittle column was based on linear and non-linear stress–strain curves, and Sahlin [12] extended the analysis to include for the possibility of the eccentricity at each end of the column being different.

Kukulski and Lugez [13] have overcome the difficulty of integrating the differential equation for a column with limited or no tensile strength by putting it in the form:

$$\frac{d^2e}{dx^2} = -\frac{\varepsilon_1 - \varepsilon_2}{d} \tag{5.7}$$

ε_1 and ε_2 are the strains in the extreme fibres of the section. If the stress–strain relationship for the material is known, it is possible to represent the variation of $\Delta\bar{\varepsilon} = \bar{\varepsilon}_1 - \bar{\varepsilon}_2$ as a function of the eccentricity ratio, $\bar{e} = e/h$, of the force acting on the section being considered for given values of the mean stress f_0. This stress divided by the compressive strength of the masonry f'_m may be represented by $\bar{f}_0$. On this basis, Kukulski and Lugez have obtained the curves shown in figure 5.9 for the relationship between $\Delta\bar{\varepsilon}$ and $\bar{e}$ for various values of $\bar{f}_0$, assuming the logarithmic stress–strain function in figure 5.10. The full line cutting off the $\bar{f}_0$ curves corresponds to the achievement of the ultimate strain in the material.

It will be seen that the $\bar{f}_0$ curves below 0.6 show a discontinuity which in fact corresponds to the point at which cracking of the section takes place. (In this example, tensile resistance to the extent of $0.15f'_m$ has been assumed.) The locus of such points is indicated by a chain broken line which becomes asymptotic to the $\bar{e}$ axis. In the absence of tensile strength this line would intersect the axis at $\bar{e} = 0.166$. Up to the cracking line, the $\bar{f}_0$ curves

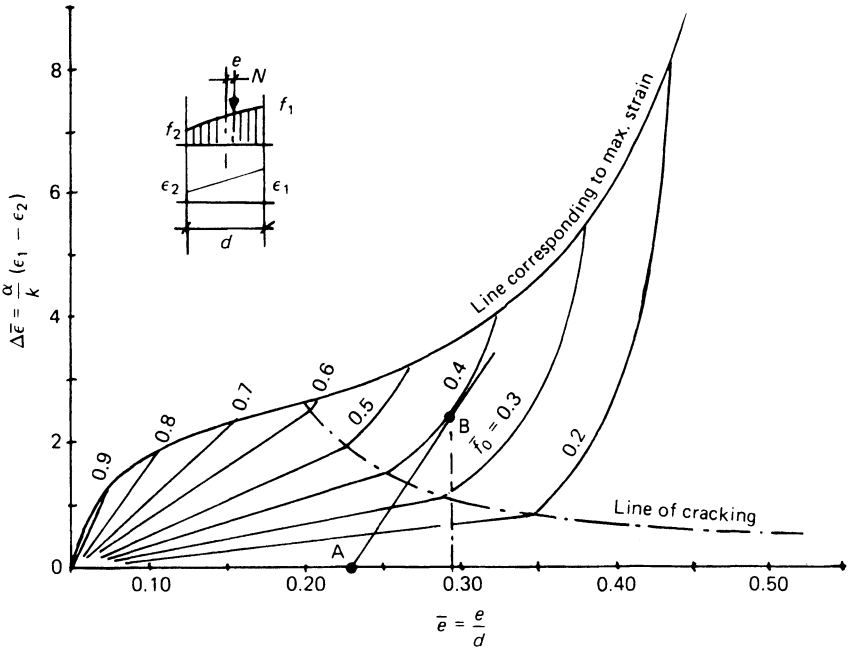

Figure 5.9 Variation of $\Delta\bar{\epsilon}$ against $\bar{e}$ in a rectangular section for various values of $\bar{f}_0 = f_0/f'_m$. Plotted for parameters $k = 1.1$ and $n = -0.15$ (see figure 5.10)

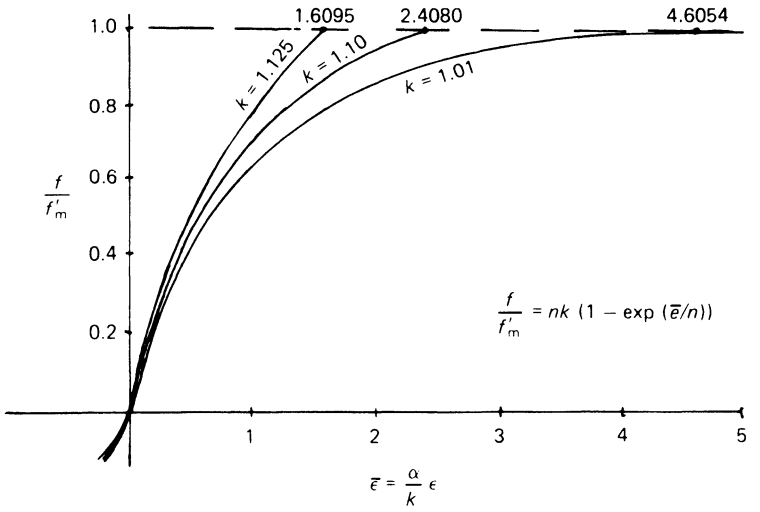

Figure 5.10 Assumed stress–strain relationship. Plotted for $n = 0.15$ and three values of k. $\alpha = E_0/f'_m$

are approximately linear. Beyond this, they may be represented by an equation of the form

$$\Delta\bar{\varepsilon} = \frac{1}{\left(a_1 - a_2\bar{e}\right)^2} \tag{5.8}$$

where a_1 and a_2 are constants which may be found for each value of $\bar{f}_0$, having regard to the coordinates of the curve at the cracking line and at the failure line.

Thus the following differential equations are obtained:

$$\text{For uncracked sections: } \frac{\mathrm{d}^2\bar{e}}{\mathrm{d}x^2} = -a\bar{e} \tag{5.9}$$

$$\text{For cracked sections: } \frac{\mathrm{d}^2\bar{e}}{\mathrm{d}x^2} = -\frac{1}{\left(a_1 - a_2\bar{e}\right)^2} \tag{5.10}$$

These equations can be integrated, with the introduction of the end eccentricities ($\bar{e} = \bar{e}_0$ at $x = \pm h/2$) and the eccentricity $\bar{e}_r$ corresponding to failure. This leads to the value of $\bar{f}_0$ at failure, which is the same as the capacity reduction factor, ϕ. This, however, does not take into account the possibility of buckling failure, which can be found from the curves of figure 5.9 in the following manner. If the end eccentricity ratio (at $x = \pm h/2$) in a slender wall is $\bar{e}_A$, then for $\bar{f}_0 = 0$ the eccentricity ratio at mid-height of the wall is also $\bar{e}_A$. As the load is increased, the variation of $\bar{e}_m$ is represented by a curve having positive slope (AB in figure 5.9). If at some point such as B this curve is a tangent to one of the $\bar{f}_0$ curves, a point of instability is defined, since, if $\bar{e}_m$ increases beyond B the corresponding value of $\bar{f}_0$ is reduced and, unless the load is reduced, collapse will take place.

From the above analysis Kukulski and Lugez have produced graphs of the slenderness reduction factor ϕ for a variety of cases, one of which is shown in figure 5.11. The base of the graph is the parameter $\lambda = l/(h\sqrt{\alpha})$ where $\alpha = E_0/f'_m$, E_0 being the tangent modulus of the material.

Kirtschig and Anstotz [14] have shown good agreement with tests on calcium silicate and lightweight aggregate masonry specimens with equal end eccentricities. The theory is, however, strictly valid only if equations (5.9) and (5.10) and the assumed stress–strain function correctly represent the characteristics of the material of the wall. This limitation could of course be overcome if numerical integration of appropriate functions for $\Delta\bar{\varepsilon}$ was used along with an experimentally determined stress–strain relationship.

Romano *et al.* [15] have also produced a solution of the differential equation for a masonry column based on non-linear stress–strain curves. Payne *et al.* [16] have developed a method of analysis combining finite element and finite difference procedures which has permitted investigation of the tensile strength of the brick units, non-linear behaviour of the mortar and deviations from initial straightness.

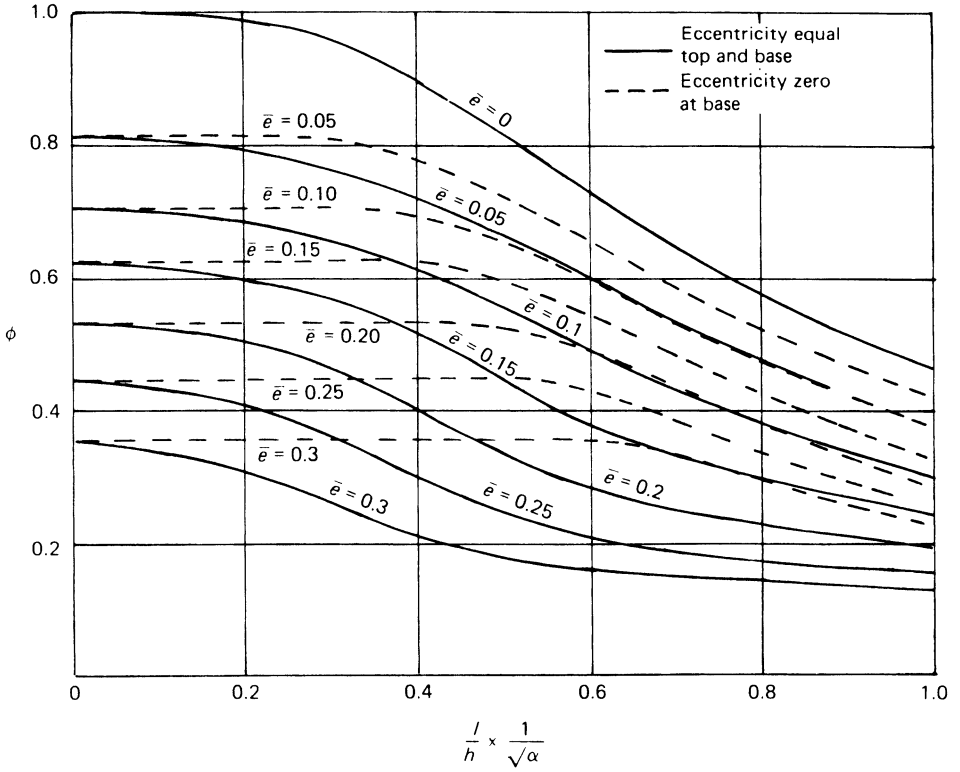

Figure 5.11 Slenderness/eccentricity reduction factors by theory of Kukulski and Lugez. Plotted for $k = 1.1$ and assuming tensile strength of masonry equal to 0.125 of compressive strength

5.3.2 *Solutions assuming deflection and stress–strain curves*

Haller's theory [4] is based on the assumption of a sinusoidal lateral deflection curve and a non-linear stress–strain relationship derived from tests on small masonry prisms. The solution is in less formal mathematical terms, and results in expressions for calculating the maximum load on the element which are rather less cumbersome than those resulting from the general solution of the differential equation. Haller's solution showed good agreement with experimental results, provided that an additional initial eccentricity of 1/1000 of the height of the test column was added to the eccentricity of the load. Although the experimental stress–strain curve used by Haller was very close to parabolic, the substitution of the latter relationship in Haller's calculation, rather surprisingly, appears to result in a considerable difference in the estimated mean failing stress as compared with that derived on the basis of the experimental curve.

Haller's theory related to specific masonry specimens and was not generalised; other investigators however, including Monk [17] and Turkstra [18] have derived general theories based on non-linear stress–strain relationships. The degree of non-linearity is defined by a factor $k = E_0\varepsilon'/f'_m$ where E_0 is the initial tangent modulus, f'_m the maximum stress and ε' the corresponding strain. Thus k is the ratio of the ultimate strain to the elastic strain at failure stress. These theories demonstrate (as did Sahlin's) that the wall strength is a function of a non-dimensional parameter $(h/d\sqrt{(f'_m/E_0)})$. Evaluation of wall strength at a given eccentricity of loading thus requires knowledge of three parameters of the stress–strain curve, namely f'_m, E_0 and k. The curves shown in figure 5.12, calculated by Turkstra, show the effect of variation in the parameter k with slenderness ratio, assuming a particular value of f'_m/E_0. Turkstra obtained reasonable agreement between test and theoretical results using values of $\sqrt{(E_0/f'_m)}$ of 15 and 19.4, and of k in the range 1.0–1.5. As shown in chapter 2 (page 46), accurately determined stress–strain curves indicate a second degree parabolic form, that is, $k = 2$, in which case, $E_0/f'_m = 2/\varepsilon'$. The maximum strain ε' is on average about 0.003, suggesting a value of the order of 24 for $\sqrt{(E_0/f'_m)}$. Monk in fact suggests values of 2 and 25.8 for these parameters and used these in deriving a set of design curves. Uncertainties concerning these parameters may

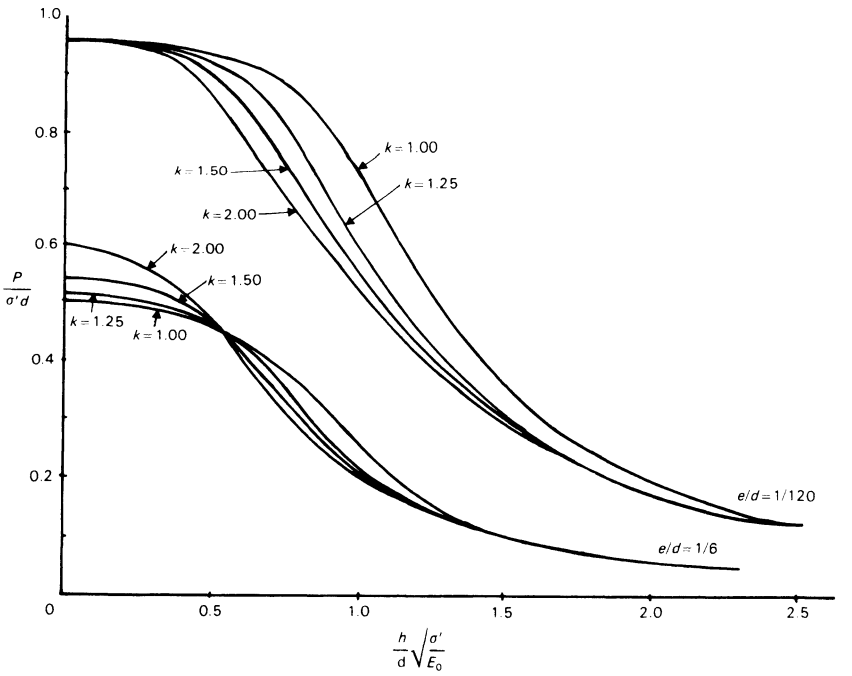

Figure 5.12 Effects of stress–strain relationships (Turkstra)

result in significant inaccuracies in the derived reduction factors, so that tests on specific materials may be required in applying these theories.

5.4 **Wall–floor slab interaction**

In the theories discussed above, it is assumed that the compression element under consideration has known end conditions and eccentricity of loading, whereas in an actual building these factors and the strength of a wall or column will be influenced by interaction between the members of the structure. Thus, as illustrated in figure 5.13, the rotation of the top of an eccentrically loaded wall will depend on the relative stiffness of the walls and floor slab, the loading conditions and the characteristics of the wall–floor slab connection. The slab-end moment will be generated by the wall loads, N_u and N_L in figure 5.13a, which will determine the slab-end rotation θ. In general, this will be greater than the rotation at the top of the wall below the joint since the latter will not be rigid. The usual assumption

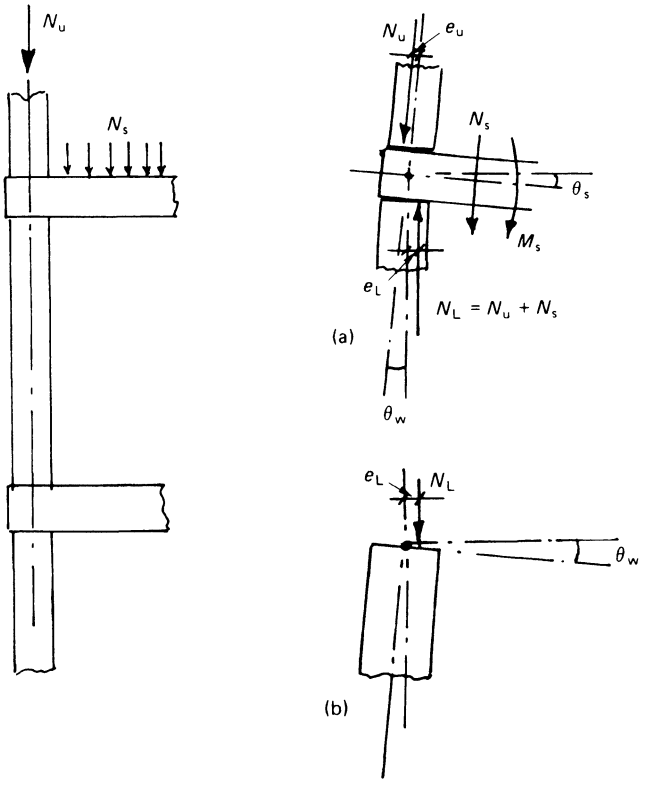

Figure 5.13 Wall–floor slab interaction

is to find the eccentricity of the load N_L (figure 5.13b) and to use this in calculating the wall strength, without regard to the angle of rotation at the top of the wall. However, the floor slab will restrain this rotation if the wall is tending to buckle, so that, in order to take into account wall–floor slab interaction, a solution is required for the strength of walls in which the rotation at the end of the wall is a variable in addition to the variables of load, eccentricity and member dimensions. The problem may be considered in two parts: (1) the strength of walls in terms of end rotation and eccentricity, and (2) the determination of eccentricities taking into account the characteristics of the wall–floor slab connection. The first of these will be considered in the following section and the second in chapter 6.

5.4.1 *Wall strength in terms of end rotation*

A number of solutions for this problem have been published. Sahlin [19], working from Angervo's solution of the differential equation for a brittle column, derived the set of parametric curves shown in figure 5.14, which connect the end rotation of a wall, the applied load and the eccentricity. These particular curves are for the case of zero eccentricity at the bottom of the wall. Superimposed on them in dimensionless terms are curves of constant edge stress so that it is possible, for a given load, to determine the maximum stress in the wall for known conditions of end rotation and eccentricity or the buckling load.

Risager [20] has produced a solution for walls compressed between floor slabs with equal angles of rotation at the ends, based on consideration of an equivalent column having a parabolic deflected form, as indicated in figure 5.15. Using the notation shown in this diagram, the deflection, y, of the column of length H_s between points of inflection is

$$y = 4y_c \frac{x}{H_s}\left(1 + \frac{x}{H_s}\right) \tag{5.11}$$

where y_c is the maximum deflection of the equivalent column and x is the distance along the load axis, measured from the point of inflection. The eccentricity and angle of rotation at the level of the lower surface of the floor slab are then, respectively

$$e = 4y_c \frac{S}{H_s}\left(1 - \frac{S}{H_s}\right) \tag{5.12}$$

and

$$\theta = 4\frac{y_0}{H_s}\left(1 - \frac{2S}{H_s}\right) \tag{5.13}$$

Introducing the following parameters

$$\varepsilon = \frac{e}{d/2} \qquad \Omega = \frac{H}{d}\theta \qquad \Phi = \frac{H}{d}\theta$$

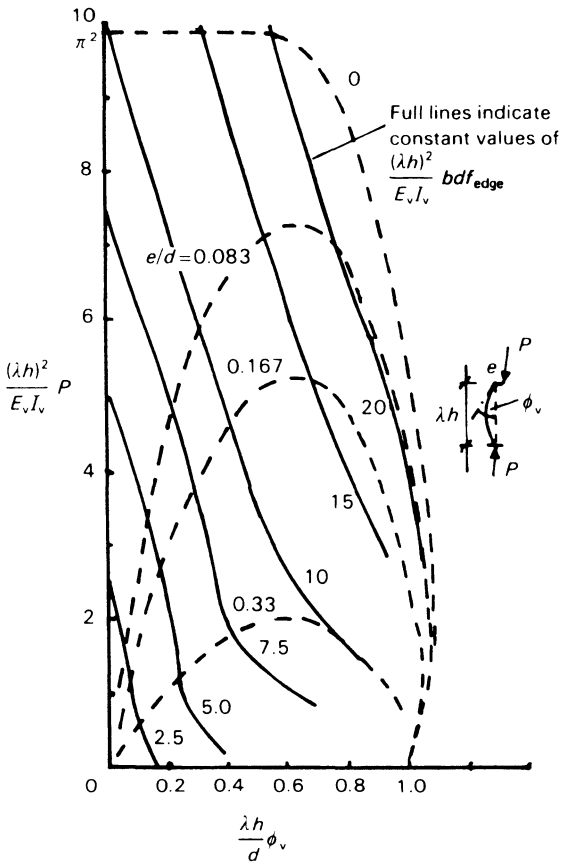

Figure 5.14 Interrelationship between load in a brittle column and angle of rotation of its upper end. Load is eccentric at top and axial at base (after Sahlin)

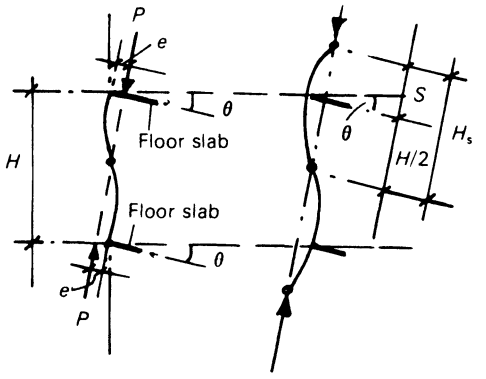

Figure 5.15 Equivalent column in Risager's analysis

it can be shown from equations 5.12 and 5.13 that

$$\Phi = \Omega\left(\frac{1}{1-2\dfrac{S}{H}}\right) = \frac{4y_c}{d/2}\,\frac{1}{\left(1+2\dfrac{S}{H}\right)^2} \tag{5.14}$$

and

$$\varepsilon = 2\Phi\frac{S}{H} \tag{5.15}$$

Consideration of the stresses in a column of rectangular section without tensile stress shows that the edge stress is

$$\sigma_{max} = \frac{2}{3}\frac{P}{b(d/2-e)} \tag{5.16}$$

and the curvature

$$\varkappa = \frac{2}{9}\frac{P}{Eb(d/2-e)^2} \tag{5.17}$$

Introducing the further parameters

$$\Psi = 7.2\left(\frac{d}{H}\right)^2\frac{E}{f'_m} \tag{5.18}$$

$$\nu = \frac{P}{bdf'_m} \tag{5.19}$$

Risager established the formulae shown in table 5.1, from which the bearing capacity, crack condition, mode of failure, eccentricity and end moments can be determined for a given column, provided that the angle of rotation at its end is known.

A similar analysis has been developed by Colville [21, 22], who extended it to include walls in single and double curvature and with several combinations of end eccentricity. This solution resulted in parametric curves of $f(P) - f(\theta)$, similar to those derived by Sahlin. The results of Colville's analysis have been found to compare reasonably well with those obtained experimentally.

Thurlimann and Schwartz [23] have obtained a solution for this problem leading to a design graph from which both ultimate and serviceability limit states can be assessed. They start with the following equation relating the curvature, of a cross-section (ϕ), under a constant normal force (N), to the deflection (w) of the wall:

$$\phi = -\frac{d^2w(x)}{dx^2} \tag{5.20}$$

Table 5.1 Formulae for bearing capacity and eccentricity (Risager)

Zone	*Bearing capacity*	*Eccentricity*
I	$\nu = 1 - \frac{1}{3}\Phi\Psi$	$\varepsilon = \frac{2}{3}\Phi\sqrt{\left(\frac{3\Psi}{3 - \Phi\Psi}\right)} - \Phi$
II	$\nu = \frac{3}{4}\frac{1}{\Phi}\frac{1}{\Psi}$	$\varepsilon = 2\sqrt{\left(\Phi - \frac{1}{\Psi}\right)} - \Phi$
III	$\nu = \frac{4}{9}\Psi$	$\varepsilon = 0$
IV	$\nu = \frac{1}{64}\Phi\Psi(4 - \Phi)^2$	$\varepsilon = 0$

Mode of failure Zones I and II: stress failure. Zones III and IV: buckling.
Wall section Zones I and III: uncracked. Zones II and IV: cracked.

Taking $w(x) = e(x)$ and introducing a reference eccentricity e_0 equation (5.20) can be rewritten as

$$-\frac{d^2\eta(x)}{dx^2}e_0 = \phi(\eta) \tag{5.21}$$

where $\eta(x) = e(x)/e_0$. This equation represents the non-linear differential equation of the deflection $w(x) = \eta(x)e_0$. A solution to this equation has been obtained by assuming that the non-dimensional eccentricity η and the curvature ϕ are related by the equation

$$\phi(\eta) = \frac{2Ne_0}{(EI)_0\pi}\tan\left(\frac{\pi}{2}\eta\right)\left[1 + \tan^2\left(\frac{\pi}{2}\eta\right)\right] \tag{5.22}$$

where $(EI)_0$ is the initial flexural stiffness of the cross-section with (N, ϕ = 0). This leads to the solution of equation (5.21):

$$\eta(x) = \frac{2}{\pi}\sin^{-1}\left[\sin\left(\eta_m\frac{\pi}{2}\right)\sin\left(\frac{\pi x}{l}\right)\right] \tag{5.23}$$

where

$$l = \pi\left[(EI)_0/N\right]^{1/2}\cos\left(\eta_m\frac{\pi}{2}\right)$$

Equation (5.23) defines a family of column deflection curves, the parameter η_m being the non-dimensional eccentricity at $x = l/2$, and l the half-wavelength of the deflection curve. It will be noted that when η_m tends to

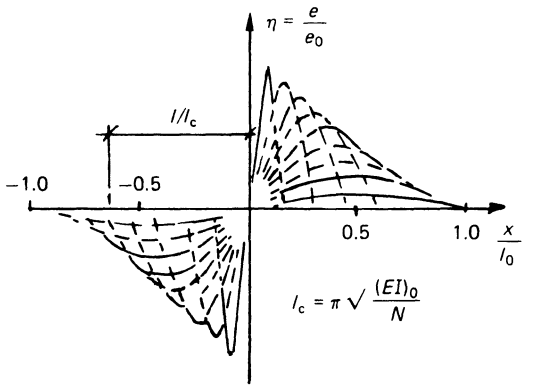

Figure 5.16 Column deflection curves for non-linear stress–strain relationship (Thurlimann and Schwartz)

zero, the η–ϕ relationship becomes linear and the deflection curve tends towards a sine wave, that is, the solution reduces to the case of elastic buckling. If the eccentricity e_m tends towards e_0, the half-wave tends towards two linear segments. These points can be seen from the curves shown in figure 5.16.

Having obtained the family of column deflection curves, it remains to relate these to the end rotation. This is achieved in the manner indicated in figure 5.17a which shows a wall loaded by a force N which has eccentricities of zero and e_u at top and bottom, respectively. Figure 5.17b shows a family of deflection curves for this case in relation to the member, and figure 5.17c the position of one of the curves which fits the specified eccentricities. The angle of rotation of the wall is then $\theta = e_u/h$. For a given value of N, the $\eta_u = e_u/e_0 - \theta$ relationship can be obtained from the corresponding family of deflection curves, as illustrated for a particular case in figure 5.18a. These curves have been shown to agree closely with the results of tests in which the end rotation of walls under constant end load, applied at various eccentricities, has been increased up to the point of failure.

The η_u–θ curves have been presented in generalised form for design purposes (figure 5.18b) by replacing η_u by $M_{w_0} = M_w/N_c e_0$ where $N_c = \pi^2(EI)_0/h^2$ and θ by $\theta_0 = l_c/e_0\theta$. Curves are shown for several values of the parameter $N_0 = N/N_c$. This design approach is based on the assumption that the eccentricity–curvature curves are affine with respect to the η-axis.

5.5 **Semi-empirical methods**

An alternative approach to the calculation of the compressive strength of masonry elements allowing for the effects of slenderness and eccentricity makes use of formulae associated with the names of Rankine, Ritter and

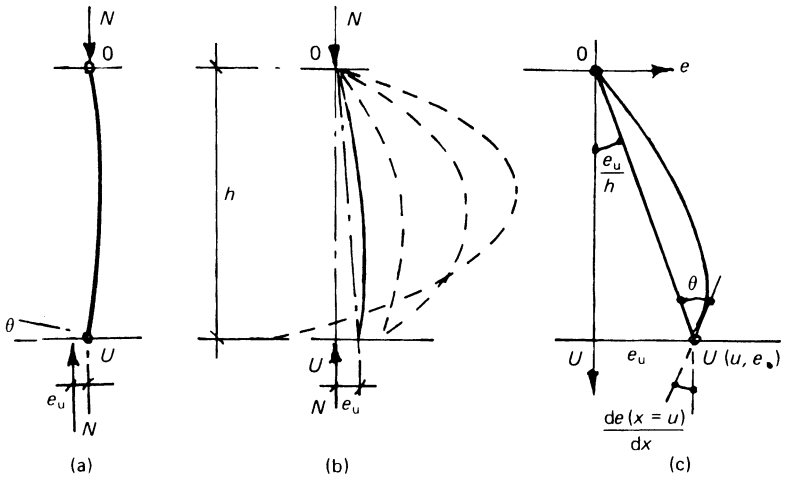

Figure 5.17 Determination of η–θ relationship

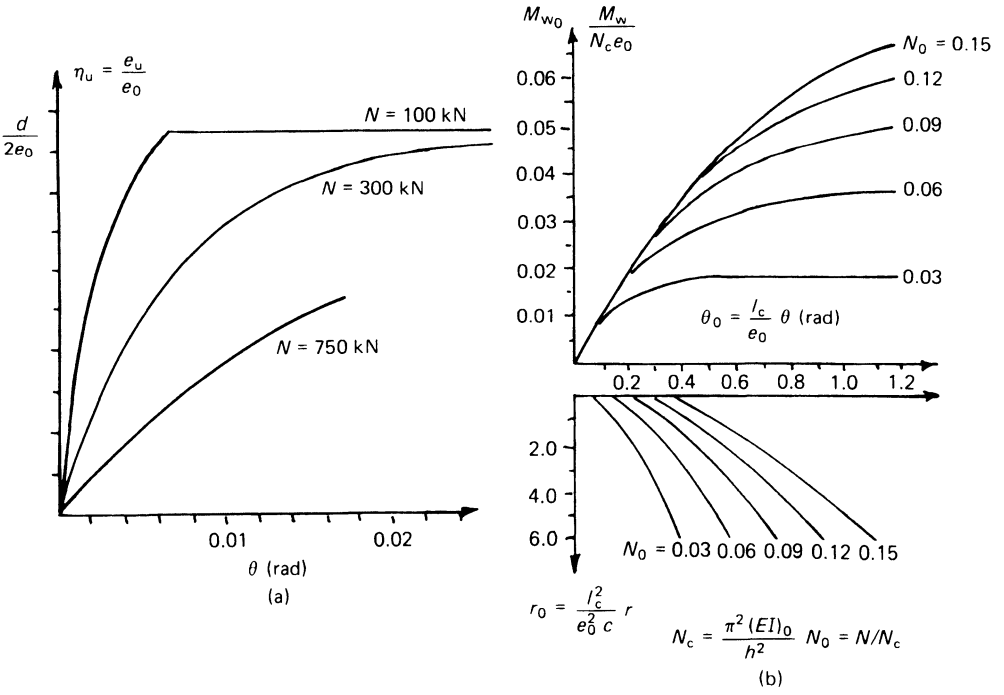

Figure 5.18 (a) Example of η_u against θ relationship. (b) Design curves for compressive strength of masonry walls related to end rotation (Thurlimann and Schwartz)

other earlier writers. The basis of these formulae is the assumption of a linear relationship between the ratios σ/f_c and σ/f_e where σ, f_c and f_e are respectively the applied compressive stress, the compressive strength of the material and the stress corresponding to the Euler buckling load. This results in an equation of the form:

$$\frac{\sigma}{f_c} = 1 - \frac{\sigma}{f_e} \tag{5.24}$$

Starting from this equation, Morton [24] has derived the following capacity reduction factor applicable to eccentricities within the core of the section:

$$\beta^* = \frac{1}{n/m + f_c/f_e} \tag{5.25}$$

where $n = 1 + (e \cdot \bar{y}/r^2)$ in which e is the eccentricity, $\bar{y}$ the distance of the extreme fibre from the neutral axis and r the radius of gyration of the section; m is a factor, suggested equal to 1.1, to allow for the apparent increase in compressive strength in bending and f_e is the Euler buckling stress. Morton adopts a value of E in calculating the Euler stress related to the characteristic strength of the masonry, suggesting $900f_k$ as being normally appropriate. He has extended the theory to apply to larger eccentricities where the section would be cracked and indicates its applicability to sections other than rectangular.

A similar approach, used in the Danish code of practice for masonry, has been described by Knutsson [25] but in this case a modified value of the elastic modulus is adopted to allow for the non-linear stress–strain relationship of the material:

$$E = E_0\left(1 - \sigma/f_c\right)$$

where E_0 is the tangent modulus at low stress levels and f_c is the compressive strength.

Both these authors demonstrate good agreement between theoretical and experimental results, and the method has the advantage of being easily understood and resulting in strength formulae that are much less cumbersome than those derived by more rigorous theories.

A fundamentally similar approach [26–28] is the 'moment magnifier' method used extensively in North America for masonry and for steel and reinforced concrete columns. In this method an interaction curve defining the strength of a short compression member subject to axial load and bending moment is first derived. This curve has the form indicated in figure 5.19 in which the vertical axis is in terms of the applied load P divided by the ultimate load, P_0, which the section can resist in the absence of bending, that is, the maximum axial load for failure. On the horizontal axis the applied moment M is divided by the moment capacity, M_k, when a load is applied at the end of the middle third, that is, at an eccentricity of $d/6$. The stress

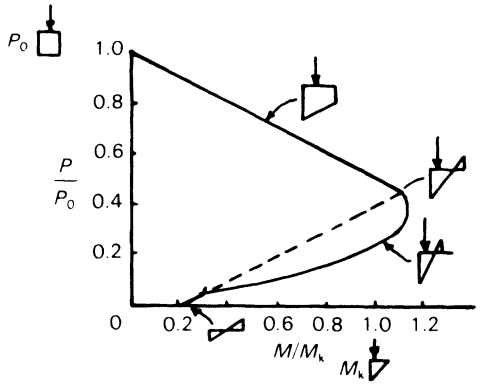

Figure 5.19 Axial load–moment interaction curve

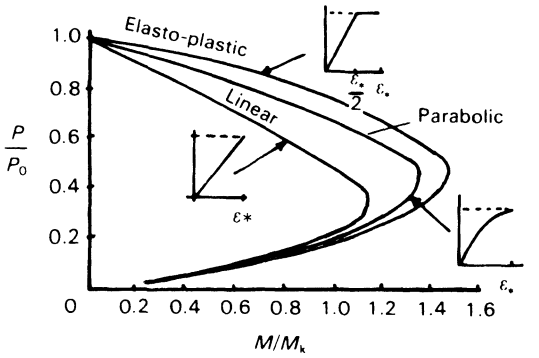

Figure 5.20 Effect of stress–strain relationship on axial load–moment interaction (Turkstra)

conditions associated with the various portions of the interaction curve are also shown. The curve in figure 5.19 is based on the assumption that the ultimate tensile strength is equal to 0.1 of the compressive strength; if, as is usual, the tensile strength is neglected, the interaction curve will pass through the origin. Turkstra and Ojinaga [26] have demonstrated the effect of different idealised stress–strain curves, assuming the same ultimate strain in each case, with the results shown in figure 5.20. Formulae for the calculation of the interaction curve for a solid rectangular section are given in table 5.2.

End conditions and slenderness are allowed for by introducing a 'moment magnifier'

$$L = \frac{C_m}{1 - P/P_e} \tag{5.26}$$

Table 5.2 Formulae for interaction curves for solid rectangular masonry sections

For an uncracked section	For a cracked section (zero tensile strength)
$M_e = \frac{2}{Ad}(Ap_0 - P)$	$M_e = \frac{Pd}{2}\left(1 - g\frac{P}{aP_0}\right)$
The cracking line is given by	$g = 2\left(1 - \frac{4I}{Ad^2}\right)$
$M_k = P_k e_k$	$P_k = \frac{aP_0}{2}$
	$e_k = \frac{2I}{Ad}$
	$P_0 = Af'_m$

where M_e is the maximum moment capacity
P compressive force on the section
A area of cross-section
I moment of inertia of the section based on the uncracked section
a flexural compressive strength coefficient
d section thickness
f'_m compressive strength of the brickwork.

in which C_m is a correction factor depending on the moment distribution in the element, and is intended to give the equivalent uniform moment in the column that would lead to the same long column strength as the actual moment diagram. P_e is the Euler critical load taking into account the effective height of the compression member. The application of the moment magnifier will be understood by reference to figure 5.21. Figure 5.21a shows a pinned column which carries a load P at an initial eccentricity e at each end. If the maximum eccentricity is Δ, the corresponding bending moment is

$$P(e + \Delta) = Pe \frac{1}{1 - P/P_e} \tag{5.27}$$

In this case $C_m = 1$ and $P_e = \pi^2 EI/h^2$.

If the moments at the lower and upper ends of the column are M_1 and M_2, respectively, the correction factor C_m is given by

$$C_m = 0.6 + 0.4M_1/M_2 \geq 0.4 \tag{5.28}$$

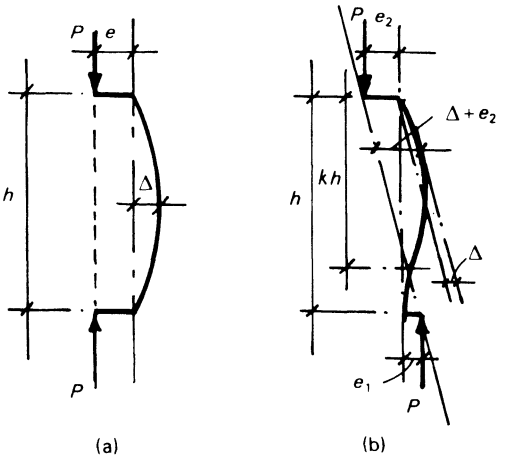

Figure 5.21 Moment magnifier method: (a) equal end eccentricities; (b) general case – eccentricities at column ends

The ratio of the moments is positive if the column is bent in single curvature, and in this case

$$P_e = \pi^2 EI/(kh)^2$$

where kh is the effective length.

Calculation of EI presents certain problems, as the stress–strain relationship is non-linear, and the value of I may be reduced by cracking of the section. The following empirical relationship has been suggested [28] for calculating the flexural rigidity of a masonry element

$$EI = E_0 I_n \left(0.2 + \frac{P}{P_e}\right) \leq 0.7 E_0 I_n \tag{5.29}$$

where E_0 is the initial tangent modulus, and I_n the moment of inertia of the uncracked section.

As mentioned in relation to Morton's adaptation of the Rankine formula, it has been found that the apparent flexural compressive strength of masonry specimens calculated on the basis of a linear stress distribution is consistently greater than the prism strength. Morton proposed an enhancement factor of 1.1 while Fattal and Cataneo [28] have given values between 1.3 and 1.4 at eccentricities between $t/12$ and $t/4$ falling to 1.18 at $t/3$.

5.6 **Special wall types**

5.6.1 *Cavity walls*

Cavity wall construction is frequently used for the outer walls of buildings in order to achieve a higher degree of weather protection and thermal

insulation than would be obtained from a solid wall of the same material thickness. Experiments [29] have shown that, for practical purposes, the inner leaf of a multi-storey cavity wall transmits by far the larger proportion of the loading from floors above, even when the floor slabs are carried through the thickness of the wall. In considering the strength and stability of a cavity wall, it will therefore be appropriate to assume that the structural effect of the outer leaf will be to stabilise the inner leaf, provided that the ties between them are sufficiently stiff, and it has been found [30] that twisted wire ties will not produce this strengthening effect.

If, however, the ties are sufficiently stiff to ensure that the two leaves deflect laterally to the same extent, thus doubling the effective stiffness of the loaded leaf, the theoretical buckling load for the leaf of a cavity wall will be twice that of a single leaf wall of the same thickness, but under eccentric loading a crack will develop in the unloaded leaf at a relatively low load. The maximum tensile stress in this leaf is given by

$$f_{ol} = \frac{3f(e/d)}{(1 - f/2f_e)} \tag{5.30}$$

where $f = P/bd$ and f_e is the Euler buckling stress.

The edge stresses in the inner leaf are given by

$$f_{il} = -f \pm \frac{3f(e/d)}{(1 - f/2f_e)} \tag{5.31}$$

The relative cracking loads for solid and cavity walls have been calculated by Sahlin [31] and are shown in figure 5.22.

The effect of cracking in the outer leaf has been discussed by Jensen [32] in relation to the following formula for the effective thickness of a cavity wall:

$$t_{th} = \sqrt[3]{\left(t_1^3 + k\frac{E_2}{E_1}t_2^3\right)}$$

where t_1, E_1 and t_2, E_2 are respectively the thickness and elastic modulus of the inner and outer leaves. The factor k lies between 1 and 0, being 1 if the outer leaf is uncracked and 0 if each and every joint is cracked. This is a useful concept but too few results are available from which to determine specific values of k.

5.6.2 *Stiffened walls*

Theoretical and experimental studies of wall strengths have generally been limited to consideration of rectangular cross-sections. However, many walls in practical situations are stiffened by piers, or returns, and recently interest has developed in the use of walls with fins or of cellular construction [33–36] as indicated in figure 5.23.

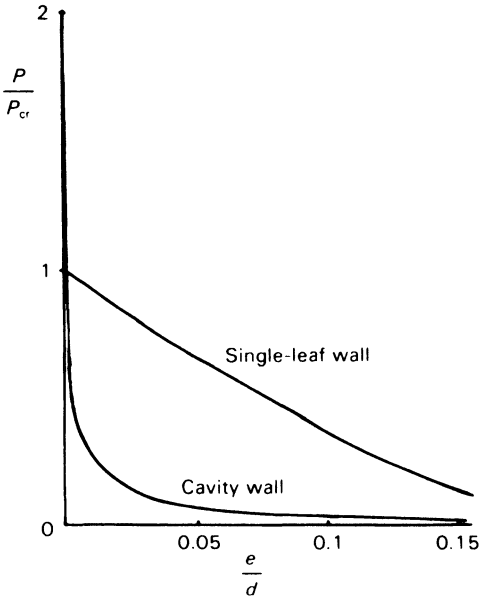

Figure 5.22 Cracking loads of single-leaf and cavity walls related to the Euler load for a single leaf (Sahlin)

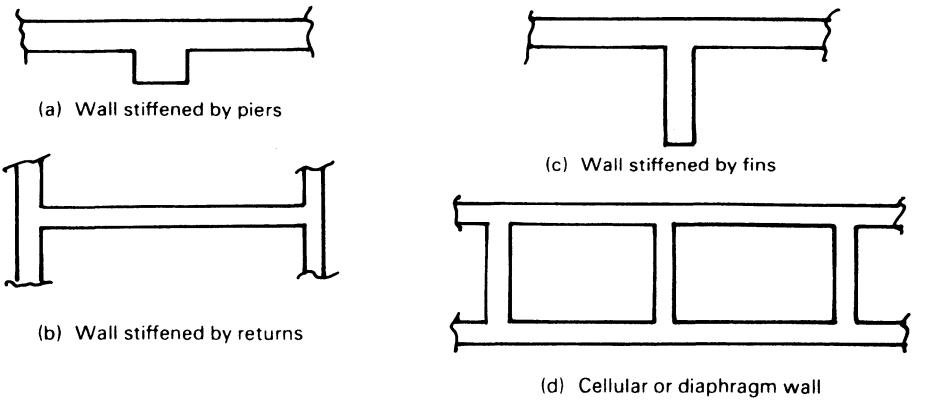

Figure 5.23 Cross-sections of stiffened walls

In principle, it would be rational to consider the compressive strength of such elements by calculating their slenderness ratios on the basis of their overall radii of gyration [37]. The strength and stability of the individual sections of wall, and the integrity of the bond between them, may however be more critical, so that information about the behaviour of brickwork panels with stiffened edges is of importance. No theoretical solution for this

problem appears to exist, but there are some experimental results [38] from tests on axially loaded walls with returns on both vertical edges. The results of these tests, some of which are summarised in table 5.3, led to the following conclusions:

(1) Walls stiffened along their vertical edges by returns did not show increased strength as compared to strip walls, up to a slenderness

Table 5.3 Test results of axially loaded strip walls and walls stiffened along their vertical edges by returns

Test no.	*Height/ length*	*Slenderness ratio*	*a* *Failure stress for strip wall (N/mm^2)*		*b* *Failure stress for walls with returns (N/mm^2)*	*Strength of walls with returns* / *Strength of strip walls (b/a)*
1	1.3	24	10.8	9.2	9.9	1.1
2	1.3	24	7.65		10.9	1.2
3	1.0	24	8.13		8.86	1.08
4	1.0	24			8.86	1.0
5	1.4	8	10.84	11.19	10.24	0.91
6	1.4	8	11.55		9.8	0.87
7	0.8	8	11.2		11.0	0.98
8	0.8	8			10.56	
9	2.8	16	11.15	11.15	10.7	0.96
10	2.8	16	11.15		10.7	
11	1.6	16	11.15		9.30	0.83
12	1.6	16			9.72	0.87
13	5.6	32	9.07	9.35	9.89	1.05
14	5.6	32	9.62		8.50	0.91
15	3.12	32	9.35		7.9	0.85
16	3.12	32			9.2	0.98
17	2.06	32	9.35		7.24	0.77
18	2.06	32			9.08	0.97
19	1.3	24	12.0	14.5	10.6	0.73
20	1.3	24	17.0		9.4	0.65
21	1.0	24			10.0	0.60
22	1.0	24	20.3	16.6	15.0	0.90
23	1.0	24	12.94		11.8	0.71
24	1.0	24			17.7	1.10
25	1.0	24			15.0	0.90

1 to 4: walls built with $\frac{1}{3}$ scale brick
17 to 18: walls built with $\frac{1}{2}$ scale brick
19 to 23: full-scale walls
Return walls not loaded
5 to 16: walls built with $\frac{1}{2}$ scale brick
24 to 25: full-scale wall
Return walls loaded

ratio of 32. It would appear therefore, that up to this limit, no increase in the bearing capacity of axially loaded walls should be made on account of their edges being stiffened by bonded returns. This conclusion holds whether or not the returns are loaded to the same extent as the main wall.

(2) Before cracking and separation of returns, the central deflections of walls with returns are smaller than those of corresponding strip walls, which indicates effective stiffening up to this point. This stiffening effect decreases with increasing aspect ratio.

(3) As returns provide effective stiffening at low axial loads, they may be effective in increasing the strength of very slender walls that may be expected to show buckling rather than strength failures.

(4) Where only the main wall was loaded, about 6 per cent of the total applied load was transferred to each of the returns. The average ultimate vertical shear stress which destroyed the bond between the main wall and returns varied between 0.35 and 0.68 N/mm^2, calculated on an area equal to the height times the thickness of the main wall.

The compressive strength of masonry columns having non-rectangular cross-sections has been investigated by Phipps *et al.* [39, 40]. Figure 5.24

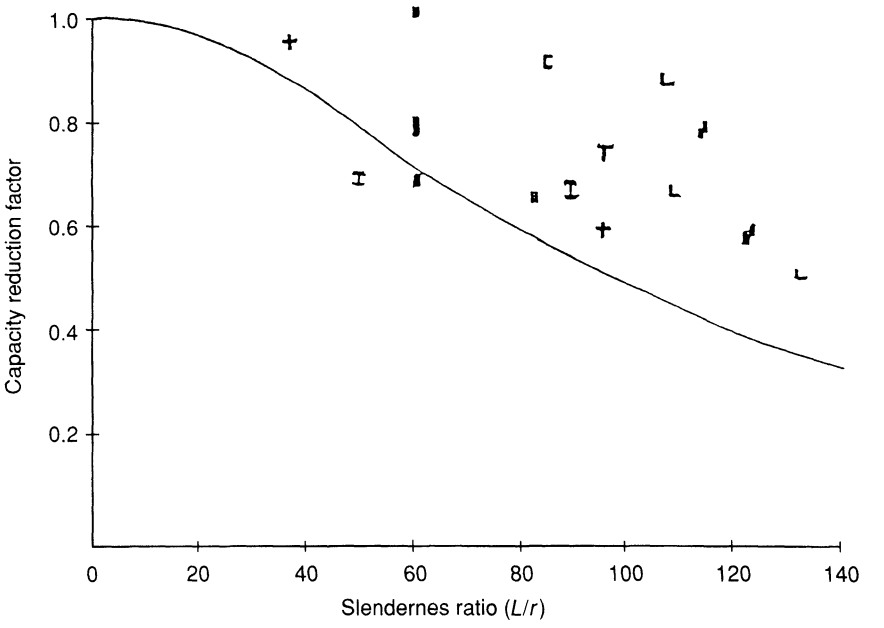

Figure 5.24 Capacity reduction factors (ratio of failure stress to prism strength) for masonry columns tested by Phipps *et al.* compared with Rankine/Morton formula. Symbols are indicative of specimen cross-sections

has been derived from some of the large number of test results and shows the ratio of the failure stress to the prism strength of the material plotted against the slenderness ratio, height/radius of gyration. All the points refer to pinned end columns with axial load.

Also shown is the reduction factor given by the Morton/Rankine theory (equation 5.25) assuming zero eccentricity. There is a considerable scatter of results but no greater than has been found in tests on rectangular section columns and walls (see for example figure 5.1, page 92). There does not appear to be any systematic difference as between the different cross-sections tested, which included rectangular, cruciform and I types and in brick and block.

Phipps *et al.* have shown that it is possible to compute the failure strength of the various columns using experimental values for materials properties but no general solution is available. However, it would appear that the Morton/Rankine reduction factors could be safely applied to non-rectangular sections with nominally axial loading. Phipps [41] has also proposed the use of the empirical formula given in the British Code of Practice BS 5628 Part 1 [42], with suitable modification. This formula is based on the assumption of a rectangular stress block at failure and no

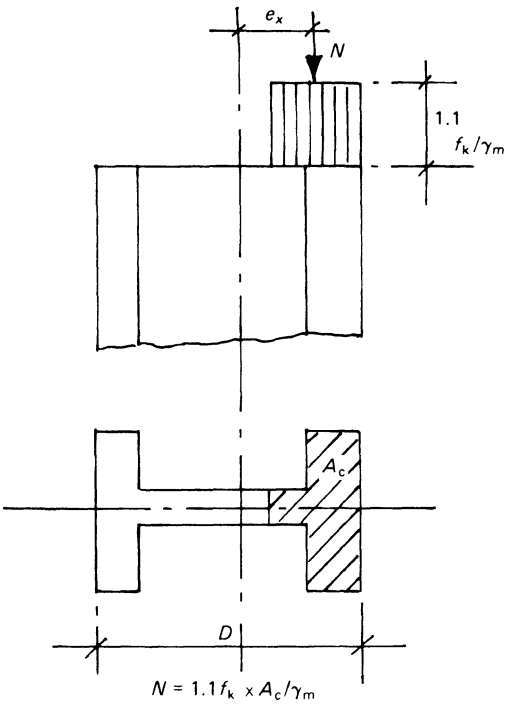

Figure 5.25 Eccentric load on non-rectangular section at design load for ultimate limit state

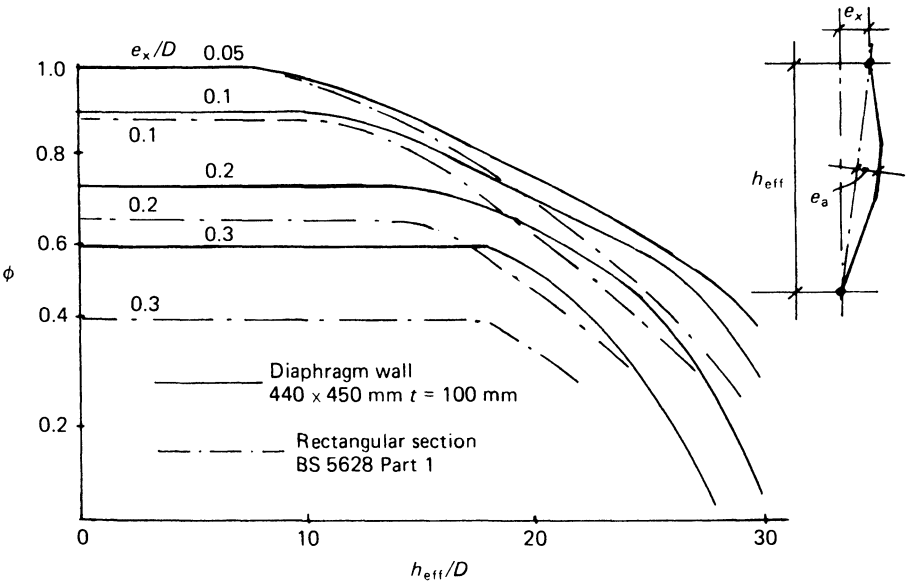

Figure 5.26 Slenderness/eccentricity reduction factors for a diaphragm wall by BS 5628 method (Phipps)

tensile resistance, as shown in figure 5.25. Second-order lateral deflection is assumed to be given by the equation:

$$e_x = D\left(\left[1/2400 \times h_{eff}/D\right]^2 - 0.015\right) \tag{5.32}$$

where D is the overall depth of the section as indicated in figure 5.25. This deflection is constant over the central fifth of the wall height and varies linearly from e_x at the top of the wall to zero at the bottom (figure 5.25). On this basis, Phipps has calculated the capacity reduction factors for a typical diaphragm wall shown in figure 5.26. The corresponding factors for a rectangular section are shown for comparison.

Allowance for slenderness and eccentricity could also be made using the moment-magnifier method although rather tedious calculatious would be required to construct the required interaction diagrams for non-rectangular sections.

References

1. C. B. Monk, 'A Historical Survey and Analysis of the Compressive Strength of Brick Masonry', *Research Report No. 12* (Structural Clay Products Research Foundation, Geneva, Ill., 1967).
2. N. Davey and F. G. Thomas, 'The Structural Use of Brickwork', *Structural Paper No. 24* (Institution of Civil Engineers, London, 1950).

3. F. G. Thomas, 'The Strength of Brickwork', *Struct. Engr.*, **31** (1953) 35–46.
4. P. Haller, 'Load Capacity in Brick Masonry', in *Designing, Engineering and Constructing with Masonry Products*, ed. F. B. Johnson (Gulf, Houston, Tex., 1969), pp. 129–49.
5. 'Compressive, Transverse and Racking Strength of Four-inch Brick Walls', *Research Report No. 9* (Structural Clay Products Research Foundation, Geneva, Ill., 1965).
6. 'Compressive and Transverse Strength Tests of Eight-inch Brick Walls', *Research Report No. 10* (Structural Clay Products Research Foundation, Geneva, Ill., 1966).
7. 'Compressive and Transverse Tests of Five-inch Brick Walls', *Research Report No. 8* (Structural Clay Products Research Foundation, Geneva, Ill., 1965).
8. S. S. Hasan and A. W. Hendry, 'Effect of Slenderness and Eccentricity on the Compressive Strength of Walls', *Proceedings of the Fourth International Brick Masonry Conference* (Brugge) 1976, Paper 4.d.3.
9. N. Royen, 'Knickfestigkeit exzentrisch beanspruchter Säulen aus Baustoff der nur gegen Druck widerstandsfähig ist', *Bauingenieur*, **18** (1937) 444.
10. K. Angervo, 'Uber die Knickung und Tragfähigkeit eines exzentrisch gedrucken Pfeilersohne Zugfestigkeit', *Publication 26* (Staatliche Technische Forschungsanstalt, Helsinki, 1954).
11. J. C. Chapman and J. Slatford, 'The Elastic Buckling of Brittle Columns', *Proc. Instn Civ. Engrs.*, **6** (1957) 107–25.
12. S. Sahlin, 'Diagrams of Critical Stress for Columns of Material without Tensile Strength', *Report No. 16/25* (Swedish National Institute for Building Research, Stockholm, 1965).
13. W. Kukulski and J. Lugez, 'Résistance des Murs en Béton non Armé soumis à des Charges Verticales', *Cahier CSTB no. 681* (1966).
14. K. Kirtschig and W. Anstotz, 'Buckling Tests on Masonry', *Proceedings of the Ninth International Brick/Block Masonry Conference* (Berlin) 1991, pp. 202–9.
15. F. Romano, S. Ganduscio and G. Zingone, 'Stability of Masonry with Non-linear Stress–Strain Relationship', *Masonry International*, **6** (2) (1992) 69–74.
16. D. C. Payne, D. S. Brooks and G. Sved, 'The Analysis and Design of Slender Brick Walls', *Masonry International*, **4** (2) (1992) 55–65.
17. C. B. Monk, 'Column Action of Clay Masonry Walls', in *Designing, Engineering and Constructing with Masonry Products*, ed. F. B. Johnson (Gulf, Houston, Tex., 1969), pp. 161–70.
18. C. J. Turkstra, 'The Capacity of Masonry Walls under Eccentric Vertical Loads', *Structural Mechanics Series No. 71-3* (Structures Laboratory, McGill University, Montreal, 1971).
19. S. Sahlin, *Structural Brickwork* (Prentice-Hall, Englewood Cliffs, N.J., 1971), pp. 91–116.
20. S. Risager, 'Structural Behavior of Linear Elastic Walls having No Tensile Strength', in *Designing, Engineering and Constructing with Masonry Products*, ed. F. B. Johnson (Gulf, Houston, Tex., 1969), pp. 257–66.
21. J. Colville, *Analysis and Design of Brick Masonry Walls* (Dept. of Civil Engineering, University of Edinburgh, 1977).
22. J. Colville, 'Simplified Design of Load Bearing Brick Masonry Walls', *Proc. Br. Ceram. Soc.*, **27** (1978) 217–34.

23. B. Thurliman and J. Schwartz, 'Design of Masonry Walls and Reinforced Concrete Columns with Column Deflection-Curves', *I.A.B.S.E.*, **P-108** (1987) 17–24.
24. J. Morton, 'An Alternative Approach to Reduction Factors for the Design of Solid Masonry Walls', *Proceedings of the Ninth International Brick/Block Masonry Conference* (Berlin) 1991, pp. 758–66.
25. H. F. Knutsson, 'Vertical Load Bearing Masonry – The Danish Approach', *Masonry International*, **5** (1) (1991) 23–6.
26. C. Turkstra and J. Ojinaga, 'The Moment Magnifier Method Applied to Brick Walls', *Proceedings of the Fourth International Brick Masonry Conference* (Brugge) 1976, Paper 4.b.3.
27. R. G. Drysdale and S. E. A. Sallam, 'Design of Masonry Walls and Columns for Combined Axial Load and Bending Moment', *Proceedings of the First Canadian Masonry Symposium* (Calgary) 1976, pp. 394–408.
28. S. G. Fattal and L. E. Cattaneo, 'Structural Performance of Masonry Walls under Compression and Flexure', *Building Science Series 73* (National Bureau of Standards, Washington, D.C., 1977).
29. B. P. Sinha, A. H. P. Maurenbrecher and A. W. Hendry, 'An Investigation into the Behaviour of a Five Storey Cavity Wall Structure', *Proc. Br. Ceram. Soc.*, **24** (1975) 147–60.
30. G. J. Edgell, 'The Compressive Strength of Cavity Walls Containing Butterfly Wire Ties', *Proceedings of the British Masonry Society*, **6** (1994) 126–9.
31. S. Sahlin, *Structural Masonry* (Prentice-Hall, Englewood Cliffs, N.J., 1971), pp. 183–91.
32. H. E. Jensen, 'Strength Tests on Lightweight Concrete Walls with Masonry Veneer Leaves', *Proceedings of the British Masonry Society*, **6** (1994) 40–3.
33. W. G. Curtin and G. Shaw, *Brick Diaphragm Walls in Tall Single-storey Buildings* (Brick Development Association, London, 1977).
34. W. G. Curtin, G. Shaw, J. K. Beck and W. A. Bray, *Design of Brick Fin Walls in Tall Single-storey Buildings* (Brick Development Association, Windsor, 1980).
35. G. Shaw and J. K. Beck, 'Design of Concrete Masonry Diaphragm Walls', *Concrete Soc. Tech. Report No. 27* (1985).
36. M. E. Phipps and T. I. Montague, *The Design of Concrete Blockwork Diaphragm Walls* (Aggregate Concrete Block Association, Leicester, 1987).
37. F. Sawko and W. G. Curtin, 'Effective Thickness and Structural Efficiency of Cellular Walls and Piers', *Proc. Instn Civ. Engrs.*, **65** (1978) 893–8.
38. B. P. Sinha and A. W. Hendry, 'Compressive Strength of Axially Loaded Brick Walls Stiffened along their Vertical Edges', *Proceedings of the Fifth International Brick Masonry Conference* (Washington) 1979, pp. 254–61.
39. M. E. Phipps, A. J. Bell and Li Yang, 'Slender Brickwork Columns', *Proceedings of the Tenth International Brick and Block Masonry Conference* (Calgary) 1994, pp. 589–96.
40. M. E. Phipps, A. J. Bell and T. Swailes, 'Masonry Column Tests', *Proceedings of the British Masonry Society*, **6** (1994) 168–72.
41. M. Phipps, 'The Design of Slender Masonry Walls and Columns of Geometric Cross-section to Carry Vertical Load', *Structural Engr.*, **65A** (12) (1987).
42. *BS 5268 Code of Practice for Use of Masonry. Part 1, Structural use of unreinforced masonry* (British Standards Institution, London).

6 DESIGN ANALYSIS OF UNREINFORCED MASONRY STRUCTURES

6.1 **General**

Three analytical problems arise in the design of masonry structures, which relate to (1) the distribution of vertical loads among the various walls in the building, (2) the determination of eccentricity of loading on walls, and (3) the distribution of lateral loads on the walls. Conventionally these problems are resolved in design calculations by rather arbitrary assumptions, but they can be treated more rationally by the methods described in this chapter.

6.2 **Vertical load analysis**

6.2.1 ***Load distribution on walls***

In simple cross-wall structures the allocation of floor loads to the supporting walls is straightforward. However, with two-way spanning slabs, and with complex wall arrangements, the problem becomes more difficult and considerable differences in estimated wall loads can arise according to the assumptions made. The most usual procedure is to subdivide the floor areas into triangles and trapeziums, as in the case of reinforced concrete beam design, and to allocate the loads from these areas to the appropriate walls. With a simple rectangular slab this is probably reasonably accurate overall, but it should be noted that the distribution of the force applied to the walls will not be uniform along their lengths, being in fact concentrated towards the centre. It is probable that this non-uniformity will gradually even out down the height of a wall, and in the lower levels of a multi-storey building there would be an approximation to uniformity.

An alternative approach described by Sutherland [1] is to divide the floors into tributary areas, the load from each being allocated to a particular wall group, taking into account any displacement of the centroid of the loaded area from the centroid of the wall group. This procedure is illustrated in figure 6.1 in which a comparison is made between the wall stresses

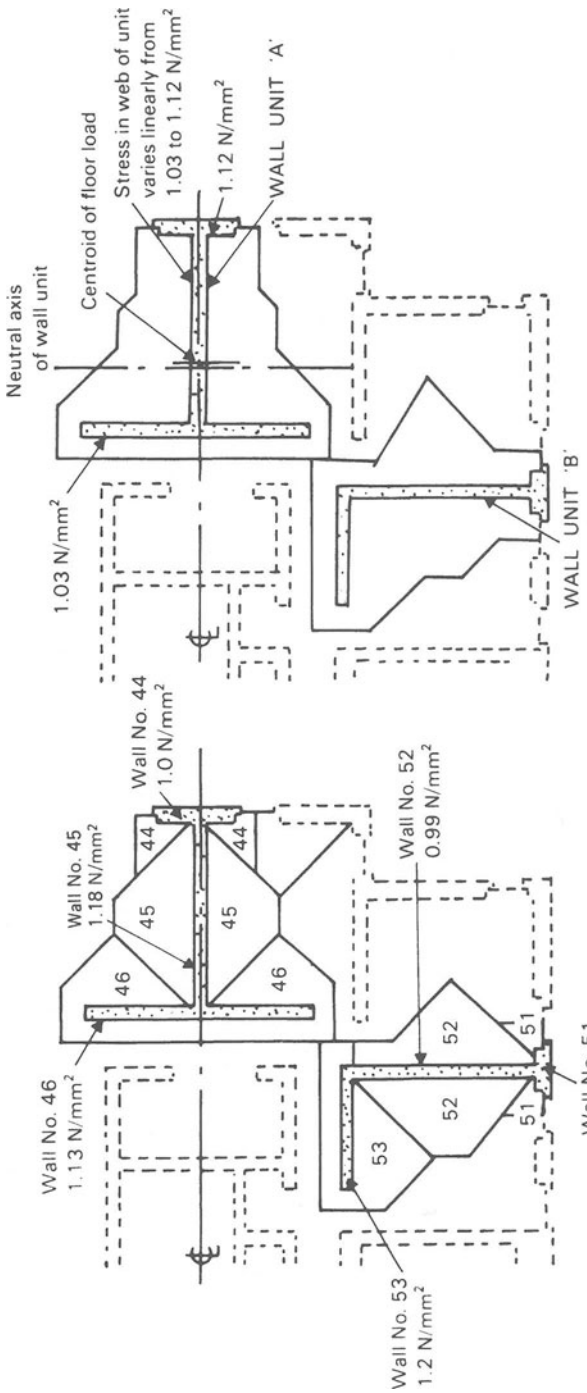

Figure 6.1 Wall stresses by alternative methods of calculating loading (Sutherland): (a) tributary areas allocated to individual walls; (b) loading allocated to wall units

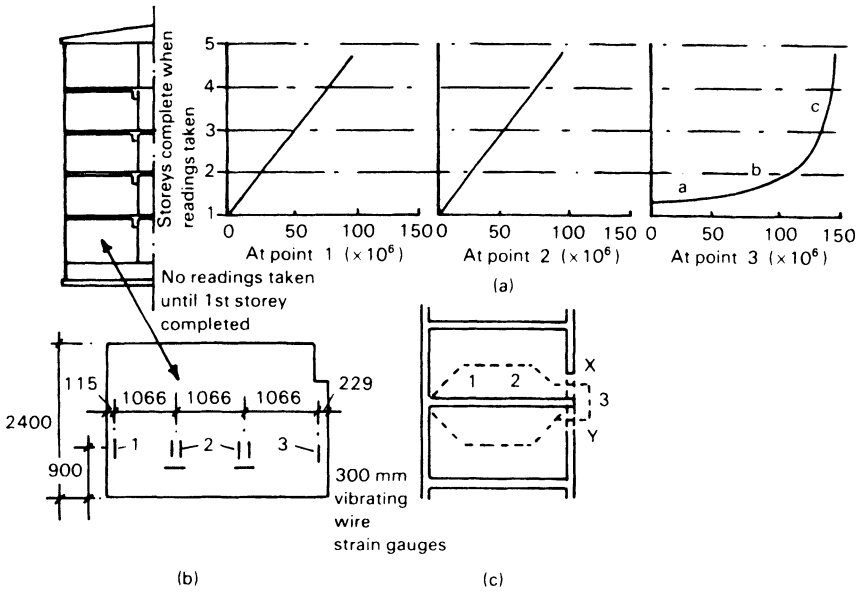

Figure 6.2 Strain measurements in a cross-wall building: (a) recorded change in strain in first-floor wall; (b) location of strain gauges (same layout on opposite face); (c) estimated tributary floor area supported

resulting from the two approaches – the 'wall unit' method is probably more accurate, but requires more lengthy calculations and the extent to which it is more accurate is uncertain.

There is some reason to believe that in rather tall buildings, say of ten storeys or more, there will be a tendency for the stresses in the lower sections of walls to even out, not only in individual walls but in wall groups as well. Some evidence for this was found by Stockbridge [2] from strain measurements taken in a five-storey cross-wall building; figure 6.2 shows a record of the strains measured in a wall of this building as the storeys above were constructed. On the basis of the load distribution indicated in figure 6.2c, it would have been expected that the reading at point 1 would have been considerably smaller than that at point 2, whereas in fact, they were almost equal. The stressing of the wall at point 3 was complicated by the presence of a lintel, XY, above the end of the wall. The effect of this lintel was initially to attract load to this area, but after construction had reached the first storey the rate of increase of strain decreased considerably until by the time the fifth floor was reached, the strains across the width of the wall were becoming much more uniform than in the earlier stages.

6.2.2 *Analytical models for vertical load analysis*

The conventional analytical model for the design of a masonry structure for vertical loads is one in which the walls and floor slabs are effectively inter-

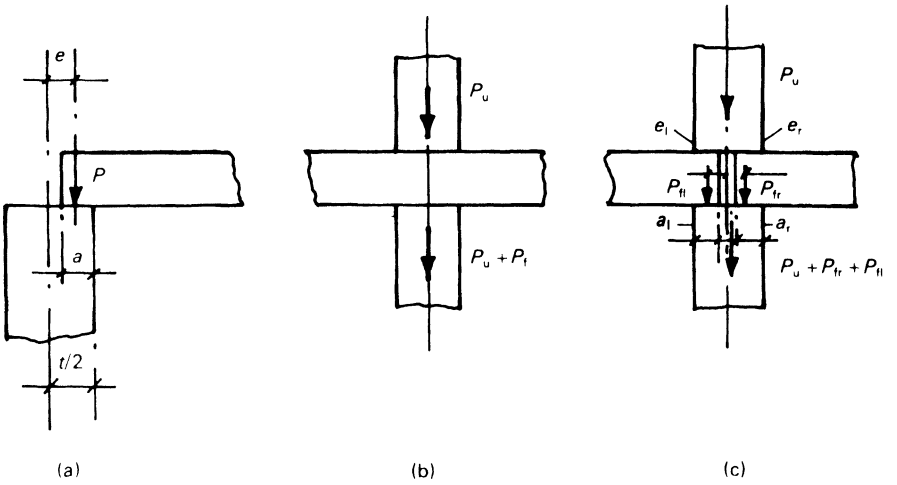

Figure 6.3 Typical assumed eccentricities in conventional analytical model: (a) slab simply supported on wall, $e = t/2 - a/2$ or $a/3$; (b) continuous floor slab, floor load P_f much smaller than P_u, $e = 0$; (c) discontinuous slabs, eccentricity of $P_u = 0$, $e_l = a_l/2$, $e_r = a_r/2$, eccentricity of load on lower wall is calculated from these assumed eccentricities

connected by hinged joints. The forces from the floor slabs are transmitted to the walls eccentrically, as indicated in figure 6.3. These eccentricities are determined by empirical rules as, for example, in the British Code of Practice for Structural Use of Masonry, BS 5628, which suggests that the load from a single floor or roof may be considered to act at one-third of the depth of the bearing area from the loaded face of the wall or, in the case of a continuous floor slab passing over a wall, each side of the floor may be taken as being supported on half of the total bearing area. In this Code, the load from the floors above the wall under consideration is assumed to be axial and correspondingly the eccentricity of loading at the lower end of a wall section is taken as zero.

This type of assumption obviously simplifies calculations and is very widely used in design, and although extremely crude and inherently inaccurate, being protected by large safety factors, it has given satisfactory results in terms of structural performance. A more rational analytical model for a masonry structure must take into account the ability of the wall–floor slab joints to transmit bending moments.

6.2.3 *Eccentricity by partial frame analysis*

Wall-end moments and thus eccentricities can be calculated in suitable cases by the application of frame analysis provided that allowance is made for the fact that wall–floor slab joints are not fully rigid; experimental

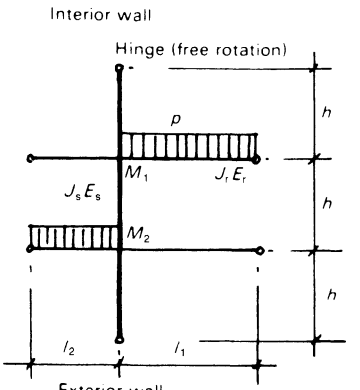

Superimposed loads

$$p l_1^2 x$$

$$M_1 = \frac{1}{4} \frac{2(1+r) - (l_2/l_1)^2}{N_1}$$

$$M_2 = \frac{1}{4} \frac{2(l_2/l_1)^2 (1+r) - r}{N_1}$$

$$r = 1 + \alpha_1 + \alpha_2$$

$$N_1 = 4(1+r)^2 - r^2$$

$$\alpha_1 = \frac{h}{l_1} \frac{J_r E_r}{J_s E_s} \qquad \alpha_2 = \frac{h}{l_2} \frac{J_r E_r}{J_s E_s}$$

Dead loads

$$g l_1^2 x$$

$$M_1 = M_2 = M$$

$$M = \frac{(2+3r)[1 - (l_2/l_1)^2]}{4N_1}$$

$$M_1 + \frac{1}{2} \frac{\alpha + 2}{N}$$

$$M_2 + \frac{1}{4} \frac{\alpha + 1}{N}$$

$$\alpha = \frac{h}{l} \frac{J_r E_r}{J_s E_s}$$

$$N = 4(\alpha + 2)^2 - (\alpha + 1)^2$$

$$M_1 = M_2 = \frac{1}{4} \frac{\alpha + 3}{N}$$

$$M_1 = M_2 = \frac{1}{8(\alpha + 3)}$$

Figure 6.4 Haller's partial frame method for calculating eccentricities

evidence relating to this will be reviewed in a subsequent section. Haller [3] has given a number of formulae for calculating wall-end moments on the basis of rigid joints between walls and floor slabs. These are summarised for internal and external walls in figure 6.4, and have been derived by the normal methods of structural mechanics. In order to apply these formulae, the *EI* values for the walls and floor slabs must be known. As far as the walls are concerned, the values given by equation 5.29 may be used, and for the floors one of the normal methods for calculating the flexural rigidity of a reinforced concrete slab may be adopted.

Haller's formulae are based on the assumption of full rigidity at the joint

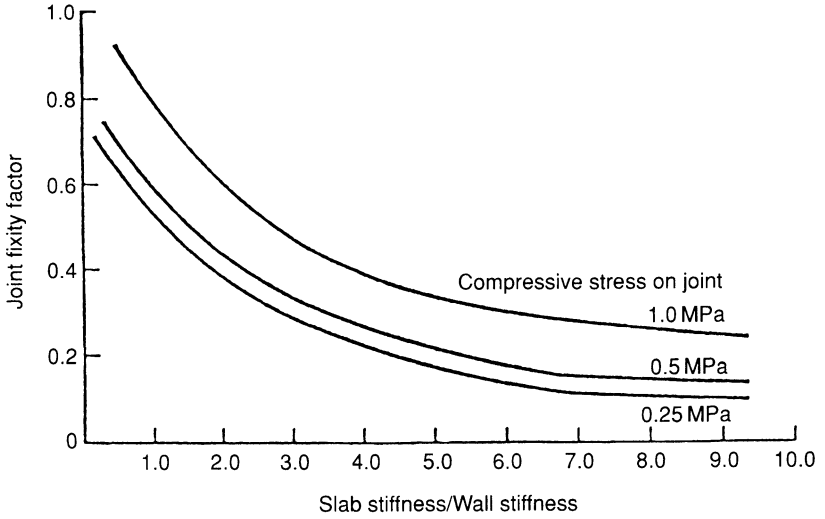

Figure 6.5 Joint fixity versus slab/wall stiffness ratio for three levels of vertical compression on joint

between the wall and the floor slab whereas it is known that this condition does not apply in practice. As a result of extensive experimental work on masonry structures, the relationship shown in figure 6.5 between slab/wall stiffness, wall precompression and joint fixity has been established which can be used to modify the rigid joint moments derived from the Haller formulae [4] in calculating eccentricities.

Vahakallio and Makela [5] have developed a method for calculating eccentricities on the basis of a simplified elastic analysis, which assumes that horizontal members have bending strength but that vertical members have no tensile strength. The distribution of moments at a joint is calculated by considering a section of the structure consisting of the floor slab panels and the walls intersecting at the joint under consideration, as indicated in figure 6.5. The end moments in the members are then obtained from the following equations:

$$M_{o1} = \alpha\left(M_q - a_{o1} \times M/A_o\right) \tag{6.1}$$

$$M_{o2} = \alpha\left(M_p - a_{o2} \times M/A_o\right) \tag{6.2}$$

$$M_{o3} = -\alpha a_{o3} \times M/A_o \tag{6.3}$$

$$M_{o4} = -\alpha a_{o4} \times M/A_o \tag{6.4}$$

where α, the carry-over factor, is 1.1 at crossed joints, 1.2 at right-angled joints, and 1.5 at T-joints

M_p and M_q are the fixed end moment due to uniformly distributed loads p and q:

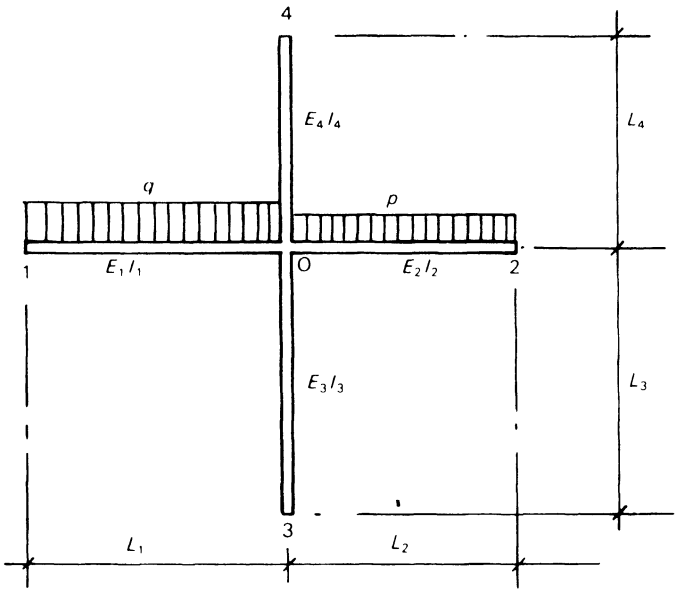

Figure 6.6 Method of Vahakallio and Makela – notation

$$M = M_q - M_p(\geq 0) \tag{6.5}$$

$$a_{oi} = k_i E_i I_i / L_i \tag{6.6}$$

where $k_i = 3$ or 4 for hinged or fixed ends respectively, for $i = 1$ or 2 in figure 6.6, and $k_i = a_i$ for $i = 3$ or 4:

$$A_o = \Sigma a_{oi} \text{ at the joint} \tag{6.7}$$

The value of $\bar{a}_i$, which makes allowance for cracking, is a function of the relative eccentricity, and is shown in figure 6.7. The dimension L_i used in calculating a_{oi} for the walls is the distance from the joint to the point of inflection in the member, that is, $\lambda_i h$. An initial value of $\lambda_i = 0.5$ may be assumed, and corrected after a trial calculation of moments. Since the value of the eccentricity has to be assumed in obtaining $\bar{a}_i$, it is evident that an iterative procedure will, in general, be required.

6.2.4 *Approximate calculation of eccentricities*

An alternative approach to the calculation of load eccentricities on bearing walls has been developed by Awni and Hendry [6] following the methods originally used by Sahlin [7] and by Colville [8].

Using the notation set out in table 6.1, Colville showed that the following relationships for the parameter $Z = PH^2/(EI)_w$ hold for cracked and uncracked walls in single and double curvature.

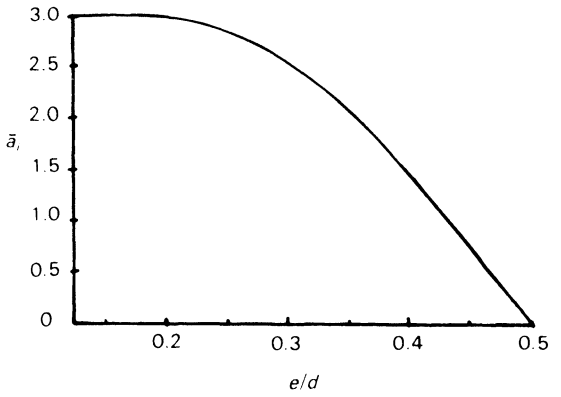

Figure 6.7 Coefficient $\bar{a}_i$ to allow for effect of cracking on wall stiffness

Table 6.1 Notation for calculation of eccentricity

θ_s is the slab rotation
θ_w is wall rotation
$\theta_j = \theta_s - \theta_w$, is the angular displacement within the joint

$$\Phi = \theta_w \frac{H}{t}$$

H, t are respectively, height and thickness of wall

$$\overline{M} = \frac{wL^2}{12}$$

w is uniform load on the slab per unit width
L is span of slab
R is a factor depending on load eccentricity, slenderness and curvature type
P_u is total load at joint from floors above
P_L is total load at joint below slab

$$\psi = \frac{P_u}{P_L}$$

β is joint stiffness

$$\bar{\beta} = \frac{2(EI)_s}{\beta L}$$

e is load eccentricity

$$\varepsilon = e/t$$

$(EI)_s$ and $(EI)_w$ are flexural rigidities of slab and wall respectively
$K = (2EI)_s H/(EI)_w L$

(a) Single curvature. (i) Uncracked section

$$Z = \frac{\pi^2 \Phi}{4\varepsilon + \Phi} \tag{6.8}$$

(ii) Cracked section

$$Z = 33.31\Phi\left(1 - 2\varepsilon - \frac{\Phi}{2}\right)^2 \tag{6.9}$$

(b) Double curvature. (i) Uncracked section

$$Z = \frac{\pi^2 \Phi^2}{\left(\Phi + \varepsilon\right)^2} \tag{6.10}$$

(ii) Cracked section

$$Z = 33.31\Phi\left[1 - \left(\frac{\left(\varepsilon + \Phi\right)^2}{2\Phi}\right)\right]^2 \tag{6.11}$$

if $\varepsilon < \Phi$, or

$$Z = 33.31\Phi\left(1 - 2\varepsilon\right)^2 \tag{6.12}$$

if $\varepsilon > \Phi$, then

$$\theta_s = \frac{wL^3}{24\left(EI\right)_s} - \frac{ML}{2\left(EI\right)_s} \tag{6.13}$$

where

$$M = \left(P_L e_L + P_u e_u\right) = \left(P_L + P_u\right)e$$

assuming $e_L = e_u = e$, thus

$$\theta_s = \frac{wL^3}{24\left(EI\right)_s} - \frac{\left(P_L e_L + P_u e_u\right)L}{2\left(EI\right)_s} \tag{6.14}$$

Letting $\theta_j = M/\beta$ and $\theta_w = (P_L e_L H)/[(EI)_w R]$ we have from the relationship $\theta_w = \theta_s - \theta_j$:

$$\frac{P_L e_L H}{\left(EI\right)_w R} = \frac{wL^3}{24\left(EI\right)_s} - \frac{\left(P_L + P_u\right)eL}{2\left(EI\right)_s} - \frac{\left(P_L + P_u\right)e}{\beta} \tag{6.15}$$

Substituting ψ and M as defined above, and solving for e:

$$e = \frac{\overline{M}}{P_L\left[\left(1 + \psi\right)\left(1 + \frac{2\left(EI\right)_s}{\beta L}\right) + \left(\frac{2\left(EI\right)_s}{RL}\frac{H}{\left(EI\right)_w}\right)\right]} \tag{6.16}$$

or

$$\varepsilon = \frac{\overline{M}}{P_L t\left[\left(1 + \psi\right)\left(1 + \overline{\beta}\right) + \overline{K}/R\right]} \tag{6.17}$$

If the joint is rigid, that is, $\theta_j = 0$, $\beta = \infty$, $\overline{\beta} = 0$ and equation 6.16 reduces to

$$\varepsilon = \frac{\overline{M}R}{P_L t\left[\left(1 + \psi\right)R + \overline{K}\right]} \tag{6.18}$$

The factor R is determined from the moment–rotation equations for double and single curvature for uncracked and cracked sections, as follows.

For an uncracked wall in single curvature, we have from equation 6.8:

$$Z = \frac{\pi^2 \Phi}{4\varepsilon + \Phi}$$

As previously defined:

$$\Phi = \theta_w \frac{H}{t} = \frac{P_L H^2}{\left(EI\right)_w} \frac{e_L}{t} \frac{1}{R} = \frac{Z\varepsilon}{R} \tag{6.19}$$

Substituting in the expression for Z:

$$Z = \frac{\pi^2\left(Z\varepsilon/R\right)}{4\varepsilon + \left(Z\varepsilon/R\right)} \tag{6.20}$$

from which

$$R = \frac{\pi^2 - Z}{4} \tag{6.21}$$

Similarly for the double curvature case

$$R = \pi\sqrt{\left(Z\right)} - Z \tag{6.22}$$

For cracked sections the derivation of R in this way results in awkward cubic expressions. To avoid this difficulty, Awni has derived relationships giving the maximum rotation capacity Φ_{max} at the buckling load in terms of ε by differentiating the various expressions for Z, and equating to zero, thus obtaining the curves shown in figure 6.8. From equation 6.19:

$$\frac{\Phi}{\varepsilon} = \frac{Z}{R} \tag{6.23}$$

that is, the slope of the Φ against ε relationship, if regarded as linear, is equal to Z/R. For the single curvature case, it will be seen from figure 6.8 that the relationship is linear and

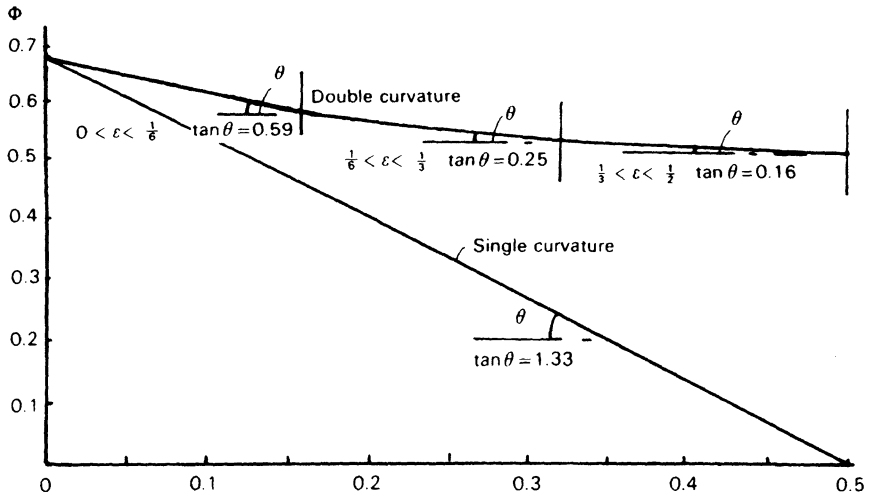

Figure 6.8 Curves of Φ against ε for double and single curvature

$$\frac{\Phi_{max}}{\varepsilon} = \frac{Z}{R} = 1.332$$

Substituting in equation 6.21 then gives

$$R = 1.85 \tag{6.24}$$

for both uncracked and cracked sections. The Φ_{max} against ε curve for the double curvature case is not linear, but taking appropriate values of the slope for the uncracked and cracked cases, and using equation 6.22 results in

$$\begin{aligned} R &= 2.345 \text{ for uncracked sections} \\ R &= 1.275 \text{ for cracked sections} \end{aligned} \tag{6.25}$$

Using these values of R it is then a simple matter to calculate ε directly from equation 6.18.

Summarising, the procedure in design is to calculate the following:

$$\overline{M} = \frac{wL^2}{12}, P_u, P_L, \psi = P_u/P_L$$

$$\overline{K} = (2EI)_s H/(EI)_w L$$

The eccentricity is then found by substituting these quantities into equation 6.17, or 6.18 if fully rigid joints can be assumed, using the appropriate value of R from equation 6.24 or 6.25. Values of the joint stiffness parameter β have been obtained from experimental results and are given in figure 6.9.

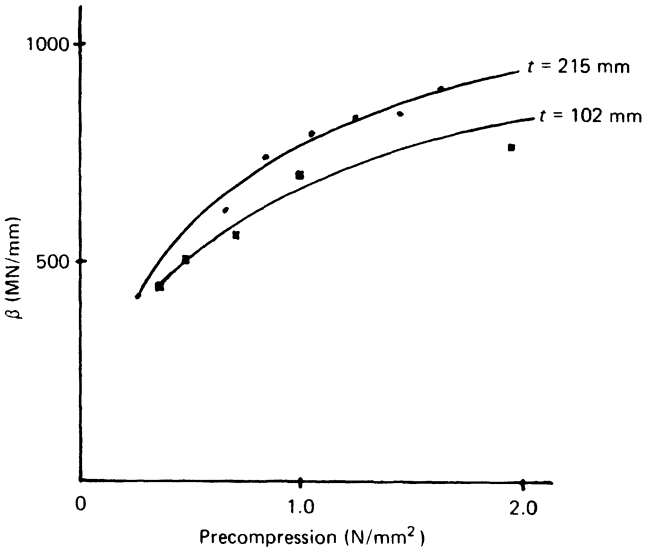

Figure 6.9 Parameter β against joint precompression

Wall-end rotation, if required for the calculation of wall strength, can be found from the relationship

$$\theta_w = \Phi \frac{t}{H}$$

The end-rotation approach of Thurlimann and Schwarz to the assessment of compressive strength, outlined in section 5.4.1 (page 107), can be used to determine eccentricity at wall–floor slab intersections using the design charts [9] which were developed from their work. The principle is indicated in figure 6.10. In this diagram the vertical axis is the eccentricity ratio *e/d* and the horizontal axis the angle of rotation at the top of the wall. A set of curves representing the relationship between the wall-end rotation and the eccentricity ratio for various values of a parameter related to the slenderness of the wall is drawn to these axes. A line representing the slab-end rotation is then superimposed: this intersects the *y*-axis at a value of *e/d* corresponding to the fixed-end moment divided by the axial load (zero end rotation). The line intersects the *x*-axis at the slab-end rotation corresponding to zero restraining moment. This line intersects the wall rotation line corresponding to the slenderness parameter where the wall and slab rotations are equal and defines the *e/d* ratio for the specified conditions.

This solution assumes that the joint is full rigid, although some adjustment of the wall-end rotation curve might be made to allow for this, and the

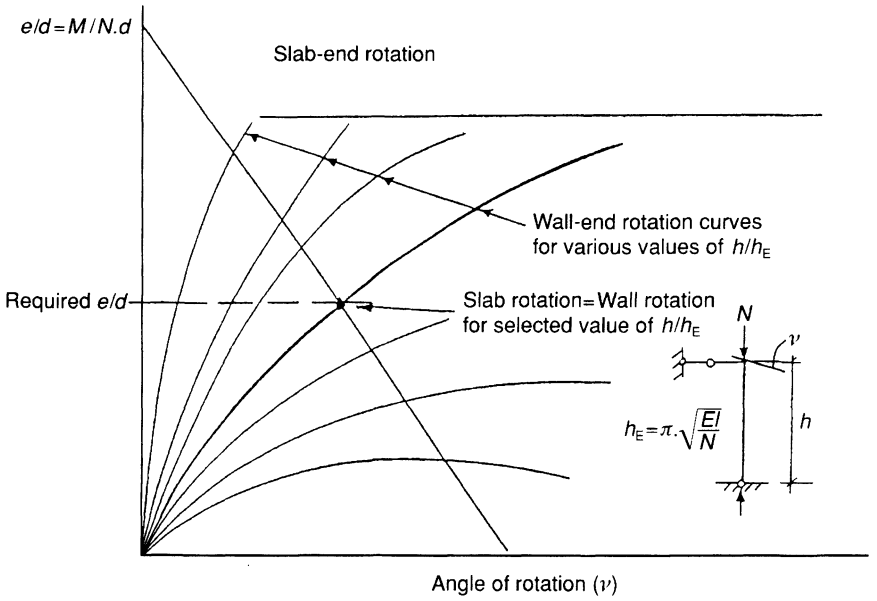

Figure 6.10 Eccentricity from wall and slab-end rotations (Swiss method)

slenderness parameter curves, calculated from experimentally determined materials properties, are specific to particular units and materials.

6.2.5 *Evaluation of methods of calculating eccentricities*

The methods of calculating structural eccentricities in multi-storey masonry buildings described in the preceding sections range from those based on simplified empirical assumptions to rather complicated analytical models which attempt to allow for at least some of the complex factors known to influence wall–floor slab interaction. Page and Sparkes [10] have carried out a study of these and other methods in which calculated values were compared with results obtained in a test on a full-scale, three-storey, two-bay structure. It was concluded that the partial frame method with correction for incomplete fixity of the joints using the fixity factors proposed by Hendry, shown in figure 6.5, gives a reasonable representation of the actual behaviour. The empirical '1/3rd rule' underestimates eccentricities while the assumption of fully rigid frame behaviour would lead to considerable overestimation.

The study also examined the effect of using the eccentricity calculated by the various methods on the ratio of the design load to the compressive capacity of the cross-section in a ten-storey building, according to the Australian code AS 3700. A wide variation in the calculated eccentricities

was found but the required compressive capacity was in most cases not greatly affected. The conclusion was therefore that a simple empirical method would be adequate for design in most cases but, where a more detailed analysis is deemed necessary, the partial frame method with allowance for incomplete fixity of the joints [4] would be appropriate. The assumption of frame action, however, will overestimate the eccentricities in lightly loaded walls, for example in low-rise buildings, or in the upper two or three storeys of tall buildings, and will not be appropriate in these situations. The eccentricity on internal walls will in general be very small and therefore seldom call for detailed investigation.

6.3 Experimental verification of frame action in masonry structures

Tests on two-storey, single-bay structures of the type shown in figure 6.11 were carried out by Colville and Hendry [11] on a full-scale structure and repeated by Awni and Hendry [12] on a half-scale equivalent. The experimental variables were slab loading, joint precompression and loading sequence.

As will be seen from figures 6.12 and 6.13, a high degree of fixity is attained in this form of wall–floor slab joint at precompressions above 0.3–

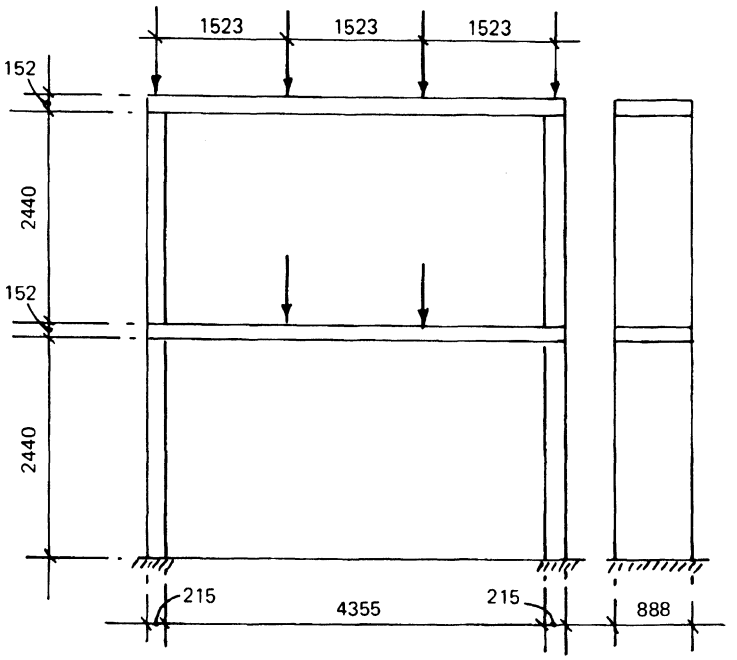

Figure 6.11 Test structure of wall–floor slab interaction

0.4 N/mm^2, but the fixity does not increase very much with precompressions in excess of this figure. It was found in these tests that the loading sequence had no effect on the joint behaviour.

Loading tests on the three-storey, two-way structure shown in figure 6.14 were conducted by Awni and Hendry [12]. In these tests, attention was concentrated on joint C2 and a jacking system was arranged so that precompression could be applied to the top of wall C. This permitted the evaluation of joint fixity at various precompressions, as shown in figure 6.15. In this case, the joint fixities attained are quite low – of the order of 30 per cent – even at relatively high precompressions. Similar results were obtained by Stokle and Bell [13] in a series of tests with a different experimental arrangement.

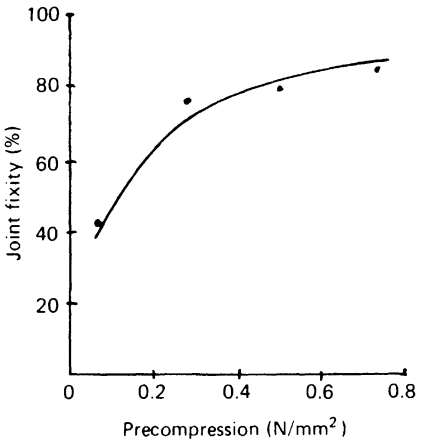

Figure 6.12 Joint fixity against precompression for 215 mm wall structure

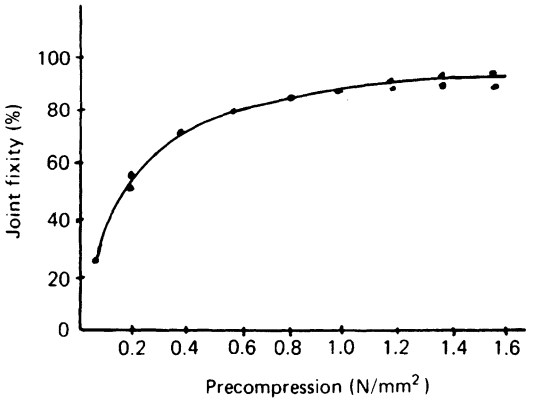

Figure 6.13 Joint fixity against precompression for half-scale structure with equivalent 215 mm thick walls

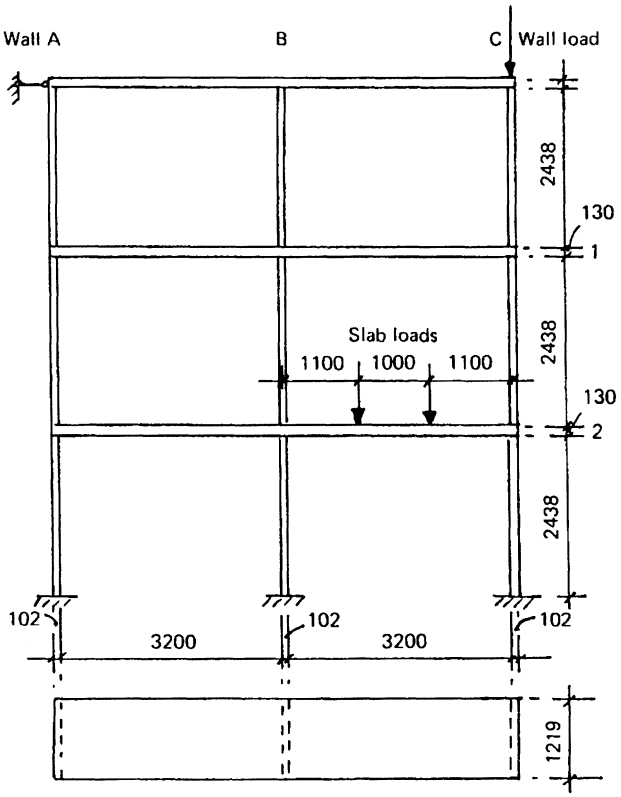

Figure 6.14 Test structure for wall–floor slab interaction: full scale with 103 mm thick walls

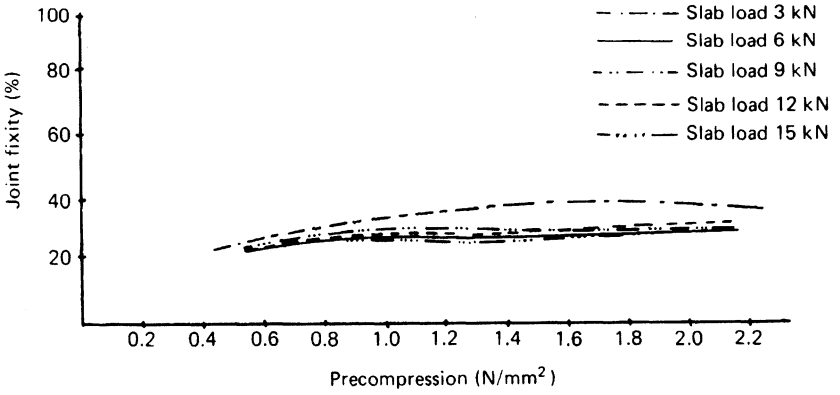

Figure 6.15 Joint fixity against precompression for 102 mm wall

Tests were also carried out by Chandrakeerthy and Hendry [14] on the single-bay structure shown in figure 6.16 in which one of the walls was single leaf 102.5 mm thick and the other a 280 mm cavity wall. The results in terms of joint fixity are shown in figure 6.17. Allowing for the difference in the form of the test structures and loading, these results are consistent with

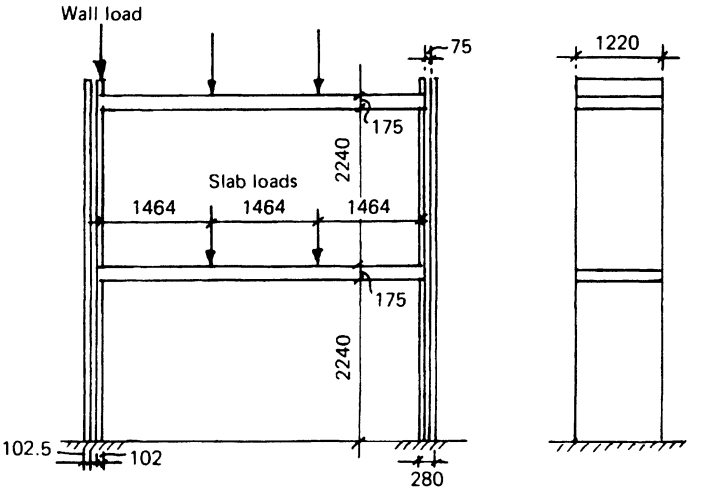

Figure 6.16 Test structure for wall–floor slab interaction with 102.5 mm single-leaf and 280 mm cavity walls

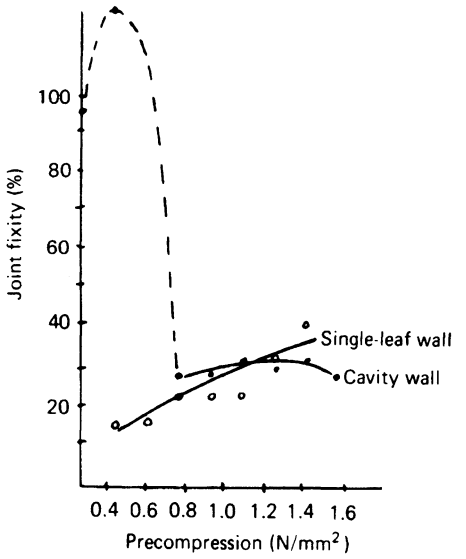

Figure 6.17 Joint fixity against precompression for cavity wall structure

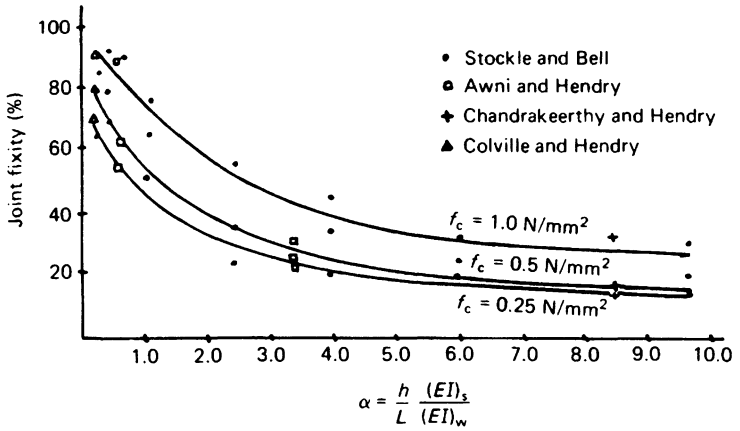

Figure 6.18 Joint fixity against slab/wall stiffness ratio

those obtained by Awni in that the fixity between the floor slab and the 102.5 mm thick wall is of the order of 30 per cent at a precompression of 1 N/mm^2.

The test on the cavity wall showed that at a precompression of up to about 0.3 N/mm^2 the joint was essentially rigid. At a slightly higher precompression, however, the fixity suddenly decreased and at higher precompressions the fixity was similar to that developed in the corresponding single-leaf tests. It is clear that the sudden decrease must have resulted from cracking of the outer leaf which, immediately prior to cracking, would have been subjected to a high bending moment from the floor slab with only nominal compression from above.

Figure 6.18 draws together the results from the tests described above by plotting the joint fixity against the ratio of wall/slab stiffness. The resulting curves formed the basis for those shown in figure 6.5 which it was suggested could be used to adjust the wall-end moments obtained on the assumption of a rigid frame.

A somewhat similar test has been reported by Germanino and Macchi [15] of a twin-bay, two-storey structure, in the form shown in figure 6.19. In this case the floor spans were quite large and the loading levels were taken up to the ultimate. An axial load of 300 kN, simulating a superimposed load of eight floors, was applied to the left-hand wall only. The elastic modulus for the masonry was determined by tests on small walls with a mean value of 7300 kN/mm^2 being adopted. An E value of 30000 kN/mm^2 was taken for the floor slab concrete. A first analysis was carried out assuming that joints 4 and 6 in figure 6.20 were hinged, that the remaining joints were rigid, and that the walls and floor slabs were uncracked. The results, however, did not agree well with those obtained experimentally, because joints 4 and 6 were capable of transmitting some bending moment and joint 3 was not fully

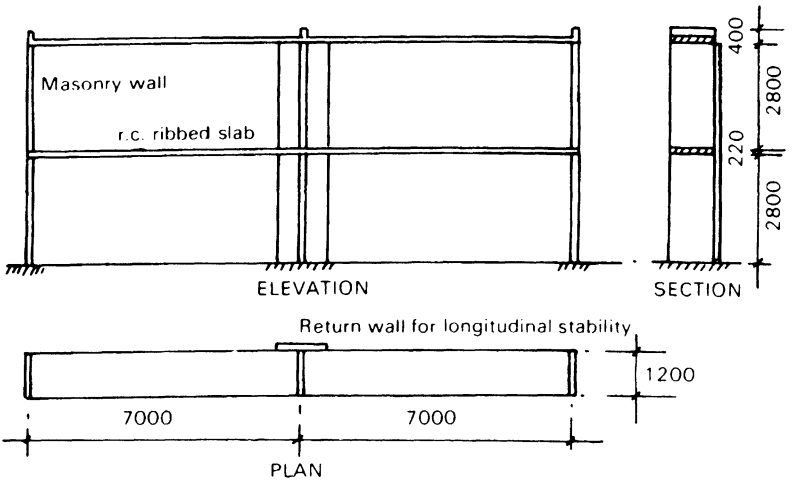

Figure 6.19 Outline of test structure for wall–floor slab interaction (Germanino and Macchi)

rigid. An improved representation of the structure was obtained by assuming all the joints as rigid, and adjusting the moments of inertia of the walls and slabs as indicated in figure 6.20. Comparison between the calculated and experimental moments for two loading cases was then found to be as follows:

Load in C2					Loads in C3–C1–C5							
Bending moment	M_{30}	M_{36}	M_{32}	M_{10}	M_{01}	M_{14}	M_{12}	M_{21}	M_{56}	M_{54}	M_{23}	M_{65}
Theoretical	2.11	3.45	5.56	4.36	2.28	2.09	6.46	13.00	10.30	9.50	6.00	2.18
Experimental	1.97	3.73	5.70	3.85	1.97	1.40	5.25	14.20	13.60	10.10	8.60	2.20

These results on the whole are reasonbly satisfactory although a rather complex adjustment of the moments of inertia was applied, and this might not give equally satisfactory results for other loading cases.

Germanino and Macchi also carried out an analysis of this structure at a load level corresponding to the ultimate limit state. This required an iterative procedure starting with a calculation on the basis of the uncracked structure described above, but with loads corresponding to the ultimate limit state. Where this analysis indicated that the floor slab would be cracked, the moment of inertia was recalculated by a method proposed by Cauvin [16], which allows for the stiffening effect of concrete on the tension side of a cracked beam or slab. The moments of inertia of wall sections were reduced when the eccentricity of load exceeded $d/6$. In this case, the effective thickness of the wall over the length in which tensile stresses appear (taken as 0.1 of the height) was $3(d/2 - e)$; if $e > d/2$, a hinge was intro-

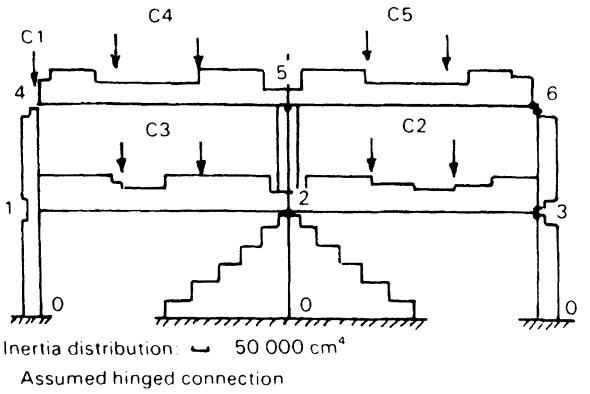

Figure 6.20 Assumed static scheme and moments of inertia for walls and floor slabs in test structure of Germanino and Macchi

duced. Calculations on this basis showed good agreement between theoretical and measured slab deflections. The tests also indicated that at collapse the assumption of hinges at the critical sections of floors and at the joints of the upper floors is justifiable.

Olatunji *et al.* [17] have investigated wall–floor slab interaction in 200 mm concrete block masonry and have concluded that, in calculating the distribution of moments at a joint, the effective EI values of the upper and lower walls should be taken as follows:

$$\text{For upper walls: } EI = E_m I_n\left(0.13 + P/P_B\right) \leqslant 0.7E_m I_n$$

$$\text{For lower walls: } EI = E_m I_n\left(0.20 + P/P_B\right) \leqslant 0.7E_m I_n$$

where $E_m = 750f'_m$, and I_n = the nominal moment of inertia of the wall. P is the load on the wall and P_B the short wall compressive strength. Within certain limitations, including a slab/wall stiffness ratio not exceeding 1.7, the use of these effective EI values gives results in reasonable agreement with those obtained in tests when applied with conventional frame analysis methods.

All the tests described above have been concerned with the effect of short-term loading. It is evident that long-term creep effects in both the walls and slabs of a building will lead to modification of the moments transmitted through the joints and also to the second-order lateral deflections resulting from compression of the walls. These effects have been investigated by Bell *et al.* [18] using test frames of the type shown in figure 6.21, loaded for periods of up to 420 days. By measuring the force in the tie at the base of the wall, it has been possible to determine directly the moment at the joint and thus the eccentricity of the resultant load over this period. Tests have been carried out on brick and block walls of various

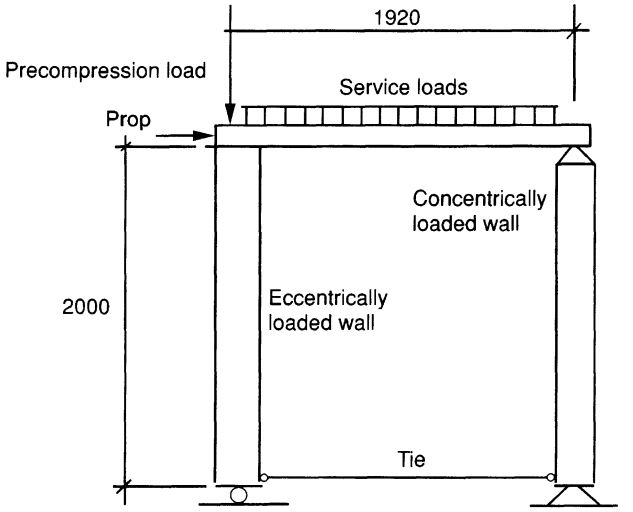

Figure 6.21 Test frame for investigation of effect of creep at wall–floor slab joint (Bell *et al.*)

thicknesses under different loading conditions. The results indicated that when walls and slabs act together and develop frame action, the moments at the joint were substantially reduced and may not be structurally significant. This is in contradistinction to the situation where the loading is applied at constant eccentricity producing a quasi-pinned end condition; in this case it is to be expected that creep in the wall material will result in an increase in the lateral deflections which might require to be taken into account in design. Where the wall loads are transmitted through floor slabs, short-term eccentricities will require to be taken into account but the effect of creep will be beneficial.

6.4 **Lateral load analysis**

Wind loading may be a serious factor in the design of multi-storey buildings and appropriate methods of lateral load analysis are required. The conventional procedure is to use what is often termed the cantilever method, which treats the structure as a series of cantilever walls interconnected by links capable of transmitting direct forces but not bending moments, as shown diagrammatically in figure 6.22b. More complex theoretical representations are possible, including storey-by-storey deflection compatibility [19], distributed shear interconnection [20] and various frame analogies [21]; these are indicated in figures 6.22c to e. Finite element analysis is also possible [22], although unlikely to be necessary for design calculations (figure 6.22f).

Analyses using these methods give quite different results for bending

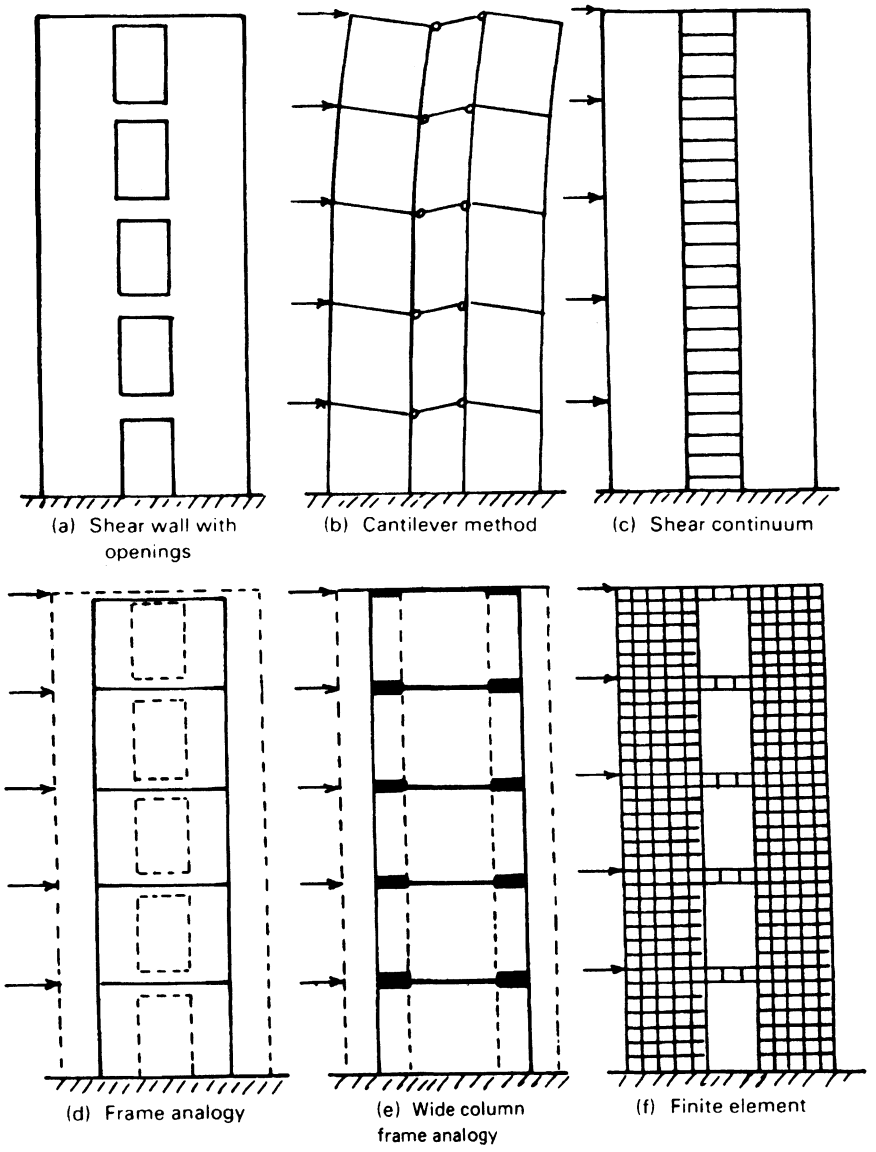

Figure 6.22 Theoretical methods for the estimation of wind stresses and deflections

moments and deflections in a particular case (see figures 6.23 and 6.24), so that a comparison with experimental results is useful in deciding the most satisfactory method for brick masonry structures. Such experiments have been carried out on full-scale and model masonry structures at Edinburgh University [23–25]. The results of these tests indicate that the simple canti-

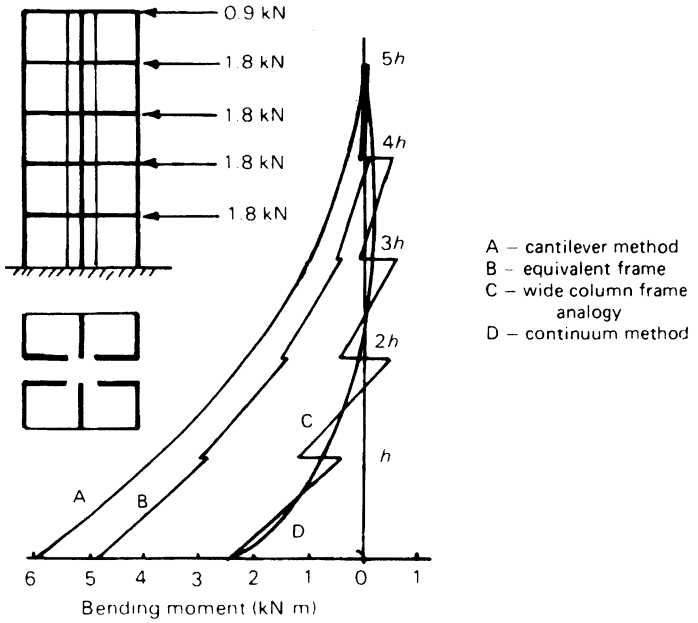

Figure 6.23 Bending moments in five-storey cross-wall structure calculated by various methods

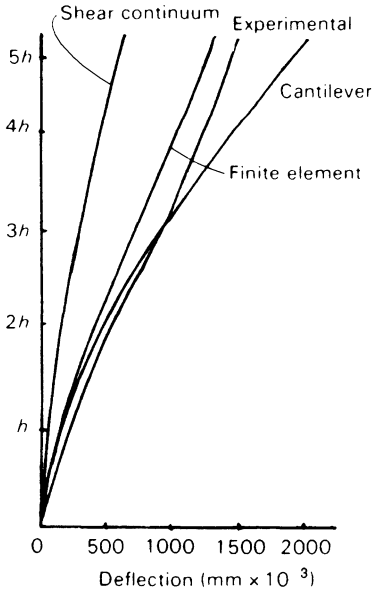

Figure 6.24 Comparison of measured and calculated deflections of shear wall structure tested at full scale

lever method overestimates the deflections and bending moments, and may therefore be used as a means of checking whether lateral loading is likely to be critical in a given case. At the same time, however, this method neglects the bending moments in the floor slabs, which could, exceptionally, crack as a result of wind loading.

6.4.1 *Frame analysis for lateral loads*

If lateral loading calculated on the basis of the cantilever approach appears to be critical, a more accurate analysis is possible on the basis of an equivalent frame using any convenient method of calculation. The shear interconnection method and the wide column frame analogy do not appear to give satisfactory results, presumably because of incomplete fixity of the interconnecting elements; attempts have been made by Michael [26] and by Soane [27] to allow for this effect.

An important problem in applying frame analysis to brickwork structures is the definition of the effective width of return walls that act as flanges to a shear wall, and of the effective width of floor slabs that interconnect these walls. Soane [27] has suggested, on the basis of model studies on a multi-storey brickwork structure, a value of $14t_f + t_w$ for T-section walls, and $7t_f + t_w$ for L-section walls. The same author found that the effective width of floor slabs could be taken as one-half of the bay width (that is, the distance between adjoining shear walls where these are regularly spaced parallel to one another). These figures are supported by the results of the full-scale and model tests on masonry structures, referred to above [23–25].

6.4.2 *Benjamin's method for irregular wall arrays*

Many masonry buildings have irregular wall arrays for which frame analysis methods for lateral loading are not readily applicable. For such cases, the approximate method described by Benjamin [19] may be appropriate. In this method, the lateral loads are allocated between the various walls in the system in proportion to their translational and torsional rigidities.

Consider a typical wall element in plan, as shown in figure 6.25, displaced Δx and Δy and rotated through an angle $\Delta\theta$ by the movement of a rigid horizontal diaphragm. The forces F_x and F_y necessary to produce the translational movements are then

$$F_x = R_x\Delta x + R_{xy}\Delta y \tag{6.26}$$

$$F_y = R_{xy}\Delta x + R_y\Delta y \tag{6.27}$$

where R_x and R_y are respectively the rigidities (force per unit displacement) of the element parallel to the X and Y axes, and R_{xy} is the force necessary to prevent displacement in the Y direction with unit displacement in the X direction. If the element is now rotated through an angle $\Delta\theta$, the forces F_x and F_y then become

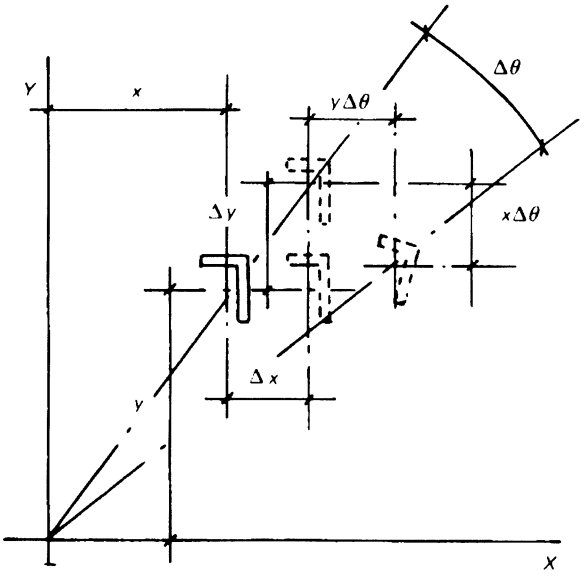

Figure 6.25 Translation and rotation of wall element

$$F_x = R_x\Delta x + R_{xy}\Delta y + yR_x\Delta\theta - xR_{xy}\Delta\theta \tag{6.28}$$

$$F_y = R_{xy}\Delta x + R_y\Delta y + yR_{xy}\Delta\theta - xR_y\Delta\theta \tag{6.29}$$

The torsional moment on the wall due to the rotation $\Delta\theta$ about its own axis is

$$T = J\Delta\theta \tag{6.30}$$

where J is the relevant torsional constant. If several walls are interconnected by the diaphragm, the total forces on the latter are

$$P_x = \Sigma F_x$$

$$P_y = \Sigma F_y$$

$$T_p = \Sigma yF_x - \Sigma xF_y + \Sigma T$$

and, substituting from equations 6.28, 6.29 and 6.30

$$P_x = \Delta x\Sigma R_x + \Delta y\Sigma R_{xy} + \Delta\theta\Sigma yR_x - \Delta\theta\Sigma xR_{xy} \tag{6.31}$$

$$P_y = \Delta x\Sigma R_{xy} + \Delta y\Sigma R_y + \Delta\theta\Sigma yR_{xy} - \Delta\theta\Sigma xR_y \tag{6.32}$$

$$\begin{aligned} T_p = {} & \Delta x\Sigma yR_x + \Delta y\Sigma yR_{xy} + \Delta\theta\Sigma y^2R_x - \Delta\theta\Sigma xyR_{xy} \\ & - \left(\Delta x\Sigma xR_{xy} + \Delta y\Sigma xR_y + \Delta\theta\Sigma xyR_{xy} - \Delta\theta\Sigma x^2R_y\right) \\ & + \Delta\theta\Sigma J \end{aligned} \tag{6.33}$$

Calculations are simplified if the reference axes are such that

$$\Sigma y R_x - \Sigma x R_{xy} = 0 \tag{6.34}$$

$$\Sigma y R_{xy} - \Sigma x R_y = 0 \tag{6.35}$$

In this case:

$$P_x = \Delta x \Sigma R_x + \Delta y \Sigma R_{xy} \tag{6.36}$$

$$P_y = \Delta x \Sigma R_{xy} + \Delta y \Sigma R_y \tag{6.37}$$

$$T_p = \Delta\theta\left(\Sigma y^2 R_x + \Sigma x^2 R_y - 2\Sigma xy R_{xy} + \Sigma J\right) \tag{6.38}$$

The total torsional rigidity of the structure is

$$J_p = \Sigma y^2 R_x + \Sigma x^2 R_y - 2\Sigma xy R_{xy} + \Sigma J \tag{6.39}$$

The procedure for finding the forces F_x, F_y and the torsional moment T on an individual wall is thus as follows:

Calculate R_x, R_y, R_{xy} and J for each wall.
Find the position of the reference axes to satisfy equations 6.34 and 6.35.
Solve equations 6.36, 6.37 and 6.38 for Δx, Δy and $\Delta\theta$.
Substitute these displacements in equations 6.28 and 6.29 for F_x and F_y, and the torsional moment on the wall is given by $T_p J/J_p$.

Wall rigidities taking account of bending and shear deformations may be calculated from

$$R = \left(\frac{1}{h^3/3EI + 1.2h/AG}\right). \tag{6.40}$$

Note that the area A is the area resisting shear, so that the 'flange' areas of an I-section, for example, are omitted.

Values of E and G are also required for this calculation. As indicated in section 2.6 the value of E for brickwork depends on the strength and on the stress level. An average value of 600–700 times the crushing strength of brickwork would, however, be reasonable. The value of G is also rather uncertain, but taking Poisson's ratio as 0.1 would give a shear modulus of $E/2.2$, which has been found to give deflections in reasonable agreement with experimental results. Similar values are likely to apply to concrete blockwork.

Calculation of torsion constants should be by the normal methods for the strength of materials [28]. The J value for a particular section depends on its type; thus, referring to figure 6.26 an 'open' section has a torsion constant equivalent to a rectangular section of the same total length and thickness and is generally relatively small. For a thin rectangular section

$$J = \frac{1}{3} b t^3 \tag{6.41}$$

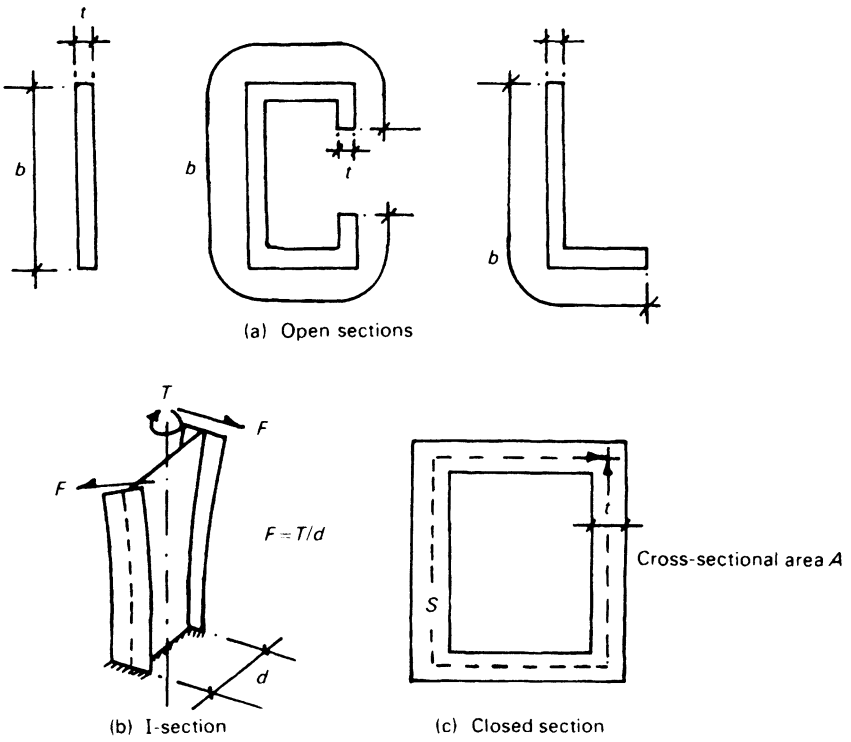

Figure 6.26 Torsion of various cross-sections

The torsional stiffness of an I-section, on the other hand, results from the flexure of the flanges, and an equivalent torsional constant should be calculated on this basis. Closed sections, that is, of tubular form, are very much stiffer in torsion than open ones and, in general terms, the torsional constant for a non-circular section of uniform thickness is

$$J = \frac{4A^2t}{S} \tag{6.42}$$

where S is the perimeter of the section.

Location of reference axes to satisfy equations 6.34 and 6.35 is achieved by taking trial axes such that the coordinates of point (x, y) are (x_1, y_1). Then

$$x = x_1 - \bar{x} \qquad y = y_1 - \bar{y}$$

where $\bar{x}$ and $\bar{y}$ are the coordinates of the desired origin related to the trial axes. Substituting in equations 6.34 and 6.35 gives

$$\bar{x}\Sigma R_{xy} - \bar{y}\Sigma R_x = \Sigma x_1 R_{xy} - \Sigma y_1 R_x \tag{6.43}$$

$$\bar{x}\Sigma R_y - \bar{y}\Sigma R_{xy} = \Sigma x_1 R_y - \Sigma y_1 R_{xy} \tag{6.44}$$

which can be solved simultaneously for $\bar{x}$ and $\bar{y}$.

If the principal axes of the wall section are parallel to the X and Y axes, $R_{xy} = 0$ and in this case

$$\Sigma y R_x = 0 \qquad \Sigma x R_y = 0 \tag{6.45}$$

$$\Delta x = \frac{P_x}{\Sigma R_x} \qquad \Delta y = \frac{P_y}{\Sigma R_y} \tag{6.46}$$

$$J_p = \Sigma y^2 R_x + \Sigma x^2 R_y + \Sigma J \tag{6.47}$$

and the actions on individual walls are

$$F_x = P_x \frac{R_y}{\Sigma R_x} + T_p \frac{y R_y}{J_p} \tag{6.48}$$

$$F_y = P_y \frac{R_y}{\Sigma R_y} T_p \frac{x R_y}{J_p} \tag{6.49}$$

$$M = T_p \frac{J}{J_p} \tag{6.50}$$

The validity of this method of calculation has been confirmed by comparison with the test results from experiments on model [26] and full-scale structures [23]. A more rigorous study of torsional effects has been presented by Keskin and Davies [29].

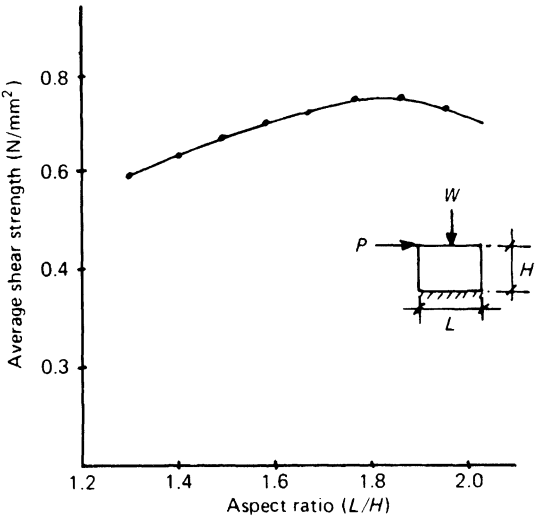

Figure 6.27 Variation of shear strength with aspect ratio of panel ($\sigma_n = 1.0\,\text{N/mm}^2$)

6.4.3 *The strength of masonry shear walls*

The strength of masonry shear walls is normally assessed in design on the basis of the Mohr–Coulomb failure criterion, as discussed in section 4.3. This will generally be sufficiently accurate although it should be noted that investigation [30] using finite element analysis in conjunction with a failure criterion based on biaxial stress tests has shown that, for a given normal stress at the bed joints, the aspect ratio (length/height) of the shear wall influences the shear strength. This is illustrated in figure 6.27 from which it may be concluded that the shear strength of the wall shown reaches a maximum, some 20 per cent greater than for a square panel, when L/H is 1.8.

References

1. R. J. M. Sutherland, 'Design Engineer's Approach to Masonry Construction', in *Designing, Engineering and Constructing with Masonry Products*, ed. F. B. Johnson (Gulf, Houston, Tex., 1969), pp. 375–85.
2. J. G. Stockbridge, 'A Study of High-Rise Load Bearing Brickwork in Britain', M. Arch. Thesis (University of Edinburgh, 1967).
3. P. Haller, 'Load Capacity of Brick Masonry', in *Designing, Engineering and Constructing with Masonry Products*, ed. F. B. Johnson (Gulf, Houston, Tex., 1969), pp. 129–49.
4. A. W. Hendry, 'The Calculation of Eccentricities in Loadbearing Walls', *Engineers File Note 3* (Brick Development Association, Windsor, 1986).
5. P. Vahakallio and K. Makela, 'Method for Calculating Restraining Moments in Unreinforced Masonry Structures', *Proc. Br. Ceram. Soc.*, **24** (1975) 161–73.
6. A. A. Awni and A. W. Hendry, 'A Simplified Method for Eccentricity Calculation', *Proceedings of the Fifth International Brick Masonry Conference* (Washington) 1982, pp. 528–34.
7. S. Sahlin, *Structural Masonry* (Prentice-Hall, Englewood Cliffs, N.J., 1971), pp. 91–116.
8. J. Colville, 'Analysis and Design of Brick Masonry Walls', *Research Report* (Dept. of Civil Engineering, University of Edinburgh, 1977).
9. Swiss Standard, *SN SIA V177/2 Design of Masonry Walls* (Swiss Society of Engineers and Architects, Zurich, 1989).
10. A. W. Page and D. R. Sparkes, 'Evaluation of the Effective Eccentricity for Masonry Walls Loaded in Compression', *Research Report No. 098.05.1994* (University of New South Wales, Australia).
11. J. Colville and A. W. Hendry, 'Tests of a Load Bearing Masonry Structure', *Proc. Br. Ceram. Soc.*, **27** (1978) 77–84.
12. A. A. Awni and A. W. Hendry, 'Joint Fixity Measurements on Load Bearing Masonry Structures', *Proc. Br. Ceram. Soc.*, **30** (1982) 149–59.
13. J. D. Stokle and A. J. Bell, 'Frame Action in Masonry Structures: An Experimental Investigation', *Masonry International*, **1** (3) (1987) 104–8.
14. S. R. de S. Chandrakeerthy and A. W. Hendry, 'Behaviour of Wall–Floor Slab

Joints in Single Leaf and Cavity Walls', *Int. J. Masonry Construction*, **3** (1) (1983) 10–13.
15. G. Germanino and G. Macchi, 'Experimental Research of a Frame Idealisation for a Bearing Wall Multi-storey Structure', *Proc. Br. Ceram. Soc.*, **27** (1978) 353–66.
16. A. Cauvin, 'Analisi non lineare di telai piani in cemento armato', *Technical Report 1st Scienza e Technica delle Construzional Pavia* (1977).
17. T. M. Olatunji, J. Warwaruk and J. Longworth, 'Stiffness Distribution at a Wall/Slab Joint in Concrete Masonry Walls', *Masonry International*, **9** (1986) 34–42.
18. A. J. Bell, M. E. Phipps and J. Mercer, 'Creep in Load Bearing Masonry Frames', *Masonry International*, **12** (1) (1998).
19. J. R. Benjamin, *Statically Indeterminate Structures* (McGraw-Hill, New York, 1959), pp. 205–71.
20. R. Rosman, 'Approximate Analysis of Shear Walls Subjected to Lateral Loads', *J. Am. Concr. Inst.*, **61** (1964) 717–33.
21. W. W. Frischmann, S. S. Prabhu and J. F. Toppler, 'Multi-Storey Frames and Interconnected Shear Walls Subjected to Lateral Loads', *Concr. Constr. Engng.*, **58** (1969) 227–34.
22. I. A. McLeod, 'New Rectangular Finite Element for Shear Wall Analysis', *J. Struct. Div. Am. Soc. Civ. Engrs.*, **95** (1969) 399–409.
23. B. P. Sinha, A. H. P. Maurenbrecher and A. W. Hendry, 'Model and Full-scale Tests on a Five-storey Cross Wall Structure under Lateral Loading', *Proceedings of the Second International Brick Masonry Conference* (Stoke-on-Trent) 1971, eds H. W. H. West and K. H. Speed (British Ceramic Research Association, Stoke-on-Trent, 1971), pp. 201–8.
24. M. Rostampour, 'Aspects of the Design of Multi-storey Buildings in Lightweight Concrete Blockwork', PhD Thesis (University of Edinburgh, 1973).
25. U. C. Kalita and A. W. Hendry, 'An Experimental and Theoretical Investigation of the Stresses and Deflections in Model Cross-Wall Structures', *Proceedings of the Second International Brick Masonry Conference* (Stoke-on-Trent) 1971, eds H. W. H. West and K. H. Speed (British Ceramic Research Association, Stoke-on-Trent, 1971), pp. 209–14.
26. D. Michael, 'The Effect of Local Wall Deformations on the Elastic Interaction of Cross Walls Coupled by Beams', in *Symposium on Tall Buildings*, eds A. Coull and B. Stafford Smith (Pergamon, Oxford, 1967), pp. 253–70.
27. A. J. M. Soane, 'Interaction of Brickwork Walls and Concrete Floors under Lateral Load', in *Designing, Engineering and Constructing with Masonry Products*, ed. F. B. Johnson (Gulf, Houston, Tex., 1969), 178–274.
28. J. Case and A. H. Chilver, *Strength of Materials* (Edward Arnold, London, 1959), pp. 282–7.
29. O. Keskin and S. R. Davies, 'The Effect of Torsion on Multi-Storey Structures', *Proc. Br. Ceram. Soc.*, **24** (1975) 127–37.
30. W. Samarsinghe, A. W. Page and A. W. Hendry, 'Behaviour of Brick Masonry Shear Walls', *Struc. Engr.*, **59B** (3) (1981) 42–8.

7 LATERALLY LOADED UNREINFORCED WALLS

7.1 General

It is possible to distinguish two categories of wall in relation to lateral strength: firstly, wall panels, the resistance of which depends primarily on the flexural strength of masonry and, secondly, those whose resistance depends on the action of in-plane forces. Walls in the first category are those found in low-rise buildings and as cladding panels in multi-storey buildings. The lateral loading on these usually arises from wind pressure, although they have to be sufficiently robust to withstand relatively small incidental loads, for example from the movement of people and equipment in a building. The second category includes walls having the degree of precompression to be expected some two or more storeys below roof level in a loadbearing masonry structure, and walls whose location in a concrete or steel structure is such that in-plane forces would be generated in them if they were subjected to lateral deflections. These walls have lateral strengths greatly exceeding the order of wind loading, and the problem of estimating their resistance is likely to be associated with that of accidental damage.

7.2 The strength of masonry walls without precompression

7.2.1 *Experimental studies*

A number of experimental studies of laterally loaded panels supported on three or four sides without precompression have been reported. Losberg and Johansson [1] and Hallquist [2] drew attention to the development of a crack pattern at failure very similar to the yield line pattern in laterally loaded concrete slabs. Several investigators [3–6] have carried out tests on model-scale panels, all of which have confirmed that failure takes place along a definite pattern of lines, dependent on the support conditions and the ratio of height to width. The patterns of these 'fracture' lines resemble

'yield' lines in corresponding laterally loaded reinforced concrete slabs, but on account of the brittle nature of masonry, the resemblance is geometrical only.

A very extensive programme of tests on laterally loaded panels was undertaken by the British Ceramic Research Association [7–11]. The work was carried out at full-scale on walls supported on three and on four sides, supplemented by tests on small specimens for the determination of the flexural strength of the brickwork used for the various panels. The results are described in references 10 and 11 from which figure 7.1 has been derived for panels built in various brick–mortar combinations and supported on three sides. There is considerable scatter of results, but the relationship between failing strength, brickwork flexural strength and aspect ratio may be represented empirically by

$$\frac{p}{f} = 1.40 - 0.82\frac{h}{L} + 2.27\left(\frac{h}{L}\right)^2 \tag{7.1}$$

where p is the failing pressure in kN/m^2

f the flexural strength of the brickwork in the stronger direction in N/mm^2

and h, L are the height and length of panel respectively (m).

Points from model tests by Kheir [4], if plotted as in figure 7.1, are in general agreement with the results of West *et al.* [7] on full-scale walls.

In a review of experimental work on laterally loaded panels, Baker [12] has pointed out that secondary effects in lateral load testing of brickwork

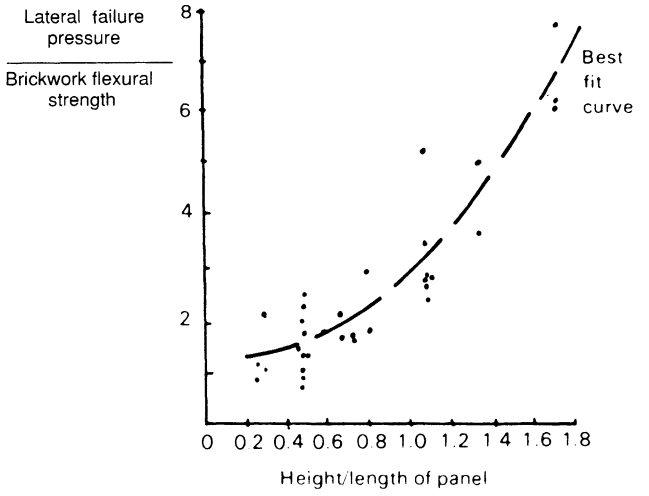

Figure 7.1 Laterally loaded panels – relationship of failing pressure to aspect ratio for walls supported on three sides (West and Haseltine)

panels can significantly affect the observed failing pressure. These effects arise mainly from unintentional, or indeterminate, restraint or yielding at the supports. Furthermore, in comparing results from diverse sources, apparent inconsistencies can arise from the use of different methods for determining the flexural tensile strength of the material from small specimens.

Anderson [13] has reported an extensive series of tests on brickwork and blockwork walls under lateral load and with a variety of boundary conditions, including return walls. It was found that for vertically spanning walls a vertical edge could be considered to have full fixity provided that it had a return of the same thickness as the main wall and equal in length to at least one-third of its height. A further major investigation of laterally loaded walls was carried out by Lawrence [14], again covering various support conditions. Resulting from this work, Lawrence plotted the ratio of failure pressure to moment of resistance of the wall section against the wall area (figure 7.2). Curves of the corresponding ratio for first cracking are also shown. The relationship of strength to area was found to be more consistent than to aspect ratio and is approximately proportional to $1/A^2$. It was noted that the influence of arching on the strength of walls was most pronounced in the case of those supported on three sides, but was very variable.

Baker [15] has made a number of observations from a review of experimental results:

(1) The strength of a single-leaf panel, simply supported on four sides, is given approximately by the sum of the strengths of vertically and horizontally spanning strips.
(2) The strength of a panel simply supported on three sides is approximately the same as that of a panel supported on four sides but twice the height.
(3) Rotational restraint at supports increases the strength of a horizontally spanning strip but not that of a vertically spanning strip.
(4) Vertical compressive stress increases the strength of both vertically and horizontally spanning strips.

On the basis of these observations, Baker [15] has suggested an approximate empirical method of assessing the strength of masonry panels without openings. In this method the strength of a vertically spanning strip is

$$W_v = \frac{\alpha_v F'_v Z}{H^2} \tag{7.2}$$

where F'_v is the modulus of rupture in the vertical direction, Z is the section modulus and H is the height of the panel. The constant α_v corresponds to the support conditions, for example, 8 for a simply supported strip.

The additional load capacity of a vertical strip due to a compressive stress F_a is

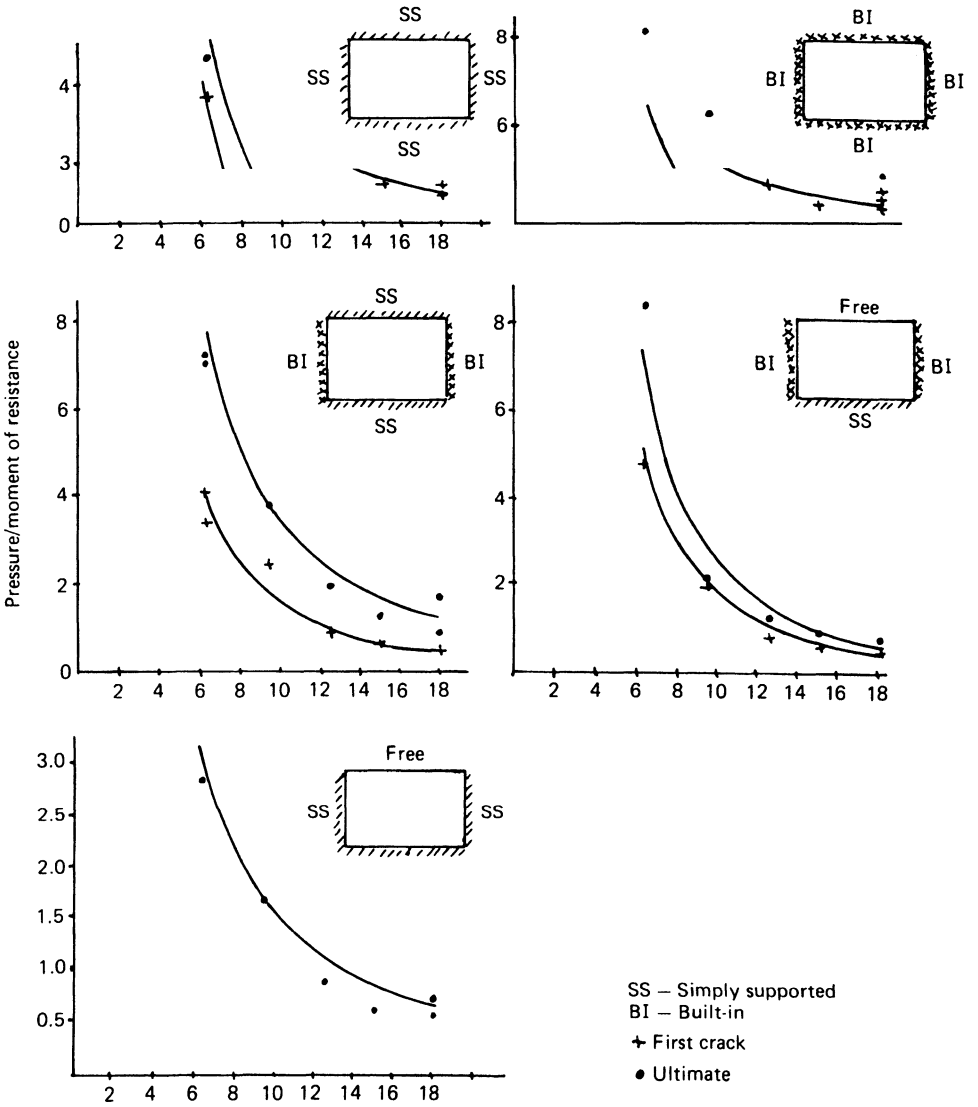

Figure 7.2 Pressure/moment of resistance for various boundary conditions against area of panel in sq. m. (Lawrence)

$$W_s = \frac{\alpha_v F_a Z}{H^2} \tag{7.3}$$

and the effective modulus of rupture in horizontal flexure, F''_h, is the lesser of

$$F'_h\left(1 + \frac{F_a}{F'_v}\right) \quad \text{or} \quad 1/9\left(4F'_b + 5F'_v\right) \lessdot F'_h \tag{7.4}$$

where F'_h is the modulus of rupture in the horizontal direction. The strength of a horizontally spanning strip is then

$$W_h = \frac{\alpha_h F''_h Z}{L^2} \tag{7.5}$$

and the lateral load capacity of the panel is given by

$$W = \left(W_v + W_h + W_s\right) \tag{7.6}$$

7.2.2 *Calculation of the strength of laterally loaded panels*

In view of the difficulties in ensuring that support conditions in lateral loading tests are in accordance with the idealised representations, and because of the uncertainty surrounding the failure criteria for brickwork or blockwork in flexure, in addition to that arising from the measurement of flexural strength, great precision in correlating the calculated strength of laterally loaded panels with experimental results is not to be expected.

Two approaches have been considered: firstly, by the application of elastic theory and secondly, by various modifications to yield line analysis. On the face of it, elastic theory would appear to be the more promising since the load–deflection relationship for laterally loaded panels is reasonably linear; however, allowance must be made for the orthotropic properties of brickwork, but this presents no difficulty in principle. The main problem relates to the criterion of failure for brickwork subjected to biaxial bending in the presence of vertical compression. Baker [16] has suggested an elliptical failure criterion which may be represented by the equation:

$$\left(F_y/F_{uy}\right)^2 + \left(F_x/F_{ux}\right)^2 = 1 \tag{7.7}$$

However, Sinha *et al.* [17] have proposed the use of the Rankine maximum stress criterion which assumes that failure will take place whenever the strength in either the horizontal or vertical direction is reached. This proposal is supported by a series of tests on cross-shaped beam specimens in which the panel of brickwork at the intersection of the cross arms was subjected to simultaneous bending moments in the X and Y directions, as indicated in figure 7.3a. The results of the tests when plotted in dimensionless form as in figure 7.3b define a biaxial failure envelope which indicates an enhancement of the strength in the weaker direction. Baker's criterion, also plotted, does not appear to be accurate but the Rankine theory could be applied as a first approximation. The tests also demonstrated that the applied load on the specimen was distributed according to the stiffness orthotropy of the brickwork and that when the failure moment in the weaker direction was reached, no further moment was transmitted in that direction. Any further increase in the applied load then depends on there being some residual strength in the stronger direction.

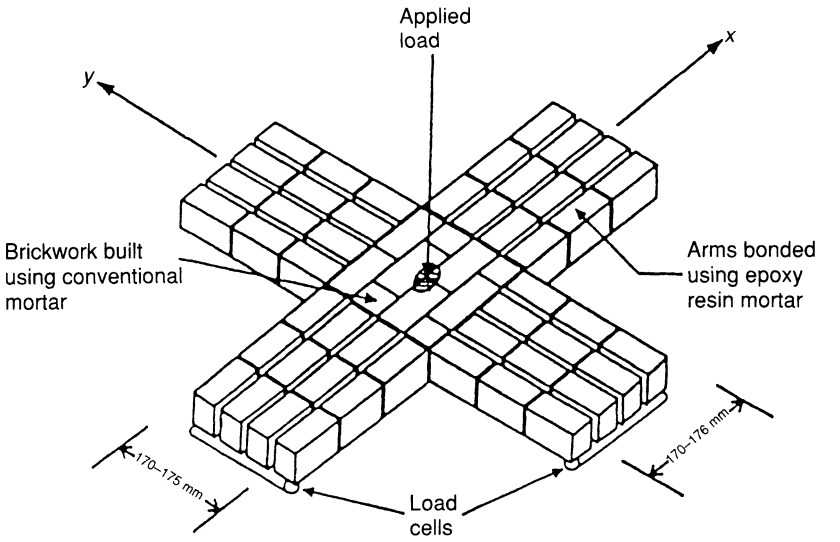

(a) Cross-shaped specimens

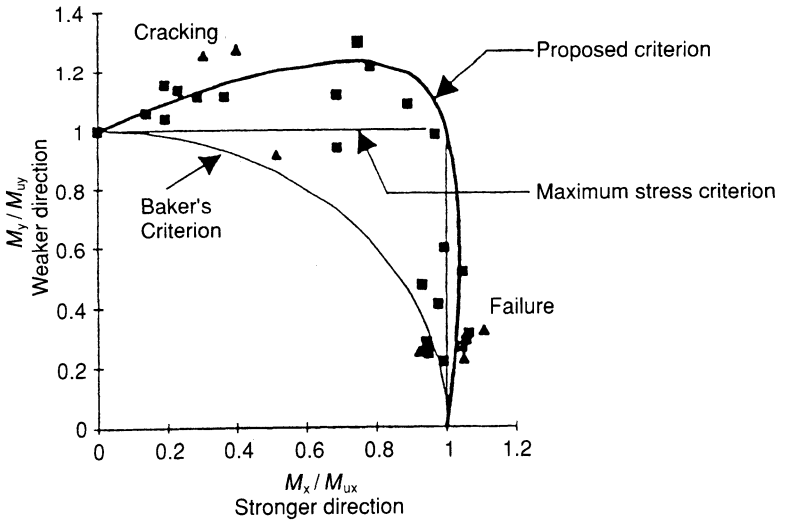

(b) Biaxial failure criterion

Figure 7.3 Experiments on laterally loaded brickwork specimens (Sinha *et al.* [17]). In points to the left and above (1, 1), specimens cracked in the weaker direction before failure. In those below (1, 1), failure occurred simultaneously with attainment of maximum moment in the stronger direction. ▲ Duarte (1993).

Elastic calculations using a suitable finite element program and relevant values of Young's moduli and Poisson's ratios in the orthogonal directions together with the appropriate failure criterion may thus be expected to give an accurate estimate of the strength of laterally loaded panels.

The failure pattern of brickwork panels, resembling the yield line pattern in reinforced concrete slabs, has prompted the application of yield line analysis to this problem, although it is obvious that the basic assumption of constant moment along a failure line cannot occur in a brittle material. Haseltine *et al.* [11] have shown that strength calculations based on yield line theory, in which the orthogonal ratio, μ, is taken as being equal to the strength ratio of the brickwork, gives results in good agreement with tests on walls supported on three or four sides, provided that flexural strength values are taken from wallette tests as established by West *et al.* [10] and that suitable allowance is made for the support conditions. A comparison between calculated and test results is shown in figure 7.4. Anderson [13] has confirmed that the use of yield line formulae gives satisfactory agreement with experimental results for panels which are simply supported or have effectively fixed-end conditions, but overestimate the strength of panels which are continuous over supports.

Other reports [15, 18] have stated that the yield line approach overestimates the strength of laterally loaded panels. The work by Sinha *et al.* [17] referred to above indicates that while this is frequently the case, the method is accurate when failure occurs similtaneously in both principal directions. This would appear to be a logical conclusion having regard to the

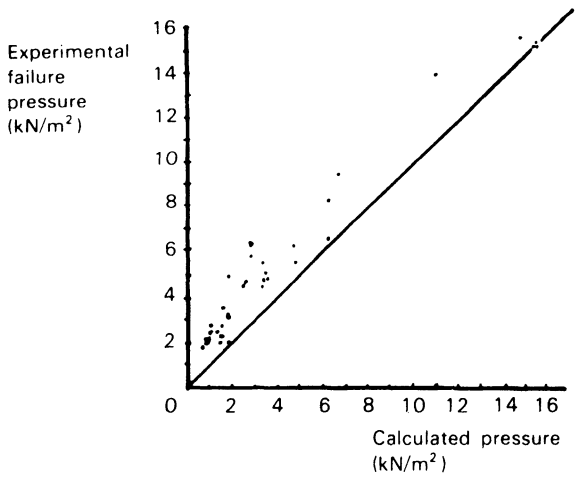

Figure 7.4 Comparison between calculated and experimental results for laterally loaded panels (Haseltine and West)

assumption in yield line theory of rigid plastic behaviour following attainment of the maximum moment in the weaker direction which, as previously noted, cannot obtain in a brittle material.

Most of the studies of laterally loaded walls have been on panels without openings whereas this is a common case in practice. Some work, however, has been done by Chong *et al.* [19] and by Duarte and Sinha [20] exploring the application of finite element and yield line methods to this problem. The latter report that for panels with a central opening the yield line method, in spite of its inherent limitations, gives reasonably accurate results. Their solutions for panels with three different boundary conditions are shown in table 7.1.

7.2.3 *Cellular and fin walls under lateral load*

Walls of cellular or T-section in plan, known as diaphragm or fin walls, have come into use for large single-cell buildings such as sports halls [21, 22]. These walls support a relatively light roof structure, but are relatively tall and the predominant load on them is from wind. The roof structure will be sufficiently stiff in the horizontal plane to enable it to transmit loads from the wall head to shear walls at the ends of the building, so that the walls can be regarded as propped cantilevers.

Bending moments in a wall of this type are therefore essentially as shown in figure 7.5a and the stresses in the wall will result from the combination of bending stresses due to wind and direct stresses from dead loads. In principle this is straightforward, but in practice problems arise from the presence of a damp-proof course at the base and from the doubtful reliability of the tensile strength of the masonry at the critical section in the upper part of the wall. A question also arises concerning the strength of the connection between the diaphragms and the outer leaves of the wall or between the wall and the fins.

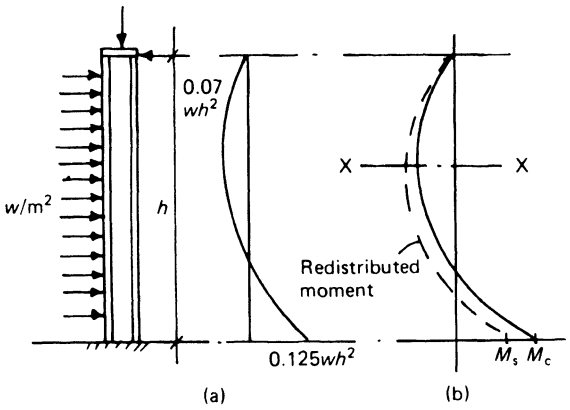

Figure 7.5 Bending moments in a propped cantilever wall

Table 7.1 Yield line formulae for laterally loaded masonry panels with central opening (Duarte and Sinha [20])

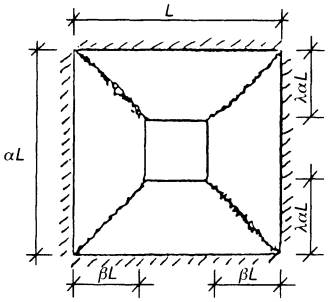

Walls with four edges simply supported containing a central opening

$$q = \frac{12m\left(\frac{\mu\lambda}{\beta} + \frac{\beta}{\alpha^2\lambda}\right)}{L^2(3 - 3\beta + 4\beta\alpha - 3\lambda)}$$

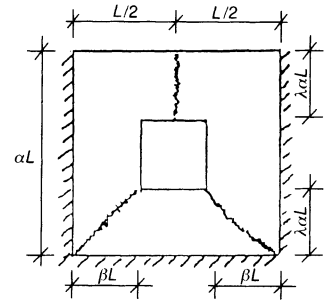

Walls with upper edge free and three other edges simply supported

$$q = \frac{24m\left(\frac{\beta^2}{\lambda\alpha^2} + 2\mu\lambda^2\right)}{L^2(3\lambda + 20\beta^2\lambda - 18\beta\lambda + 12\beta - 12\beta^2)}$$

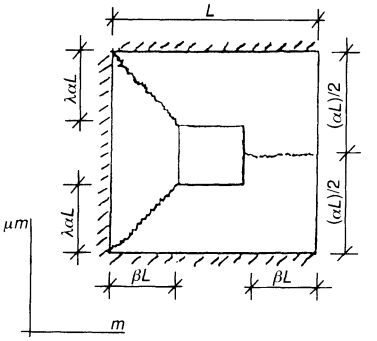

Walls with one vertical edge free and three other edges simply supported

$$q = \frac{24m\left(\frac{2\beta}{\alpha^2} + \frac{\mu\lambda^2}{\beta}\right)}{L^2(3\beta + 20\beta\lambda^2 - 18\beta\lambda + 12\lambda - 12\lambda^2)}$$

where q = applied external pressure
μ = strength orthotropy
m = ultimate moment per unit length along a yield line.

— Free edge
⌇⌇⌇ Simply supported
⌇⌇⌇ Yield line

The presence of a damp-proof course will, unless this consists of impervious bricks, limit the moment of resistance at the base to a 'no tension' or gravity situation. The 'no tension' moment is

$$M_c = NZ/A_m \tag{7.8}$$

where N = total axial load at this section, Z = section modulus and A_m = cross-sectional area of the wall. The 'gravity' moment is

$$M_s = ND/2 \tag{7.9}$$

where D = overall depth of the section. At any intermediate section in the height of the wall, the moment of resistance will be

$$M_c = Z\left(N/A + f_t\right) \tag{7.10}$$

assuming that a tensile stress of f_t can be developed.

If the wall behaves as an elastic propped cantilever, the bending moment at the base will rise until the limiting value of M_c corresponding to the tensile strength f_t is reached at the base. A crack will then be developed there and the moment of resistance will reduce to M_s, leading to a redistribution of the moments in the upper part of the wall, as indicated in figure 7.5b. Further load can be resisted until a crack occurs at a section XX. The moment at XX will, of course, not fall below the gravity moment at this section.

The condition reached when the moments at X and at the base are limited to the gravity moments represents the ultimate limit state of failure for the wall and may be found as follows (referring to figure 7.6):

Weight of top section of wall = $\varrho A_m h_t$
Weight of lower section of wall = $\varrho A_m h_b$

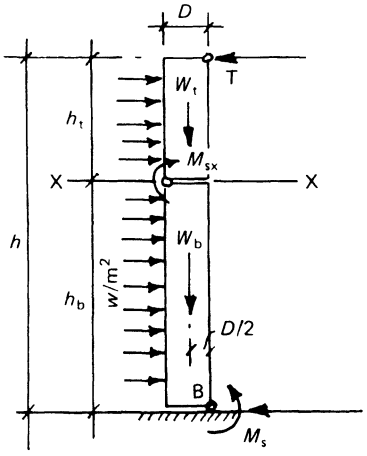

Figure 7.6 Propped cantilever masonry wall at ultimate limit level

where ϱ is the density of the material and A_m the cross-sectional area. At the base

$$N = W_t + W_b = \varrho A_m h \tag{7.11}$$

and gravity moments at B and X are

$$M_s = N \times D/2 \quad \text{and} \quad M_{sx} = W_t \times D/2 \tag{7.12}$$

If the lateral load is w/m^2, the horizontal reactions at T and B are

$$H_t = wh/2 - M_s/h \qquad H_b = wh/2 + M_s/h \tag{7.13}$$

Considering the top part of the wall and taking moments about X:

$$W_t \times D/2 + wh_t^2/2 - H_t \times h_t = 0 \tag{7.14}$$

So that, at failure:

$$w_{max} = 2\varrho A_m D(h - h_t) \tag{7.15}$$

Putting $x = h_t/h$:

$$w_{max} = 2\varrho A_m D/h(1 - x) = K/(1 - x) \tag{7.16}$$

where $K = 2\varrho A_m D/h$.

Phipps and Montague [23] have pointed out that the location of the critical section in the upper part of the wall will coincide with a bed joint and, having regard to the flat slope of the bending moment diagram in this region and the spacing of the bed joints, x could be between 0.3 and 0.45, leading to values of w_{max} in equation 7.16 of $1.4K$ to $1.8K$.

The gravity or stability calculation of the strength of a cellular or fin wall under lateral loading is conservative and some designers [21–23] include tensile resistance of the masonry at the upper section in estimating the ultimate limit state.

Experimentally [23] it has been found that the existence of tensile stress raises the failure load but as soon as the tensile bond breaks, the load reverts to that corresponding to a stability failure. It would appear prudent, having regard to the uncertain value of the tensile bond strength in more or less direct tension, to estimate strength on the stability criterion but with a considerably reduced safety factor. A figure of 1.5 for the partial safety factor when relying only on gravity forces has been suggested.

7.3 **Lateral strength of walls with precompression**

7.3.1 ***Experimental studies***

The lateral strength of brick masonry walls with precompression has been quite thoroughly investigated. An extensive series of tests by West

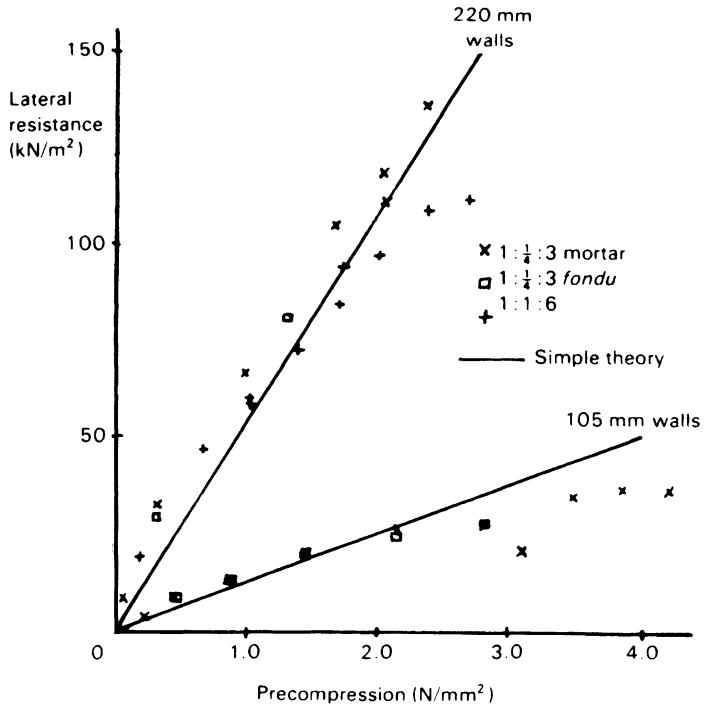

Figure 7.7 Lateral resistance of brick walls with precompression (after West *et al.*)

et al. [24] demonstrated experimentally the relationship between lateral strength and precompression of storey height strip walls of various thicknesses and materials. The results of a number of these tests are summarised in figure 7.7; they show that there is a more or less linear increase in lateral resistance for all walls up to about a precompression of $2\,N/mm^2$. Above this level of precompression, the strength tends to fall away from the linear relationship as a result of local compression at the lines of failure.

Lateral loading tests on storey height cavity walls built within a five-storey brickwork structure were reported by Hendry *et al.* [25]. These experiments showed the same strength characteristics as those indicated in figure 7.7 for strip walls, and also established experimentally the effect of returns (figure 7.8). The lateral resistance of walls of this type is usually of interest in relation to accidental loading, typically as a result of gas explosion. Morton and Hendry [26] therefore investigated the strength of strip walls with precompression subjected to a dynamic load, and demonstrated that at rates of loading equivalent to a gas explosion in a building there was no significant difference as compared with the resistance to a slowly increased load.

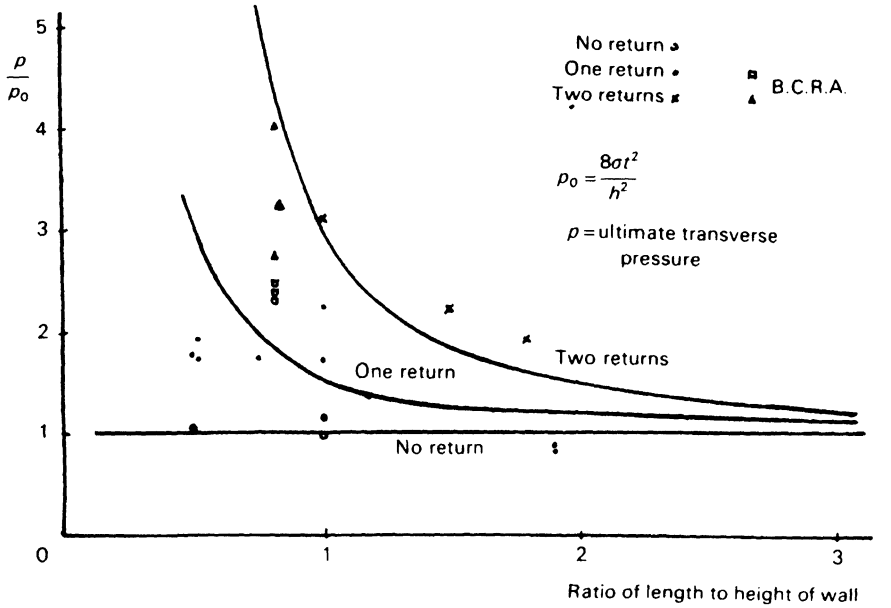

Figure 7.8 Effect of returns on the strength of laterally loaded walls with precompression

7.3.2 *Theoretical treatment*

The mechanism of failure of laterally loaded strip walls with precompression is indicated in figure 7.9. If the tensile bond of the mortar to brick is neglected, and if no local crushing takes place at the 'hinges', the system can be represented statically by a three-hinged arch so that the lateral pressure at failure is given by

$$p_c = \frac{8\sigma}{S^2} \tag{7.17}$$

where p_c is the ultimate lateral pressure
σ is the precompression
$S = H/t$, which is the slenderness ratio.

As previously observed, this relationship agrees closely with experimental results up to precompressions of the order of $2\,N/mm^2$, but above this level a more elaborate analysis is required taking into account the compression of the brickwork and possible local failure. The following approach was developed by Morton [27], based on the following assumptions:

(1) The tensile bond between the bricks and mortar, and the self-weight of the wall are neglected.

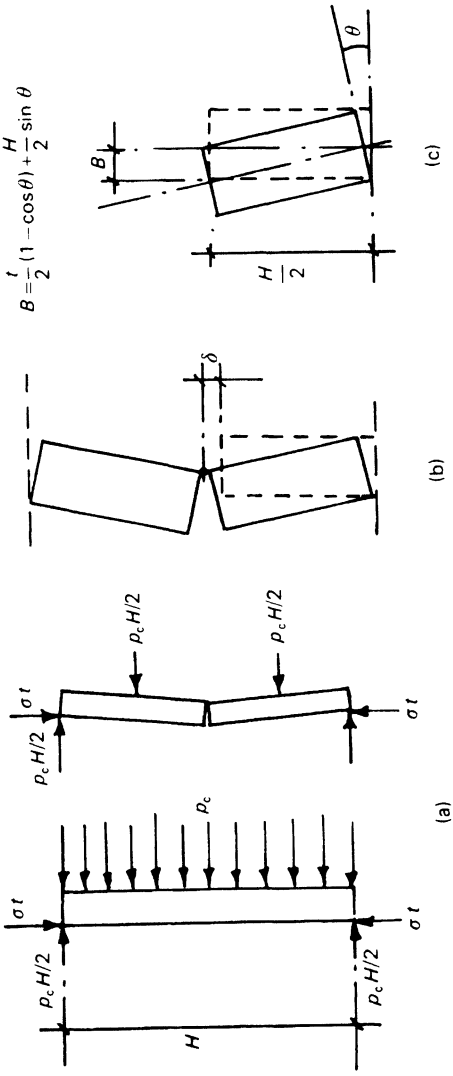

Figure 7.9 (a) Failure mechanism of laterally loaded wall with precompression. (b) Lift of half-height of wall at failure. (c) Rotation geometry of half-height of wall

(2) The top of the wall is supported against lateral movement without impeding vertical movement.
(3) The precompression remains constant.

Referring to figure 7.9:

$$\text{work done by lateral force at failure} = \frac{p_c H t}{4} \tag{7.18}$$

$$\text{work done in lifting a mass above top of wall} = 2\delta\left(\sigma t + \frac{w}{2}\right) \tag{7.19}$$

where 2δ is the maximum lift at the top of the wall taking into account elastic deformations
w is the weight per unit length of wall.

Equating 7.18 and 7.19:

$$p_c = \frac{4}{Ht}\left(\sigma t + \frac{w}{2}\right)2\delta \tag{7.20}$$

The vertical distance through which the mass above the wall is lifted is equal to the geometric distance calculated on the basis of a rigid material, less the shortening due to the elastic deformation. To evaluate the shortening, it is necessary to relate θ, the angle of rotation of the wall to the lateral deflection at the point of instability, the precompression σ, the compressive strength of the brickwork σ_c and the slenderness ratio S. Defining $u = B/t$, where B is the horizontal deflection of the centre line of the wall at mid-height, it can be shown that, if it is assumed $u = 1 - \sigma/\sigma_c$, the following equation for $\cos\theta$ is obtained:

$$\cos^2\theta\left(1 + S^2\right) + 2\left(1 - \frac{2\sigma}{\sigma_c}\right)\cos\theta + \left[\left(1 - \frac{2\sigma}{\sigma_c}\right)^2 - S^2\right] = 0 \tag{7.21}$$

The positive square root of equation 7.21 gives the value of θ at which the restoring moment becomes zero. The various stress conditions at failure shown in figure 7.10 can be identified, and from these Morton has calculated the elastic shortening Δ. Thus in figure 7.10, cases 2 and 3

$$\Delta = \frac{\sigma_{av}}{E}H \tag{7.22}$$

and in case 4

$$\Delta = \frac{H}{2E}\sqrt{\left(\sigma_{max}^2 - 2\sigma_{av}t\tan\theta\right)} \tag{7.23}$$

where σ_{max} is the maximum compressive stress in the material and σ_{av} the average stress. The lift is then

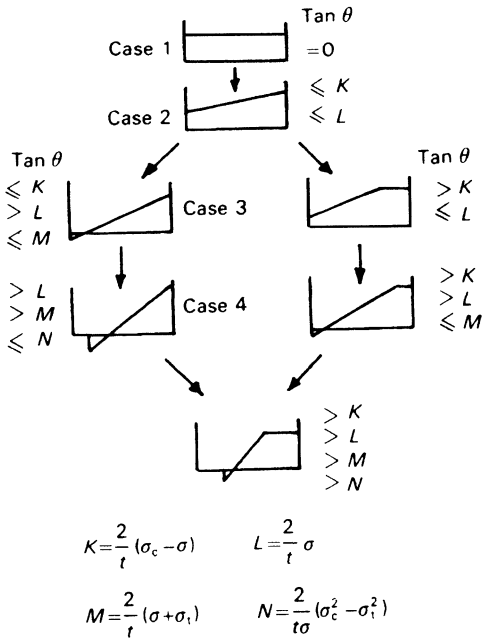

Figure 7.10 Failure stress patterns related to angle of rotation of half-wall in Morton's theory

$$2\delta = 2\left\{\left[\left(\frac{H}{2}\right)^2 + t^2\right] - \frac{H}{2}\right\} - \Delta \qquad (7.24)$$

If the compressive stress at the extreme fibre equals the ultimate stress, it is assumed that the mass above the wall has been displaced to its limit and further rotation causes the corner of the masonry to be progressively crushed while the displacement remains at its maximum. On this basis, the curves shown in figure 7.11 have been calculated for the following materials properties:

Ultimate strain: 0.001	Density of brickwork: 1700 kg/m^3
Ultimate tensile strength: 0.35 N/mm^2	E: 7000 N/mm^2

These curves show the relationship between lateral strength and slenderness ratio for various precompressions. An alternative presentation of the results given by this theory is presented in figure 7.12, which shows the lateral resistance of storey height walls (2.6 m) plotted against precompression for various values of E, which may in turn be related to brickwork strength. These results have been found to correlate well with experimental values.

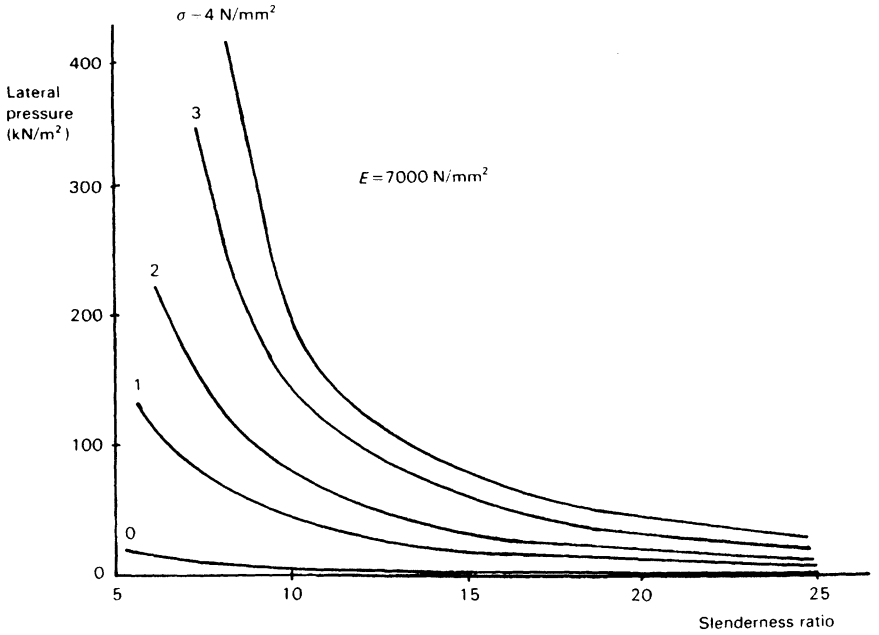

Figure 7.11 Relationship between lateral strength and slenderness ratio for various precompressions

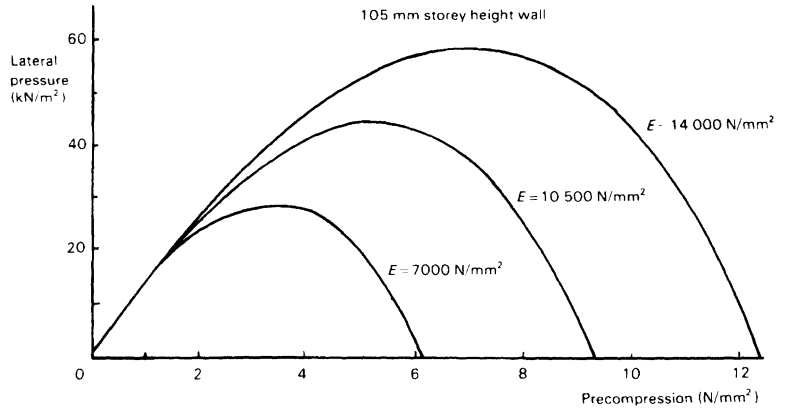

Figure 7.12 Lateral strength of storey height (2.6 m) walls against precompression for various values of E

7.4 The lateral strength of infill panels

7.4.1 *Arching theories for strip walls*

A masonry panel built into a steel or concrete frame can develop very high resistance to lateral pressure as a result of 'arching' effects in the wall. A solution for the lateral strength of such panels subject to blast loads was produced by McDowell *et al.* [28] and McKee and Sevin [29]; further experimental and theoretical studies of the resistance of masonry walls to blast loading have been reported by Wilton, Gabrielsen and others [30–35]. These extensive investigations, carried out on full-scale walls in a large shock-tunnel, are summarised in reference 36.

McDowell *et al.* derived equations for the resistance of a laterally loaded wall deflecting between unyielding supports, as indicated in figure 7.13. The theory is based on the following assumptions as to material properties:

(1) the tensile resistance is negligible;
(2) the material has an elasto-plastic stress–strain relationship;
(3) there is no strength recovery beyond the elastic range, that is, a slight decrease in strain in the plastic range results in an instantaneous drop in stress to zero and a permanent set equal to the plastic strain in the material.

The wall is assumed to deflect in such a way that each half-wall rotates about the first point in contact with the support, as indicated in figure 7.13. Referring to this diagram:

$$a = \frac{H}{4}\frac{1 - \cos\theta}{\sin\theta}$$

and

$$B = H\frac{1 - \cos\theta}{\sin\theta}$$

Thus

$$a = \frac{B}{4}$$

Putting $u = B/t'$ and $S = H/t'$, then

$$\sin\theta = \frac{2u}{S\left[1 + \left(u/S\right)^2\right]}$$

$$\cos\theta = \frac{1 - \left(u/S\right)^2}{1 + \left(u/S\right)^2}$$

The fraction of the half-depth in contact with the support is

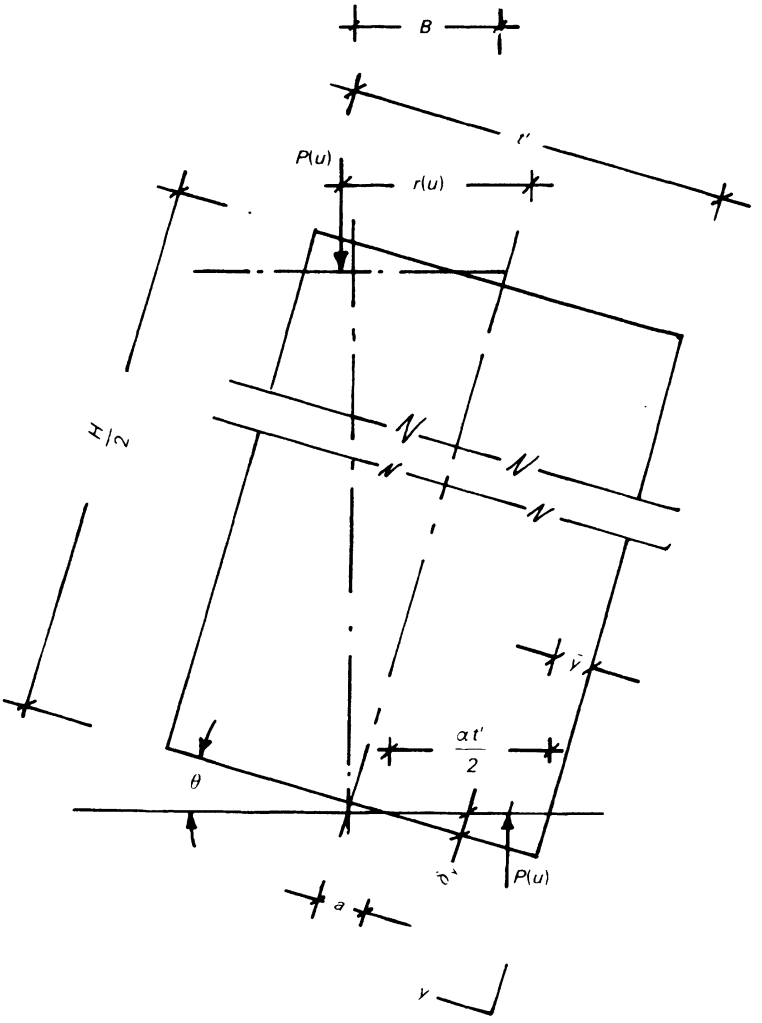

Figure 7.13 Analysis of laterally loaded strip wall with rigid boundary condition (McDowell *et al.*)

$$\alpha = \frac{1 + (u/S)^2}{1 - (u/S)^2} (1 - u/2)^2 \tag{7.25}$$

The shortening of the material at any position y is then

$$\delta_y = \frac{ut'(1 - 2g/t' - u/2)}{S\left[1 - (u/S)^2\right]} \tag{7.26}$$

The average strain along a fibre of the beam at a distance y from the bottom surface is

$$\varepsilon_{av} = \frac{2}{H}\delta_y \tag{7.27}$$

Each fibre of the half-wall is unstressed at one end where a crack develops, and the assumption is made that the strain varies linearly to zero at this end. The strain at the contact end is then given by

$$\begin{aligned}\varepsilon_y &= 2\varepsilon_{av} = \frac{4}{H}\delta_y \\ &= \frac{4u}{S^2}\frac{\left(1 - 2y/t' - u/2\right)}{\left[1 - \left(u/S\right)^2\right]}\end{aligned} \tag{7.28}$$

Introducing the non-dimensional parameter $R = (\varepsilon_c/4)S^2$ where ε_c is the maximum compressive strain in the material at failure, the following expression gives, to a close approximation

$$\varepsilon_y = \frac{u\varepsilon_0}{R}\left(1 - 2y/t' - u/2\right) \tag{7.29}$$

This equation expresses the distribution of strain along the contact area at the supports and at mid-height of the wall, and hence the distribution of stress. The arching force is then evaluated as the resultant of the stress distribution along the contact area by integrating across the depth of the wall. On the basis of this equation and the assumed material properties, the stress patterns shown in table 7.2 have been derived in terms of the deflection parameter u. The corresponding values of the arching force $P(u)$ are also shown. When the force $P(u)$ is known, the resistance moment is given by

$$M(u) = P(u)r(u) \tag{7.30}$$

where $r(u)$ is the lever arm, given approximately by

$$r(u) = t(1 - u - 2y/t') \tag{7.31}$$

From these equations and a knowledge of the maximum compressive strain at failure it is possible to calculate the resistance of the wall to lateral pressure. McDowell *et al.* used these relations to calculate the resistance of panels to blast from atomic explosions. Morton [27] produced a similar solution for the pressure pulse resulting from a gas explosion, and Wilton *et al.* [33] modified the original theory in applying it to the results of their shock-tunnel experiments.

7.4.2 *Walls supported on four sides*

The theory described in section 7.4.1 relates to a strip wall. If the wall is similarly restrained on its vertical edges, the problem becomes con-

Table 7.2 Solution for strip wall laterally loaded between unyielding supports [28]

Range of R	*Range of u*	*Stress patterns*	$\frac{8}{\sigma_c t'} P(u)$	$\frac{16}{\sigma_c (t')^2} M(u)$
$R \geqslant \frac{1}{2}$ $R < \frac{1}{2}$	$u \geqslant 0$ $0 \leqslant u \leqslant 1 - \sqrt{(1-2R)}$	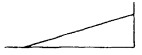	$\frac{2u}{R}\left(1-\frac{u}{2}\right)^2$	$\frac{8u}{3R}\left(1-\frac{5u}{4}\right)\left(1-\frac{u}{2}\right)^2$
$R < \frac{1}{2}$	$1-\sqrt{(1-2R)} \leqslant u < \sqrt{(2R)}$	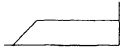	$4\left(1-\frac{u}{2}-\frac{R}{2u}\right)$	$4\left(1+\frac{R}{2}+\frac{3u^2}{4}\right)-2u-\frac{R^2}{3u^2}$
	$\sqrt{(2R)} \leqslant u < 1$	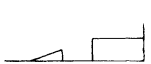	$4(1-u)+\frac{u}{2R}\left[2\sqrt{(2R)}-u\right]^2$	$4(1-u)^2+\frac{u}{6R}\left[2\sqrt{(2R)}-u\right]^2\left(5u-4\sqrt{2R}\right)$
$\frac{1}{8} \leqslant R < \frac{1}{2}$	$1 \leqslant u < 2\sqrt{(2R)}$	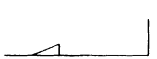	$\frac{u}{2R}\left(2\sqrt{(2R)}-u\right)^2$	$\frac{u}{6R}\left[2\sqrt{(2R)}-u\right]^2\left(5u-4\sqrt{2R}\right)$
	$u \geqslant 2\sqrt{(2R)}$		0	
	$\sqrt{(2R)} \leqslant u < 2\sqrt{(2R}$	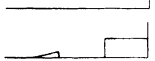	$4(1-u)+\frac{u}{2R}\left[2\sqrt{(2R)}-u\right]^2$	$4(1-u)^2+\frac{u}{6R}\left[2\sqrt{(2R)}-u\right]^2\left(5u-4\sqrt{2R}\right)$
$R < 1/8$	$2\sqrt{(2R)} \leqslant u < 1$	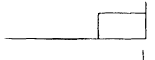	$4(1-u)$	$4(1-u)^2$
	$u \geqslant 1$	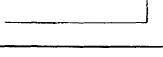	0	0

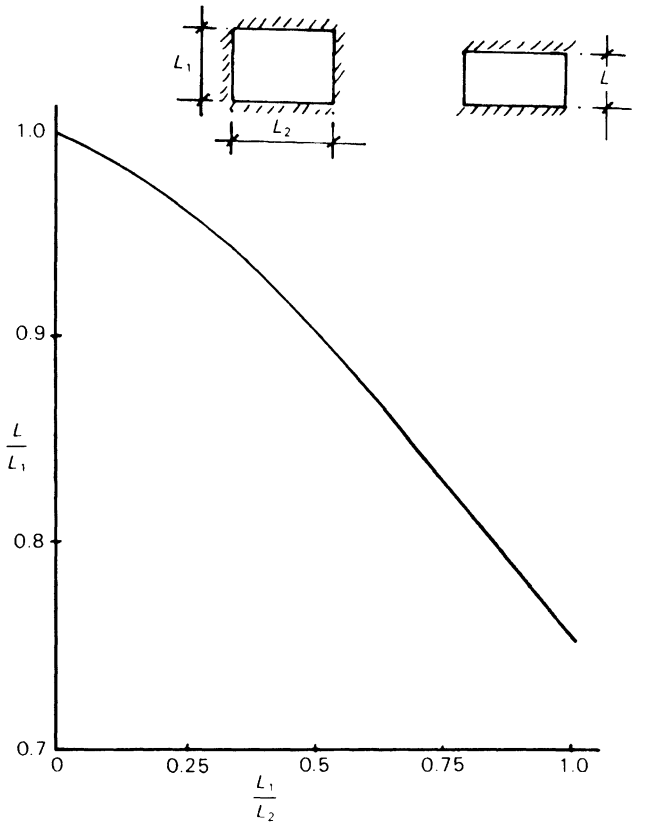

Figure 7.14 Equivalent one-way spanning panel for wall simply supported on four sides (McKee and Sevin)

siderably more complicated; McKee and Sevin [29] have proposed the empirical curve shown in figure 7.14 which permits the substitution of an equivalent 'one-way' panel for one of side and base dimensions L_1 and L_2. Taking values of $\sigma_c = 7\,\text{N/mm}^2$, $\varepsilon_c = 0.001$ in Morton's solution and using the equivalent wall coefficient gives the curve of lateral pressure at failure against slenderness ratio S shown in figure 7.15. Also shown in this diagram are curves indicating the limitation of lateral resistance which results from the wall being pushed out of the restraining structure by shear failure around its perimeter, which is liable to occur at low values of S.

A few experimental test results have been plotted on figure 7.15. Three of these, reported by Thomas [37] were 'static' tests in which panels were built into a concrete encased steel frame and loaded by hydraulic jacks. Two others were obtained as part of an extensive investigation into the effects of gas explosions, carried out by the British Ceramic Research

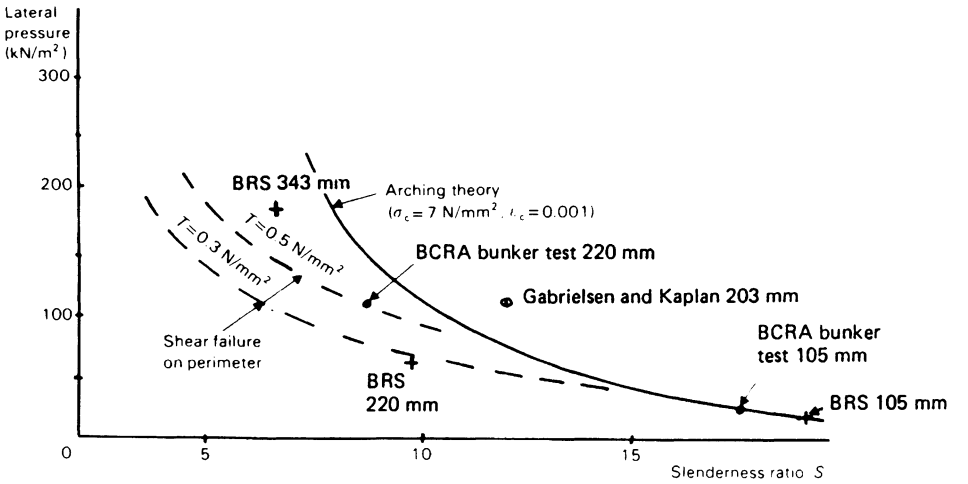

Figure 7.15 Lateral strength of infill panels restrained on four sides (after Morton)

Association [38]. In these cases, the walls were built into the end of a heavy concrete bunker and loaded by exploding a gas–air mixture in the bunker. The remaining result is from the tests reported by Gabrielsen and Kaplan [39].

In the case of walls having a slenderness ratio of 10 or less, there was evidence of shear failure around the perimeter. The other walls showed very clearly that failure followed the 'yield line' pattern of fracture lines also noted in the tests on simply supported panels. It would appear from these results that the lateral resistance of fully restrained panels can be estimated with fair accuracy, even though there is some uncertainty about the ultimate strength and strain values that should be used in the calculation.

In the foregoing it has been assumed that the brickwork panel is tightly built into the surrounding structure. If there is a gap between the wall and the restraining structure it is still possible for arching to develop after initial cracking of the brickwork. Gabrielsen and Kaplan [39] have investigated this case and have shown that a wall with a small gap between the top edge and the support frame developed about 16 per cent of the strength of a fully restrained wall. This, however, was still some three times the strength of a corresponding wall tested with simple support conditions.

7.4.3 *An approximate theory for infill panels*

The analysis described in section 7.4.2 is rather complex, and for approximate calculations Hodgkinson *et al.* [40] have suggested the simple analytical model shown in figure 7.16. This assumes that, at failure, the bearing

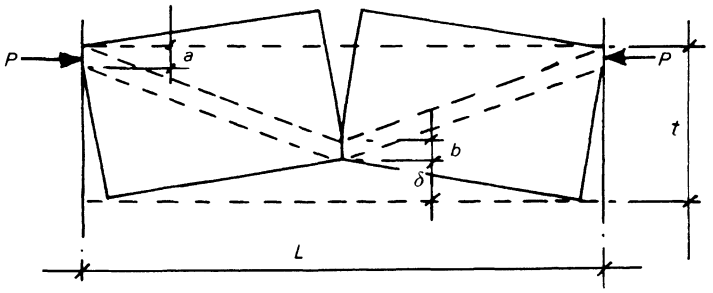

Figure 7.16 Approximate arching theory (Hodgkinson *et al.*)

width at the supports and at the centre of the wall is a and the lateral pressure at failure is given by

$$p_a = \frac{8P(t - a - \delta)}{L^2} \tag{7.32}$$

where P is the arch thrust
t is the wall thickness
L is the span
δ is the deflection at mid-height.

Appropriate values of a and of the compressive strength f_k under the conditions in an arching situation have been suggested on the basis of experimental results. A number of walls were tested, spanning horizontally between rigid supports 2.72 m apart, with the results summarised in table 7.3.

The thrust has been calculated from equation 7.32 for two assumed values of a and taking the deflection either as found experimentally or zero. The thrust stress has been related to the characteristic strength for the brickwork as given in BS 5628. As a result, it is suggested that for design purposes the bearing width a should be taken as $t/10$, the deflection omitted

Table 7.3 Summary of arching tests on horizontally spanning walls

Brick type	*Characteristic strength of brickwork, f_k (N/mm^2)*	*Failure pressure of wall (kN/m^2)*	*Deflection at failure (mm)*	*Thrust stress/f_k*			
				Including deflection Assumed a		*Excluding deflection*	
				t/10	*t/5*	*t/10*	*t/5*
A	16.0	32.9	20	2.5	1.5	2.0	1.1
B	6.4	21.0	27	4.6	2.7	3.3	1.8

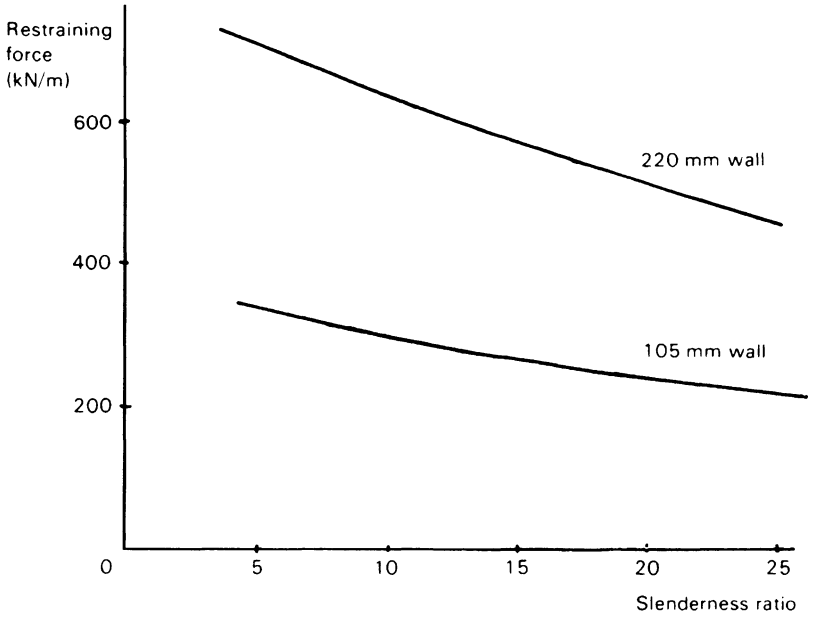

Figure 7.17 Forces required to develop full strength of 105 mm and 220 mm walls by arching action

and the thrust stress limited to 1.5 times the value of f_k. These proposals are of a tentative nature, but could be applied with reasonable confidence to panels spanning between two rigid supports, and in particular to those spanning horizontally which are unsupported on their top edges, and which rest on a damp-proof course at their bases.

Attention should be drawn to the magnitude of the restraining forces generated by arching action; by way of illustration, the curves of figure 7.17 have been derived from Morton's theory. From this figure it will be seen that considerable forces are required to develop the full strength of an infill panel and, conversely, large forces may be imposed on the surrounding structure if a brickwork panel is loaded to failure by lateral pressure.

References

1. A. Losberg and S. Johansson, 'Sideways Pressure on Masonry Walls of Brickwork', *CIB Symposium on Bearing Walls* (Warsaw) 1969.
2. A. Hallquist, 'Lateral Loads on Masonry Walls', *Reprint 172* (Norwegian Building Research Institute, Oslo, 1970).
3. K. M. H. Satti, 'Model Brickwork Panels under Lateral Loading', PhD Thesis (University of Edinburgh, 1972).

4. A. M. A. Kheir, 'Brickwork Panels under Lateral Loading', M.Phil. Thesis (University of Edinburgh, 1975).
5. L. R. Baker, 'Flexural Strength of Brickwork Panels', *Proceedings of the Third International Brick Masonry Conference* (Essen) 1973, eds L. Foertig and K. Gobel (Bundesverband der Deutschen Ziegelindustrie, Bonn, 1975), pp. 378–83.
6. B. P. Sinha, M. D. Loftus and R. Temple, 'Lateral Strength of Model Brickwork Panels', *Proc. Instn Civ. Engrs.*, **67** (1979) 191–8.
7. H. W. H. West, H. R. Hodgkinson and W. F. Webb, 'Lateral Loading Tests on Walls with Different Boundary Conditions', *Proceedings of the Third International Brick Masonry Conference* (Essen) 1973, eds L. Foertig and K. Gobel (Bundesverband der Deutschen Ziegelindustrie, Bonn, 1975), pp. 180–6.
8. H. W. H. West and H. R. Hodgkinson, 'The Lateral Load Resistance of Brickwork without Precompression', *Proc. Br. Ceram. Soc.*, **24** (1975) 101–13.
9. H. W. H. West and B. A. Haseltine, 'The Design of Laterally Loaded Walls', *Proceedings of the Fourth International Brick Masonry Conference* (Brugge) 1976, Paper 4.b.10.
10. H. W. H. West, H. R. Hodgkinson and B. A. Haseltine, 'The Resistance of Brickwork to Lateral Loading, Part 1, Experimental Methods and Results of Tests on Small Specimens and Full Sized Walls', *Struct. Engr.*, **55** (1977) 411–21.
11. B. A. Haseltine, H. W. H. West and J. N. Tutt, 'The Resistance of Brickwork to Lateral Loading, Part 2, Design of Walls to Resist Lateral Loading', *Struct. Engr.*, **55** (1977) 422–30.
12. L. R. Baker, 'The Lateral Strength of Brickwork – An Overview', *Proc. Br. Ceram. Soc.*, **27** (1978) 169–88.
13. C. Anderson, 'Transverse Laterally Loaded Tests on Single Leaf and Cavity Walls', *Proceedings of the Third International Symposium on Wall Structures, C.I.B.* (COBPBO, Warsaw) 1984, pp. 93–103.
14. S. J. Lawrence, 'Behaviour of Brick Masonry Walls under Lateral Loading' PhD Thesis (2 volumes) (University of New South Wales, 1983).
15. L. R. Baker, 'Lateral Loading of Masonry Panels – A State of the Art Report', *Seminar/Workshop on Planning, Design, Construction of Load Bearing Brick Buildings for Developing Countries* (Delhi) 1981 (Dept. of Civil Engineering and Building Science, University of Edinburgh, 1981), pp. 168–88.
16. L. R. Baker, 'A Failure Criterion for Brickwork in Bi-axial Bending', *Proceedings of the Fifth International Brick Masonry Conference* (Washington) 1979.
17. B. P. Sinha, C. L. Ng and R. F. Pedreschi, 'Failure Criterion and Behaviour of Brickwork in Biaxial Bending', *J. Mat. Civ. Eng. A.S.C.E.*, **9** (2) (1997).
18. B. P. Sinha, 'A Simplified Ultimate Load Analysis of Laterally Loaded Model Orthotropic Brickwork Panels of Low Tensile Strength', *Struc. Eng.*, **56** (4) (1978) 81–4.
19. V. L. Chong, C. Southcombe and I. M. May, 'The Behaviour of Laterally Loaded Masonry Panels with Openings', *Proc. Br. Masonry Soc.*, **6** (1994) 178–82.
20. R. B. Duarte and B. P. Sinha, 'Lateral Strength of Brickwork Panels with Openings', *Proc. Inst. Civ. Eng. Structs Buildings*, **94** (1992) 397–402.

21. W. G. Curtin and G. Shaw, *Brick Diaphragm Walls in Tall Single-Storey Buildings* (Brick Development Association, 1977).
22. W. G. Curtin and G. Shaw, *Design of Brick Fin Walls in Tall Single-Storey Buildings* (Brick Development Association, Windsor, 1980).
23. M. Phipps and T. I. Montague, *Diaphragm Walls* (Aggregate Concrete Block Association, Leicester, 1987).
24. H. W. H. West, H. R. Hodgkinson and W. F. Webb, 'The Resistance of Brick Walls to Lateral Loading', *Proc. Br. Ceram. Soc.*, **21** (1973) 141–64.
25. A. W. Hendry, B. P. Sinha and A. H. P. Maurenbrecher, 'Full Scale Tests on the Lateral Strength of Brick Cavity Walls', *Proc. Br. Ceram. Soc.*, **21** (1973) 165–80.
26. J. Morton and A. W. Hendry, 'An Experimental Investigation of the Lateral Strength of Brickwork Panels with Precompression under Dynamic and Static Loading', *Proceedings of the Third International Brick Masonry Conference* (Essen) 1973, eds L. Foertig and K. Gobel (Bundesverband der Deutschen Ziegelindustrie, Bonn, 1975), pp. 362–9.
27. J. Morton, 'A Theoretical and Experimental Investigation of the Static and Dynamic Lateral Resistance of Brickwork Panels with Reference to Damage by Gas Explosion', PhD Thesis (University of Edinburgh, 1970).
28. E. L. McDowell, K. E. McKee and E. Sevin, 'Arching Action Theory of Masonry Walls', *J. Struct. Div. Am. Soc. Civ. Engrs.*, **123** (1958).
29. K. E. McKee and E. Sevin, 'Design of Masonry Walls for Blast Loading', *Trans. Am. Soc. Civ. Engrs.*, **124** (1959) 457–71.
30. A. B. Willoughby, C. Wilton, B. L. Gabrielsen and J. V. Zaccor, 'Loading Structural Response and Debris Characteristics of Wall Panels, *URS 680-5* (URS Research Co., San Mateo, Calif., 1969).
31. C. Wilton, B. Gabrielsen, J. Edmunds and S. Bechtel, 'Loading and Structural Response of Wall Panels', *URS 709-4* (URS Research Co., San Mateo, Calif., 1969).
32. C. Wilton and B. L. Gabrielsen, 'Shock Tunnel Tests of Preloaded and Arched Wall Panels', *URS 7030-10* (URS Research Co., San Mateo, Calif., 1973).
33. C. Wilton, B. Kaplan, B. L. Gabrielsen and J. V. Zaccor, 'Blast/Fire Interaction, Blast Translation and Toxic Gases', *SSI 743-8* (Scientific Services Inc., Redwood City, Calif., 1976).
34. B. L. Gabrielsen and C. Wilton, 'Shock Tunnel Tests of Arched Wall Panels', *URS 7030-19* (URS Research Co., San Mateo, Calif., 1974).
35. B. L. Gabrielsen, K. Kaplan and C. Wilton, 'A Study of Arching in Non-Reinforced Masonry Walls', *SSI 748-1* (Scientific Services Inc., Redwood City, Calif., 1975).
36. B. L. Gabrielsen, C. Wilton and K. Kaplan, 'Response of Arching Walls and Debris from Interior Walls Caused by Blast Loading', *URS 7030-23* (URS Research Co., San Mateo, Calif., 1975).
37. F. G. Thomas, 'The Strength of Brickwork', *Struct. Engr.*, **31** (1953) 35–46.
38. N. F. Astbury, 'Gas Explosions in Load Bearing Brickwork Structures', *Special Publication No. 68* (British Ceramic Research Association, Stoke-on-Trent, 1970).
39. B. L. Gabrielsen and K. Kaplan, 'Arching in Masonry Walls Subjected to Out-of-plane Forces. Earthquake Resistant Masonry Construction: National

Workshop', *NBS Building Science Series No. 106* (Boulder, Colo., 1976), pp. 283–313.

40. H. R. Hodgkinson, B. A. Haseltine and H. W. H. West, 'Preliminary Tests on the Effect of Arching in Laterally Loaded Walls', *Proceedings of the Fourth International Brick Masonry Conference* (Brugge) 1976, Paper 4.a.5.

8 REINFORCED AND PRESTRESSED MASONRY

8.1 **The application of reinforced and prestressed elements**

The brittle nature of masonry is no great disadvantage in situations where the load to be transmitted is vertical and compressive stresses predominate. It does, however, put severe restrictions on its use for elements in which significant tensile stresses are developed, and to overcome this limitation it may be useful to use reinforced or prestressed members. Special problems also arise in structures in seismic areas and in relation to resistance to accidental damage which may necessitate the use of reinforcement.

There are three basic ways of introducing reinforcing steel into brickwork construction: by placing it

(a) Within the mortar joints
(b) In specially formed pockets
(c) In a grouted cavity between skins of brickwork.

Similar possibilities exist for reinforcing blockwork construction, but in this case there is greater scope for the use of specially shaped units and for the incorporation of reinforcement in the cores of hollow blocks. These methods are illustrated in figure 8.1.

The flexural limitations of masonry can also be overcome by the use of prestressing techniques, although practical application of this method has so far been limited.

8.2 **Reinforced masonry flexural elements**

Early research work [1–10] indicated that the principles underlying the design of reinforced concrete could be applied also to reinforced masonry, provided that suitable adjustments are made for the differences in material properties.

Reinforced masonry may thus be designed on the basis of linear elasticity

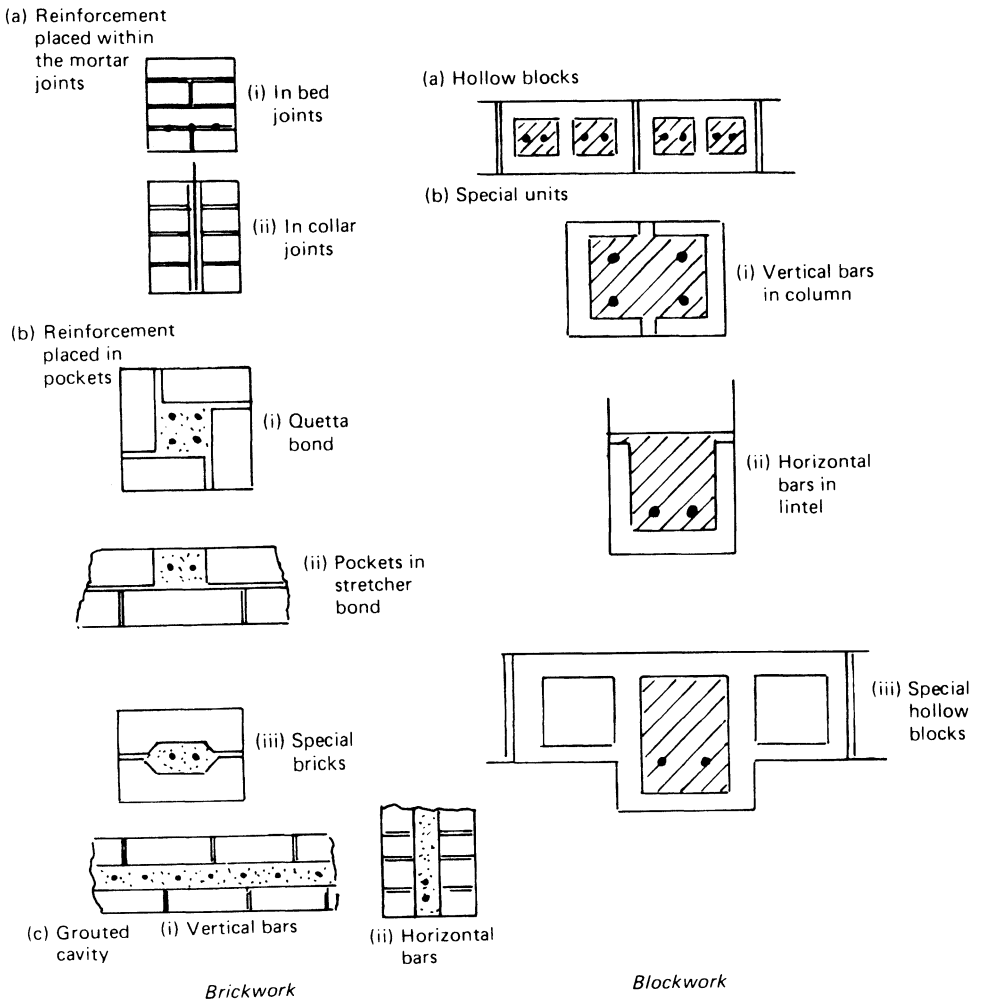

Figure 8.1 Methods of reinforcing brickwork and blockwork

or in relation to ultimate strength. Calculations relating to the serviceability limit state of deflection will be based on elastic behaviour, while those relating to the ultimate limit state will require assumptions as to the stress–strain relationship up to the ultimate load. Values for the elastic modulus, and discussion of actual stress–strain curves, may be found in chapter 2; idealised stress–strain curves for masonry and reinforcing steel will be discussed in section 8.2.2. It is usual to assume that in flexural elements, plane sections remain plane after bending and that the tensile strength of masonry may be neglected.

8.2.1 *Flexural strength of reinforced masonry*

On the above assumptions it is possible to derive expressions for the moment of resistance of a reinforced masonry section in the same way as for reinforced concrete. Thus, on the basis of linear elastic theory, for a rectangular section

$$M = \frac{1}{2} b x f_{bc} \left(d - \frac{x}{3} \right) = A_s f_s \left(d - \frac{x}{3} \right) \tag{8.1}$$

where b is the width of section
x is the depth of neutral axis
f_{bc} is the permissible compressive stress in masonry
d is the effective depth of section
A_s is the area of steel reinforcement
f_s is the permissible tensile stress in steel.

The depth of the neutral axis can be calculated from the equation

$$bx^2 + 2\alpha_e x A_s - 2\alpha_e d A_s = 0 \tag{8.2}$$

where α_e is the modular ratio.

If the steel area is such that f_{bc} and f_s are reached simultaneously:

$$\frac{x}{d} = \frac{1}{1 + \left(f_s / \alpha_e f_{bc} \right)} \tag{8.3}$$

Values of permissible stresses are specified in design codes for various mortar combinations. The modular ratio is a function of the compressive strength, and will lie in the range 10–40 for strong to relatively weak masonry.

Design codes are now tending to be based on limit state principles, and thus for consideration of the ultimate limit state a non-linear stress block has to be considered. In this case the section analysis again follows the precedent of reinforced concrete. Thus, referring to figure 8.2 and following the theory described by Kong and Evans [11] for a singly reinforced beam, we have

$$k_1 f_k b x = A_s f_s$$

or

$$f_s = \frac{k_1 f_k b}{A_s} x \tag{8.4}$$

and

$$x = \frac{\varepsilon_k}{\varepsilon_k + \varepsilon_s} d \tag{8.5}$$

Combining equations 8.4 and 8.5 gives

$$f_s = \frac{k_1 f_k}{\varrho} \frac{\varepsilon_k}{\varepsilon_k + \varepsilon_s} \tag{8.6}$$

where ϱ is the steel ratio A_s/bd.

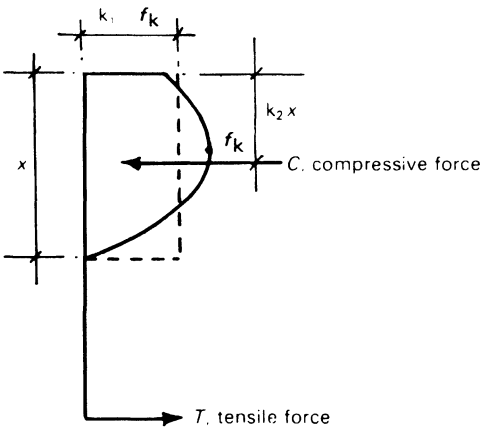

Figure 8.2 Stress distribution in singly reinforced beam

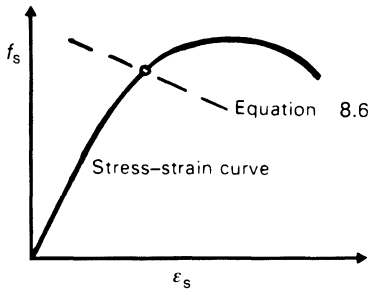

Figure 8.3 Intersection of equation 8.6 with stress–strain curve for steel

At the ultimate limit state, the values of f_s and ε_s must satisfy equation 8.6, and also define a point on the stress–strain curve for the steel, as indicated in figure 8.3. The moment of resistance is then

$$M_u = A_s f_s (d - k_2 x)$$
$$= A_s f_s \left(1 - \varrho \frac{k_2}{k_1} \frac{f_s}{f_k}\right) d \qquad (8.7)$$

The term within the brackets in equation 8.7 is the lever arm factor for the beam.

As in reinforced concrete, the mode of failure of a masonry beam, reinforced with steel having a definite yield point, depends on the steel ratio ϱ. If the steel and masonry strains reach ε_y and ε_k simultaneously this is termed a 'balanced' section, in which

$$\frac{x}{d} = \frac{\varepsilon_k}{\varepsilon_k + \varepsilon_y} \qquad (8.8)$$

Substituting in equation 8.6 gives the steel ratio for this condition as

$$\varrho = k_1 \frac{f_k}{f_y} \frac{\varepsilon_k}{\varepsilon_k + \varepsilon_y} \tag{8.9}$$

If the steel ratio is less than this, failure of the beam, described as 'under-reinforced', is initiated by yielding of the steel, but the beam will continue to resist increased bending moment until the strain in the brickwork reaches ε_k. Conversely, in an over-reinforced beam, failure will follow the attainment of ε_k in the brickwork. In this case it can be shown that

$$\frac{k_1 f_k}{\varepsilon_s}\left(\frac{x}{d}\right)^2 + \varepsilon_k\left(\frac{x}{d}\right) - \varepsilon_k = 0 \tag{8.10}$$

The neutral-axis factor x/d can be calculated from this equation, and the moment of resistance from

$$M_u = k_1 f_k bx(d - k_2 x) \tag{8.11}$$

In practice, over-reinforced masonry beams are to be avoided on account of their brittle mode of failure.

In the above discussion, the stress block for reinforced masonry beams has been characterised by the two ratios k_1 and k_2. Investigation of the stress–strain relationship for brick masonry, as discussed in chapter 2, has indicated that this may be represented by a second-degree parabola in which the strain at maximum stress is ε_m and at failure ε_u. Depending on the ratio of ε_u to ε_m, the values of k_1 and k_2 are as follows:

$\varepsilon_u/\varepsilon_m$	1.0	1.5	1.75
k_1	0.667	0.75	0.729
k_2	0.375	0.417	0.45

An average value of $\varepsilon_u/\varepsilon_m$ of 1.5 would be appropriate for practical purposes.

In design codes it is usual to adopt an equivalent rectangular stress block and the actual parabolic form may be represented, as shown in figure 8.4, by taking either (a) a mean stress which will give the same area within the enclosed rectangle or (b) by taking a maximum strain ordinate to give the same effect.

Rewriting equation 8.7 in the form

$$\frac{M}{bd^2 f_k} = \varrho \frac{f_y}{f_k}\left(1 - X\varrho \frac{f_y}{f_k}\right) \tag{8.12}$$

the values of X for a parabola and for approximations (a) and (b) are as follows:

Parabola	$X = 0.617$
Approximation (a)	$X = 0.685$
Approximation (b)	$X = 0.50$

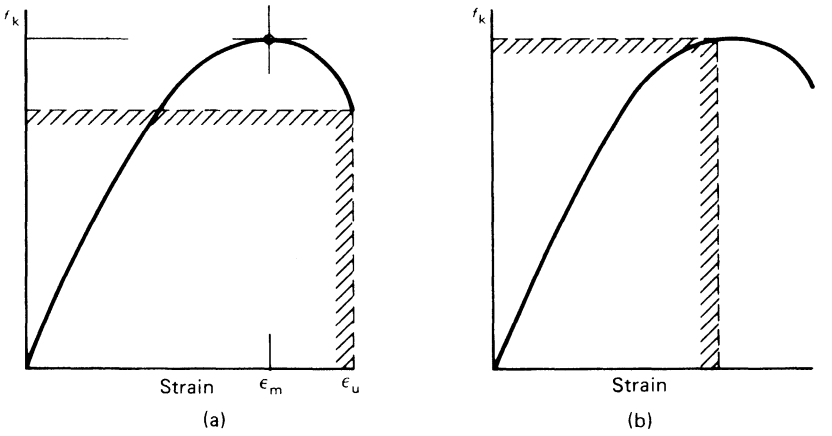

Figure 8.4 Alternative approximations for parabolic stress block

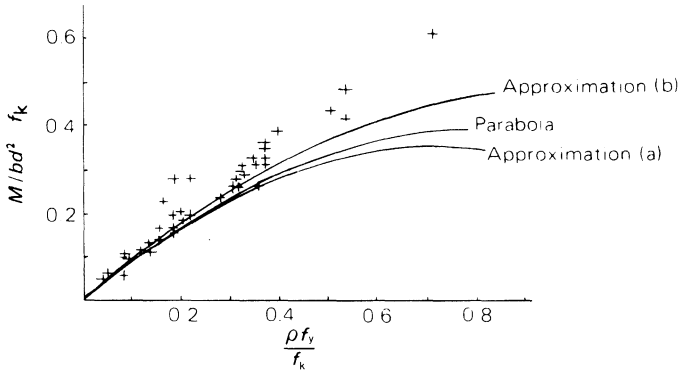

Figure 8.5 Test results for reinforced brickwork beams

A comparison between equation 8.12 and the collected experimental results is presented in figure 8.5 from which it will be seen that for values $\varrho \times f_y/f_k$ up to 0.5 there is little difference between the three cases. At higher values of $\varrho \times f_y/f_k$, taking $X = 0.50$ results in closer agreement with test results but such values are unlikely to occur in practice. Similar results have been obtained for reinforced blockwork [12].

Introducing partial safety factors for steel (γ_{ms}) and masonry (γ_{mm}) gives the following limit state design formula for rectangular section beams:

$$M_d = \varrho \frac{f_y}{\gamma_{ms}} bd^2 \frac{z}{d} \tag{8.13}$$

where

$$\frac{z}{d} = \left(1.0 - 0.5\varrho \frac{f_y}{f_k} \frac{\gamma_{mm}}{\gamma_{ms}}\right) \not> 0.95 \tag{8.14}$$

To avoid brittle failure, the value of M_d in equation 8.13 should be limited to

$$0.4\frac{f_k}{\gamma_{mm}}bd^2 \tag{8.15}$$

8.2.2 *Shear strength of reinforced masonry beams*

The shear strength of reinforced beams of various types has been studied by a number of investigators and, although the general pattern of behaviour is similar to that of reinforced concrete, there are a number of significant differences arising from the physical characteristics of the materials. Sinha and de Vekey [13] have shown that the shear resistance of grouted cavity brickwork beams is influenced by the shear span ratio and the percentage of reinforcement, and to a lesser extent by the brick and mortar strengths. Osman and Hendry [14] attempted to assess the contribution of compression zone transmission, aggregate interlock and dowel effect in developing shear resistance in this type of beam, the result for a typical test being shown in figure 8.6. As the latter two of these effects are likely to take place almost entirely in the concrete filling, it follows that the shear strength will depend on the width of the cavity [15] and that for beams of the same overall cross-section and reinforcement, grouted cavity beams will be intermediate between reinforced concrete and all-brick sections. This is shown in figure 8.7 where the shear strength is plotted against the shear span ratio for three different beam types.

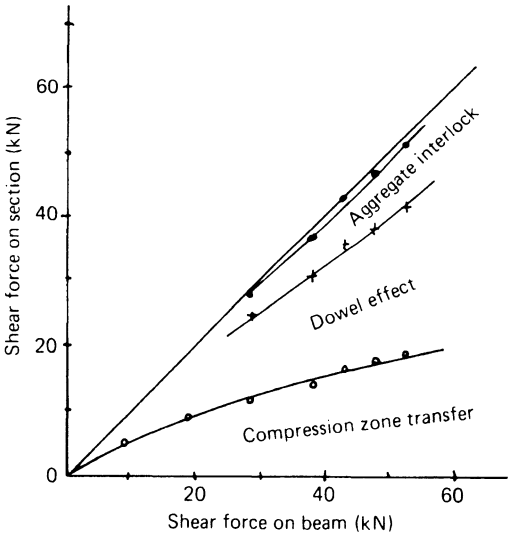

Figure 8.6 Shear transmission by different mechanisms in a grouted cavity beam

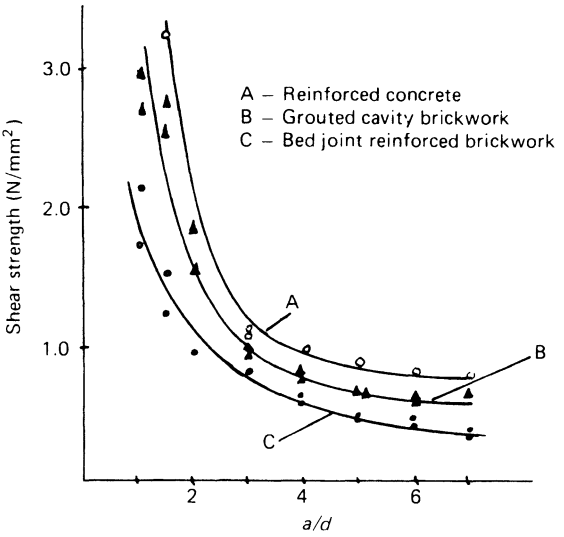

Figure 8.7 Shear strength of grouted cavity brickwork against shear span ratio (Suter and Keller)

Brickwork beams in which the reinforcement was placed in the lowermost bed joint were investigated by Suter and Hendry [16, 17] with the result shown in figure 8.8. Examination of collected test results for such beams confirmed that the steel ratio had no significant effect on the shear strength, presumably as dowel effect is not developed. Although there is considerable scatter in the results, there is a clear trend of increasing shear strength with decreasing ratio of shear span to effective depth (*a/d*). This effect is marked at *a/d* ratios of less than 2, and results from the mode of failure. Thus, at higher *a/d* ratios, shear failure follows from the development of a typical diagonal crack, whereas in beams with a low *a/d* ratio, cracking is followed by the development of a tied arch effect – the lower the shear span ratio the greater the arching effect and thus the apparent shear resistance.

The shear strength of reinforced concrete blockwork beams has been reviewed by Rathbone [18]. Where the beams are built in concrete-filled hollow blocks, the shear strengths are more closely related to corresponding reinforced concrete sections and there is an appreciable increase with steel percentage, as may be seen in figure 8.9. The effect of steel percentage for various types of beams is illustrated in figure 8.10. The *a/d* ratio for each beam is shown and approximate lines have been drawn for $a/d = 2, 4$ and 6 for beams in which the reinforcement is embedded in concrete. As already noted, where the reinforcement is placed in the lowermost bed joint of a brickwork section, there is no increase in shear strength with steel percentage. The British Code of Practice BS 5628: Part 2 gives a formula representing the lines shown in figure 8.9 for the shear strength of reinforced masonry

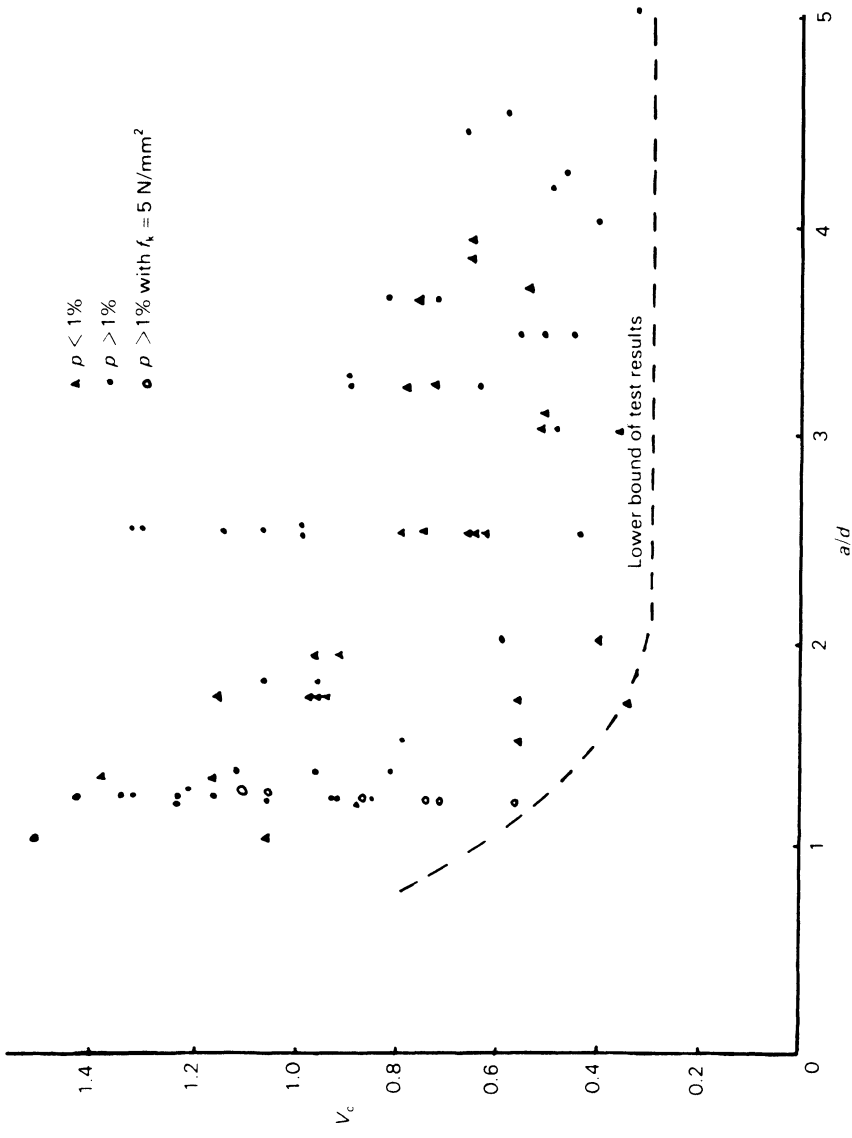

Figure 8.8 Collected test results for shear strength of reinforced brickwork beams against shear span ratio

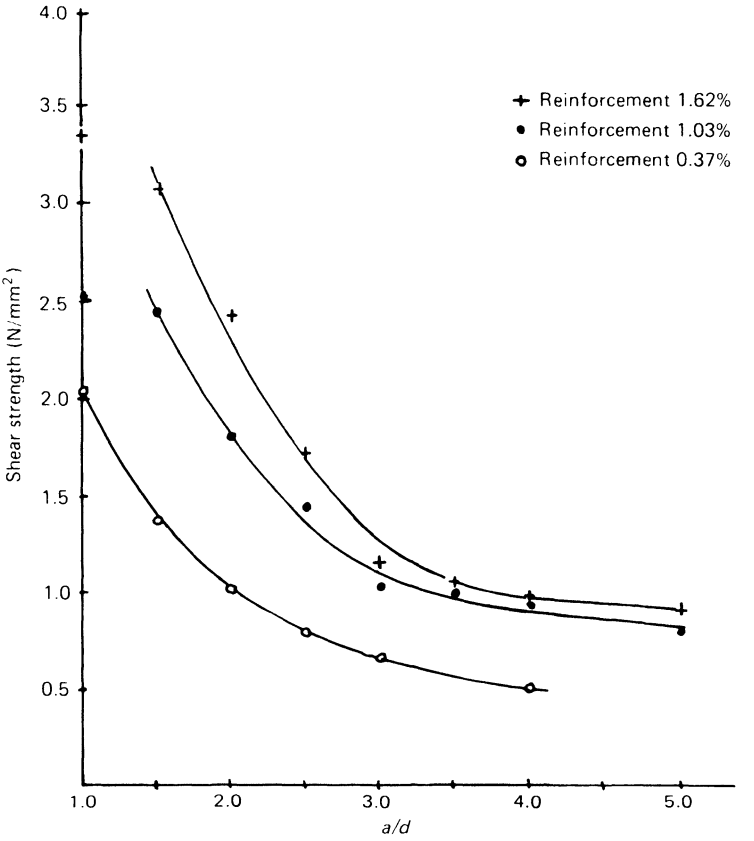

Figure 8.9 Shear strength of reinforced concrete blockwork beams against shear span ratio for three steel percentages (Rathbone)

in which the reinforcement is placed in concrete. Songbo Li *et al.* [19] have suggested that the validity of this formula is limited to beams having moderate amounts of reinforcement and moderate span/depth ratios. These authors recommend the use of the following equation derived from an analysis of test results for the shear capacity of a beam, V, which includes a parameter, R, relating to the material properties of the masonry:

$$V = \alpha Rbd\left[0.173 + 0.056\ln\left(\frac{A_s f_y}{Rbd}\right)\right] \tag{8.16}$$

where $\alpha = 1.996 - 0.994\ln(a/d)$

$R = 0.131R_1 + 0.277\sqrt{R_1 R_2}$

R_1 = block strength

R_2 = mortar strength.

The inclusion of shear reinforcement is possible in certain types of reinforced masonry beams, such as grouted cavity and concrete-filled hollow

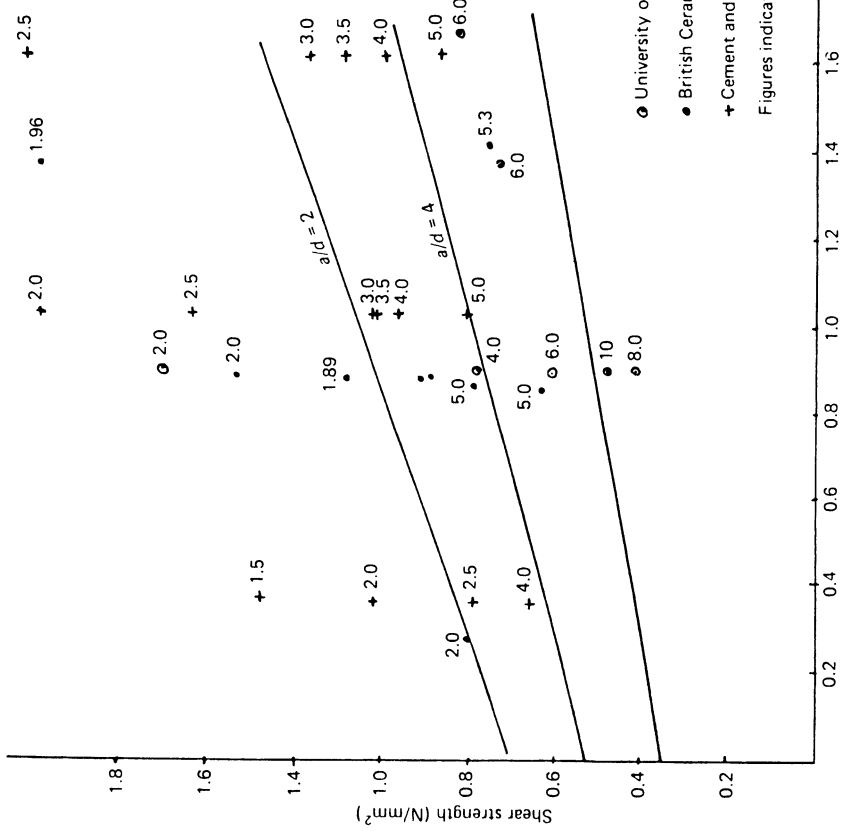

Figure 8.10 Shear strength of reinforced masonry beams showing effect of steel percentage and shear span ratio

blockwork. In brickwork sections it may be possible to form pockets in which vertical shear steel can be placed or a limited amount of reinforcement can be accommodated in the collar joint. There is very little experimental information as to the effectiveness of shear reinforcement apart from a series of tests carried out by the Structural Clay Products Institute [20] on three sets of beams, two of which had shear steel in the collar joints and the other had a grouted cavity construction. These results are summarised in table 8.1 from which it will be seen that the experimental shear strengths are considerably in excess of those to be expected without shear reinforcement. These enhanced shear strengths can be estimated with fair accuracy using the standard formula for the spacing of vertical stirrups. Omitting partial safety factors this formula is

$$f_{sv} = \left(f_v + A_{sv} f_y / b s_v\right) \tag{8.17}$$

where f_v = shear strength without shear steel
A_{sv} = shear steel area
f_y = yield stress of shear steel
b = breadth of section
s_v = spacing of stirrups.

In all but one case this gives a result in reasonable agreement with the experimental values in table 8.1.

For flexural design of reinforced masonry beams it is convenient to define a limit on failure by tensile yielding of the reinforcement beyond which shear failure may be expected in the absence of shear steel. Thus the shear stress in the beam, V/bd, must not exceed the shear strength f_v. Then if the shear span is taken as

$$a = M_{max}/V \tag{8.18}$$

the limiting condition for shear failure is

$$\frac{M_{max}}{(a/d)bd^2} \not> f_v \tag{8.19}$$

or

$$M_{max}/bd^2 \not> f_v(a/d) \tag{8.20}$$

This condition can be superimposed [12] on a design diagram in which the parameter M/bd^2 is plotted against the masonry strength. An example is shown in figure 8.11. From this it is evident that shear will be a limiting factor unless the steel ratio is less than about 0.003. Masonry compressive strength, on the other hand, has a rather limited influence on the moment of resistance.

8.2.3 *Calculation of deflection of reinforced masonry beams*

Tests on reinforced masonry beams have shown that the load–deflection relationship is bi-linear with a discontinuity occurring when the masonry

Table 8.1 SCPI tests on reinforced brickwork beams with shear reinforcement

Beam no.	*b (mm)*	$100A_{sv/bd}$	A_{sv} *(mm²)*	s_y *(mm)*	*Ult. shear stress (N/mm²)*	*Estimated shear strength** (N/mm²)*
S.7*	199	2.2	70.9	75	1.26	1.54
J.1†	349	1.99	258	75	2.40	2.81
J.2	324	2.09	258	75	2.51	3.00
J.3	324	2.09	258	75	1.9	3.00
AN4‡	229	1.38	200	203	1.44	1.43
AN5	229	1.38	200	203	1.86	1.43

*Brick compressive strength 63.4 N/mm², mortar mix 1:0.78:4.7.
†Brick compressive strength 18.1 N/mm², mortar mix 1:0.16:3.
‡Brick compressive strength 85.1 N/mm², mortar mix 1:0.5:4.5.
**$f_{sv} = (f_{vk} + A_s f_{yv}/bs_v)$ where $f_{vk} = 0.35\,\text{N/mm}^2$ and $f_y = 250\,\text{N/mm}^2$.

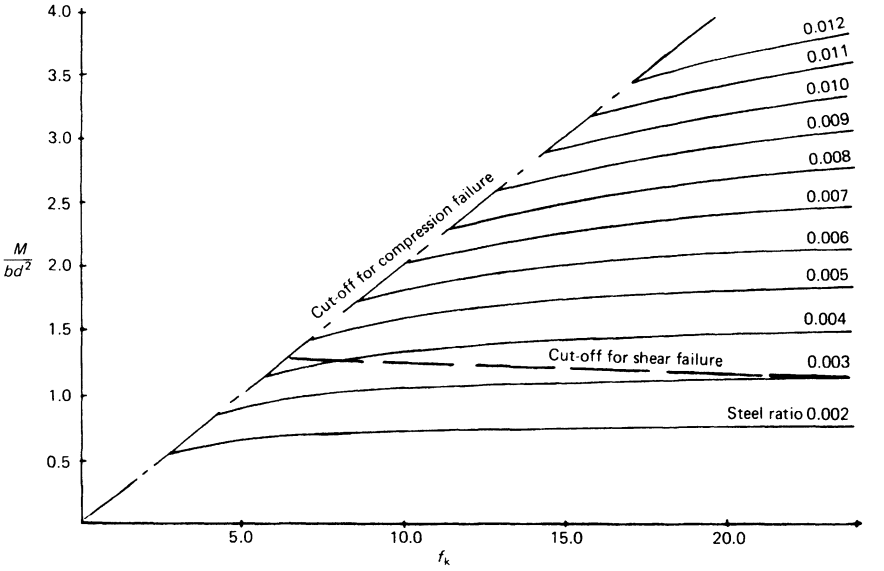

Figure 8.11 Limitation on flexural design of reinforced masonry beams by compression and shear failures (f_y = 460N/mm^2; γ_{ms} = 1.15; γ_{mm} = 2.0; γ_{mv} = 2.0)

cracks. Thus, initial deflection may be calculated on the basis of an uncracked section. Beyond this stage, a cracked section should be assumed and the following relationships for the neutral-axis depth and second moment of area are applicable, where ϱ is the steel ratio and α_e the modular ratio:

$$\frac{x}{d} = -\alpha_e \varrho + \sqrt{\left(\alpha_e^2 \varrho^2 + 2\alpha_e \varrho\right)} \tag{8.21}$$

and

$$I = \left[\frac{1}{3}\left(\frac{x}{d}\right)^3 + \alpha_e \varrho\left(1 - \frac{x}{d}\right)^2 + \alpha_e \varrho\left(\frac{x}{d}\right)^2\right] bd^3 \tag{8.22}$$

In practice, the effective second moment of area will vary along the length of a beam as the extent of cracking changes along the span, in the manner suggested in figure 8.12. Furthermore, tensile stresses will be developed in the material below the neutral axis between the cracks, and result in a stiffening effect. In reinforced concrete beams this effect can be allowed for by assuming the existence of a limited tensile stress in the concrete below the neutral axis, which reduces the moment on the cracked section used in calculating deflection by an amount equal to

$$\frac{1}{3}\frac{b(h-x)^3}{(d-x)} \times \text{tensile stress in concrete} \tag{8.23}$$

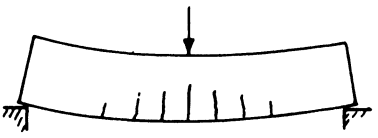

Figure 8.12 Variation of crack depth along the length of a beam

where h is the overall depth of the beam. In principle, this could be applied to reinforced brickwork beams, but experimental confirmation is lacking.

An alternative procedure [21] is to use the following moment curvature relationship:

$$\theta = \frac{M}{EI_u} + \frac{M - M_{cr}}{0.85EI_{cr}} \tag{8.24}$$

where M is the applied moment, EI_u the flexural rigidity of the transformed uncracked section, EI_{cr} the flexural rigidity of the transformed cracked section, M_{cr} the cracking moment equal to $I_u f_t/(H - d)$, f_t being the flexural tensile strength of the masonry, H the overall depth of the section, and d the neutral-axis depth. The relationship between curvature and mid-span deflection for various load conditions is as follows:

Concentrated load at mid-span	$\Delta = \theta L^2/12$
Uniformly distributed load	$\Delta = \theta L^2/9.6$
Equal end moments	$\Delta = \theta L^2/8$

The value of Young's modulus for brickwork is discussed in section 2.6. An approximate value of 900 f_k has been suggested for medium-strength reinforced clay brickwork, and this would be applicable to short-term loading but should be reduced by a factor of 2.0 when calculating long-term deflections. This is based on results reported by Wyatt *et al.* [22] and is confirmed by long-term loading experiments on grouted cavity cantilever walls carried out by Sinha [23, 24]. If, in the case of a cantilever wall, there is a non-rigid damp-proof course near the base, the creep deflections may be doubled.

8.3 **Reinforced masonry compression elements**

The strength of reinforced masonry compression elements has not been extensively investigated, presumably because in most practical situations it is possible to meet design requirements with unreinforced walls or columns. With axial loading, the addition of a low percentage of reinforcing steel will result in only a small increase in the load capacity of the member but, if more extensive use is made of reinforced masonry, the use of beam columns or walls transmitting substantial bending moments in addition to axial loads

may become more widespread and a knowledge of the strength of such elements will be required.

Tests [25, 26] on axially loaded reinforced masonry columns have confirmed that their strength could be regarded as the sum of the compressive strength of the masonry and of the steel at its yield point. The presence of lateral ties was found to add slightly to the strength of the column and to prevent complete collapse at the maximum load. Thus in limit state terms, the design capacity of a short compression member would be

$$N = \frac{f_k A_b}{\gamma_{mm}} + \frac{0.8 f_y A_{sc}}{\gamma_{ms}} \tag{8.25}$$

where A_b and A_{sc} are, respectively, the areas of brickwork and steel, and γ_{mm} and γ_{ms} are partial safety factors for these materials which have, respectively, characteristics f_k and f_y.

Consideration of the strength of reinforced masonry members under combined axial load and bending moment will be facilitated by referring to direct load–moment interaction diagrams, similar in principle to those referred to in section 5.5 for plain masonry. For this case, assuming for simplicity a rectangular stress block, and using the notation shown in figure 8.13

$$N_{bwk} = f_k b d_c \tag{8.26}$$

$$M_{bwk} = N\left(\frac{h}{2} - \frac{d_c}{2}\right) = 0.5 f_k b d_c (h - d_c) \tag{8.27}$$

or, in dimensionless form

$$\alpha_{bwk} = \frac{N_{bwk}}{f_k b h} = \frac{d_c}{h} \tag{8.28}$$

$$\beta_{bwk} = \frac{M_{bwk}}{f_k b h^2} = 0.5 \frac{d_c}{h}\left(1 - \frac{d_c}{h}\right) \tag{8.29}$$

By calculating α_{bwk} and β_{bwk} at various values of d_c/h between 0 and 1.0, the axial load–moment interaction curve shown in figure 8.14 is obtained.

If now an area of reinforcement A_{s2} is introduced at a depth of d_2 from the lower face of the beam as shown in figure 8.13b, this will contribute to the axial force by an amount

$$N(A_{s2}) = A_{s2} f_{s2} \tag{8.30}$$

where f_{s2} is the stress in the steel corresponding to a strain ε_{s2}. The moment about the mid-depth contributed by the steel is

$$M(A_{s2}) = -A_{s2} f_{s2}\left(\frac{h}{2} - d_2\right) \tag{8.31}$$

In dimensionless terms:

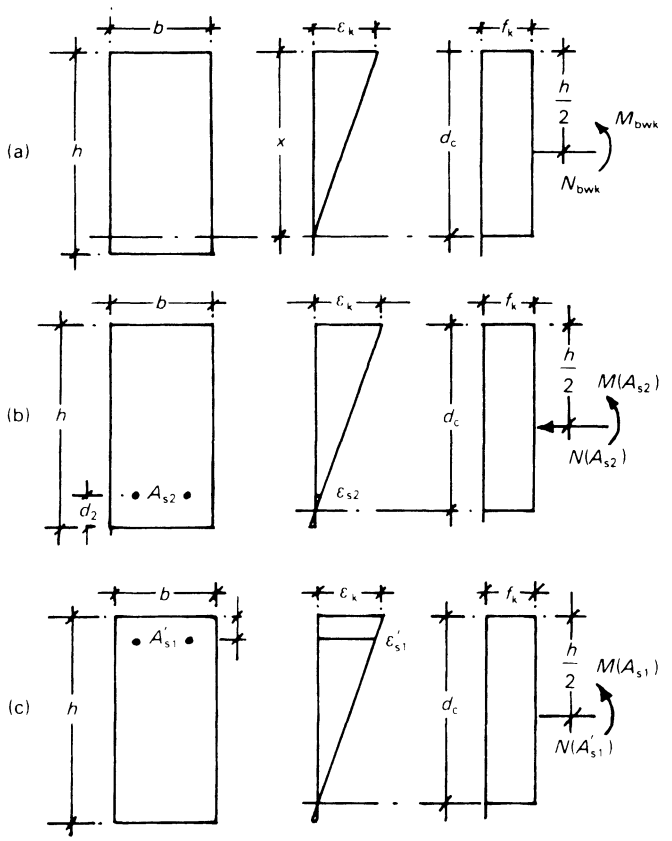

Figure 8.13 Strain and stress distributions: (a) in plain section; (b) with reinforcement A_{s2}; (c) with reinforcement A'_{s1}

$$\alpha_{s2} = \frac{N(A_{s2})}{f_k bh} = \frac{A_{s2}}{bh}\frac{f_{s2}}{f_k} \tag{8.32}$$

$$\beta_{s2} = \frac{M(A_{s2})}{f_k bh^2} = -\left(\frac{1}{2} - \frac{d_2}{h}\right)\alpha_{s2} \tag{8.33}$$

These parameters can be calculated for a given section using the relationship

$$\frac{\varepsilon_{s2}}{\varepsilon_k} = \frac{d_2 - (h - d_c)}{d_c} = \frac{d_c/h - (1 - d_2/h)}{d_c/h} \tag{8.34}$$

Thus, $f_{s2} = E_s\varepsilon_{s2}$, and hence α_{s2} and β_{s2} can be evaluated for various values of d_c/h. The effect of the reinforcement on the interaction diagram is represented by a vector $\sqrt{[(\alpha_{s2})^2 + (\beta_{s2})^2]}$ as shown in figure 8.14.

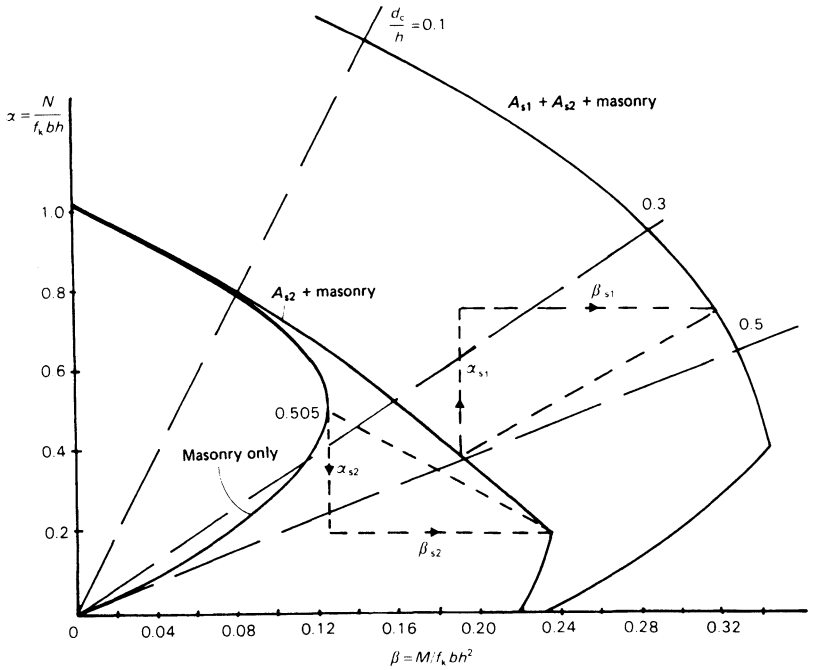

Figure 8.14 Axial force/bending moment interaction diagrams for plain and reinforced masonry sections

If reinforcement is introduced near the upper face of the beam, as shown in figure 8.13c, corresponding values of α_{s1} and β_{s1} are as follows:

$$\alpha_{s1} = \frac{N(A'_{s1})}{f_k bh} = \frac{A'_{s1}}{bh}\frac{f'_{s1}}{f_k} \tag{8.35}$$

$$\beta_{s1} = \frac{M(A'_{s1})}{f_k bh^2} = \left(\frac{1}{2} - \frac{d'}{h}\right)\alpha_{s1} \tag{8.36}$$

Also

$$\frac{\varepsilon_{s1}}{\varepsilon_k} = \frac{d_c - d'}{d_c} = \frac{d_c/h - d'/h}{d_c/h} \tag{8.37}$$

The effect of this reinforcement in addition to A_{s2} is then represented on the interaction diagram, figure 8.14, by the vector $\sqrt{[(\alpha_{s1})^2 + (\beta_{s2})^2]}$.

Figure 8.14 is based on illustrative values of the various terms; although the characteristics of these curves are fully discussed in reference 11, the following points may be noted:

(1) Considering the interaction diagram for A_{s2} steel when $d_c/h = 1 - d_2/h$, 0.85 for the example shown, the steel strain is zero, both α_{s2} and β_{s2} are zero and the steel is inactive.

(2) For the steel to reach the yield stress f_y in this case, $\varepsilon_s = 0.00205$. This occurs at a value of $d_c/h = 0.505$ for the example shown. This point defines the maximum value of β on the interaction diagram and corresponds to a 'balanced' failure, in which the steel and brick reach their limiting values simultaneously. In load–moment (N–M) combinations above this point, the brickwork will reach its limit before the steel and vice versa below this point.
(3) When both A'_{s1} and A_{s2} steel reinforcement is present, the maximum β again corresponds to the balanced failure condition.
(4) Load–moment combinations corresponding to specific eccentricity ratios lie on straight lines, as indicated in figure 8.14.

The interaction diagrams described above relate to short compression members. As mentioned in section 5.5, these curves can be modified using the moment magnifier method or otherwise to allow for the second-order effects from slenderness.

Experimental confirmation of the calculated interaction diagrams for reinforced brickwork is limited, but a series of tests by Anderson and Hoffman [27] showed good agreement with experimental results up to an eccentricity ratio of 0.34, as may be seen from figure 8.15. Other experimental investigations of reinforced brickwork and blockwork columns have been carried out by Drysdale and Sallam [28], Hatzinikolas *et al.* [29] and Davies and El Traify [30]. Again reasonable agreement is shown between test results and calculated interaction diagrams. Davies and El Traify have extended consideration to the case of biaxial eccentricity and have developed a computer program for the analysis of columns subjected to this loading condition. This results in the production of a set of interaction diagrams such as the one shown in figure 8.16, which is for an axial load ratio $P = N/(f_m BT)$ with the notation shown in the figure. The axes of the diagram are, respectively, $M_x/f_m BT^2$ and $M_y/f_m BT^2$. Curves are plotted on these axes for various values of the parameter A_s/BTf_m. Diagrams of this type can be used in two ways: firstly, if the values of M_x and M_y and the load ratio P are known, using an appropriate chart, the amount of reinforcement required can be determined. Secondly, if the axial load and reinforcement are known, acceptable combinations of M_x and M_y can be defined. In a design situation it would, of course, be necessary to introduce the relevant material partial safety factors.

8.4 **Reinforced masonry shear walls**

Reinforced masonry shear walls are usually adopted to meet the requirement for seismic resistant structures but could be used more generally where the shear strength of plain masonry walls is found to be insufficient. Shear reinforcement may be placed in the core of grouted cavity walls, in collar and bed joints or in the cores of hollow block units. It has been suggested [31] that horizontal bars are more effective than vertical on the

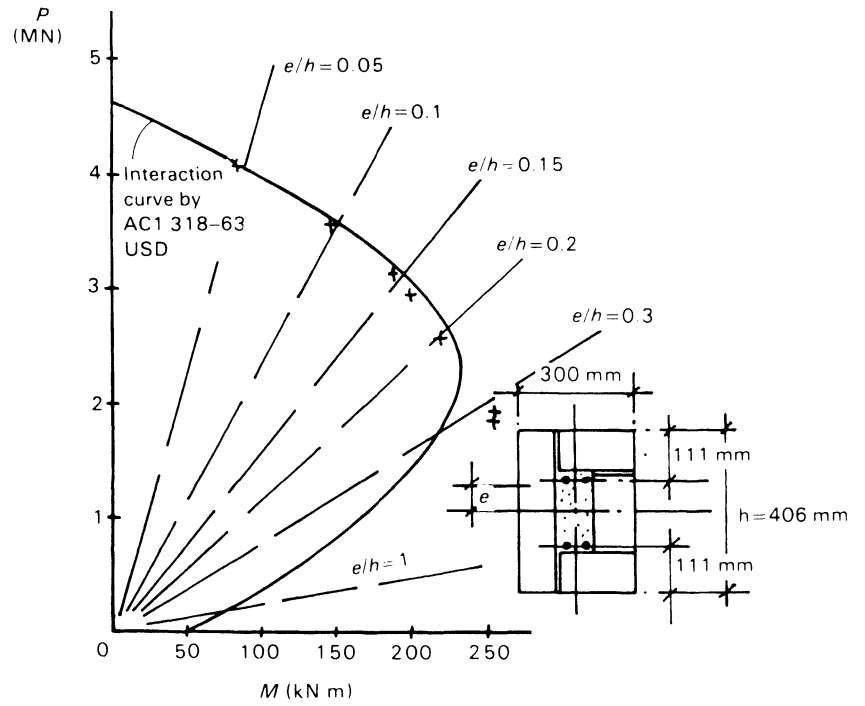

Figure 8.15 Results of tests on eccentrically loaded reinforced brickwork columns compared with calculated interaction curve (Anderson and Hoffman). Brick strength 93 N/mm^2; mortar ASTM 270 type S; grout 25 N/mm^2 av.; masonry strength 36 N/mm^2; steel ASTM A 15–4, f_v = 275 N/mm^2, 4 no. 16 mm dia. bars

basis that under racking shear, a wall will fail by the development of a diagonal crack; relative movement across the crack is resisted by dowel action by vertical steel, but by direct tension by horizontal reinforcement. This would apply where the horizontal steel is fully embedded in concrete fill, as in a grouted cavity wall, but would not be reliable where the reinforcement was placed in the bed joints of a brick masonry wall where the presence of steel may weaken the resistance of the masonry to vertical tensile stresses which will be present.

The strength of reinforced shear walls is influenced by the ratio of height to length, *h/l*, the amount and distribution of reinforcement and masonry strength. These effects have been investigated [32] experimentally and it has been shown that the shear strength increases with decrease in *h/l* ratio, with increase in vertical load and, in the case of filled hollow blockwork, with the grouting of the unreinforced cavities.

Scrivener [33] has reported shearing strengths for grouted concrete blockwork walls of approximately square aspect ratio of the order of 0.7–1.3 N/mm^2 with reinforcement ratios from 0.1 to 0.47 per cent. This com-

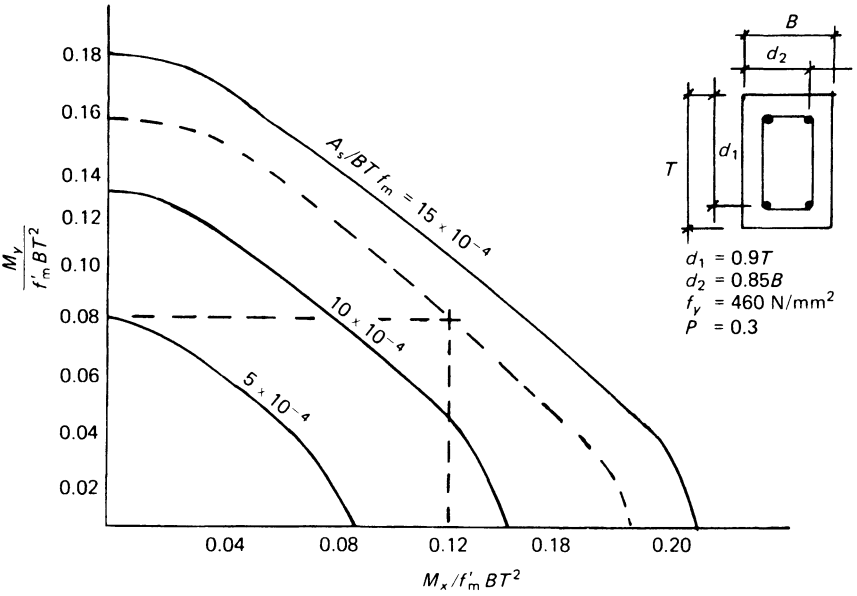

Figure 8.16 Interaction diagram for biaxial eccentricity of loading on a reinforced masonry column (Davies and El Traify)

pared with a shear strength of $0.33\,N/mm^2$ without reinforcement. In this case it was found that vertical and horizontal reinforcing were equally effective. A series of tests [34] on reinforced brickwork walls with vertical reinforcement in the collar joints showed very similar results.

The flexural strength of a shear wall may be predicted [35] by assuming that all the vertical reinforcement has yielded and that the compression zone is located at the 'leeward' toe of the wall.

The behaviour of reinforced shear walls has been extensively investigated [32] under cyclic loading in relation to seismic resistance. Investigators in this area recommend that flexural resistance should be kept lower than shear strength in order to develop ductility, which is essential in this context.

8.5 **Prestressed masonry**

The application of prestressed masonry has recently attracted increased attention in practice and in research. It has been shown that the same principles as apply to prestressed concrete are valid for post-tensioned masonry and that this form of construction has certain advantages over reinforced masonry, including avoidance of cracking under load and greater efficiency in the use of the material. Both beam and wall elements have

been investigated with most practical applications being to walls subjected to predominantly lateral loading.

8.5.1 *Post-tensioned masonry beams*

In the design of post-tensioned beams, conditions are investigated at transfer of prestress and under service loading assuming elastic behaviour. Thus, for a section having section moduli at bottom and top fibres of Z_1 and Z_2 respectively, at initial transfer, the stress at the top of the section will be

$$f_{2i} = P/A - Pe_s/Z_2 + M_i/Z_2 \tag{8.38}$$

and at the bottom of the section

$$f_{1i} = P/A + Pe_s/Z_1 - M_i/Z_1 \tag{8.39}$$

where P is the prestressing force, e_s its eccentricity from the centroidal axis and M_i the moment due to the self-weight of the beam. The initial prestressing force will be reduced as a result of various losses so that when considering the condition under the service load, P will be reduced to αP, where α is a loss factor which will be discussed in section 8.5.3 below. Top and bottom stresses at service will then be

$$f_{2s} = \alpha\left(P/A - Pe_s/Z_2\right) + M_s/Z_2 \tag{8.40}$$

$$f_{1s} = \alpha\left(P/A + Pe_s/Z_1\right) - M_s/Z_2 \tag{8.41}$$

where M_s is the bending moment at the serviceability limit state. These stresses have to be considered at the critical sections in each, usually at mid-span, and shown not to exceed allowable levels.

The shear strength of post-tensioned brickwork beams of up to 6.5 m span has been investigated by Pedreschi and Sinha [36, 37] with the results shown in figure 8.17. Prestressing results in a reduction of the diagonal tensile stress at the centroid of the section and comparison with reinforced masonry shows that the shear strength is considerably increased by post-tensioning.

The ultimate strength of post-tensioned masonry beams after cracking is similar to that of reinforced masonry and depends on whether the tendon is bonded or unbonded. In the former case it can be shown [38] that the stress in the tendon at failure, f_{pb}, is given by the equation

$$f_{pb} = \frac{k_1 f_m bd}{A_{ps}} \frac{\varepsilon_{mu}}{\varepsilon_{pb} + \varepsilon_{mu} - \varepsilon_{mp} - \varepsilon_{pe}} \tag{8.42}$$

where ε_{mu} = ultimate compressive strain in masonry
ε_{pb} = ultimate compressive strain in tendon
ε_{mp} = masonry strain due to prestress
ε_{pe} = strain in tendon due to effective prestress.

Then, referring to figure 8.18, the ultimate moment is:

$$M_u = A_{ps} f_{pb}\left(d - k_2 d_c\right) \tag{8.43}$$

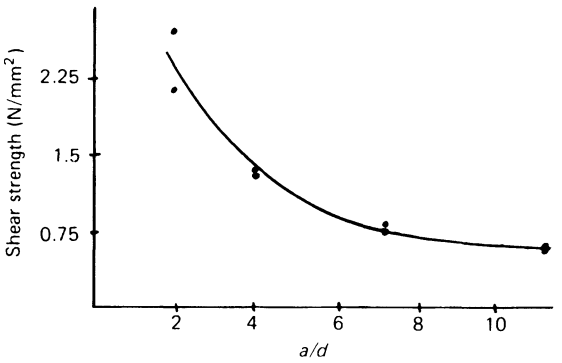

Figure 8.17 Shear strength of prestressed brickwork beams against shear span ratio (Pedreschi and Sinha).

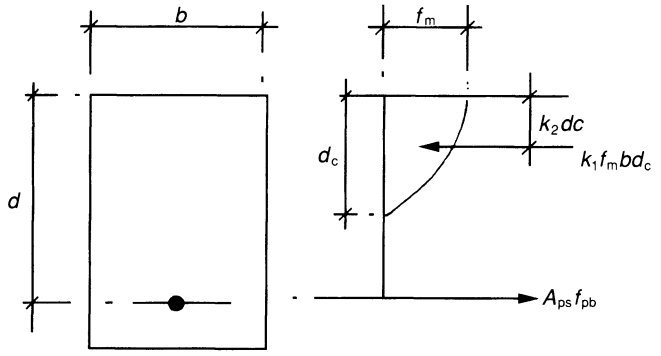

Figure 8.18 Prestressed beam at ultimate load condition

In an unbonded section the steel strain will be less and equation 8.42 will be modified.

Walker and Sinha [39, 40] have applied the technique of partial prestressing to brickwork beams, with a view to overcoming certain of the limitations inherent in the application of prestressing to this material, such as the restriction of the prestressing force to avoid splitting in the anchorage zone and the development of undesireably large crack widths. Again it has been found possible to predict the behaviour of the beams by standard procedures based on those used for prestressed concrete.

8.5.2 *Post-tensioned walls*

The application of post-tensioning to masonry walls is primarily to overcome the limitations imposed by the relatively weak flexural strength of the material and thus to walls which are predominantly subjected to lateral

load. The principles are the same as described in the previous section for beams with the difference that the post-tensioning of beams is likely to be parallel to the bed joints of the masonry whereas it will be normal to that direction in walls.

Curtin *et al.* [41] reported tests on cavity walls prestressed with 12 mm rods in connection with their use as spandrel walls in school buildings, required to resist lateral loads from continuous glazing units above. The prestressing was effected by tightening a nut on each rod against a steel plate bridging the two leaves of the wall.

A major application of prestressing is to walls of cellular and T cross-section which have to carry a combination of vertical and lateral loading. These walls are designed on the assumption of elastic behaviour and the basic equations are similar to those for beams with the addition of compressive stress arising from the external vertical loads [38].

Shear failure may take place in diaphragm walls either between the diaphragm and the outer leaves of the section or in the diaphragms. In the former case, the shear is transmitted either by a masonry unit bond or by metal ties. Only a limited amount of information is available regarding the shear resistance of masonry units, but Tsui *et al.* [42] have reported brick masonry shear strengths of the order of 1.5–3.0 N/mm^2 when using bricks of crushing strength between 30 and 60 N/mm^2 set in 1:$\frac{1}{4}$:3 or 1:1:6 mortar. Al-Hashemi and Curtin [43] obtained somewhat higher strengths for very high strength brickwork (167 N/mm^2 bricks in 1:$\frac{1}{4}$:3 mortar) which, however, decreased as the precompression normal to the bonded connection increased.

In the case of unbonded diaphragm walls, shear transmission between the diaphragms and outer walls is by metal ties embedded in the bed joints. Phipps and Montague [44] suggest that the limiting shear transmission is determined by the formation of plastic hinges in the ties at a distance $j = 6t$ apart, where t is the thickness of the tie. The corresponding shear on one tie is thus $V_t = t_w v s = 2m_t/j$ where m_t is the plastic moment of a tie (equal to $f_t b t^2/4$), t_w the thickness of the diaphragm, v the shear stress at the interface and s the spacing. The required spacing of ties is then

$$s = \frac{m_t}{3tvt_w} \tag{8.44}$$

Roumani and Phipps [45, 46] have shown that the shear force required to cause diagonal cracking in the web of a T or I section can be predicted on the criterion of maximum tensile principal stress. Using the conventional formulae for shear stress and principal stress resulting from combined shear and direct stress, the shear force at first crack is

$$V_{cr} = \frac{Ib}{A\bar{y}}\sqrt{\left(f_{tf}^2 + f_p f_{tf}\right)} \tag{8.45}$$

where $0.25 < f_{tf} = (2.25 - a/d) < 1.25\,\text{N/mm}^2$, and f_p is the average compressive stress due to prestress. Failure occurs when inclined cracks penetrate into the compression flange and may be estimated from a modification of equation (8.45):

$$V_u = \frac{Ib}{A\bar{y}}\sqrt{\left(f_{tf}^2 + f_{pu} f_{tf}\right)} \tag{8.46}$$

where f_{tf} is as above and

$$f_p < f_{pu} = \left(2.5 f_p - f_p^2\right) < 2 f_p \tag{8.47}$$

Post-tensioning of masonry shear walls has been proposed by Page and Huizer [47] who have demonstrated that the horizontal shear stress at failure can be several times that of a plain masonry wall. The strength of a post-tensioned wall can be estimated on the basis of the failure criteria discussed in section 4.4.

8.5.3 *Loss of prestress*

Loss of prestress may result from elastic, shrinkage and creep deformations of the masonry, anchorage slip, frictional effects and relaxation in the tendon and in some situations ambient temperature variations. These effects may be assessed separately and combined to give an overall loss factor.

Alternatively, the following formula derived by Lenczner [48] for the percentage loss of prestress may be used:

$$P_R = 100 f_b A_b \frac{\left(\varepsilon_m + C_c \dfrac{f_b}{E_b}\right)\dfrac{h}{L} E_s A_s}{f_b A_b} \tag{8.48}$$

where f_b = stress in brickwork at transfer
A_b = cross-sectional area of brickwork (mm^2)
ε_m = moisture strain (+ve for shrinkage)
C_c = creep ratio
E_b = elastic modulus of brickwork
h = height of member
E_s = elastic modulus of steel
L = length of prestressing bars
A_s = area of prestressing bars.

In the above, Lenczner takes

$$C_c = 4.46 - 0.33\sqrt{f_b'} \text{ for walls} \tag{8.49}$$

$$C_c = 1.73 - 0.14\sqrt{f_b'} \text{ for columns} \tag{8.50}$$

$$E_b = 3750\sqrt{f_b'} - 10\,000 \tag{8.51}$$

where f'_b is the compressive strength of the bricks. Good agreement has been shown between experimental results and estimates of prestress loss by the above formulae.

Phipps and Montague [49] have examined prestress losses, including relaxation of stress in tendons and temperature effects. Theoretically it would appear to be possible to have a 46 per cent loss in a particular case in which the tendons were stressed to 70 per cent of their characteristic strength, but laboratory measurements on diaphragm walls showed losses of between 13 and 22 per cent. This was of the same order as observed by Lenczner [48] over a similar period of about 14–16 months. In a test on a heavy diaphragm wall relating to a bridge abutment, Garrity and Garwood [50] reported a loss of prestress of 5 to 6 per cent over a five month period. It would appear from these data that in practice an allowance of 25 per cent would be adequate in most cases.

References

1. A. Brebner, 'Notes on Reinforced Brickwork Tests, Theory and Actual Construction of Reinforced Brickwork in India', *Technical Paper No. 38* (Government Public Works Dept, London, 1923).
2. Reports of Committee on Reinforced Brick Masonry of the National Brick Manufacturers Research Foundation: No. 3 'Method of Testing Reinforced Brick Masonry Demonstration Structure', *J. Am. Ceram. Soc.*, **15** (1932) 300–5. No. 4 'Results of Tests on Ten Reinforced Brick Masonry Demonstration Structures with Summary Covering Tests on Thirteen Structures', *J. Am. Ceram. Soc.*, **15** (1932) 273–99. No. 6 'Preliminary Outline of Program of Comprehensive Research in Reinforced Brick Masonry', *J. Am. Ceram. Soc.*, **15** (1932) 305–13. No. 7 'Tentative Specifications for Reinforced Brick Masonry', *J. Am. Ceram. Soc.*, **15** (1932) 313–20. No. 8 'Results of Tests on Seven Demonstration Structures with Summary Covering Tests on Twenty Structures', *Bull. Am. Ceram. Soc.*, **12** (1933) 166–97.
3. H. Filippi, *Brick Engineering – Reinforced Brick Masonry Principles of Design and Construction*, Vol. 3 (Brick Manufacturers Association of America, Cleveland, Ohio, 1933).
4. L. B. Lent, 'Reinforced Brick Masonry', *J. Am. Ceram. Soc.*, **14** (1931) 469–81.
5. J. W. Whittemore and P. S. Dear, 'An Investigation of the Performance Characteristics of Reinforced Brick Masonry Slabs', *Bull. Va Polytech. Inst. Engng Exp. Stn*, **9** (1932).
6. J. W. Whittemore and P. S. Dear, 'A Comparison of the Performance Characteristics of Reinforced Brick Masonry Slabs and Reinforced Concrete Slabs', *Bull. Va Polytech. Inst. Engng Exp. Stn*, **15** (1933).
7. M. O. Withey, 'Tests of Brick Masonry Beams', *Proc. Am. Soc. Test. Mater.*, **33** (1933) 651–65.
8. D. E. Parsons, A. H. Strang and J. W. McBurney, 'Shear Tests of Reinforced Brick Masonry Beams', *J. Res. Natn Bur. Stand.*, **9** (1932) 749–68.
9. F. G. Thomas and L. G. Simms, 'The Strength of some Reinforced Brick Masonry Beams in Bending and in Shear', *Struct. Engng*, **17** (1939) 330–49.

10. C. W. Hamann and L. W. Burridge, 'Reinforced Brickwork', *Struct. Engng*, **17** (1939) 198–250.
11. F. K. Kong and R. H. Evans, *Reinforced and Prestressed Concrete*, 3rd edn (van Nostrand Reinhold (U.K.), Wokingham, 1987), pp. 86–9.
12. S. R. Davies and A. W. Hendry, 'Reinforced Masonry Beams', *Proc. Br. Masonry Soc.*, **1** (1986) 73–6.
13. B. P. Sinha and R. C. de Vekey, 'Factors Affecting the Shear Strength of Reinforced Grouted Brickwork Beams and Slabs', *Proceedings of the Fifth International Brick Masonry Conference* (Rome) 1982, pp. 831–42.
14. Y. Osman and A. W. Hendry, 'Shear Transmission in Reinforced Grouted Cavity Brickwork Beams', *Proceedings of the Fifth International Brick Masonry Conference* (Rome) 1982, pp. 817–30.
15. G. T. Suter and H. Keller, 'Shear Strength of Grouted Reinforced Masonry Beams', *Proceedings of the Fourth International Brick Masonry Conference* (Brugge) 1976, Paper 4.c.2.
16. G. T. Suter and A. W. Hendry, 'Shear Strength of Reinforced Brickwork Beams', *Struct. Engnr*, **53** (1975) 249–53.
17. G. T. Suter and A. W. Hendry, 'Limit State Shear Design of Reinforced Masonry Beams', *Proc. Br. Ceram. Soc.*, **24** (1975) 191–6.
18. A. J. Rathbone, 'The Shear Behaviour of Reinforced Concrete Blockwork Beams', *Proceedings of Symposium on Draft BS 5628, Part 2* (Institution of Struct. Engnrs (London)) 1981, pp. 17–28.
19. Songbo Li, A. N. Fried and J. J. Roberts, 'Analysis of Shear Strength for Reinforced Concrete Blockwork Beams', *Proceedings of the Tenth International Brick and Block Conference* (Calgary) 1994, pp. 1021–35.
20. J. G. Gross, R. D. Dikkers and J. C. Grogan, *Recommended Practice for Engineered Brick Masonry* (Structural Clay Products Institute, McLean, Va., 1969), pp. 314–26.
21. Y. A. A. Osman, 'Behaviour of Reinforced Grouted Cavity Brickwork Beams and Walls', PhD Thesis (University of Edinburgh, 1983).
22. K. Wyatt, D. Lenczner and J. Salahuddin, 'The Analysis of Creep Data in Brickwork', *Proc. Br. Ceram. Soc.*, **24** (1975) 11–20.
23. B. P. Sinha, 'Reinforced Brickwork: Grouted Cavity Shear Tests', *S.C.P.16* (Structural Clay Products Ltd, Hertford, 1978).
24. B. P. Sinha, 'Long Term Tests on Reinforced Clay Brick Masonry Grouted Cavity Vertical Cantilever Walls', *S.C.P.14* (Structural Clay Products Ltd, Hertford, 1979).
25. I. Lyse, 'Tests of Reinforced Brick Masonry Columns', *J. Am. Ceram. Soc.*, **16** (1933) 584–97.
26. M. O. Withey, 'Tests of Reinforced Brick Masonry Columns', *Proc. Am. Soc. Test. Mater.*, **34** (1934) 387–405.
27. D. E. Anderson and E. S. Hoffmann, 'Design of Brick Masonry Columns', in *Designing, Engineering and Constructing with Masonry Products*, ed. F. B. Johnson (Gulf, Houston, Tex., 1969), pp. 94–100.
28. R. G. Drysdale and S. E. A. Sallam, 'Design of Masonry Walls for Combined Axial Load and Bending Moment', *Proceedings of the First Canadian Masonry Symposium* (Calgary) 1976, pp. 394–408.
29. M. Hatzinikolas, J. Longworth and J. Warwaruk, 'The Analysis of Eccentri-

cally Loaded Masonry Walls by the Moment Magnifier Method', *Proceedings of the Second Canadian Masonry Symposium* (Ottawa) 1980, pp. 245–8.
30. S. R. Davies and E. A. El Traify, 'Uniaxial and Biaxial Bending of Brickwork Columns', *Proceedings of the Sixth International Brick Masonry Conference* (Rome) 1982, pp. 843–54.
31. M. J. N. Priestley and D. O. Bridgeman, 'Seismic Resistance of Brick Masonry Walls', *Bull. New Zealand Soc. for Earthquake Engineering*, **7** (4) (1974).
32. R. R. Schneider and W. Dickey, 'Reinforced Masonry Design' (Prentice-Hall Englewood Cliffs, N.J., 1980), pp. 528–563.
33. J. C. Scrivener, 'Static Racking Tests on Concrete Masonry Walls' in *Designing, Engineering and Constructing with Masonry Products*, ed. F. B. Johnson (Gulf, Houston, Ta., 1969), pp. 185–91.
34. J. C. Scrivener and D. Currie, 'Shear Strength of Reinforced Brick Walls', *Masonry International*, **2** (1984) 24–31.
35. J. C. Scrivener, 'Reinforced Masonry in a Seismic Area – Research and Construction Development in New Zealand', *Proceedings of the First Canadian Masonry Symposium* (Calgary) 1976, pp. 371–82.
36. R. F. Pedreschi and B. P. Sinha, 'Development and Ultimate Load Behaviour of Pre-stressed Brickwork Beams', *Struct. Engnr.*, (Sept. 1982) 63–7.
37. R. F. Pedreschi and B. P. Sinha, 'The Shear Strength of Pre-stressed Brickwork Beams', *Proc. Br. Masonry Soc.*, **1** (1986) 114–16.
38. A. W. Hendry (ed.), *Reinforced and Prestressed Masonry* (Longman, Harlow, 1991), p. 87.
39. P. Walker and B. P. Sinha, 'Development and Structural Behaviour of Partially Pre-stressed Brickwork Beams', *Proceedings of the Seventh International Brick Masonry Conference* (Melbourne) 1985, pp. 1015–29.
40. P. Walker and B. P. Sinha, 'Comparative Studies of Reinforced, Fully and Partially Pre-stressed Brickwork Beams', *CIB Congress* (Washington DC) 1986, Vol. 6, pp. 2661–71.
41. W. G. Curtin, S. Adams and M. Sloan, 'The Use of Post-tensioned Brickwork in the SCD System', *Proc. Br. Ceram. Soc.*, **24** (1975) 235–45.
42. K. Y. Tsui, W. J. Harvey, J. M. Morton and G. Shaw, 'A Preliminary Investigation of the Vertical Shear Strength Brick Masonry', *Proceedings of the Sixth International Brick Masonry Conference* (Rome) 1982, pp. 33–44.
43. A. K. Al-Hashemi and W. G. Curtin, 'Principal Tensile Strength and Vertical Shear Resistance of High Strength Brickwork', *Proceedings of the Eighth International Brick/Block Masonry Conference* (Dublin) 1988, pp. 571–82.
44. M. E. Phipps and T. I. Montague, *The Design of Concrete Blockwork Diaphragm Walls* (Aggregate Concrete Block Association, Leicester, 1987).
45. N. Roumani and M. E. Phipps, 'The Shear Strength of Prestressed Brickwork I and T Sections', *Proceedings of the Seventh International Brick Masonry Conference* (Melbourne) 1985, pp. 1001–14.
46. N. Roumani and M. E. Phipps, 'The Shear Strength of Prestressed Brickwork I Sections', *Proc. Br. Masonry Soc.*, **1** (1986) 110–13.
47. A. W. Page and A. Huizer, 'Racking Tests on Prestressed and Hollow Clay Masonry Walls', *Proceedings of the Eighth International Brick/Block Masonry Conference* (Dublin) 1988, pp. 538–47.
48. D. Lenczner, 'The Loss of Prestress in Post-tensioned Brick Masonry Members', *Masonry International*, **5** (1985) 9–12.

49. M. E. Phipps and T. I. Montague, *The Design of Concrete Blockwork Diaphragm Walls* (Aggregate Concrete Blockwork Association, Leicester, 1987).
50. S. W. Garrity and T. G. Garwood, 'The Construction and Testing of a Full Scale Clay Brickwork Diaphragm Wall Bridge Abutment', *Proc. Br. Masonry Soc.*, **4** (1990) 24–9.

9 THE RESISTANCE OF MASONRY STRUCTURES TO ACCIDENTAL DAMAGE

9.1 **Abnormal loading incidents**

It is not generally possible to carry out a normal structural analysis relating to abnormal loading arising from such causes as gas explosion, vehicle impact or bomb blast since the location and magnitude of the load effect resulting from such incidents are unpredictable, and in some cases it would in any case be impracticable to design elements to resist the forces involved. It is necessary, however, to design buildings so that any damage resulting from such an incident remains localised. Concern about this problem arose as a result of a gas explosion on the eighteenth floor of a block of flats in London in 1968. This building, called Ronan Point, was of large panel precast concrete construction. The explosion blew out one of the external wall panels and, as a result, part of the five floors immediately above the explosion collapsed on to the eighteenth floor. This in turn, was unable to sustain the debris load and collapsed on to the floor below and so on almost to ground level. The tribunal [1] which investigated the accident gave this sequence of events the name 'progressive collapse'.

Prior to the Ronan Point accident, no specific consideration was given to accidental forces and associated liability to collapse in the design of masonry bearing wall structures, although the problem had been indirectly recognised in relation to large panel concrete structures [2, 3]. However, Ronan Point drew attention to the problem in a forcible manner, and consideration had to be given to the possibility of damage to masonry structures on a scale disproportionate to the magnitude of any accidental forces likely to be experienced.

In the decade following Ronan Point considerable attention was devoted to the problem through accident statistics [4], field studies [5], experiments on structures [6–8] and structural elements [9–11]. On the basis of this work, various design strategies for minimising the effects of accidental damage have been put forward, and these have been categorised as follows:

(1) Event control
(2) Direct design
(3) Indirect design.

By event control is meant the reduction of the risk of structural damage by eliminating exposure to a particular hazard (for example, by excluding potentially explosive materials from buildings), providing specific protection (for example, bollards to prevent vehicle impact) or by incorporating features in a building which will limit the severity of a hazard (for example, venting to limit the pressure developed by a gas explosion). While ordinary prudence may encourage the adoption of some of these precautions, they are generally outside the control of structural designers. The alternatives, however, are matters of structural design: the direct approach is to design a structure to resist certain specified forces or amounts of damage without collapse, while the indirect approach is to achieve this objective by specifying minimum levels of strength and continuity.

9.2 **Direct design for accidental damage**

As previously stated it is not possible to specify the loading associated with structural accidents with any certainty, so that in applying the direct design approach the forces to be resisted are of an idealised nature and arbitrary magnitude. Thus the Building Regulations in the United Kingdom require that any element on which the stability of a structure is to depend following an accident must be able to withstand a pressure of $34\,kN/m^2$ from any direction. Various other abnormal load criteria have been proposed, and have been compared by Leyendecker and Ellingwood [4].

Resistance of masonry walls to accidental damage is related to their lateral strength, and may be calculated using the methods discussed in chapter 7.

In the second direct design procedure, sometimes referred to as the 'alternate path method', specified elements, or parts of elements, are assumed to have failed and the stability of the remaining structure is investigated. It is not generally possible to assess the amount of damage that will result from a particular hazard and, as in the case of pressures arising from accidental causes, some kind of idealisation has to be adopted. The British Code of Practice for the Structural Use of Masonry, BS 5628: 1992 requires that the effect of removing vertical and horizontal elements one at a time should be considered. It has then to be demonstrated that the 'damaged' structure has adequate residual stability and that collapse of any significant portion of the structure is unlikely to occur.

Examination of a wide variety of existing designs by Morton *et al.* [12] has identified three particular situations which may be critical in relation to accidental damage. These are:

Case A Where there is an outside wall without returns, or only one internal return

Case B Where there is an internal wall without returns

Case C Where the removal of a section of a wall imposes high local bearing stresses on a return wall or walls.

In case A (figures 9.1a and b) the removal of a panel of masonry will leave the remaining sections of the wall supported by the floor slabs above. In case B (figures 9.1c and d) the walls above the damaged wall will have to be carried by the floor slabs supported around their perimeter by the remaining walls. Case C (figure 9.1e) arises where the unsupported masonry spans or cantilevers across the opening left by the removal of a wall panel, resulting in the application of a concentrated load on the return wall. It may also be necessary to examine the stressing of a masonry cantilever, such as that shown in figure 9.1e, to ascertain whether or not it can be assumed to act as a unified structure; if not, it must be considered under case A.

In cases where the support of the walls above an opening is dependent on a remaining return wall, it is necessary to calculate the bearing stress in the brickwork. The assumptions in the previous paragraph are based on normal methods of structural mechanics. Thus in case A, it may be necessary to assess whether a storey height length of outside wall can be supported by a floor slab when the wall directly below is assumed to have been removed. In a typical case the situation may be as represented as in figure 9.2, and using the notation shown in this diagram, yield line analysis may be applied as follows:

$$E = p\left(\frac{\beta L^2}{6} + \frac{\alpha L^2}{3}\right) - \frac{P(2L - C)C}{2L} \tag{9.1}$$

where E is the work done by the external loads per unit displacement of the mechanism

p is the weight of the floor slab plus the uniformly distributed imposed load

P is the weight of wall per unit length

L and C are dimensions as shown in figure 9.2.

The internal work done in the yield lines is given by

$$D = m\left(4\alpha + \frac{\mu}{\alpha - \beta} + 4i_1\alpha + \frac{i_2}{\alpha - \beta}\right) \tag{9.2}$$

Equating D and E, and substituting known values of α, μ, i_1 and i_2 gives an expression for m, the minimum designed moment for the slab, in terms of β. The value of β corresponding to the minimum value of m can then be found by putting $dM/d\beta = 0$. Finally m is calculated and compared with the actual moment of resistance of the slab. Other cases can be dealt with in a similar manner and solutions are given in standard textbooks on reinforced concrete.

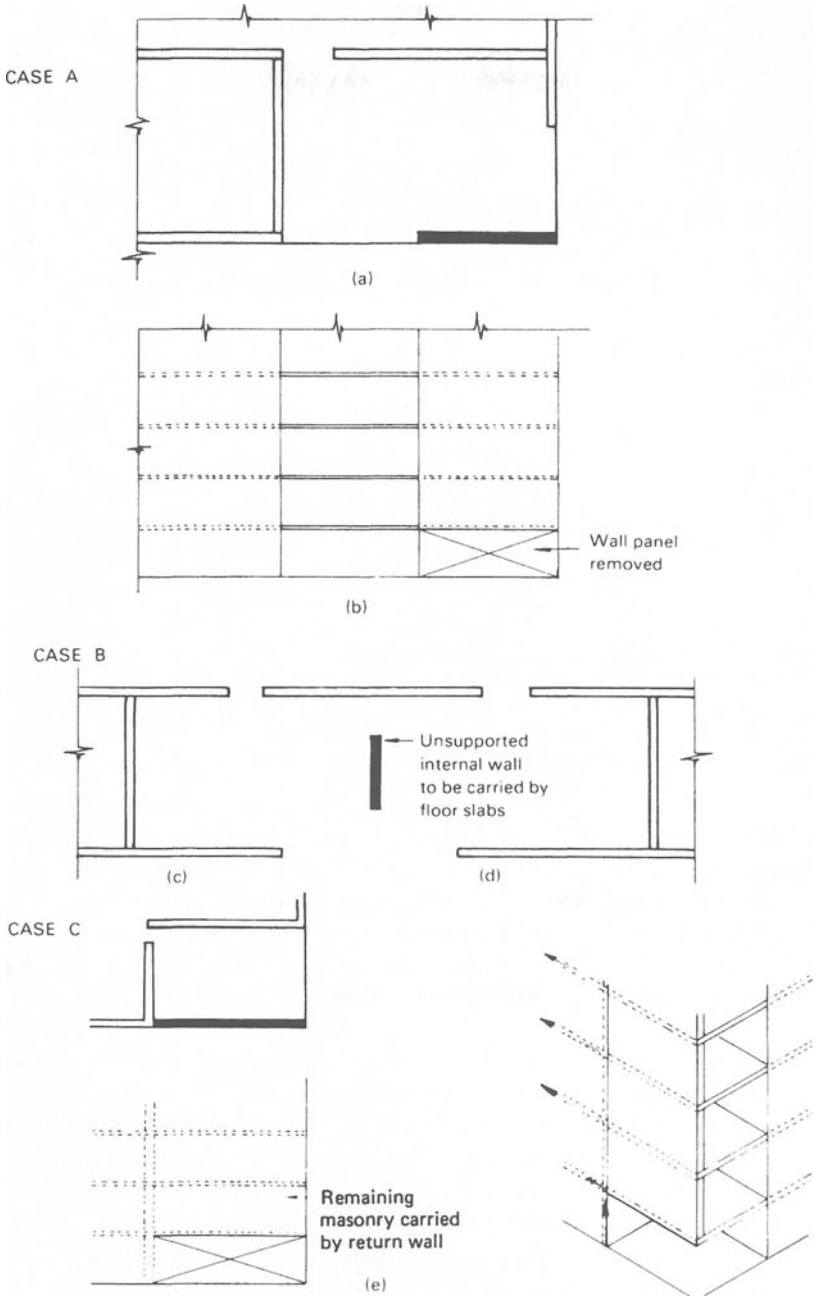

Figure 9.1 Situations requiring special attention in relation to accidental damage

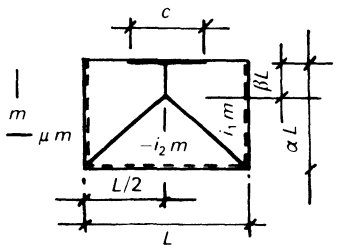

Figure 9.2 Yield line analysis of floor slab carrying wall load on edge

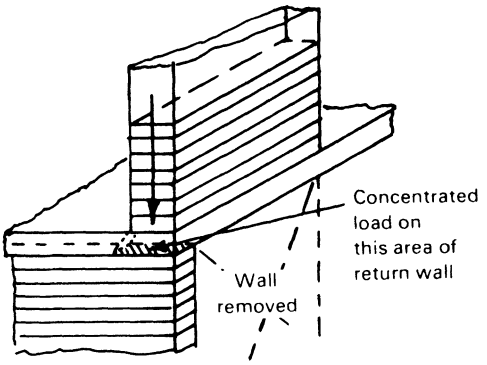

Figure 9.3 Wall bearing on a return

In case C, the bearing stress on a return has to be considered, as indicated in figure 9.3. The force transmitted to the return wall resulting from the dead and superimposed loads on the structure above it is calculated by statics. The bearing stress in the masonry is then determined, allowing for spread of the load through the floor slab and, in a design situation, compared with the maximum bearing stress for the material under accidental damage conditions.

Consideration of the removal of floor slab elements gives rise to rather intractable conceptual problems, for example, it is difficult to see how a reinforced concrete floor slab in a brickwork structure could be removed without there being serious damage to the brickwork. It is, therefore, more practical to design floors whose removal does not have to be considered, either by direct design to meet the hypothetical accidental damage loads, or by indirect design by incorporating a sufficient degree of continuity.

9.3 **Indirect design for accidental damage**

The indirect approach [4, 13, 14] to the control of accidental damage does not depend on the representation of the forces likely to be encountered, or

on the assessment of the effect of limited damage. Instead, the idea is to design the building on an empirical basis to possess certain minimum levels of strength, continuity and ductility as will enable it to survive accidental forces in an acceptable manner. The terms 'robustness' and 'structural integrity' are sometimes applied in this context, and these were satisfactorily achieved in traditional forms and methods of construction. In terms of modern masonry structures, the first step in securing general stability is the adoption of a satisfactory wall layout, as discussed in chapter 1. Following this, comes the need to ensure continuity of the floor system. In this respect, *in situ*, two-way spanning reinforced concrete slabs, continuous over internal walls, afford the highest degree of protection. Least satisfactory would be simply supported precast planks without lateral ties. The British Code of Practice BS 5628: 1992 sets out requirements for ties in floors to meet all reasonable continuity criteria and, in terms of this Code, avoids the requirement to consider removal of such elements in a direct design approach.

The corresponding provision of vertical ties is a more doubtful procedure. Firstly, it is in practice difficult to build in ties in unreinforced masonry walls and, secondly, their effect is uncertain. Indeed, in an experimental study of a large panel loadbearing wall structure of model-scale, Beak [15] showed that continuous vertical ties could promote progressive collapse by pulling out wall panels at levels above and below that at which an explosion took place. Thus, if vertical ties are to be used at all they should not be continuous from one storey to the next.

Indirect design considerations further require [14] that walls should be adequately stiffened by returns and piers, as appropriate, and that roof structures as well as floors should be constructed in such a way as to promote the spreading of lateral loads among the walls. These elements must also be adequately tied, or strapped, to the walls to provide lateral support.

The indirect approach is in fact applicable to all building design and is likely to be sufficient for low-rise buildings. Tall buildings, on the other hand, may require more detailed consideration on a semi-quantitative basis by direct design methods to ensure that no weaknesses exist in their resistance to accidental forces.

9.4 Experimental studies of accidental damage

A great deal of information about the behaviour of masonry structures can be obtained from a systematic study of the buildings damaged in gas explosions and other accidents [5]. However, it is only possible to infer the forces involved and the material properties in such cases; other relevant factors may be difficult to ascertain. The results of controlled experiments are therefore of value in verifying the basis for assessment of new designs, the effectiveness of structural precautions and in affording information on the response of building structures to accidental damage.

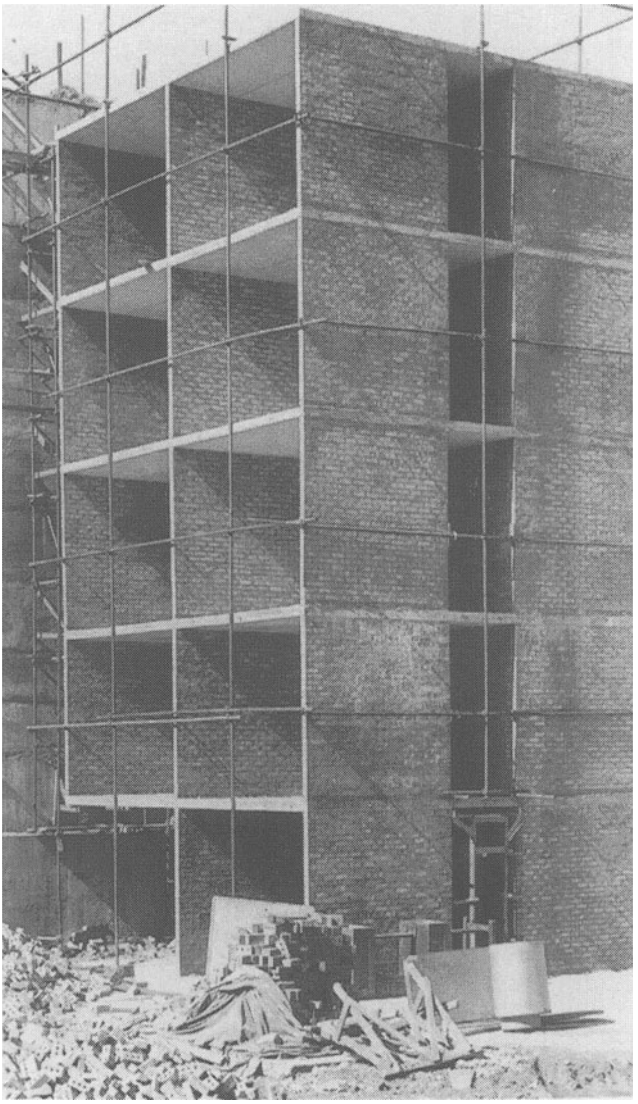

Figure 9.4 Wall removal test on five-storey brickwork structure simulating accidental damage

A number of tests [7] were carried out at Edinburgh University on the full-scale experimental structure shown in figure 9.4 with the object of confirming that a cross-wall structure of this type could survive the removal of a major bearing wall. The floors were of 50 mm precast slabs containing the main reinforcement with 75 mm of *in situ* concrete topping, giving an

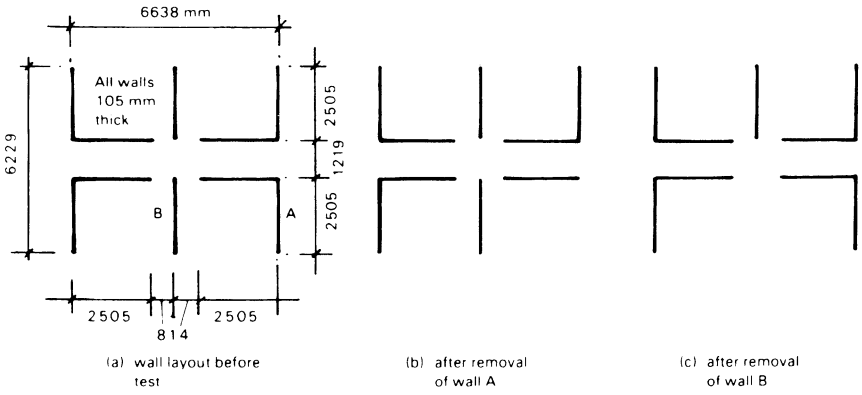

Figure 9.5 Wall removal tests on brickwork structure

overall slab depth of 125 mm. In the tests, the outer cross-wall (A in figure 9.5) was first removed by lateral loading applied by hydraulic jacks. This wall was then rebuilt and a second test carried out by removing one of the internal panels (B in figure 9.5) in the same way. Deflections were measured, and these showed that the maximum deflection of the floor slab after the first test was 4 mm, and after the second test 5.4 mm. No damage was observed anywhere in the structure except immediately above the wall that had been removed, where the joint between the first floor slab and the wall was broken and the wall appeared to be partly hanging from the second floor slab and partly supported by the first floor slab. The structure appeared to be stable after the removal of a main bearing wall, and this was confirmed by calculation which indicated that there would be a load factor of 1.94 on the dead load plus 1.9 kN/m^2 superimposed load after the removal of the centre cross-wall, and 2.44 after the removal of the end cross-wall. It should be emphasised that this structure was not designed with progressive collapse in mind and represented what was considered to be sound construction in accordance with the then current Code of Practice. Naturally, no general conclusions could be based on a single case, but the inference for future designs was that brick masonry structures could without difficulty be made resistant to progressive collapse as a result of accidental damage.

The experiment described was intended as a demonstration of feasibility. It was on the lines of the direct design approach described in section 9.2, in which stability following the removal of a section of bearing wall was considered but, of course, it did not afford any information about the behaviour of a masonry building subjected to accidental forces and in particular to a gas explosion. An extensive series of tests was undertaken by the British Ceramic Research Association and the Brick Development

Association in order to explore this problem and to obtain information which would have a bearing on structural design. The investigation has been described in detail in references 6 and 8, and included gas explosion experiments in a specially designed building representing the top three storeys of a tall cross-wall structure. These tests were supported by a series of tests in a bunker, the front of which was closed by brick walls or cladding panels of various kinds. Details of the experimental building are shown in figure 9.6, from which it will be seen that it consisted of three loadbearing cross-walls at approximately 3.8 m centres with 127 mm reinforced concrete floor slabs. The outer walls were of 280 mm brick cavity construction, with various window and cladding arrangements on the non-loadbearing walls. Internally the space was subdivided by 103 mm brick walls with communicating doors between two pairs of rooms.

Gas was introduced into one or more of the rooms for each test and ignited to simulate a domestic gas explosion. Town gas was used in most experiments since it has a high proportion of hydrogen, and would be thus expected to produce higher explosion pressures than natural gas, which is mostly methane. In some cases a gas–air mixture was contained in a polythene balloon before ignition, in others the gas was mixed with air in the room or introduced in such a way as to produce a layered concentration from floor to ceiling. It was expected that an explosion originating in one room and spreading to an adjoining gas-filled room would result in higher pressures in the latter, as a result of the turbulent mixing of burning gas with the unignited gas in the second stage of the explosion. A number of tests were therefore arranged in which this effect took place.

A large number of explosion tests were carried out, in most of which gas pressures of less than 14 kN/m^2 were generated by quantities of gas, which had they been fully confined would have resulted in pressures of up to 119 kN/m^2. These low pressures were, of course, observed because of the venting effect of the glazing or cladding, which blew out and thus limited the maximum pressures. In these tests no damage to the brickwork was observed. In a further experiment, however, in which two rooms (1 and 2 in figure 9.6) were filled with gas, an explosion initiated in room 1 resulted in a maximum pressure of 22.7 kN/m^2 in room 2 and the outer loadbearing cavity wall in room 2 was damaged but did not collapse. In fact, considerable difficulty was subsequently experienced in demolishing it prior to reconstruction.

As this was a significant result the experiment was repeated after rebuilding the damaged wall. In this repeat case the average pressure recorded in room 2 was slightly lower at 18.47 kN/m^2, and only minor damage was caused to the brickwork. A similar test was subsequently carried out in rooms 3 and 4, which had smaller venting areas than rooms 1 and 2. The gas was ignited in room 3 and maximum measured pressures of 16.9 kN/m^2 and 15.84 kN/m^2 were produced in rooms 3 and 4, respectively. It was considered that local pressures may have been as high as 24 kN/m^2 in room 4

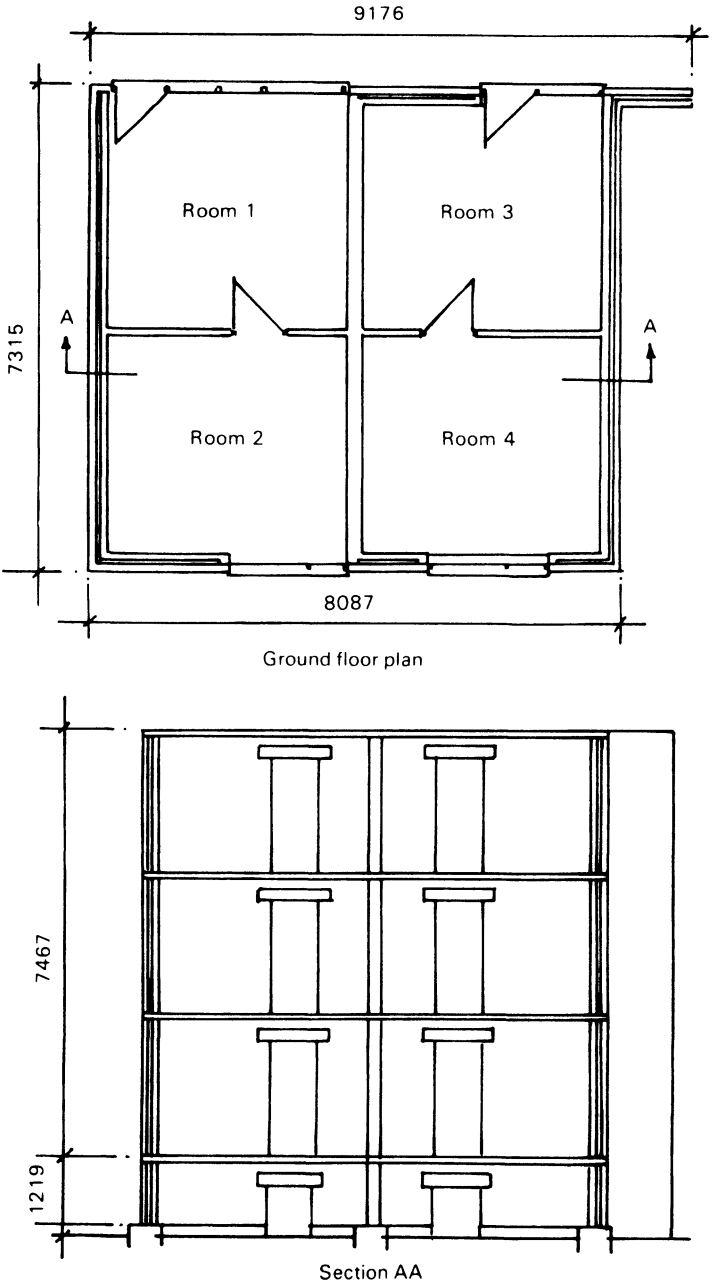

Figure 9.6 Details of BCRA explosion test structure

and considerable damage to the brickwork resulted. The outer cross-wall showed a characteristic roof-shaped fracture pattern similar to the yield line pattern in a laterally loaded concrete slab but, in spite of this, the building did not collapse and the damaged brickwork was subsequently demolished only with difficulty.

From these, and some subsidiary experiments [16], it may be concluded that it is possible under rather exceptional circumstances for a pressure of the order of 34 kN/m^2 to be generated in a domestic gas explosion. In the vast majority of such incidents, however, the venting effect of doors, windows and other circumstances will preclude such a possibility, and pressures are unlikely to exceed 24 kN/m^2. The provision of the Building Regulations requiring that elements which are necessary for the continued stability of a building after it has been subjected to accidental forces is thus seen to be well on the safe side, as least as far as gas explosions in residential buildings are concerned. Both the University of Edinburgh and the BCRA tests confirm that multi-storey brickwork structures, as normally designed in the United Kingdom, can withstand severe structural damage without it resulting in progressive collapse.

9.5 **Resistance to earthquake damage**

The problem of design of masonry buildings against accidental damage from impact and explosions has been discussed. Seismic design may be regarded as an extension of this concept since the forces involved are likely to have a small probability of occurrence but are of such a magnitude as to subject the structure to forces well beyond the normal serviceability range. From this point of view, therefore, design for seismic conditions will have the primary aim of controlling the resulting damage. In particular, design will aim to avoid total collapse or more localised failure which would carry a high risk of death or serious injury to people within or around the building. A secondary objective will be the economic one of 'repairability'.

Few areas can be regarded as completely free from earthquakes, although in many they may be very slight. The point is well illustrated by the experience of Newcastle, New South Wales, a part of Australia where until 1989 the danger of seismic activity was not regarded as calling for any precautionary measures. On 28 December of that year, the city experienced an earthquake of magnitude 5.6 on the Richter scale, the effect of which in some parts was magnified by the presence of underlying alluvial deposits. Loss of life was fortunately relatively small but considerable damage was caused to masonry buildings of various types. The effects of the earthquake have been described by Melchers [17] and by Page [18], and it is possible to draw conclusions of general application from these accounts.

The first is for the need for general robustness in the design of a building, on the lines discussed in chapter 1, in particular to avoid unsymmetrrical

wall layouts and 'soft' ground floor arrangements, that is to say, open plans accommodating parking garages and the like lacking adequate bracing walls. Certain details such as free-standing parapets are vulnerable unless reinforced or braced, and cladding panels require to be securely tied to the main structure. A very common, if not surprising, source of failure in Newcastle was the absence or corroded state of wall ties in cavity walls and other manifestations of bad design, poor workmanship or lack of maintenance. Given attention to these matters, and with the measures recommended in the British Code of Practice described above, masonry buildings can be expected to perform satisfactorily in earthquakes at least of the severity of that experienced in Newcastle.

In many areas where the risk of severe earthquakes is known to be greater, more specific measures will be required and for small domestic buildings these have discussed by Arya and Chandra [19], and in greater detail in reference 20. The essential requirement is to tie the elements of the building together and develop the necessary strength and ductility by suitable reinforcement. The overall layout of the building must be such as to provide adequate resistance to lateral forces along both principal axes. Vulnerable points include the jambs of openings and the corners of shear walls, where vertical reinforcement should be provided. This reinforcement in conjunction with bands at window lintel and roof levels provides very effective strengthening of simple brickwork buildings against earthquake forces.

It is well known that multi-storey, plain masonry buildings are liable to suffer considerable damage in a severe earthquake [21]. New high-rise masonry buildings in areas of high seismic risk are now invariably of reinforced construction and considerable progress has been made in applying the methods developed for reinforced concrete to these structures [22]. This forms a specialised branch of structural engineering and only an indication of the basic principles involved can be given here.

Conventional design codes have been based on the concept of elastic behaviour but the dynamic response characteristics of masonry buildings are such that it is not feasible to design for the extremely high lateral force levels which elastic response would imply. It has to be accepted therefore that under earthquake loading the structure will attain its ultimate load and that a considerable degree of ductile deformation will have to be accommodated. A factor, μ, equal to the ratio of the elastic displacement at ultimate lateral load divided by the elastic displacement at design load, is used to define the 'ductility demand'. This factor is typically about 4. Such ductile deformation will have to be sustained over several cycles without excessive loss of strength or stiffness.

In this context, the choice of structural form is critical. Where coupled shear walls are employed, their behaviour will depend on the nature of the interconnecting elements. If these are flexible floor slabs (figure 9.7a), energy dissipation will occur at the base of the walls and be accommodated

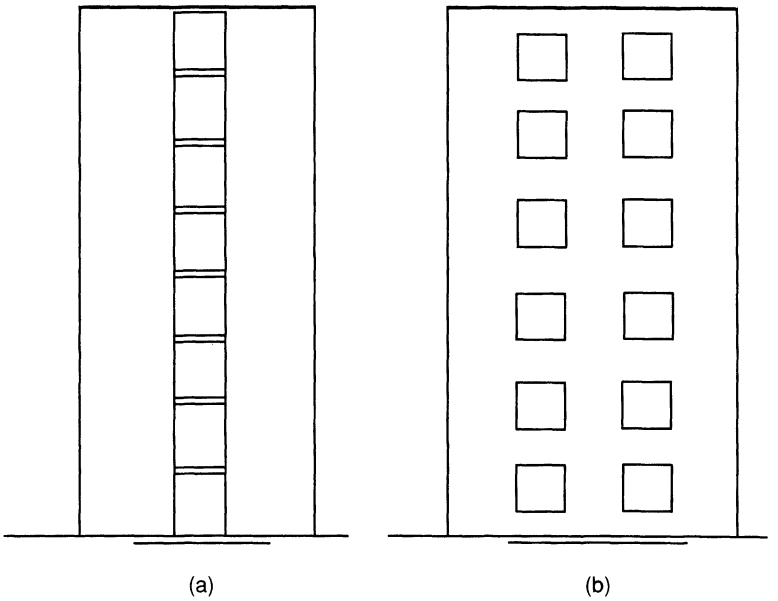

Figure 9.7 Coupled shear walls: (a) interconnection by floor slabs – ductility provided by flexural yielding of reinforcement distributed across width of walls; (b) interconnection by spandrel walls – ductile yielding of spandrels or columns in lower storeys

by carefully detailed plastic hinges where ductility is best provided by flexural rather than shear yielding of distributed steel. If the interconnection is through spandrel walls (figure 9.7b), plastic deformation is either in these or in the columns, depending on the configuration. In either case, the reinforced elements concerned would have to be designed to accommodate the required lateral displacement, generally concentrated in the lowermost storeys. In this situation, the ductility factor is correspondingly concentrated and where the pier-height is half the storey-height this factor is given by

$$\mu_p = 2n(\mu - 1) + 1 \tag{9.3}$$

where n is the number of storeys and μ is the structure ductility factor [22]. Thus for a ten-storey building, μ_p would be 61. As this would be very difficult to achieve, the indication is that wall systems of this type are unlikely to be satisfactory in seismic zones.

For design purposes, information is required relating to the strength/deformation properties of reinforced masonry elements under cyclic loading and their stiffness beyond the elastic range. Design can then be undertaken on the basis of assumed earthquake forces allowing for a selected ductility demand.

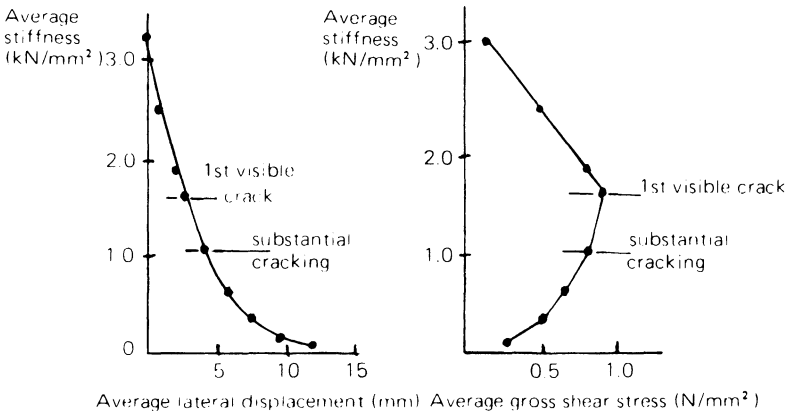

Figure 9.8 Typical performance of a reinforced masonry shear wall under cyclic loading (Mayes and Clough)

A considerable number of experimental investigations have been carried out to determine the behaviour of various forms of masonry under cyclic loading. Figure 9.8 shows the result of a test by Mayes *et al.* [23] illustrating the degradation of stiffness and strength in a typical reinforced masonry wall. Modena [24] has derived simplified analytical models for the cyclic behaviour of masonry walls and related these to the dynamic and ductility parameters required in design. Although these are for particular walls, the methodology could be adapted for other types of masonry.

The mathematical modelling of masonry structures subjected to seismic effects, based on the observed characteristics of walls, has been developed by Braga and Dolce [25]. In their analysis, the walls of the building are subdivided, as shown in figure 9.9, into horizontal strips and vertical elements which may fail in predetermined modes. The response of the structure is calculated by a step-by-step procedure in which incremental displacements are applied to each floor in turn, the element characteristics being adjusted to allow for cracking as the analysis proceeds. The method is approximate but offers a practical approach to the problem suitable for assessing the performance of low to medium-rise buildings in relation to specified seismic loadings.

The interaction between masonry panels and concrete or steel structural frames is discussed in chapter 10 for static loading. It is shown that infill walls may substantially increase the stiffness of the frame but where seismic loading has to be allowed for, the presence of infill walls may result in damage to the members or joints of the frame through forces being applied to it which were not taken into account in the design. It is advisable to allow for combined action as reliable isolation of infill panels is difficult whilst providing for their lateral support.

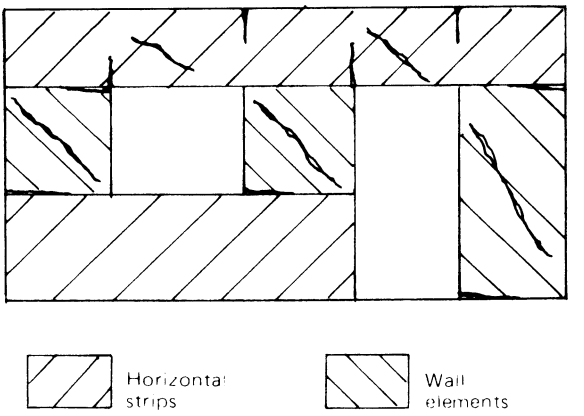

Figure 9.9 Representation of a wall with openings for assessment of resistance to in-plane seismic forces, showing assumed crack pattern (Braga and Dolce)

References

1. *Report of the Inquiry into the Collapse of Flats at Ronan Point, Canning Town* (HMSO, London, 1968).
2. 'International Recommendations for the Design and Construction of Large Panel Structures', *Bulletin No. 60* (CEB, Paris, 1967).
3. J. Despeyroux, 'L'Effondremont de L'immeuble de Ronan Point et ses Conséquences en Matière du Codification, *Annls Inst. Tech. Bâtim.*, No. 263 (1969) 1800–3.
4. E. V. Leyendecker and B. R. Ellingwood, 'Design Methods for Reducing the Risk of Progressive Collapse in Buildings', *NBS Building Science Series No. 98* (Washington, 1977).
5. R. J. Mainstone, 'Accidental Explosions and Impact: Some Lessons from Recent Incidents', *Proceedings of the Symposium on Stability of Low-rise Buildings of Hybrid Construction* (Institute of Structural Engineers, London, 1978), pp. 13–23.
6. N. F. Astbury, H. W. H. West, H. R. Hodgkinson, P. A. Cubbage and R. Clare, 'Gas Explosions in Load-bearing Brickwork Structures', *Special Publication No. 68* (British Ceramic Research Association, Stoke-on-Trent, 1970).
7. B. P. Sinha and A. W. Hendry, 'The Stability of a Five-storey Brickwork Cross-wall Structure Following the Removal of a Section of a Main Load-bearing Wall', *Struct. Engr.*, **49** (1971) 467–74.
8. N. F. Astbury, H. W. H. West and H. R. Hodgkinson, 'Experimental Gas Explosions: Report of Further Tests at Potters Marston', *Special Publication No. 74* (British Ceramic Research Association, Stoke-on-Trent, 1972).
9. A. W. Hendry, B. P. Sinha and A. H. P. Maurenbrecher, 'Full Scale Tests on the Lateral Strength of Brick Cavity Walls with Precompression', *Proc. Br. Ceram. Soc.*, **21** (1974) 165–79.
10. H. W. H. West, H. R. Hodgkinson and W. F. Webb, 'The Resistance of Brick Walls to Lateral Loading', *Proc. Br. Ceram. Soc.*, **21** (1974) 141–64.

11. J. Morton and A. W. Hendry, 'An Experimental Investigation of the Lateral Strength of Brickwork Panels with Precompression under Dynamic and Static Loading', *Proceedings of the Third International Brick Masonry Conference* (Essen) 1973, eds L. Foertig and K. Gobel (Bundesverband der Deutschen Ziegelindustrie, Bonn, 1975), pp. 362–9.
12. J. Morton, S. R. Davies and A. W. Hendry, 'The Stability of Load-bearing Brickwork Structures Following Accidental Damage to a Major Bearing Wall or Pier', *Proceedings of the Second International Brick Masonry Conference* (Stoke-on-Trent) 1971, eds H. W. H. West and K. H. Speed (British Ceramic Research Association, Stoke-on-Trent, 1971), pp. 276–81.
13. R. J. M. Sutherland, 'Principles for Ensuring Stability', *Proceedings of the Symposium on Stability of Low-rise Buildings of Hybrid Construction* (Institute of Structural Engineers, London, 1978), pp. 28–33.
14. J. F. A. Moore, 'The Stability of Low-rise Masonry Construction', *Proceedings of the Symposium on Stability of Low-rise Buildings of Hybrid Construction* (Institute of Structural Engineers, London, 1978), pp. 38–46.
15. R. Beak, 'Explosion Tests on a $\frac{1}{4}$-scale Model of an 18-storey Large Panel Structure', *BRE Note N149/76* (Building Research Establishment, Watford, Herts, 1976).
16. D. J. Rasbash, K. N. Palmer, Z. W. Ragowski and S. Ames, *Gas Explosions in Multiple Compartments* (Directorate General of Development, Dept of the Environment, London, 1971).
17. R. E. Melchers (Ed.), *Newcastle Earthquake Study* (Institute of Engineers, Australia), 1990.
18. A. W. Page, 'The Newcastle Earthquake – Behaviour of Masonry Structures', *Masonry International*, **5** (1) (1991) 11–18.
19. A. S. Arya and B. Chandra, 'Behaviour of Masonry Building for Earthquake Forces', *Proceedings of the International Seminar/Workshop on Planning, Design, Construction for Load-Bearing Brick Buildings for Developing Countries* (Department of Civil Engineering, University of Edinburgh) 1981, pp. 142–67.
20. *Basic Concepts of Seismic Codes, Vol. 1* (The International Association for Earthquake Engineering, Tokyo, 1980).
21. R. E. Klingner (ed.), *Performance of Masonry Structures in the Northridge, California, Earthquake of January 17, 1994* (The Masonry Society, Boulder, Co.) 1994.
22. A. W. Hendry (Ed.), *Reinforced and Prestressed Masonry* (Longman Scientific & Technical, Harlow), 1991, Ch. 8, pp. 183–208.
23. R. L. Mayes, Y. Omote and R. W. Clough, *Cyclic Shear Tests of Masonry Piers. Test Results* (University of California, Berkley, 1976). See also R. R. Schneider and W.L. Dickey, *Reinforced Masonry Design* (Prentice-Hall, Englewood Cliffs, N.J., 1980), p. 559.
24. C. Modena, 'Seismic Behaviour of Masonry Structures: Experimentally Based Modelling', Parts 1 and 2, *Masonry International*, **6** (2) (1992) 57–68.
25. F. Braga and M. Dolce, 'A Method for the Analysis of Antiseismic Masonry Multistorey Buildings', *Proceedings of the Sixth International Brick Masonry Conference* (Rome) 1982, pp. 1088–99.

10 MASONRY WALLS IN COMPOSITE ACTION

10.1 Composite wall–beam elements

10.1.1 *Structural action of wall–beams*

It has long been recognised that structural interaction takes place between a masonry wall and a supporting steel or concrete beam. In simplest terms this has been represented by assuming that the beam supports only part of the brickwork represented by a triangular load intensity diagram with zero ordinates at the supports and maximum loading at mid-span. The loading from the remainder of the brickwork was assumed to be transmitted to the support points by arching action as indicated in figure 10.1a. While this is essentially a correct reflection of the structural behaviour of the system as far as it goes, it is of limited quantitative value because it fails to give any indication of the concentrated compressive stresses in the wall, which may be critical, or of the actual bending moments in the beam.

A number of theoretical and experimental studies of the problem have shown quite clearly that the vertical and shear stresses at the wall–beam interface are concentrated towards the supports, as indicated in figure 10.1b. Both the shear and vertical stress distributions in these areas can be approximately represented by a triangular diagram, and the more flexible the beam, the more concentrated these stresses are towards the supports. Although the shear force tends to counteract the downward deflection of the beam, there is a tendency for this element to deflect downwards away from the wall, with the possible development of a crack between the top of the beam and the bottom of the wall. The shear force also induces an axial tension in the beam, the magnitude of which varies across the span.

Within the wall an arching action is developed and the vertical stresses are heavily concentrated towards the supports.

The type of behaviour described in the previous paragraphs has been found to take place with walls having a ratio of height to length greater than

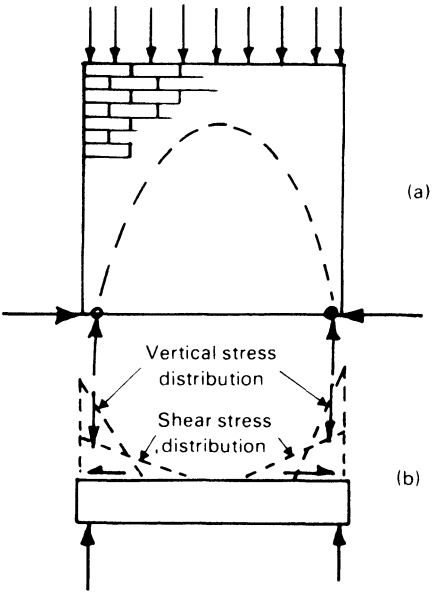

Figure 10.1 Structural action in composite wall–beam: (a) arching forces in wall; (b) vertical and shear forces in beam

about 0.6. Below this ratio, the shear becomes greater than can be resisted at the wall–beam interface and, although composite action is still possible, the element must eventually be treated as a purely flexural member.

10.1.2 *Theoretical solutions*

Using essentially the conceptual model described above, and against a background of theoretical and practical research [1], Wood and Simms [2] put forward a simple method for the calculation of composite wall beams. Instead of the triangular distribution of vertical compressive stress in the vicinity of the supports, a rectangular stress block was assumed, extending a distance x into the span from each end of the beam. Thus the ratio of the average compressive stress in the wall to the maximum in the area of the rectangular stress blocks is $C = L/2x$. The bending moment in the central section of the beam is then

$$M = \frac{WL}{k} = \frac{W}{2}\frac{x}{2} = \frac{Wx}{4} \tag{10.1}$$

from which $C = k/8$ and $x/L = 4/k$. Taking possible values of the bending moment coefficient, k, leads to the corresponding values for the extent of the stress block and the stress concentration factor:

k	x/l	C	
8	1/2	1	No composite action
12	1/3	1.5	
24	1/6	3	
48	1/12	6	
100	1/25	12.5	Maximum allowable composite action

This indicates that for composite action to be possible, the average compressive stress in the wall must be relatively small. On the basis of these values of C, it is possible to derive values of k which are consistent with the design stresses prescribed by any particular code of practice.

Thus in terms of BS 5628: 1992, the design strength per unit area of a wall will be $\beta f_k/\gamma_m$, where β is a reduction factor for slenderness, f_k and γ_m respectively the characteristic strength and partial safety factor for the material. If the average stress in the wall is less than the design stress by a factor F, and if the design strength may be increased by 50 per cent in the region of concentrated stress at the support, then

$$CF\beta\frac{f_k}{\gamma_m} \geqslant 1.50\frac{f_k}{\gamma_m} \tag{10.2}$$

Since $C = k/8$, this equation leads to the bending moment factor for the beam

$$k \geqslant 12/F\beta \tag{10.3}$$

when $M = WL/k$. This will have the effect of limiting the interactive effect according to the compression in the wall as a proportion of the design strength.

This simple analysis has been elaborated by Wood and Simms to allow for the effect of axial tension in the beam on the assumption that a parabolic line of thrust is developed in the wall. A limitation on the tensile stress in the reinforcing steel was also suggested as a means of limiting its extension when acting as a tie to the arching forces in the brickwork.

This approximate solution is useful as a means of obtaining a quantitative feel for the problem and, regulated by detailed analysis and experimentation, as a basis for simple design rules. Theoretical solutions for composite wall–beam systems have in fact been produced [1, 3–7], based on a variety of elastic analysis techniques. Finite element methods have also been applied [8–17] and, together with experimental studies, have resulted in a satisfactory understanding of the problem and in proposals for suitable methods for design analysis.

Stafford Smith and Riddington [10, 11] developed a finite element programme for the problem using a four-node rectangular element, with two degrees of freedom at each node and with linearly varying displacement functions along the boundaries. The programme also allows for tensile

cracking at the wall–beam interface. This work confirmed that the total behaviour of the system remains unchanged when the height-to-length ratio exceeds 0.7. These investigators pointed out that the composite wall–beam is the same type of problem as the beam on an elastic foundation and the infilled frame in so far as the distribution of stresses between the elements depends on their relative stiffness. Also, in these problems separation of the elements is possible, the lengths remaining in contact being a function of the relative stiffness. It is therefore essential that this parameter should enter into the analysis. Thus representing the length of contact between wall and beam as αL:

$$\alpha \propto \sqrt[4]{\left(\frac{EIL}{E_w t}\right)} \tag{10.4}$$

where EI is the flexural rigidity of the beam
E_w is the elastic modulus of the wall material in compression
t is the thickness of the wall
L is the length of the wall.

From this

$$\frac{\alpha}{L} \propto \sqrt[4]{\left(\frac{EI}{E_w t L^3}\right)} \tag{10.5}$$

or

$$\frac{\alpha}{L} = \frac{B}{K} \tag{10.6}$$

where $K = \sqrt[4]{(E_w t L^3/EI)}$ and B is a constant, found as a result of experimental investigation to have an average value of unity, in which case

$$\alpha = \frac{L}{K} \tag{10.7}$$

It will be seen from the above that the stiffer the beam relative to the wall, the longer the length of contact x, and this in turn increases the bending moment in the beam and reduces the wall stresses.

Finite element analysis permitted the definition of the vertical compressive and horizontal shear stress distributions over the contact lengths, and these were found to be approximated reasonably well by triangular diagrams. The investigation also indicated that the peak compressive stress in the wall could be represented by

$$\sigma = 1.63\frac{W_w}{L_t}\left(E_w t L^3/EI\right)^{0.28} \tag{10.8}$$

where W_w is the total vertical loading at the wall–beam interface.

The effect of the axial stiffness of the beam was also considered, and it was found that an increase in this property increased the tie force, thereby

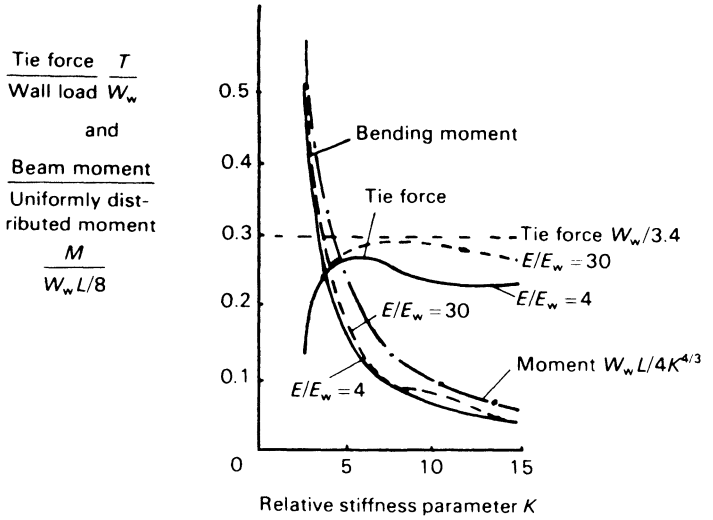

Figure 10.2 Maximum bending moments and tie force in beam (Stafford Smith and Riddington)

reducing the bending moment in the beam and increasing the peak wall stresses.

The results of Stafford Smith and Riddington's study covering a wide range of wall–beam combinations are summarised in figure 10.2. It was found that conservative estimates of the stresses in the wall and in the beam could be calculated from the following formulae:

$$\text{Maximum stress in wall} \quad 1.63\frac{W_w}{Lt}\left(E_w tL^3/EI\right)^{0.28} \tag{10.9}$$

$$\text{Maximum bending moment in beam} \quad \frac{W_w L}{3\left(E_w tL^3/EI\right)^{1/3}} \tag{10.10}$$

$$\text{Maximum tie force in beam} \quad W_w/3.4 \tag{10.11}$$

The effect of extending the beam into the surrounding brickwork was also examined, and this led to the conclusion that the stresses in both elements would be reduced in this case, although negative bending moments could be induced in the beam near its supports. Design procedures have been derived [12] from this investigation applicable to walls resting on steel and concrete beams.

Extensive finite element studies have also been carried out by Ahmed [13], on the basis of which an approximate solution for the composite wall–beam problem has been derived by Davies and Ahmed [14]. In this solution a relative stiffness parameter

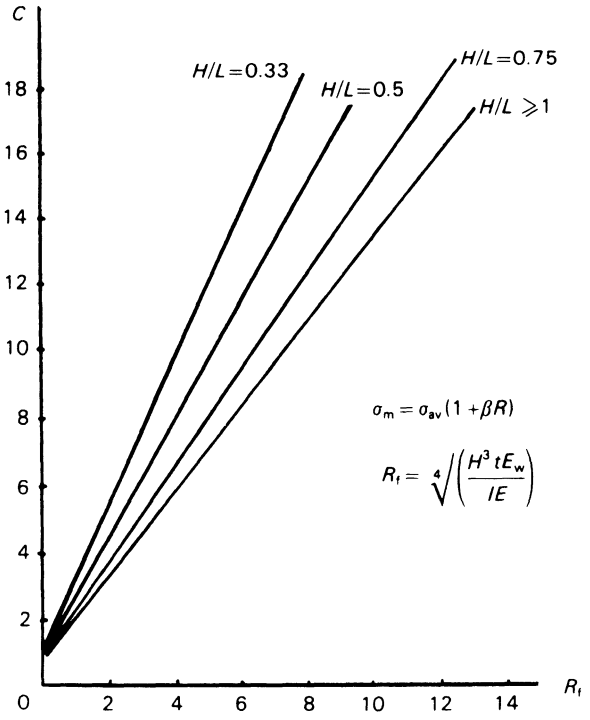

Figure 10.3 Vertical stress concentration factor plotted against parameter R_f (Davies and Ahmed)

$$R_f = \sqrt[4]{\left(\frac{E_w t H^3}{EI}\right)} \tag{10.12}$$

is introduced. This is similar to the corresponding parameter K of Stafford Smith and Riddington, but has been preferred by Davies and Ahmed on the grounds that it directly represents the ratio of the wall to the beam stiffnesses. The ratio C of the maximum to the average compressive stress in the brickwork, as derived for different H/L ratios by finite element calculations, was then plotted with the result shown in figure 10.3. This indicates a linear correlation, giving

$$C = 1 + \beta R_f \tag{10.13}$$

The coefficient β, derived from figure 10.3, can be plotted against H/L as shown in figure 10.4. The maximum vertical stress in the wall is then

$$\sigma_m = \frac{W_w}{Lt}\left(1 + \beta R_f\right) \tag{10.14}$$

The distribution of the vertical stress at the interface depends on the parameter R_f, as shown in figure 10.5.

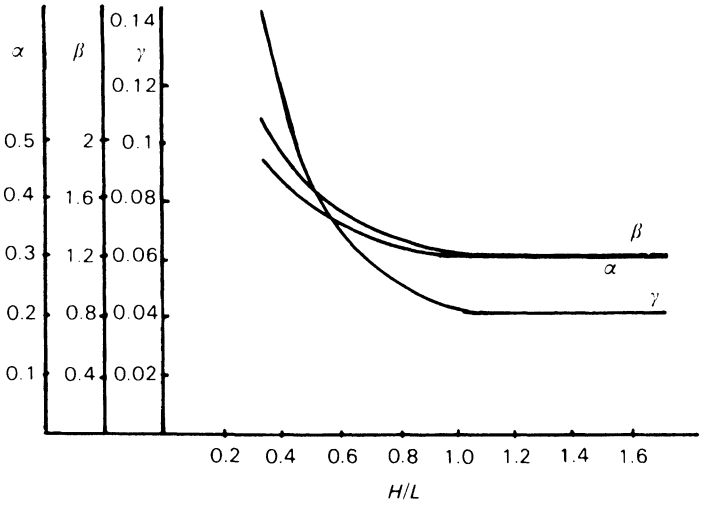

Figure 10.4 Parameters α, β and γ for composite wall beam in Davies and Ahmed's solution

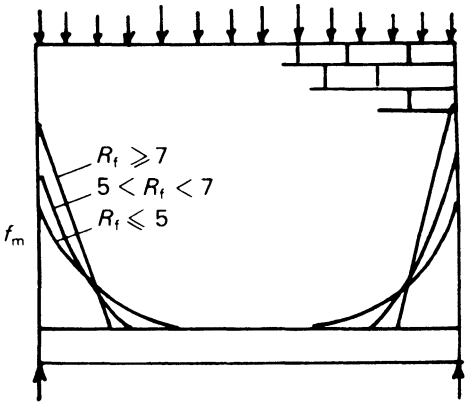

Figure 10.5 Vertical stress distribution at wall–beam interface

A similar procedure is used to calculate the beam axial force, and in this case, an axial stiffness ratio parameter

$$R_a = \frac{E_w t H}{EA} \tag{10.15}$$

is used, where A is the area of the beam. From finite element results the ratio T/W_w is plotted against R_a, as shown in figure 10.6, resulting in a relationship of the type

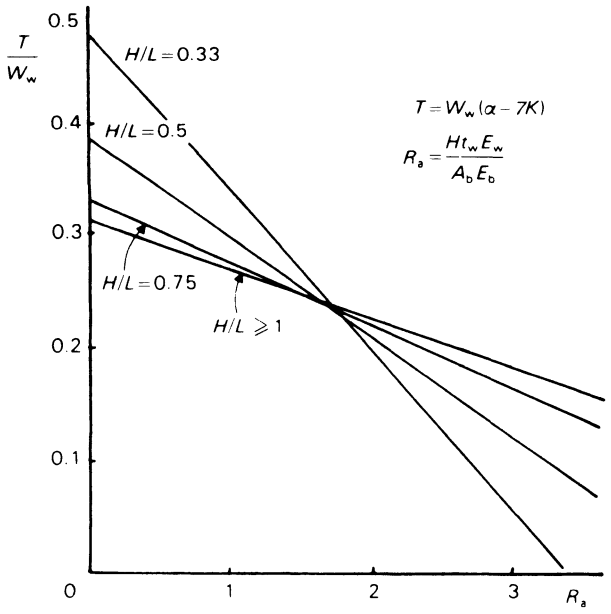

Figure 10.6 Ratio of tie force to total vertical load related to parameter R_a

$$\frac{T}{W_w} = (\alpha - \gamma R_a) \tag{10.16}$$

The coefficients α and γ are plotted against H/L in figure 10.4.

Assuming a triangular distribution of the vertical stress at the supports, of length l_v, it will be seen that

$$W_w = \sigma_m l_v t \tag{10.17}$$

or from equation 10.14

$$l_v = \frac{L}{(1 + \beta R_f)}$$

The finite element analyses showed that the shear stress acts over a length two to three times that of the vertical stress, that is

$$l_s = \frac{2L}{(1 + \beta R_f)} \tag{10.18}$$

Again assuming a triangular stress distribution

$$\frac{1}{2}\tau_m l_s t = T \tag{10.19}$$

and, since $T = W_w(\alpha - \gamma R_a)$, we have

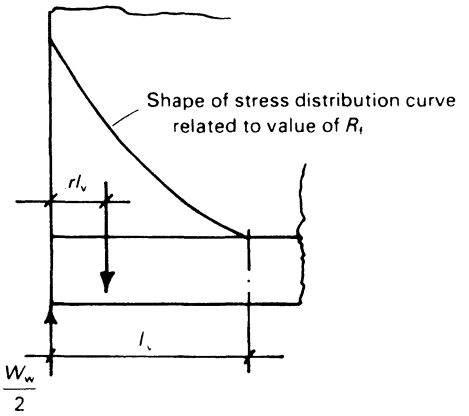

Figure 10.7 Vertical loading on beam

$$\tau_m = \frac{W_m(\alpha - \gamma R_a)(1 + \beta R_f)}{Lt} \tag{10.20}$$

The bending moment at any section in the beam results from the vertical loading and the horizontal shear at the interface, which is eccentric to the axis. Thus referring to figure 10.7, the bending moment over the central region of the beam due to the vertical load is given by

$$M_v = \frac{W_w r l_v}{2} \tag{10.21}$$

where rl_v is the distance of the support reaction to the centroid of the stress diagram. Also

$$\frac{W_w}{2} = \lambda \sigma_m l_v t \tag{10.22}$$

where λ is a coefficient which depends on the shape of the stress diagram. From equations 10.14, 10.20, 10.21 and 10.22:

$$M_v = \frac{W_w L r}{4\lambda(1 + \beta R_f)} \tag{10.23}$$

Davies and Ahmed have found that the axial tension varies along the length of the beam, approximately as shown in figure 10.8, so that the force T_x at a distance x from the support is

$$T_x = \frac{2xT}{L} \tag{10.24}$$

and the bending moment due to this force is, on substituting for T from equation 10.16

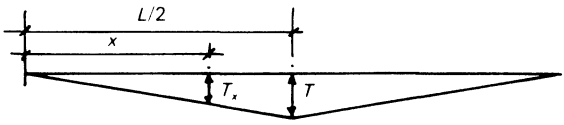

Figure 10.8 Assumed variation of tie force across span of beam (Davies and Ahmed)

$$M_H = \frac{W_w dx}{L}\left(\alpha - \gamma R_a\right) \tag{10.25}$$

The total bending moment at $x = l_v$, assumed to approximate to the maximum value on the span, is then

$$M_m = \frac{W_w Lr - 2W_w d\left(\alpha - \gamma R_a\right)}{4\left(1 + \beta R_f\right)\lambda} \tag{10.26}$$

and at mid-span

$$M_c = \frac{W_w Lr - 2W_w d\left(\alpha - \gamma R_a\right)\left(1 + \beta R_f\right)}{4\left(1 + \beta R_f\right)\lambda} \tag{10.27}$$

The values of r and λ depend on the shape of the stress distribution diagrams, which in turn depend on R_f. Appropriate values and the corresponding bending moment formulae are shown in table 10.1.

Davies and Ahmed [15] also investigated a range of wall–beam structures in which the walls were perforated by window or door openings. This work showed that centrally placed openings have only a small effect on the strength of wall–beam structures, and this is illustrated in figure 10.9, which shows the bending moments in the supporting beam of a typical structure calculated by a finite element analysis. On the other hand, an opening close to a support results in considerably greater bending moments in the beam, and much higher stresses in the wall. In the latter case, Davies and Ahmed suggested that the columns of brickwork between the opening and the end of the wall should be designed to carry half of the loading on the wall–beam structure.

10.1.3 *Experimental results and verification of wall–beam theories*

A considerable amount of experimental investigation of wall–beam structures has been reported [1, 17–21], the results of which confirm the conclusions of the theoretical analyses described in section 10.1.2 and contribute information concerning the behaviour of wall–beams at ultimate load.

Burhouse [20] showed that in the majority of cases failure took place by crushing at the lower corners of the panel, followed by failure of the supporting beam. Similar results were reported by Stafford Smith *et al.* [21]

Table 10.1 Formulae for beam bending moments [15]

Case 1

$R_f \leqslant 5$ stiff beam

$r = 0.2$ and $\lambda = 0.25$

$$M_m = \frac{WL - 10Wd(\alpha - \gamma R_a)}{5(1 + \beta R_f)}$$

and $$M_c = \frac{WL - 2.5Wd(\alpha - \gamma R_a)(1 + \beta R_f)}{5(1 + \beta R_f)}$$

Case 2

$5 < R_f < 7$ flexible beam

$r = 0.25$ and $\lambda = 0.33$

$$M_m = \frac{WL - 8Wd(\alpha - \gamma R_a)}{5.33(1 + \beta R_f)}$$

and $$M_c = \frac{WL - 2.66Wd(\alpha - \gamma R_a)(1 + \beta R_f)}{5.33(1 + \beta R_f)}$$

Case 3

$R_f \geqslant 7$ very flexible beam

$r = 0.33$ and $\lambda = 0.5$

$$M_m = \frac{WL - 6Wd(\alpha - \gamma R_a)}{6(1 + \beta R_f)}$$

and $$M_c = \frac{WL - 3Wd(\alpha - \gamma R_a)(1 + \beta R_f)}{6(1 + \beta R_f)}$$

for structures having 'light' to 'medium' supporting beams, that is, as shown by analysis, where the wall arching forces are heavily concentrated at the ends of the beam. With a very heavy support beam, local damage to the brickwork in the vicinity of the supports was much less severe and, at the ultimate load, failure took place by the development of vertical and diagonal cracks away from the supports. Model experiments by Davies and Ahmed [14] showed cracks radiating from the support points, typical of the failure patterns observed in experiments on concentrated loading on brickwork.

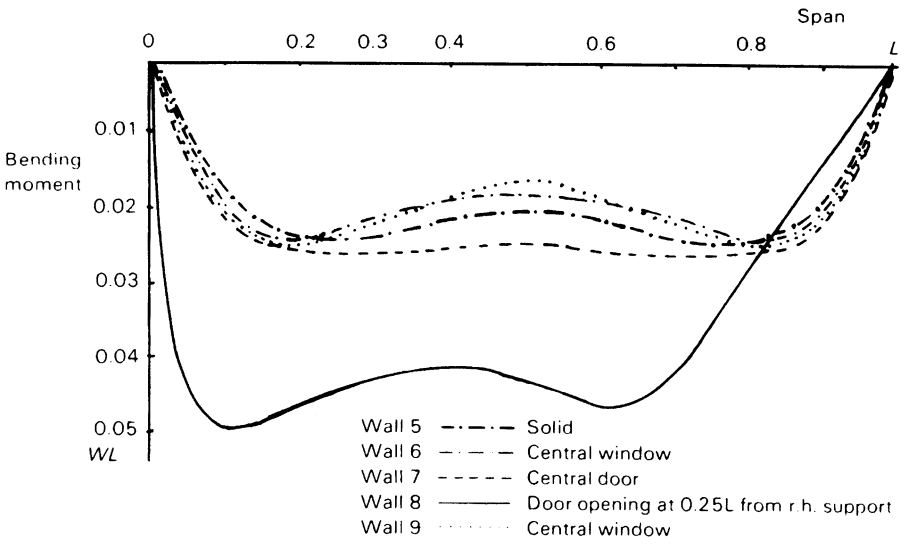

Figure 10.9 Bending moments in wall–beams with openings (Davies and Ahmed)

It is clear from the foregoing that the critical condition for failure will be, in most cases, the concentrated vertical stress distribution around the supports. This can be estimated by one or other of the methods described in the preceding section. If the beam is of exceptionally heavy section the stress concentration will be greatly reduced, and in such a case overall compressive failure of the wall may be the critical condition.

Some comparisons are possible between experimental results and the values calculated by the theories referred to in the previous paragraph – thus table 10.2 shows comparisons of vertical compressive stress concentration factors for five wall–beams tested by Burhouse [20]. In this case, the beams were reinforced concrete sections of 3658mm span, and the walls were 105mm thick single-leaf brickwork. Various parameters for the wall–beam combinations are shown in table 10.2, along with the ratios of maximum-to-average compressive stress as calculated by the approximate methods of Wood and Simms, Stafford Smith and Riddington, and Davies and Ahmed. These may be compared with the reported experimental values – the Davies and Ahmed method appears to give the most consistent agreement with experimental results, while the formula given by Stafford Smith and Riddington gives a very high result for these beams. The very approximate method of Wood and Simms gives values of the correct order of magnitude, but agreement or otherwise with the experimental results may be somewhat fortuitous, as the calculation depends on values of material strength and slenderness reduction factor from a particular code of practice, in the present case BS 5628: 1978.

Table 10.2 Comparison of calculated and experimental vertical stress concentration factors [20]

Test no.	*H/L*	*K**	R_f†	R_a‡	*Stress concentration factor*			
					S.S. & R.	*D. & A.*	*W. & S.* §	*Exp.*
6	0.58	8.48	5.05	1.5	17.86	8.58	6.4	8.33
7	0.58	8.48	5.05	1.5	17.86	8.58	6.4	9.18
8	0.83	8.48	6.83	2.25	17.86	9.89	8.85	8.72
9	0.33	8.48	3.0	0.75	17.86	7.6	8.5	9.39
10	0.81	8.48	6.69	2.19	17.86	9.7	4.75	10.89

* $K = \sqrt[4]{\left(\frac{E_w t L^3}{EI}\right)}$ – Stafford Smith and Riddington.

† $R_f = \sqrt[4]{\left(\frac{E_w t H^3}{EI}\right)}$ – Davies and Ahmed.

‡ $R_a = \frac{E_w t H}{EA}$ – Davies and Ahmed.

§ Calculated on the basis of BS 5628 values for f_k and slenderness reduction factor β (Wood and Simms).

Some further comparisons are given in table 10.3 for three wall–beams tested by Stafford Smith *et al.* [21] where the beams were steel sections encased in concrete of 2500mm span. These results also indicate that the vertical stress concentration factor can be estimated with a fair degree of accuracy by the various methods. Comparisons are also shown in this table for beam bending moment coefficients, and again the three methods of calculation give similar results. The experimental values, however, were of rather doubtful accuracy for the light and medium support beams since the experimentally derived bending moment diagrams were irregular and markedly unsymmetrical; the coefficients quoted refer to the maximum values from these diagrams.

Calculated and experimental values are also shown for the tie force in the beam in table 10.2, where agreement between the various methods is less satisfactory, with only the Davies and Ahmed solution reflecting differences in the tie force, as a fraction of the applied load, between the light, medium and heavy beams. This, however, is borne out by comparing the average tie forces shown by the experimental results, and agreement between these and the Davies and Ahmed values is good for the medium and heavy beams.

Table 10.3 Comparisons between calculated and experimental values for vertical stress concentration factors, bending moment and tie force coefficients [21]

Test no.	*H/L*	*K*	R_f	R_a	*Vertical stress concentration factors*				*Bending moment coefficients**				*Tie force coefficients†*			
					S.S. & R.	*D. & A.*	*W. & S.‡*	*Exp.*	*S.S. & R.*	*D. & A.*	*W. & S.*	*Exp.*	*S.S. & R.*	*D. & A.*	*W. & S.*	*Exp.*
1	0.8	7.9	5.4	3.49	10.12	8.02	7.33	8.4	62.8	49.9	58.7	156	6.8	22	8.8	11.5
2	0.8	6.2	4.33	1.97	5.16	6.63	5.13	5.3	45.5	39.6	41.1	56	6.8	10.8	8.8	9.1
3	0.8	3.7	2.59	0.87	2.9	4.36	2.85		22.8	28	22.8	20	6.8	7.8	8.8	7.8

* $M = W_w L$/Bending moment coefficient.

† $T = W_w$/Tie force coefficient. Coefficients quoted are for average values of tie force.

‡ Values calculated on ratio of brick work stress at failure/brickwork strength and slenderness reduction coefficient from BS 5628: 1978.

10.2 **Infilled frames**

10.2.1 ***Structural action of infill panels***

Many steel and reinforced concrete frames are built with a brickwork infill which adds considerably to the strength and rigidity of the structure as a whole. A considerable amount of research work has been carried out on the stiffening effect of infill panels although very little use of this appears to be made in practical design, possibly because of the uncertainty of the composite action when, as is usual, the brickwork is not completely bonded to the frame and there is the fear that infill panels may be removed at some stage in the life of a building. Despite these difficulties there may well be circumstances in which designers may wish to take account of the effect of infilling as, for example, in resisting exceptional forces where some degree of cracking would be unimportant.

The general nature of the structural interaction between frame and infill has been clarified, and is illustrated in figure 10.10. On first application of a racking load there may be full composite action between the frame and wall if these are bonded together. At a comparatively early stage, however, cracks will develop between the two components, except in the vicinity of two of the corners where the infill panel will lock into the frame and there will be transmission of compressive forces into the brickwork. At this stage, it is convenient to consider that the brickwork is acting as a compression diagonal within the frame, the effective width of which depends on the relative stiffness of the two components and on the ratio of the height to the width of the panel. This action continues until the shear resistance of the brickwork is overcome and a crack, slightly inclined to the horizontal, is developed. Several more or less parallel cracks of this type may develop with further increase in load and failure may finally result from the loss of rigidity of the infill as a result of these cracks, or from local crushing or spalling of the brickwork in the region of the concentrated loads. In some cases the strength of the structure may be limited by the strength of the frame members or joints.

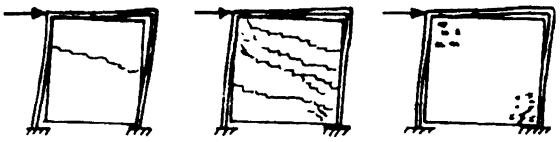

(a) First shear crack (b) Propagation of cracks (c) Crushing and spalling

Figure 10.10 Failure of infilled frames

10.2.2 *Calculation of strength and stiffness of infilled frames*

Although the analysis of infilled frame structures has been attempted using the theory of elasticity [22, 23] and by finite element analyses [24–26], the rather uncertain boundary conditions between the brickwork and the frame suggest that an approximate solution would be appropriate. Various approximations [27–29] have been proposed, the most highly developed being that based on the concept of an equivalent diagonal strut, which was originally proposed by Polyakov [30] and subsequently developed by other investigators [31–34].

The essential problems in this approach are (1) to determine the contact lengths between the frame and the brickwork, (2) to find an effective width for the equivalent strut and (3) to establish the mode of failure and strength of the brickwork. The contact length depends on the relative stiffness of the frame and infill, and on the geometry of the panel. Stafford Smith [34] first developed the analogy with a beam on an elastic foundation, by which the column of an unfilled frame under lateral load may be regarded as one half of a beam on an elastic foundation (figure 10.11a) which under a central concentrated load, P, remains in contact with the foundation over a length l_c known as the characteristic length. The general solution for the beam on an elastic foundations is

$$y = \exp(\lambda x)(A\cos\lambda x + B\sin\lambda x) + \exp(-\lambda x)(C\cos\lambda x + D\sin\lambda x)$$

where $\lambda = \sqrt[4]{(k/EI)}$, k is the foundation modulus, and A, B, C and D are constants depending on the loading and end conditions. The characteristic

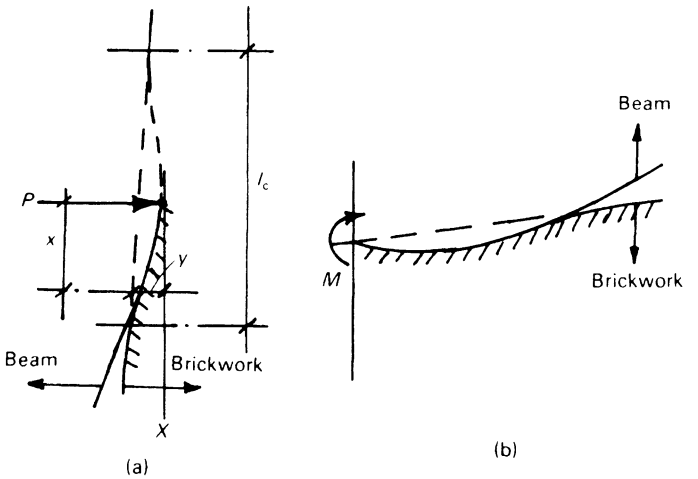

Figure 10.11 Beam on elastic foundation analogy for contact length between infill and frame

length is defined when $\lambda I_c = \pi$ in the general solution and the contact length in the case of the column of an infilled frame is half of this, leading to a parameter

$$\alpha_h = \frac{\pi}{2\lambda_h} \tag{10.28}$$

where

$$\lambda_h = \sqrt[4]{\left(\frac{E_w t \sin 2\theta}{4EI_h h}\right)} \tag{10.29}$$

in which E_w, E are the elastic moduli of the wall and frame materials respectively
t is the wall thickness
I_h is the second moment of area of the column
h is the height of the wall
l is the length of the beam
$\theta = \tan^{-1}(h/l)$.

Similarly the beam member of the infilled frame may be represented as a beam on an elastic foundation loaded by a moment M, figure 10.11b, giving rise to a corresponding parameter

$$\alpha_l = \frac{\pi}{\lambda_l} \tag{10.30}$$

where

$$\lambda_l = \sqrt[4]{\left(\frac{E_w t \sin 2\theta}{4EI_l l}\right)} \tag{10.31}$$

in which I_l is the second moment of area of the beam. The parameters λ_h and λ_l have the dimension $(\text{length})^{-1}$, and α_h and α_l have the dimension of length, so that it is convenient to multiply the first two and to divide the second two by l or h as appropriate to obtain the dimensionless graphs shown in figure 10.12, from which the contact lengths can be found for any given system.

A value for the effective width of the equivalent diagonal strut can be obtained on the basis that the compression band is defined by the lengths α_h and α_l, as shown in figure 10.13. The distribution of compressive stress between the two limiting points will not be uniform, and on the assumption that it is triangular with a maximum on the diagonal, the effective width may be taken as

$$w = \frac{1}{2}\sqrt{(\alpha_l^2 + \alpha_h^2)} \tag{10.32}$$

$$= \frac{\pi}{2}\sqrt{\left[\left(\frac{1}{\lambda_l}\right)^2 + \left(\frac{1}{2\lambda_h}\right)^2\right]} \tag{10.33}$$

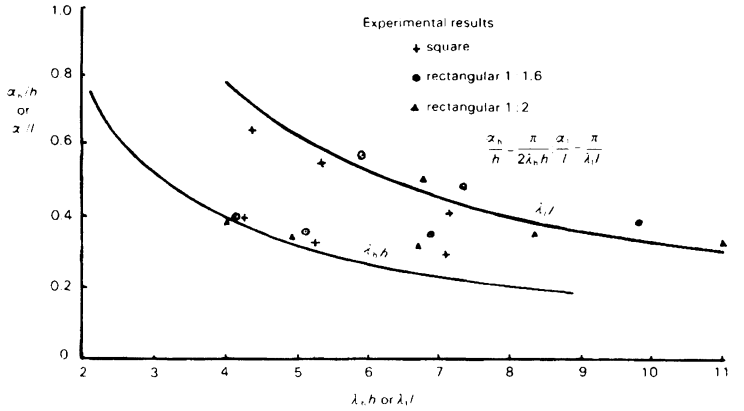

Figure 10.12 Parametric plots for infilled frames

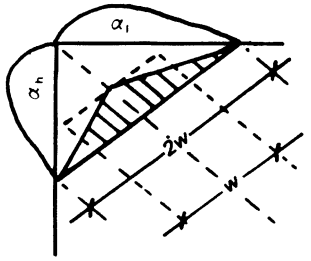

Figure 10.13 Effective width of equivalent diagonal strut

As previously noted, failure of the brickwork takes place by shear cracking along the joints between the bricks, which may be followed by crushing near the loaded corner. The cracking load of the brickwork can be estimated on the basis of the following relationship for shear strength

$$\tau = \tau_0 + \mu\sigma_n \tag{10.34}$$

where τ_0 is the shear bond strength
μ is the apparent coefficient of friction
σ_n is the normal stress on the bed joint.

If R_{cr} is the force acting on the equivalent diagonal, then the shear stress and normal stress at the centre of the panel are approximately

$$\tau = \frac{R_{cr}\cos\theta}{lwt} \tag{10.35}$$

$$\sigma_n = \frac{R_{cr}\sin\theta}{lwt}\frac{\alpha_1}{l_w} \tag{10.36}$$

The latter relationship has been suggested by Kadir [26] following work by Seddon [35] on partially loaded concrete walls. Substituting in equation 10.34 and putting $\alpha_1/l_w = \pi/\lambda_1 l_w$ gives for the horizontal load on the wall at the point of cracking:

$$P_w = R_{cr}\cos\theta = \frac{\tau_0 l_w t}{1 - \mu\tan\theta\left(\dfrac{\pi}{\lambda_1 l_w}\right)} \tag{10.37}$$

Kadir has carried out an elastic analysis to obtain a relationship giving the percentage of the total force applied to the frame–wall system carried by the wall, in terms of $\lambda_h h$. The result is shown in figure 10.14 and, from this and equation 10.37, it is possible to calculate the total cracking load on the structure, assuming that the frame remains elastic up to this point.

Following initial cracking of the brickwork, and again assuming the frame does not fail, the brickwork will resist increased lateral loading on the frame by friction, wedging and arching actions within the frame. It is not possible to apply rigorous methods of analysis to the structure in this state, but as an approximation it might be assumed that crushing failure of the equivalent diagonal strut takes place over the effective width, w. If the lateral load P_{wu} is applied along a length of the column equal to $w\cos\theta$ and it is assumed that the loading varies linearly, as shown in figure 10.15, then the ultimate load carried by the infill is

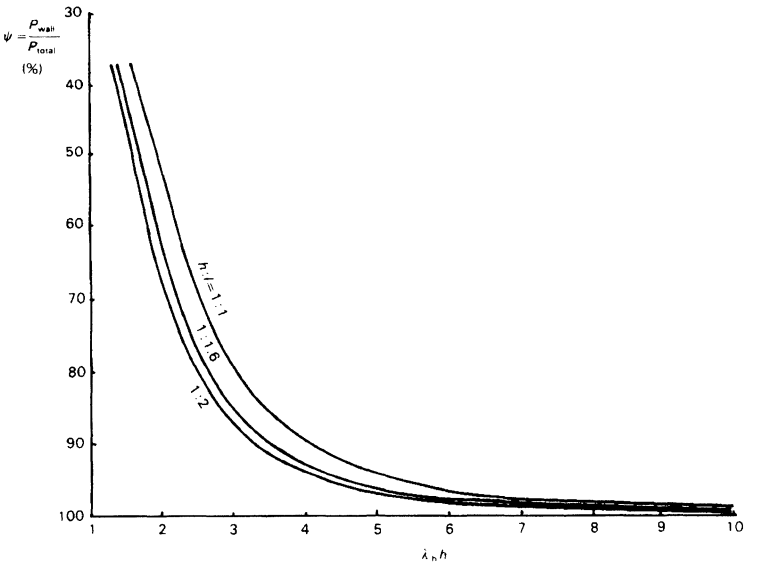

Figure 10.14 (P_{wall}/P_{total}) per cent as a function of $\lambda_h h$

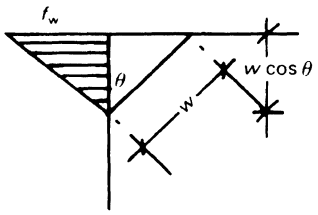

Figure 10.15 Distribution of lateral stress at ultimate load

$$P_w = \frac{1}{2} f_w t w \cos\theta \tag{10.38}$$

where f_w is the ultimate compressive strength of the brickwork. To this load must be added the resistance of the frame at the deflection, δ_f, corresponding to the maximum load in the brickwork. If the frame remains elastic, its stiffness can be calculated by normal methods of analysis; thus for a rectangular frame

$$P_f = \delta_f \frac{12EI_c}{h^3} \left[\frac{6I_l h + I_h l}{3I_l h + 2I_h l} \right] \tag{10.39}$$

Estimation of δ_f is difficult but, as an approximation based on experimental results, it could be calculated on the basis of an assumed brickwork strain at failure of 0.003.

The analysis described above is based on many simplifications, but as experimental results show considerable variation in terms of stiffness, initial cracking load and strength, the method is possibly as accurate as the situation allows. Comparisons between Kadir's approximate theory and the results of tests on one-third scale brickwork panels in steel frames are shown in figures 10.16, 10.17 and 10.18. Kadir also found that the equivalent diagonal strut method could be applied to multi-storey frames with reasonable accuracy.

10.2.3 *Infill panels with openings*

Infill panels frequently contain door or window openings, which will obviously reduce their effectiveness in stiffening the surrounding frame to an extent dependent on their size. Experiments by a number of investigators [22, 31, 36, 37] have indicated that centrally located openings may reduce the strength and stiffness of an infilled frame by about 50 per cent and 70 per cent respectively. The results of a number of model-scale tests by Kadir [26] are summarised in table 10.4, and these illustrate the effect of various sized centrally placed openings in a square infilled panel. The load at first cracking was reduced by approximately 50–80 per cent, and the ultimate load by 0–40 per cent, as compared with a corresponding frame without

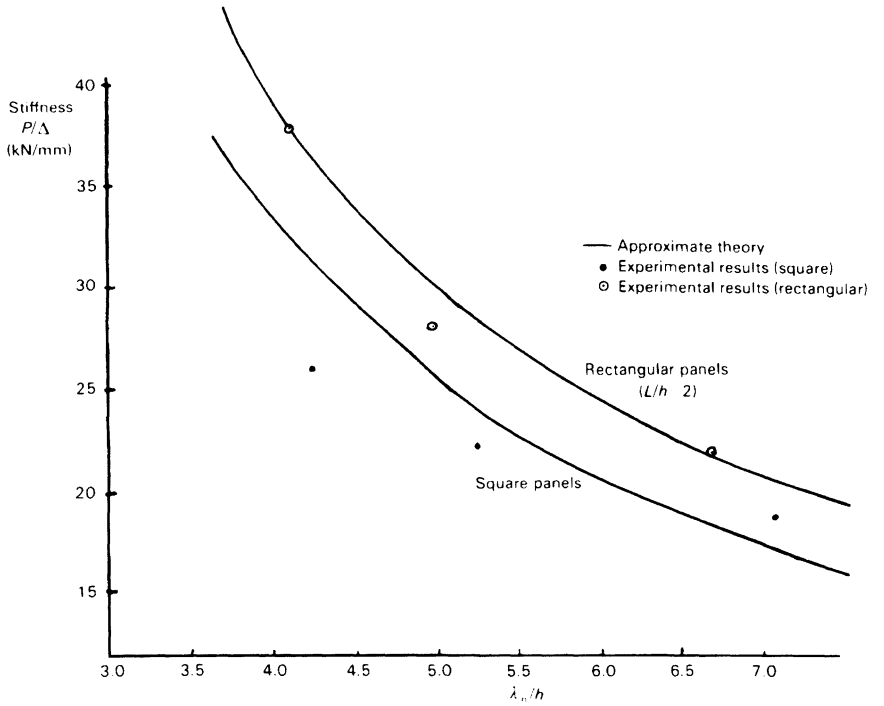

Figure 10.16 Lateral stiffness as a function of $\lambda_h h$

openings. However, because of the variability in the test results and the small number of experiments, no definite conclusions could be drawn.

Kadir suggested an approximate method of analysing infilled panels with openings in which the panel is replaced by a diagonal member of equivalent stiffness, and the stiffness of this diagonal can be calculated by considering the brickwork as a frame from the relationship

$$K_w = \frac{48E_w}{h'_w\left(h'_w + h_f\right)}\left(\frac{J_l J_h}{J_l h'_w + J_h l'_w}\right) \tag{10.40}$$

where J_h and J_l are the moments of inertia of the vertical and horizontal sections of the brickwork 'frame' shown in figure 10.19. The stiffness of the frame plus infill is then

$$K = \frac{12EI_h}{h^3 f}\left(\frac{6I_l h + I_h l}{3I_l h + 2I_h l}\right) + \frac{48E_w}{h'_w\left(h'_w + h_f\right)}\left(\frac{J_l J_h}{J_l h'_w + J_h l'_w}\right) \tag{10.41}$$

in which the first term is the frame stiffness.

Liauw and Lee [37] have put forward a method for the calculation of the stiffness and strength of infilled frames with openings that uses a strain

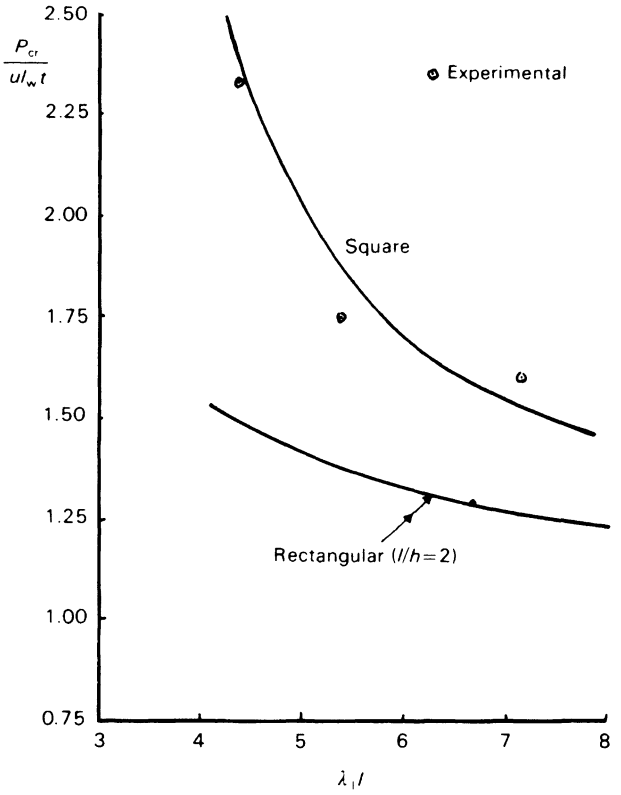

Figure 10.17 Cracking strength as a function of $\lambda_1 l$

energy method to establish the area of the equivalent diagonal strut. Referring to figure 10.20, an infill with a centrally placed door opening is replaced by two members, one horizontal and one vertical, of effective lengths L_1 and L_2 respectively and connected by a rigid joint. Interactive forces between the surrounding frame and the infill are assumed to be concentrated at two diagonally opposite corners and transmitted to this 'frame' by rigid arms. The effective length of the beam and height of the column are

$$L_1 = B + C_1$$

$$L_2 = H + C_2 \leqslant L_2'$$

where L_2' is the distance from the bottom of the wall to the centroidal axis of the beam, and C_1 is taken as half the depth of the beam. Then from consideration of the total strain energy, the deflection in the direction of the load is

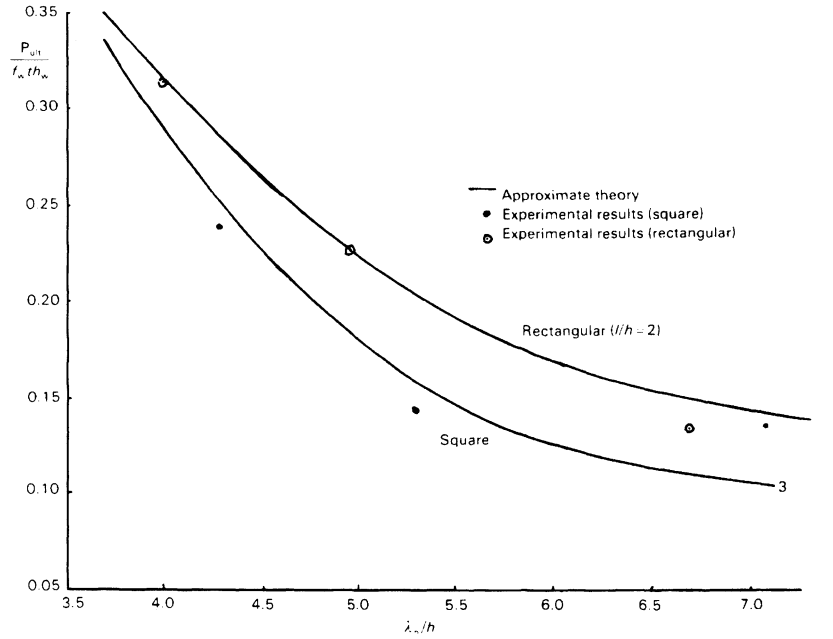

Figure 10.18 Ultimate strength as a function of $\lambda_h h$

Table 10.4 Infilled frames with openings (frame members 1.5 × 0.75 in. section in all tests)

Test no.	$h_w \times l_w$ *(in.)*	*Opening a × b (in.)*	*Strength*		*Exp. stiffness*		*Est. stiffness (approx.) (ton/in.)*
			Crack (ton)	*Ultim. (ton)*	*Initial (ton/in.)*	*Post-cr. (ton/in.)*	
—	15.75 × 15.75	No opening	1.05	4.02	55.5	—	—
WW5		3.375 × 3.126	0.35	4.52	64	22.7	97.0
WW6		3.375 × 3.126	0.375	4.32	80	25.0	97.0
WW1		6.75 × 6.25	0.35	2.75	28.5	19.6	31.7
WW3		6.75 × 6.25	0.25	2.85	33	18.5	31.7
WW2		11.25 × 9.50	0.20	2.025	6.3	5.4	6.06
WW4		11.25 × 9.50	0.15	1.98	9.7	5.7	6.06
—	15.75 × 25.25	No opening	1.27	5.28	68.0	—	—
WWA		4.5 × 6.5	0.45	4.45	83.0	29.5	73.0
WWA1		4.5 × 6.5	0.40	5.22	98.0	45.0	73.0
WWB		6.875 × 9.45	0.30	4.00	57.0	20.7	31.6
WWB1		6.875 × 9.45	0.20	3.94	82.0	18.0	31.6
WWC		9.0 × 15.75	0.125	2.20	18.75	13.0	11.0
WWC1		9.0 × 15.75	0.20	2.275	38.4	14.0	11.0
—	15.75 × 15.75	No opening	1.05	4.02	55.5	—	—
WD1		11.25 × 6.25	0.40	2.50	20.5	7.90	28.5
WD2		11.25 × 6.25	0.35	2.20	21.5	8.60	28.5

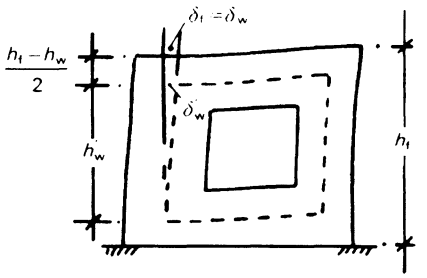

Figure 10.19 Dimensions of equivalent brickwork frame

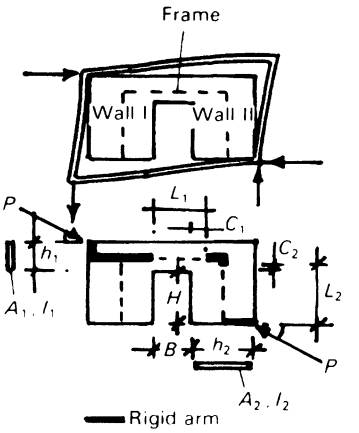

Figure 10.20 Analysis of infilled frame with opening (Liauw and Lee)

$$\Delta = \frac{P}{3E}\left\{\frac{\sin^2\theta}{I_1}\left[\left(L - m_1\right)^3 - m_1^3\right] + \frac{\cos^2\theta}{I_2}\left[\left(L_2 - m_2\right)^3 + m_2^3\right]\right.$$
$$\left. + \frac{1.2E}{G}\left(\frac{L_1\sin^2\theta}{A_1} + \frac{L_2\cos^2\theta}{A_2}\right) + \frac{L_1\cos^2\theta}{A_1} + \frac{L_2\sin^2\theta}{A_2}\right\} \tag{10.42}$$

where $m_1 = (h_1/2)\cot\theta$ and $m_2 = (h_2/2)\tan\theta$.

The diagonal stiffness of the infill is then equal to the reciprocal of the deflection Δ when $P = 1$. The stiffness of the equivalent diagonal strut is then given by

$$k = EA_e/L_d \tag{10.43}$$

and its cross-sectional area $A_e = L_d/E\Delta$. The infilled frame is then represented by a diagonally braced frame using these equivalent struts.

Liauw and Lee suggest calculating the strength of the frame, when the opening lies below the compression diagonal, with reference to the equivalent area A_e and the ultimate compressive stress of the infill material. If the opening extends above the compression diagonal the infill is subjected to bending, shear and compression, and it is necessary to assess the strength of the brickwork under diagonal loading. This will usually be limited by the bending or shear strength of one of the beam elements and may be calculated approximately on this basis. Liauw and Lee reported reasonable agreement between the results calculated in this way and those obtained experimentally.

10.2.4 *Reinforced masonry infill*

A series of tests on steel frames with reinforced brickwork or blockwork masonry infill under monotonic loading has been reported by Hendry and Liauw [38]. The brickwork infilled panels had various amounts of bed joint reinforcement which did not significantly increase the racking strength of the frame. The presence of bed joint reinforcement in fact reduced the load at which first cracks appeared from 66 per cent maximum load with the unreinforced infill to 44 per cent. Before cracking, the behaviour of the composite frame was linear so that elastic analysis could be applied up to this point. Beyond this, however, the crack pattern was exceedingly complicated (figure 10.21) making any analytical representation very uncertain.

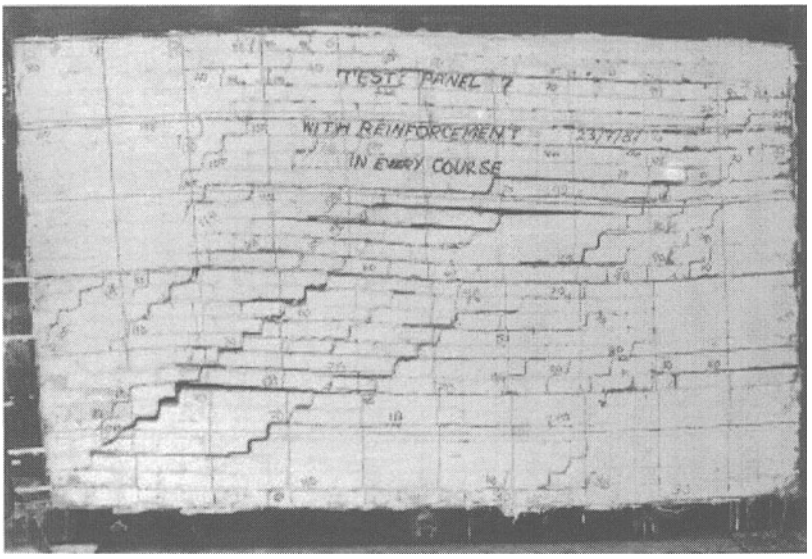

Figure 10.21 Steel frame with brickwork infill reinforced in every joint

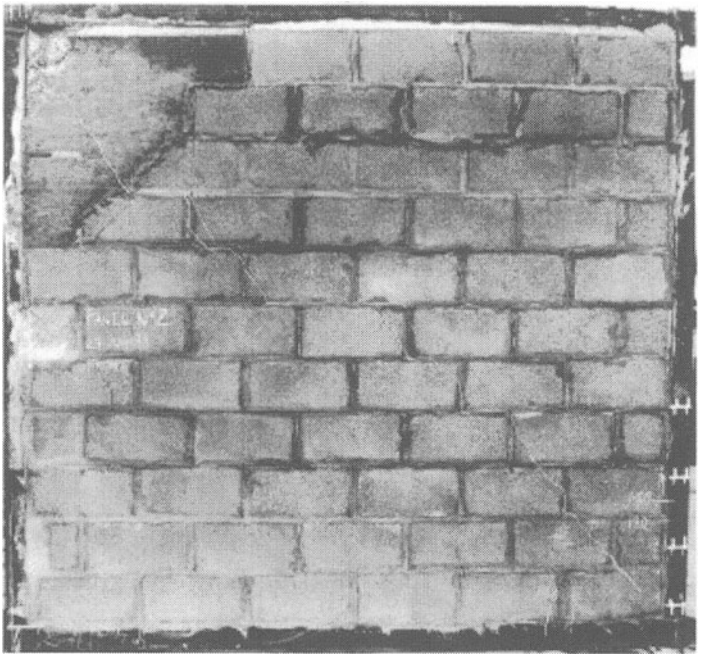

Figure 10.22 Steel frame with hollow concrete blockwork infill with 0.4 per cent vertical reinforcement in cores. Splitting of block at loaded corner

Reinforcement of hollow concrete blockwork with vertical bars through the cores was considerably more promising, provided that local failure of the blocks at the loaded corner of the frame could be prevented. Cracking of the concrete blockwork panels, apart from local crushing, was confined to the loaded diagonal as may be seen in figure 10.22. In this case, behaviour was linear up to the maximum load making the application of elastic analysis more appropriate.

References

1. R. H. Wood, 'Studies in Composite Construction. Part 1, The Composite Action of Brick Panel Walls Supported on Reinforced Concrete Beams', *National Building Studies Research Paper 13* (HMSO, London, 1952).
2. R. H. Wood and L. G. Simms, 'A Tentative Design Method for the Composite Action of Heavily Loaded Brick Panel Walls Supported on Reinforced Concrete Beams', *BRS CP26/69* (Building Research Station, Watford, Herts., 1969).
3. S. Rosenhaupt, 'Stresses in Point Supported Composite Walls', *J. Am. Concr. Inst.*, **61** (1964) 795.
4. A. Coull, 'Composite Action of Walls Supported on Beams', *Bldg Sci.*, **1** (1966) 259.

5. J. R. Colbourne, 'Studies in Composite Construction: An Elastic Analysis of Wall–Beam Structures', *BRS CP15/69* (Building Research Station, Watford, Herts., 1962).
6. A. L. Yettram and M. J. S. Hirst, 'An Elastic Analysis for the Composite Action of Walls Supported on Simple Beams', *Bldg Sci.*, **6** (1971) 151–9.
7. M. Levy and E. Spira, 'Analysis of Composite Walls with and without Openings', *Rep. Wkg Commn Int. Ass. Bridge Struct. Engng*, **33-1** (1973) 143–66.
8. D. J. Male and P. F. Arbon, 'A Finite Element Study of Composite Action in Walls', *Second Australasian Conference on Mechanics of Structures and Materials* (University of Adelaide) August 1969.
9. D. R. Green, 'The Interaction of Solid Shear Walls and their Supporting Structures'. *Bldg Sci.*, **7** (1972) 239–48.
10. B. Stafford Smith and J. R. Riddington, 'The Composite Behaviour of Masonry Wall on Steel Beam Structures', *Proceedings of the First Canadian Masonry Symposium* (Calgary) 1976, pp. 292–303.
11. B. Stafford Smith and J. R. Riddington, 'The Composite Behaviour of Elastic Wall–Beam Systems', *Proc. Instn Civ. Engrs*, **63** (1977) 377–91.
12. J. R. Riddington and B. Stafford Smith, 'Composite Method of Design for Heavily Loaded Wall/Beam Structures', *Proc. Instn Civ. Engrs*, **64** (1978) 137–51.
13. A. E. Ahmed, 'A Study of the Composite Action between Masonry Panels and Supporting Beams', PhD Thesis (University of Edinburgh, 1977).
14. S. R. Davies and A. E. Ahmed, 'An Approximate Method for Analysing Composite Wall/Beams', *Proc. Br. Ceram. Soc.*, **27** (1978) 305–20.
15. S. R. Davies and A. E. Ahmed, 'Composite Action of Wall–Beams with Openings', *Proceedings of the Fourth International Brick Masonry Conference* (Brugge) 1976, Paper 4.b.6.
16. C. B. Saw, 'Linear Elastic Finite Element Analysis of Masonry Walls on Beams', *Bldg Sci.*, **9** (1974) 299–307.
17. C. B. Saw, 'Composite Action of Masonry Walls on Beams', *Proc, Br. Ceram. Soc.*, **24** (1975) 139–46.
18. S. Rosenhaupt, 'Experimental Study of Masonry Walls on Beams', *J. Struct. Div. Am. Soc. Civ. Engrs*, **S73** (1962) 137–66.
19. S. Rosenhaupt and Y. Sokal, 'Masonry Walls on Continuous Beams', *J. Struct. Div. Am. Soc. Civ. Engrs*, **91** (1965) 155–71.
20. P. Burhouse, 'Composite Action between Brick Panel Walls and their Supporting Beams', *Proc. Instn Civ. Engrs*, **43** (1969) 175–94.
21. B. Stafford Smith, M. A. H. Khan and H. G. Wickens, 'Tests on Wall Beam Structures', *Proc. Br. Ceram. Soc.*, **27** (1978) 289–303.
22. S. Sarchanski, 'Analysis of the Earthquake Resistance of Frame Buildings Taking into Consideration the Carrying Capacity of the Filling Masonry', *Proceedings of the Second World Conference on Earthquake Engineering*, **III** (1960) 2127–41.
23. T. C. Liauw, 'Elastic Behaviour of Infilled Frames', *Proc. Instn Civ. Engrs*, **46** (1970) 343–9.
24. T. Karamanski, 'Calculating Infilled Frames by the Method of Finite Elements', in *Symposium on Tall Buildings*, eds A. Coull and B. Stafford Smith (Pergamon, Oxford, 1967), pp. 455–61.

25. D. V. Mallick and R. T. Severn, 'The Behaviour of Infilled Frames under Static Loading', *Proc. Instn Civ. Engrs*, **38** (1967) 639–56.
26. M. R. A. Kadir, 'The Structural Behaviour of Masonry Infill Panels in Framed Structures', PhD Thesis (University of Edinburgh, 1974).
27. R. H. Wood, 'The Stability of Tall Buildings', *Proc. Instn Civ. Engrs*, **11** (1958) 69–102; discussion, **12** (1959) 502–22.
28. J. R. Benjamin and H. A. Williams, 'The Behaviour of One-Storey Brick Shear Walls', *J. Struct. Div. Am. Soc. Civ. Engrs*, **84** (ST4) (1958), Paper 1728.
29. T. C. Liauw, 'An Approximate Method of Analysis for Infilled Frames with or without Openings', *Bldg Sci.*, **7** (1972) 233–8.
30. S. V. Polyakov, 'Masonry in Framed Buildings', *Gosudalst-Vennoe Izdatel' stvo Literature po Straitel'stvu i Arkitecture*, Moskva, 1956, trans. G. L. Cairns (Building Research Station, Watford, Herts., 1963).
31. M. Holmes, 'Steel Frames with Brickwork and Concrete Infilling', *Proc. Instn Civ. Engrs*, **19** (1961) 473–8.
32. B. Stafford Smith, 'Lateral Stiffness of Infilled Frames', *J. Struct. Div. Am. Soc. Civ. Engrs*, **88** (ST6) (1962) 183–9.
33. R. J. Mainstone, 'On the Stiffness and Strengths of Infilled Frames', *Proc. Instn Civ. Engrs*, Supplement IV, Paper 73605 (1971) 57–90.
34. B. Stafford Smith, 'Behaviour of Square Infilled Frames', *J. Struct. Div. Am. Soc. Civ. Engrs*, **92** (ST1) (1966) 381–403.
35. A. E. Seddon, 'The Strength of Concrete Walls under Axial and Eccentric Loads', *Symposium on Strength of Concrete Structures* (Cement and Concrete Association, London, 1956), pp. 445–73.
36. J. R. Benjamin and H. A. Williams, 'Behaviour of One-Storey Walls Containing Opening', *J. Am. Concr. Inst.*, **30** (1958) 605–18.
37. T. C. Liauw and S. W. Lee, 'On the 'Behaviour and the Analysis of Multi-Storey Infilled Frames subject to Lateral Loading', *Proc. Instn Civ. Engrs*, **63** (1977) 641–56.
38. A. W. Hendry and T. C. Liauw, 'Tests on Steel Frames with Reinforced Masonry Infilling', *Proc. Br. Masonry Soc.*, **6** (1994) 108–14.

11 THE STRENGTH OF MASONRY ARCH STRUCTURES

11.1 **General**

Masonry arches were in use for bridges and in buildings for many centuries. Their design, until the Seventeenth Century, was determined entirely by rules of proportion evolved by trial and error. A more scientific approach emerged with the realisation by Poleni and by Hooke that an arch, or segment of a dome, would be stable provided that the flexible cable carrying suspended weights, representing that of the structure, when inverted could be contained within the depth of the masonry. This concept was highly developed through the Nineteenth Century in terms of the line of thrust, reflecting the fact that the arch problem is primarily one of equilibrium rather than of material strength. Elastic analysis was applied to arches but the state of stress is very sensitive to small changes in conditions, for example at the abutments, so that the state of stress in an arch cannot be calculated with any great certainty. Furthermore, the stresses occurring in these structures are generally small and do not, in general, provide a useful safety criterion.

For various reasons, including relative costs, design philosophy and changing fashions in the use of materials, masonry arches largely fell out of use in the Twentieth Century. However, there is renewed interest in the use of arches in building and in the performance of existing masonry arch bridges. Given the exceptional durability with minimum maintenance associated with masonry arches, it is possible that there will be a revival in their use. This will be dependent on the development of methods of analysis stated in contemporary terms. Heyman [1, 2] has presented the essential principles on which an understanding of masonry arches and domes can be based. In essence, he suggests that these principles are statical equilibrium and the theorem of plastic theory which states that if any one configuration of the line of thrust can be contained within the arch, the structure is stable and collapse can never occur.

It has to be stated, however, that in practice the behaviour of masonry arch structures is extremely complicated. The following discussion therefore gives only an outline of basic principles and problems and a summary of the results of a number of experimental investigations.

11.2 **The line of thrust**

The line of thrust in an arch defines the path followed by the resultant of the forces acting on an arch across its span, including self-weight and external actions. Statically, it corresponds to the shape which would be taken up by a suspended cable subjected to the same forces but, of course, inverted. The line of thrust can be constructed using the funicular polygon construction as shown in figure 11.1a. To draw the funicular polygon, it is necessary to select a position for the pole, O, such that its horizontal distance from the vector line representing the vertical forces on the arch is, to the same scale, proportional to the arch thrust H and located vertically to correspond with the vertical reactions R_R and R_L. The polygon ACDEB is then constructed by drawing links parallel to the vectors O_1, O_2, etc.

It is possible to proceed by selecting an arbitrary position for the pole at, say, O_1 in figure 11.1b, and drawing the funicular polygon $AC_1D_1E_1B$. Since the polygon is required to pass through B, it is now redrawn using pole O_2 located by drawing a parallel to AB_1 through O_1; the new pole is then at the intersection of the horizontal and vertical lines O_1O_2 and XO_2, and the redrawn polygon is ACDEB as before. If it is required in addition that the funicular polygon should pass through a third point, say D_2, the pole must be moved horizontally to O_3 so that

$$O_3X = \frac{dD_1}{dD_2} O_2X$$

11.3 **Analysis of arches**

11.3.1 ***Arch stability in terms of the line of thrust***

It has long been understood that if the line of thrust for an arch for a particular load condition lies within the middle-third of the arch depth, the material of the arch will be entirely in compression. Theoretically, the arch would fail if the loads were raised proportionally to such a level that the compressive strength of the material was reached. In practice, however, the stresses in masonry arches will rarely reach the compressive strength of the material and failure under this condition is improbable.

It is commonly assumed that the joints between the masonry units in an arch possess no tensile resistance and therefore if the line of thrust lies outside the middle-third, cracks will appear on one side or the other of the

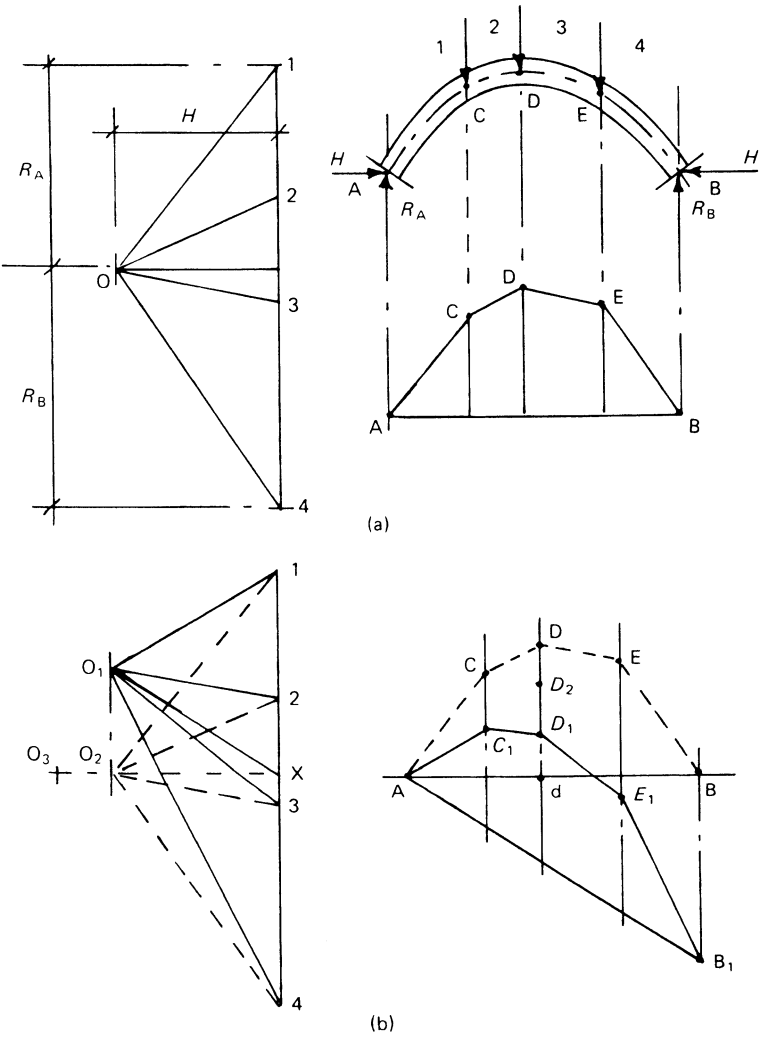

Figure 11.1 Funicular polygon construction

arch. The appearance of such cracks does not, however, imply failure. Compressive stresses may well be higher than in an uncracked arch but will still be relatively small compared with the strength of the material. It is, in fact, usually assumed that the material is infinitely strong in compression and that a failure condition is reached when the line of thrust reaches the outer faces of the masonry at four points, converting the structure into a kinematic mechanism by the formation of hinge points where the line of thrust coincides with the intrados or extrados of the arch.

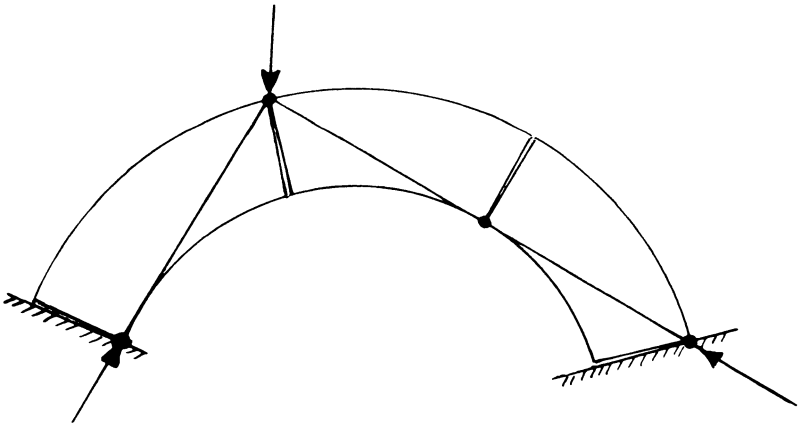

Figure 11.2 Arch failure mechanism

The failure condition is illustrated in figure 11.2 for an elementary loading case, from which it will be seen that hinge points are formed on alternate sides of the arch. A graphical procedure [2] (Fuller's construction) is available which can be used to determine whether the line of thrust can be contained within the depth of an arch. This construction relies on replacing the funicular polygon by two straight lines related to a distorted arch geometry and is shown in figure 11.3. In this diagram the funicular polygon for the loads W_1 to W_5 has been drawn on a horizontal base using the statically calculated vertical reactions at A and B and an arbitrary pole position (or horizontal thrust). Straight lines are drawn from point q, the highest point on the polygon, to points A′ and B′, any points on the horizontal base line. The distorted arch shape is then determined by drawing horizontal intercepts such as Pp′ from the node points of the original

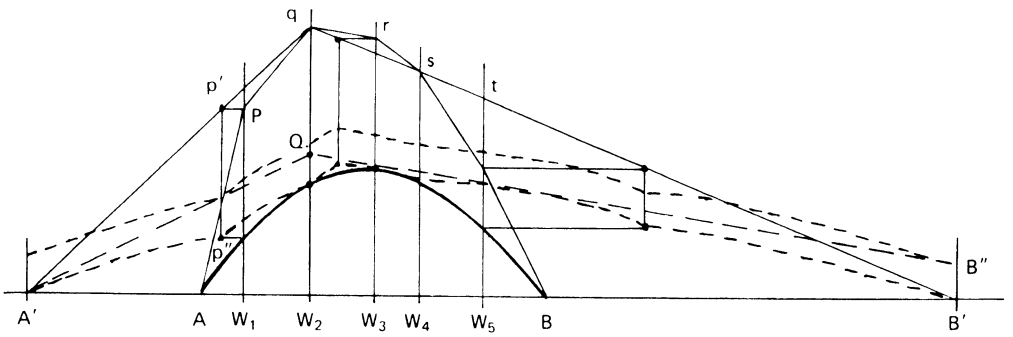

Figure 11.3 Fuller's construction (after Heyman)

polygon to intersect A′q or B′q, and verticals such as p′p″ are dropped equal in length to the distance from the original polygon to the arch profile. The point p″ is then a point on the distorted arch. This is repeated for the other node points. If AB is the intrados of the arch. A′B′ defines the intrados of the distorted arch, the extrados being defined by a parallel curve. For the given loading, a line of thrust for the arch lying within the depth of the masonry can be found if two straight lines A′Q and B″Q can be drawn. Alternatively, the minimum depth of masonry to contain a line of thrust for the given loading can be found from the construction. Heyman [2] has proposed the concept of a geometrical safety factor, defined as the ratio of the actual depth of masonry to the minimum depth required to contain the line of thrust, as discussed above. This at least gives assurance that, for values of the geometrical safety factor greater than unity, failure will not take place for the given load system. A safety factor of the order of 2.0 is suggested for practical situations but does not, of course, give a direct measure of the margin of safety in terms of proportionately increased load.

11.3.2 *Load capacity of arches by the mechanism method*

As pointed out in the preceding section, failure of an arch follows the formation of four hinge points. If the position of the hinge points is known, it is possible to calculate the failure load P for an arch such as that shown in figure 11.4, or, alternatively, the minimum depth of arch to sustain a stated value of P and thus the geometric safety factor.

This is done by taking moments about the hinge points C, D and B to give three equations in V, H, d and P. Elimination of H and V gives an equation in d and P and, given one of these, the other can be found. The

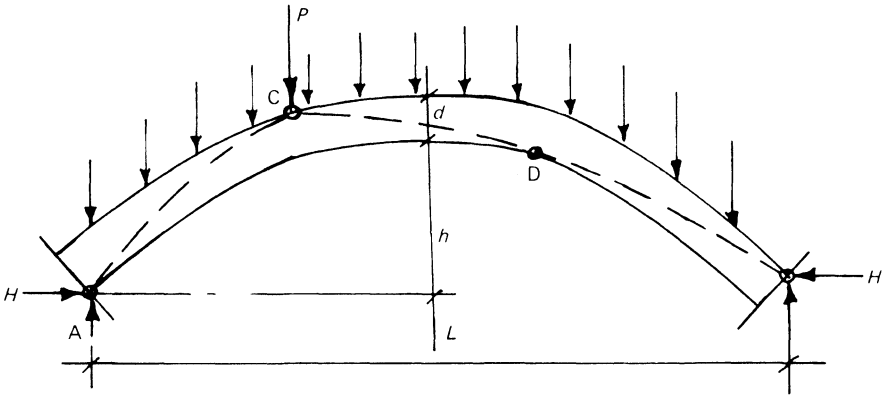

Figure 11.4 Line of thrust and location of hinge points

equations are, however, rather ill-conditioned and numerical accuracy is essential.

This solution pre-supposes that the hinge positions have been determined for the given loading, as they may be by drawing a line of thrust. Alternatively, Davies [3] has devised a computer solution for the mechanism method which determines the line of thrust by an iterative process and can accommodate both horizontal and vertical loads on the arch. Similar methods have been put forward by Harvey [4] and by Cabrera *et al.* [5].

The concept of assessing the failure load of an arch structure in a building on the basis of statics, and consideration of possible failure mechanism, has long been recognised. Thus in the structure shown in figure 11.5 the effect of the surrounding masonry and the abutments cannot be separated from the actual arch. Possible crack locations can be identified by constructing a line of thrust, thereafter considering the limiting equilibrium of the blocks into which the structure would break.

11.3.3 *Other methods of arch analysis*

Elastic analysis has been applied to masonry arches, originally by Castigliano [6], later by Pippard *et al.* [7, 8] and recently by Hughes and

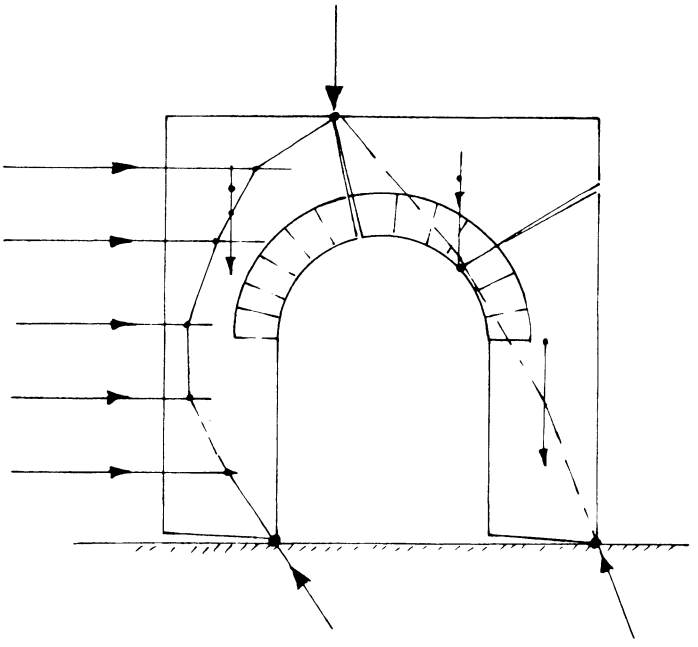

Figure 11.5 Line of thrust and failure mechanism in a building arch under vertical and horizontal loading

Vilnay [9] who have developed a computer-based method using the same strain energy principles. The latter approach has overcome the difficulty of the heavy arithmetical work and permits investigation of support movement and other secondary effects not allowed for in line of thrust or mechanism methods.

A number of authors [10–14] have applied finite element methods to arch analysis which have sucessfully reflected the behaviour of arch bridges for which test results have been available.

11.3.4 *Limitations on the analysis of masonry arch structures*

While there has been considerable development of analytical methods for masonry arch structures in recent years, the complexity of the problem means that many uncertainties remain and indeed may not be capable of complete resolution. This was recognised at the end of the Nineteenth Century [15] when there was considerable expertise in the design and construction of masonry arch bridges. Thus in a textbook of the time, Baker [16] listed a range of elements which he considered could not be stated "accurately or adequately in a mathematical formula." These included:

> uncertainties concerning the amount and distribution of the external forces
> the indeterminateness of the position of the line of resistance
> the influence of adhesion of the mortar and the elasticity of the material
> lack of knowledge concerning the strength of the masonry
> indeterminateness of the stresses in the arch owing to variations in the materials, the effect of imperfect workmanship in dressing and bedding the stones, to the action of the centre – its rigidity, the method and rapidity of striking it – and to the spreading of the abutments.

The uncertainties relating to material properties particularly affect the more sophisticated methods of analysis which attempt to estimate stresses and deformations in the arch. Line of thrust and mechanism methods on the other hand assume rigid materials, zero tensile strength, initially perfectly fitting blocks and disregard sliding failures, although methods have been proposed by Gilbert and Melbourne [17] and by Boothby [18] to overcome the last mentioned limitation.

In addition to these inherent problems there are further analytical difficulties arising from interaction between the arch and the fill and from the influence of the spandrel masonry and wing walls. While allowance for fill pressure has been made in various theoretical approaches, little attention has been given to the stiffening effect of spandrel and wing wall masonry. This converts the basic arch vault, customarily treated as a two-dimensional strip, into a three-dimensional structure.

A further level of difficulty is presented by skew span bridges and at present only rather tentative solutions have been produced [19].

11.4 Experimental studies of arch behaviour

11.4.1 *Small-scale tests*

The literature of the Nineteenth Century contains a number of reports on experimental studies of arch behaviour using model structures; these are summarised in references 1 and 2. Pippard and co-workers carried out an extensive series of tests on voussoir arches on model scale which are comprehensively described in *National Building Studies Paper No. 11* [28]. These experiments clarified the mechanics of this type of arch and demonstrated clearly the formation of successive hinge points along the arch. It was found that the limited tensile strength of mortar between the voussoirs can delay the appearance of a crack until the line of thrust is well outside the middle-third and, in fact, raised the ultimate load beyond that calculated on the assumption of zero tensile strength. The last three hinges were found to develop long after the crack under the load point, appearing almost simultaneously close to the collapse load. Some evidence of compression failure was observed, indicating that the assumption of infinite compressive strength in masonry arch material could not always be assumed. Repeated application of loads was examined but did not lead to significant reduction in the strength of the arches tested. Pippard's experiments were carried out on model voussoir arches rather than on complete structures. Royles and Hendry [20] used model structures to investigate the effects of the various elements of a masonry arch bridge on the strength of the complete structure. Thus a test programme was devised to determine the strength of a complete bridge, the bridge with spandrels but without wing walls, the bridge with fill retained by substitute spandrels not attached to the vault, and finally the vault only with weights equivalent to that of the fill but without interactive effect. Three different arches were tested in this way, based on the dimensions of actual full-scale structures. These are shown in figures 11.6a to c. Line loads were applied by hydraulic jacks at quarter or third span sections, and deflections were measured at key sections. The recorded failure loads are shown in table 11.1 and typical load–deflection curves in figure 11.7. Figure 11.8 illustrates the effect on arch strength of wing walls, spandrels and fill for the three different arches.

It was concluded from this test programme that there is a substantial strengthening effect on a masonry arch from the spandrels and wing walls, increasing as the span/rise ratio decreases. The fill by itself adds to the strength and stiffness of the vault although to a considerably less degree. Any method of assessing the strength of an arch bridge would need to take these effects into account. The model structures were built in various materials but their strength was not greatly affected by this, failures taking

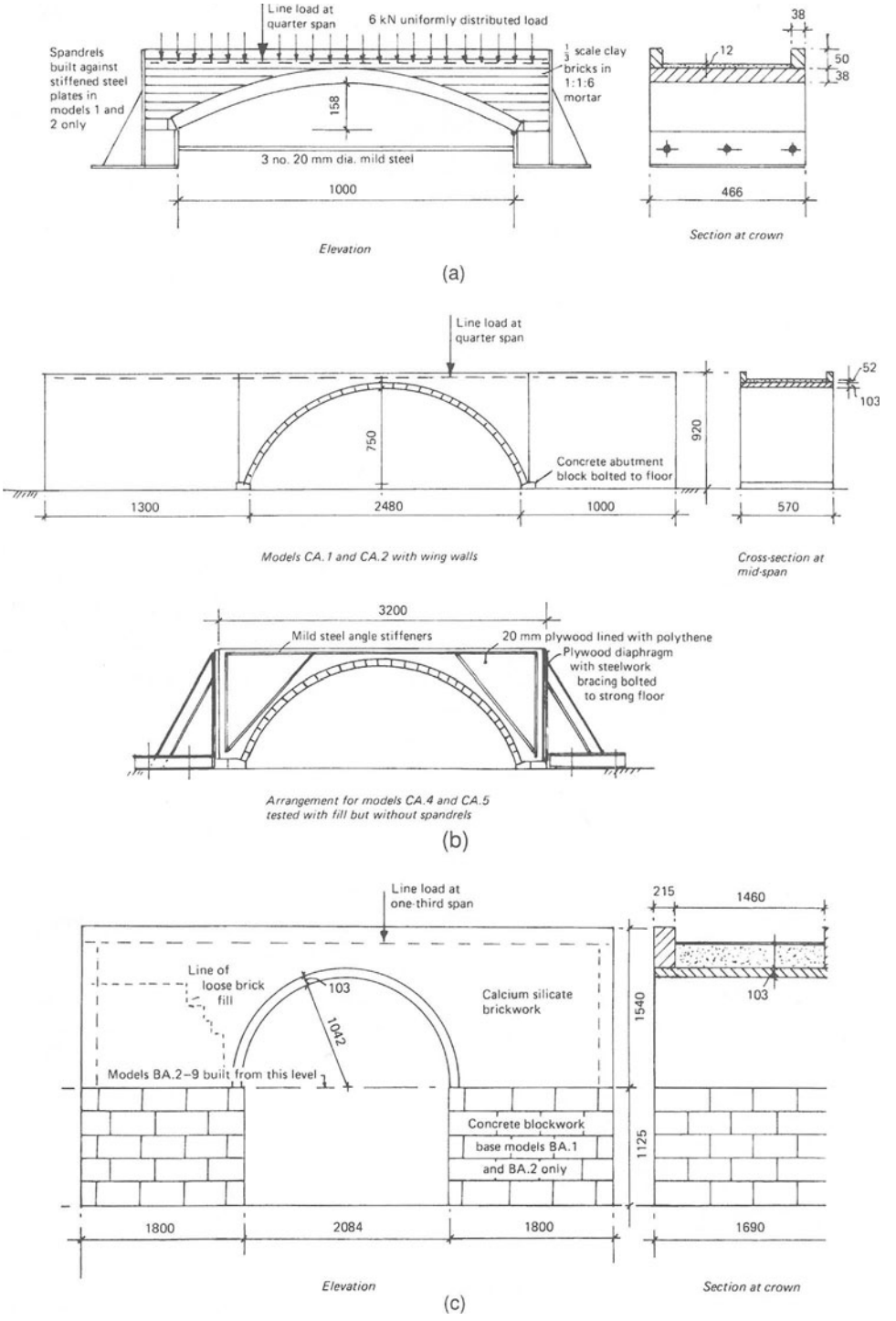

Figure 11.6 Model arch bridges tested by Hendry and Royles: (a) BM series; (b) CA series; (c) BA series

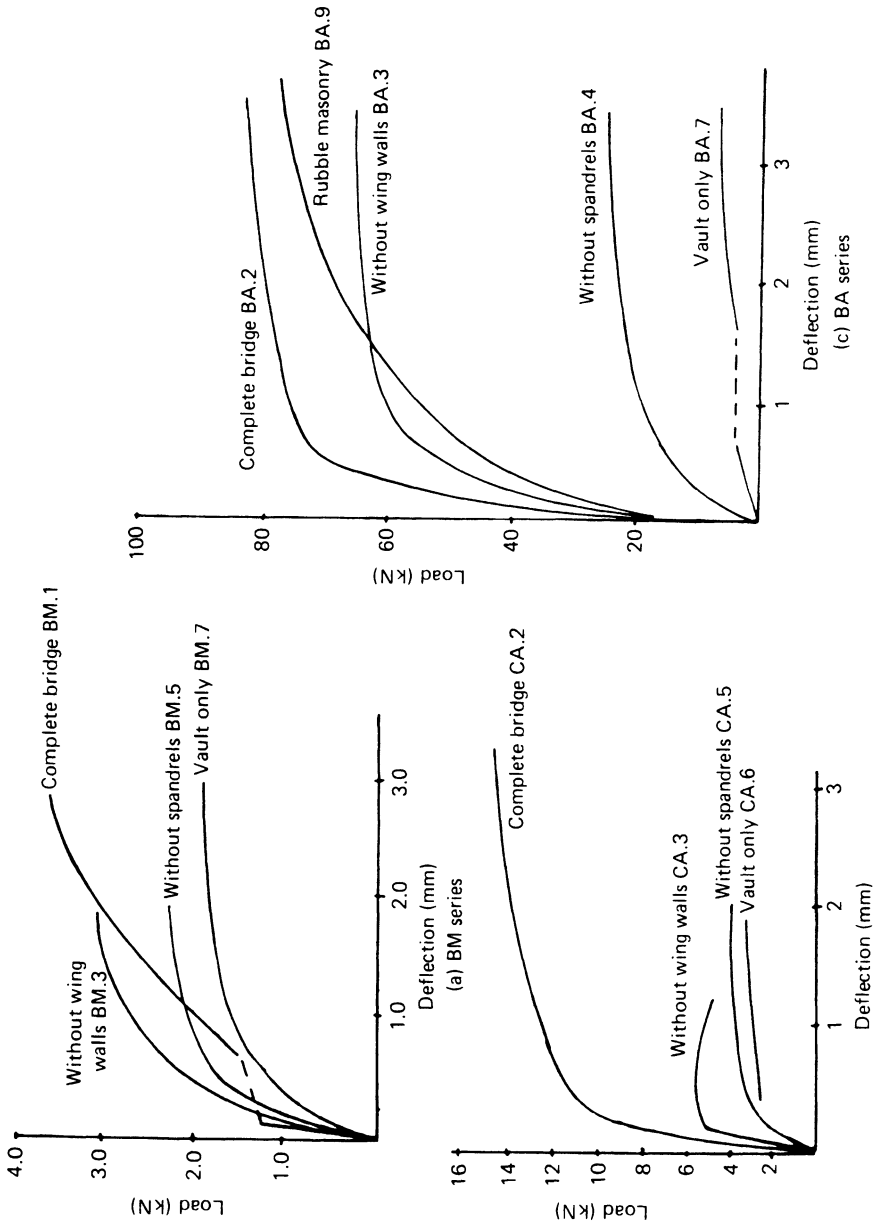

Figure 11.7 Load–deflection curves

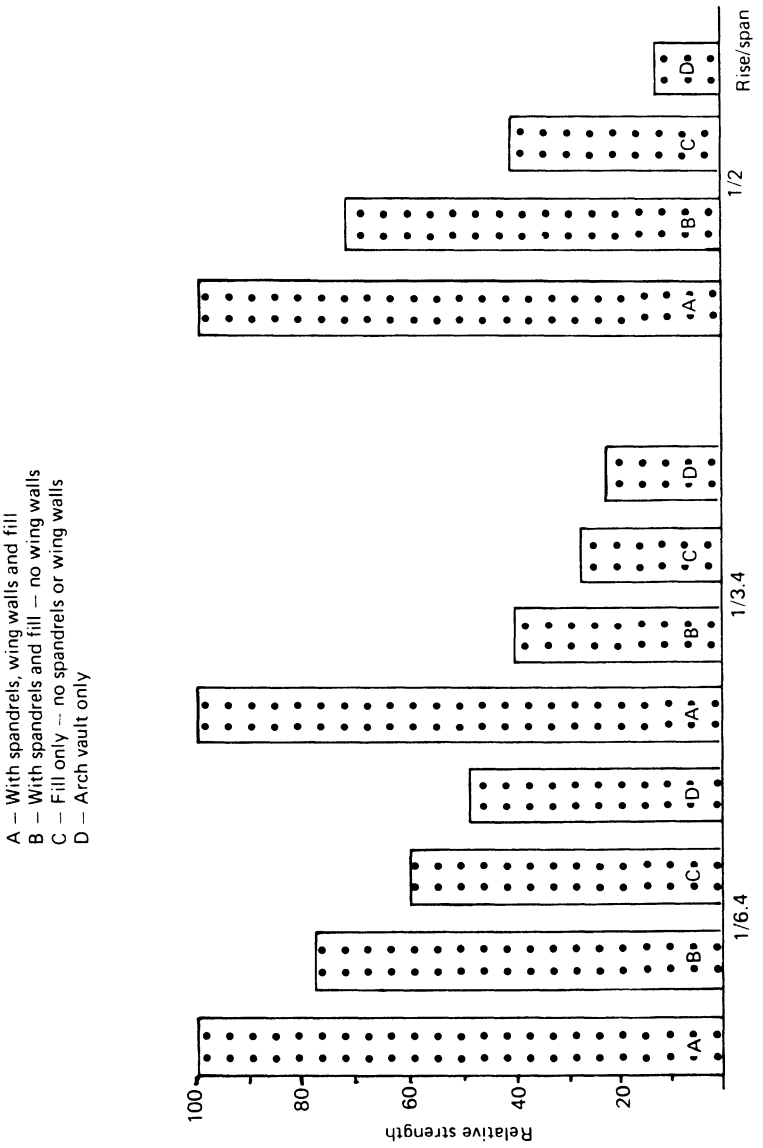

Figure 11.8 Effect on arch strength of wing walls, spandrels and fill

Table 11.1 Summary of tests

Model no.	*Span (mm)*	*Rise (mm)*	*Width (mm)*	*Depth of fill at crown (mm)*	*Vault thickness (mm)*	*Failure load (kN) (Ratio to full bridge = 100 in [ ] brackets)*			
BM.1	1000	158	466	12	38	4.05	3.9	[100]	With spandrels restrained
2						3.75			
3						3.10		[77]	With spandrels unrestrained
4	Span/rise 6.4 – parabolic					2.50			
5	Fill density: 14 kN/m^3 + 3.08 kN uniformly distributed load					2.25	2.3	[59]	No spandrels; with fill
6	(Approximate scale ratio 1 : 18)					2.15			
7						2.0			
8						1.75	1.88	[48]	Vault only
CA.1	2480	750	570	52	103	12.0			
2						15.0	13.5	[100]	With spandrels, wing walls and fill
3	Span/rise 3.4 – circular					5.5		[41]	With spandrels unrestrained and fill
4	Fill density: 14 kN/m^3					3.5			
5						4.0	3.75	[28]	Without spandrels; with fill
6	(Approximate scale ratio 1 : 10)					2.6			
7						4.0	3.3	[24]	Vault only + dead load equivalent to fill
BA.1	2084	1042	1690	240	103	90	89	[100]	With spandrels and wing walls
2						88			With spandrels and wing walls – with reduced strength materials used for vault
3	Span/rise 2 – circular					65		[73]	Spandrels – unrestrained
4	Fill density: 14 kN/m^2					32.5			
5						41.5	37	[42]	No spandrels; with fill
6	(Approximate scale ratio 1 : 5.4)					5.25			
7						8.75	7.0	[16]	Vault only + dead load equivalent to fill
8						50.0			Spandrels unrestrained: half width loaded
9						80		[90]	Rubble masonry: spandrels unrestrained

place by the formation of hinges with only limited evidence of compressive failure of the masonry.

The model tests on arch bridges indicated that considerable increase in strength results from the restraints provided by the spandrel and wing wall masonry. This effect is produced because, following the formation of hinge points, the unloaded half of the arch ring tends to move upwards and away from the load point. To do so, the weight of the spandrel masonry has to be overcome and the entire spandrel tends to rotate about the springing. If there is a wing wall or other restraint present, this rotation is prevented and a horizontal force is generated about half-way up the rise of the arch resulting in a further increase in the strength of the structure. The effect of backfill pressure and spandrel restraint has been discussed by Melbourne and Walker [21] in relation to similar model-scale tests but has not been fully resolved analytically.

The literature contains reports of many other model-scale tests on arches, some of up to 5.0 m span, and are reviewed in some detail in reference 22 up to 1993. Subsequently, further model tests have been carried out by Melbourne *et al.* on multi-ring brickwork arches [23], on skew spans and on multi-span bridges [24]. The limitations of small-scale tests on arch bridges in relation to the simulation of gravity forces has been pointed out [25] but such tests undoubtedly give a great deal of information on the behaviour of these structures.

11.4.2 *Tests on full-scale arch bridges*

As a result of interest in the development of realistic methods of assessing the strength of masonry arch highway bridges, a number of tests have been carried out on full-scale bridges. Load tests were carried out by Chettoe and Henderson [26] and by Davey [27], in the latter case to failure, with loads applied at the crown.

A series of full-scale tests on a number of masonry bridges, varying in span between about 4 m and 18 m, was promoted by the Transport Research Laboratory as a means of obtaining an insight into the behaviour of actual bridges against which to compare the results of laboratory tests and calculations. A large amount of information was obtained and is summarised in reference 22. Table 11.2 shows the leading dimensions and characteristics of these bridges and also the maximum line load carried and mode of failure. Currently, permissible axle loads on highway bridges in the UK are assessed by a procedure known as the MEXE method and for each of the bridges tested the permitted axle load so assessed is shown. The ratio between the maximum line load and the permitted axle load is generally between 6 and 8 but much higher in two cases. The level of safety so indicated is probably satisfactory as regards ultimate load although it is necessary to ensure that initial cracking does not take place at service loads.

The four hinge mode of failure was clearly identified in only two of the

Table 11.2 Full-scale tests on arch bridges (after Page [22])

	Bridge							
	A	*B*	*C*	*D*	*E*	*F*	*G*	*H*
Span	18.3	10.0	4.95	6.55	4.9	6.16	9.43	8.53
Angle of skew (deg.)	0	16	17	0	0	0	0	29
Rise (m)	2.85	5.18	1.64	1.43	1.16	1.19	2.99	1.70
Arch thickness at crown (m)	0.71	0.56	0.36	0.22	0.34	0.39	0.60	0.45
Arch shape	Parabolic	Segmental	Elliptical	Segmental	Segmental	Segmental	Segmental	Segmental
Arch material	Sandstone	Sandstone	Sandstone	Brickwork	Brickwork	Stone	Stone	Sandstone
Width of bridge (m)	8.30	8.68	5.70	3.80	7.80	7.03	5.81	9.80
Fill depth at crown (m)	0.203	1.20	0.38	0.17	0.25	0.22	0.41	0.29
Maximum load (kN)	3100	5600	2100	228	1080	2524	1325	2900
Mode of failure	Hinge formation	Material crushing	Hinge formation and material crushing		3-hinged 'snap thru'	Hinge formation	Material failure	3-hinged 'snap thru'
MEXE permissible axle load (kN)	181	643	298	27.3	146	375	197	164

tests. In other cases although hinge formation was evident before failure, this was complicated by local crushing of the masonry under the load or by more general collapse of sections of the masonry. Two bridges failed by what the investigators describe as a 'snap through' failure which, however, must have involved the formation of hinges at the point of collapse.

These tests further brought out the complex behaviour of masonry arch bridges and the difficulty of developing reliable analytical methods capable of allowing for three-dimensional effects, possible abutment movements, and uncertain material properties.

References

1. J. Heyman, 'Poleni's Problem', *Proc. Instn Civ. Engrs*, **84** (1) (1988) 737–60.
2. J. Heyman, *The Masonry Arch* (Ellis Horwood, Chichester, 1982).
3. S. R. Davies, 'The Influence of Certain Parameters on the Assessment of Masonry Arch Bridges', *Proceedings of the International Conference on Structural Faults and Repair*, Vol. 2 (Engineering Technics Press, Edinburgh, 1987), pp. 305–9.
4. W. J. Harvey, 'Application of the Mechanism Analysis to Masonry Arches', *Struct. Eng.*, **66** (5) (1988) 77–84.
5. J. G. Cabrera, A. W. Beeby and D. J. van der Cruyssen, 'Mechanism Analysis of Masonry Arch Bridges with Lateral Soil Pressure', *Proceedings of the Seventh International Conference on Structural Faults and Repair* (Edinburgh) 1997, ed. M. C. Forde, pp. 97–103.
6. C. A. P. Castigliano, 'Théorie de l'équalitive des systèmes élastiques et ses applications' (August Federico Negro, Turin, 1879), *Elastic Stresses in Structures*, trans. E. S. Andrews (Scott, Greenwood & Sons, London, 1919).
7. 'A Study of the Voussoir Arch', *National Building Studies Research Paper No. 11* (HMSO, London, 1951).
8. A. J. S. Pippard, E. Tranter and L. Chitty, 'The Mechanics of the Voussoir Arch', *J. Instn Civ. Engrs*, **4** (1936) 281.
9. T. G. Hughes and O. Vilnay, 'The Analysis of Masonry Arches', *Proceedings of the Eighth International Brick/Block Masonry Conference* (Dublin) 1988, pp. 1311–18.
10. M. A. Crisfield, 'Computer Methods for the Analysis of Masonry Arches', *Proceedings of the Second International Conference on Civil and Structural Engineering Computing*, Vol. 2 (Civil Comp. Press, Edinburgh, 1985), pp. 213–220.
11. K. D. S. Towler, 'The Non-Linear Finite Element Analysis of Bridgemill Masonry Arch Bridge', *Masonry International*, **5** (1985) 38–48.
12. B. S. Choo, M. G. Coutie and N. G. Gong, 'Finite Element Analysis of Masonry Arch Bridges using Tapered Elements', *Proc. Instn Civ. Engrs*, **91** (Part 2) (1991) 755–70.
13. Yew-Chaye Loo, 'Collapse Load Analysis of Masonry Arch Bridges', *Proceedings of the First International Conference on Arch Bridges*, ed. C. Melbourne (Thomas Telford, London, 1995), pp. 167–74.
14. E. A. W. Maunder, 'Thrust Line Solutions for Masonry Arches derived from

Finite Element Models', *Proceedings of the First International Conference on Arch Bridges*, ed. C. Melbourne (Thomas Telford, London, 1995), pp. 215–24.
15. A. W. Hendry, 'Masonry Arch Design at the End of the 19th Century', *Proc. Br. Masonry Soc.*, **7** (1995) 140–4.
16. I. O. Baker, *A Treatise on Masonry Construction* (Wiley, New York, 1st edn 1899, 10th edn 1910).
17. M. Gilbert and C. Melbourne, 'Analysis of Multi-Ring Brickwork Arches', *Proceedings of the First International Conference on Arch Bridges*, ed. C. Melbourne (Thomas Telford, London, 1995), pp. 225–38.
18. T. E. Boothby, 'Collapse Modes of Masonry Arch Bridges', *Masonry International*, **9** (2) (1995) 62–9.
19. H. W. Chandler and C. M. Chandler, 'The Analysis of Skew Arches Using Shell Theory', *Proceedings of the First International Conference on Arch Bridges*, ed. C. Melbourne (Thomas Telford, London, 1995), pp. 195–204.
20. R. Royles and A. W. Hendry, 'Model Tests on Masonry Arches', *Proc. Instn Civ. Engrs*, **91** (Part 2) (1991) 299–321.
21. C. Melbourne and P. J. Walker, 'Load Tests to Collapse of Model Brickwork Arches', *Proceedings of the Eighth International Brick/Block Masonry Conference* (Dublin) 1987, pp. 991–1002.
22. J. Page (Ed.), *Masonry Arch Bridges*, Transport Research Laboratory (HMSO, 1993), pp. 55–70.
23. C. Melbourne and M. Gilbert, 'The Behaviour of Single and Multi-span Arch Bridges', *Proceedings of the Tenth International Brick/Block Masonry Conference* (Calgary) 1994, pp. 339–447.
24. C. Melbourne and J. A. Hodgson, 'The Behaviour of Skewed Brickwork Arch Bridges', *Proceedings of the First International Conference on Arch Bridges*, ed. C. Melbourne (Thomas Telford, London, 1995), pp. 309–320.
25. M. C. R. Davies, T. G. Hughes and P. R. Taunton, 'Considerations in the Small-scale Modelling of Masonry Arch Bridges', *Proceedings of the First International Conference on Arch Bridges*, ed. C. Melbourne (Thomas Telford, London, 1995), pp. 365–374.
26. C. S. Chettoe and W. Henderson, 'Masonry Arch Bridges: A Study', *Proc. Instn Civ. Engrs*, **7** (1957) 723–55.
27. N. Davey, 'Tests on Road Bridges', *National Building Studies Res. Paper 16* (HMSO, London, 1953).
28. A. J. S. Pippard and L. Chitty, 'A Study of the Voussoir Arch', *National Building Studies Res. Paper 11* (HMSO, London, 1951).

12 TESTING OF MASONRY MATERIALS AND ELEMENTS

12.1 General

The testing of masonry materials and elements is undertaken for a variety of purposes including:

(a) the derivation of material strengths for structural design
(b) manufacturing and site quality control
(c) structural research.

In relation to any test, it is necessary to consider the following criteria:

(1) The result required, such as shear strength, water absorption, etc.
(2) The purpose for which the result is required, that is, (a), (b) or (c) above.
(3) The practicability of the proposed test in terms of time required to obtain results, generally available equipment and levels of skill, reproducibility and accuracy of results.
(4) The cost relative to the purpose of the test.

Three categories can be distinguished in relation to the structural properties of masonry:

A – Tests on materials
B – Small specimen tests on masonry
C – Tests on complete masonry elements.

In addition, a range of tests is required for the assessment of existing structures.

12.2 Categories of test

12.2.1 *Category A tests*

Under this category may be included tests on brick, blocks, natural stone, mortar, concrete, damp-proof course materials, wall ties and fixings which are relevant to structural behaviour.

The primary material strength tests for structural masonry is the unit compression test, standard procedures for which exist in various national standards. There are variations between these standards in terms of capping and other test conditions and it is necessary to specify sampling procedures, number of specimens required and the basis for calculating compressive strength. The compression test is used for all three purposes specified in section 12.1.

Flexural tensile (modulus of rupture) tests or splitting tests on bricks and blocks are sometimes carried out; the result may be relevant to the strength of laterally loaded panels.

Water absorption, measured in various ways, and initial rate of absorption of structural units have an important influence on the water regime in mortar as it sets and cures. This, in turn, influences the adhesion between brick and mortar and thus has implications for structural performance. Moisture also has an important bearing on creep behaviour.

Various tests exist for mortar and its component materials, the most widely used being for compressive strength. In this case, the size and form of specimen and curing conditions are significant. In structural design, the mortar is usually specified by mix for which a minimum compressive strength, in terms of a particular test, is quoted. Mortar compression tests may also be used as a site quality control, although this is only partially effective as it does not cover such factors as failure to fill the joints, etc.

As discussed in section 2.3, it is possible to assess masonry strength from unit strength for a given type of mortar. This is based on the results of numerous tests in which masonry strength has been correlated with unit strength. Statistical correlation is moderately satisfactory and the method is undoubtedly the simplest in terms of test procedures, but the relationship depends on the method of test both of the masonry and its component materials.

12.2.2 *Category B tests*

This category of tests refers to those carried out on small specimens of masonry for the purpose of determining strength and other properties of the composite material.

In some countries, prism tests are used as the basis of design strength of masonry, either instead of or as an alternative to unit strength plus mortar mix. There is a certain amount of experimental evidence in support of the prism test but considerably less than for the unit strength method. A need for small specimen compressive tests has, however, been identified in connection with the design of reinforced and prestressed masonry since, in this type of construction, units may be stressed in directions other than normal to the bed joints and it has been found that the unit compressive strength in such cases, even when measured in the relevant direction, does not always give a realistic indication of masonry strength.

Small specimens of masonry will also be required for determination of deformation properties such as elastic moduli, creep, moisture and thermal movements.

The British Code BS 5628, Part 1 prescribes small specimens, for the measurement of flexural tensile strength of masonry, as an alternative to a series of tabular values based on water absorption of clay bricks and compressive strength of concrete blocks. These values were derived from extensive tests on small specimens. A different form of test for this purpose has been proposed using a prism type of specimen and measuring the flexural strength of the joints between successive bricks.

Shear bond strength has also been measured using small couplet or triplet specimens and the results have been shown to be consistent with those from tests on full-size walls. Recently, more elaborate small specimen tests have been used in research to define the biaxial strength of brickwork, and the results have been applied to the assessment of the strength of shear walls. The same technique has been used for concrete blockwork but in that case the specimens were quite large. The advantage of this type of test is that it gives basic information on material strength which can be applied to a range of structures arising in practical construction.

12.2.3 *Category C tests*

Category C tests include full-scale tests on wall panels under compression, shear or lateral loading. As such test are very expensive, they are unlikely to be employed for the establishment of design strengths except in rather exceptional circumstances, such as the introduction of a new type of structural unit.

In research, however, the use of full-size walls is often essential, and a considerable amount of experimental work is still required on shear strength especially of shear walls under dynamic loading. Also included in this category are tests on sections of structure intended to evaluate interactive effects. Thus, tests may be carried out to determine wall–floor slab joint characteristics and the effect of these on wall strengths.

12.3 **Tests on masonry units**

12.3.1 *Compressive strength*

The factors affecting the apparent strength of masonry units are fairly limited and include rate of testing, and the method of preparation, whether by grinding, capping or by the use of packing material between the specimen and the machine platens.

Harding *et al.* [1] found that for typical blocks and rates of loading differing considerably from a specified 15 N/mm^2/min. (from 7 to 40 N/mm^2/min.) a statistically significant, but not large, variation in apparent strength was shown. It may be assumed, therefore, that any departure from

the normal rate of loading likely to occur in practice will not be of great importance.

The influence of various methods of preparation has been extensively studied. Kelch and Emme [2] showed that the application of different types and thicknesses of gypsum or sulphur as a capping material to the loaded faces of bricks has a considerable effect on the apparent crushing strength. The time of testing after application of the capping material may also be significant. Some indication of the magnitude of these effects may be obtained from figure 12.1.

Khalaf and Hendry [3] have reported the results of comparative tests on several types of bricks and blocks using mortar and plaster cappings and also plywood packing. Again considerable differences in the compressive strengths as between the various test methods were found. Comparison was also made with specimens tested with ground surfaces which were some 25 per cent stronger than those tested with mortar capping. Similar results were obtained by Templeton and Edgell [4]. Other investigations have indicated that the size [5] and material [6] used for packings have an effect on the apparent compressive strength of a specimen.

It follows from these observations that for comparability the method of preparation of units in compression tests must be standardised.

In an effort to overcome the problem of restraint from testing machine platens, Hilsdorf [7] devised brush platens in which the compressive load is transmitted to the specimen through a large number of slender steel rods which have low lateral rigidity and thus do not impose significant lateral restraint on the specimen. This method of test is likely to be useful in research but may be unsuitable for routine testing.

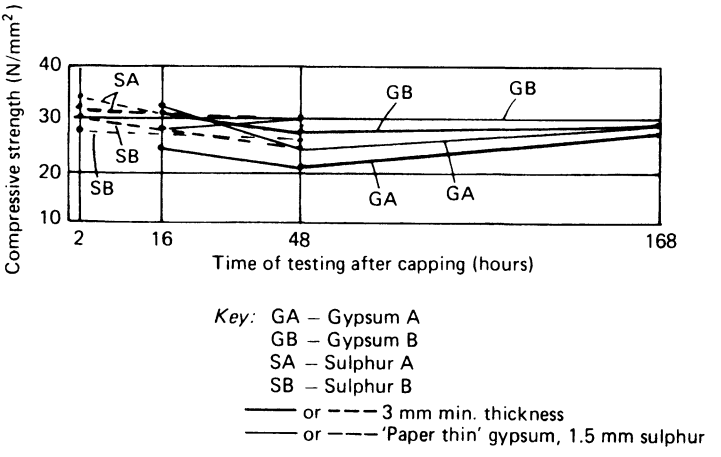

Figure 12.1 The effect on apparent crushing strength of building bricks of various capping materials and thicknesses

As mentioned in section 2.3 in connection with the determination of masonry strength, the apparent compressive strength of a unit depends on its dimensional proportions so that it is convenient to convert the measured strength to an equivalent 100 mm cube strength, as discussed in section 2.3 (page 31).

This approach has been developed for solid and perforated units but for hollow blocks there are additional complications because, in practice, they are likely to be loaded only through the face shells, whereas the standard test procedure is to load the unit over its whole area. The testing of such units has been discussed by Page and Kleeman [6] and by Ridinger *et al.* [8]. The latter have suggested the testing of small cores cut from the unit at the intersection of the cross-webs and face shells. The compressive strength of these cores was found to correlate well with that of units capped and loaded on the face shells through friction-reducing layers.

12.3.2 *Tensile strength*

In a number of countries, tests on the tensile strength of units are carried out. A direct tensile test is difficult to contrive – although it has been attempted [9] on bricks – so that flexural and splitting tests are used.

The result of a flexural tensile test is conventionally expressed as the modulus of rupture, calculated at the section of maximum bending moment by linear elastic theory. Some variations in test conditions are possible, for example, the method of ensuring that the load and support forces do not introduce torsional effects, but these are likely to be secondary. The assumption of linear elastic behaviour, however, is doubtful and may result in misleading values for units of different thicknesses. The use of the test is likely to be restricted to a qualitative comparison between similar units rather than as a measure of true material strength.

It is known that the modulus of rupture is considerably higher than the direct tensile strength of mortar and, by inference, of clay brick material. The splitting test, however, gives a closer measure of direct tensile strength and is thus likely to be more useful where information about this property is required. This point is illustrated in figure 12.2 which is based on tests by Morsy [10].

If it is considered desirable to standardise a tensile strength test, the indirect splitting test appears to provide the most likely basis. On the other hand, if the result is required for calculation of the lateral resistance of wall panels, the modulus of rupture test will be relevant. Thus definition of the purpose of the test is required.

12.3.3 *Water absorption tests*

The absorption characteristics of masonry units, particularly clay bricks, are of interest in relation to the development of mortar strength and bond as well as certain non-structural properties of masonry.

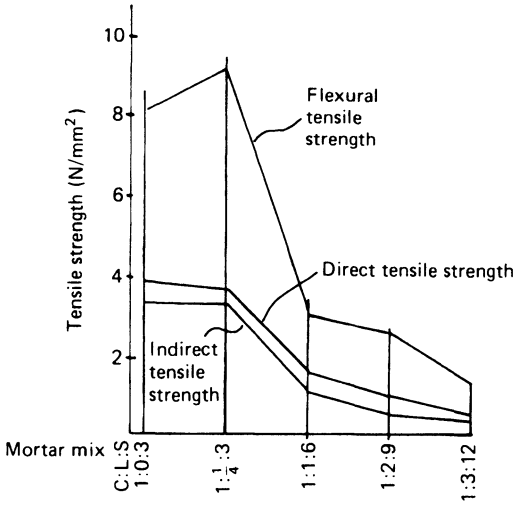

Figure 12.2 Tensile strengths of mortar

Various methods are in use for the measurement of overall water absorption, including immersion for several hours in boiling water, 24 hour immersion in cold water and vacuum extraction of air before immersion. The result obtained is obviously susceptible to the detailed test procedures, such as the preparation of the specimen, time of immersion, etc.

The initial rate of absorption (IRA) is measured by the partial immersion of the unit for a short time, for example, to a depth of 3mm for 1 minute. The IRA is measured in kg/m^2/min.

Absorption test results have been correlated with unit compressive strength [8] and with flexural tensile strength of clay brickwork [11]. More indirectly, the extraction of water from mortar by bricks having a high suction rate has been shown [12] to result in low compressive strength of slender walls.

It is significant that this effect is considerably less with a cement: lime:sand mortar than with a cement mortar, no doubt as a result of the increased water retentivity of the mortar containing lime.

Water absorption is thus a useful indicative property in relation to the structural design of clay brick masonry in particular, and suitable tests are necessary both for total absorption and IRA.

12.4 **Small specimen tests on masonry**

12.4.1 *General*

Tests on small masonry specimens are frequently undertaken as a convenient and economical means of establishing structural properties. These

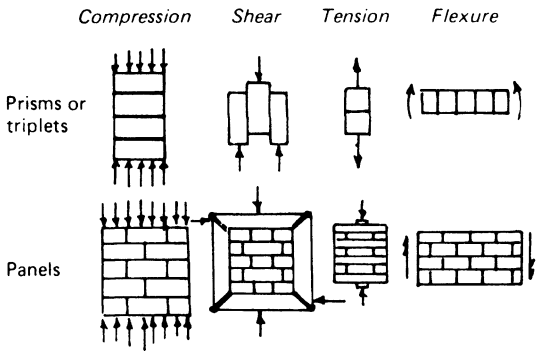

Figure 12.3 Small specimen tests

properties include compressive, shear, tensile and flexural strengths, and may be carried out on specimens consisting of only a few units or of a small panel of masonry, as summarised in figure 12.3.

In addition to the range of tests indicated in figure 12.3, small panel tests have also been used in recent years for investigation of the strength of masonry under biaxial stress.

12.4.2 *Prism tests for compressive strength*

The prism test is adopted in some codes of practice as the basis for the assessment of the design strength of masonry in compression. This is the case, for example, in North America and in Australia. A number of studies [13–17] have been undertaken on the use of prism specimens and on the effect of a variety of test procedures on the result obtained. Thus Maurenbrecher [13] has reported the results of tests relating to:

1. The effect of height-to-thickness ratio
2. Effect of capping
3. Face-shell and full mortar bedding
4. Workmanship
5. Loading, etc.
6. Stack against running bond.

It is pointed out that the effect of workmanship on the strength of prisms, for example, incomplete filling of joints, may outweigh other influences. The conclusion to be drawn from this would appear to be that, for comparative results, specimens should be jig built. This procedure would also provide a basis of comparison for site control tests in which specimens would be laid by normal procedures.

An important factor in this type of test is the height of the prism in relation to its thickness, and it is generally considered that a height-to-

thickness ratio of about 5 is necessary to eliminate platen effects and to given an accurate measure of masonry compressive strength. Correction factors have been suggested for specimens having a lower *h/t* ratio than this, but these are of doubtful validity [16] and would be sensitive to the use of capping or packing materials between the specimens and the machine platens. The other effects mentioned by Maurenbrecher are likely to be of lesser importance, although it will in general be necessary to represent the actual masonry under study correctly in terms of jointing. It would appear that a stack-bonded prism gives a somewhat higher value of masonry strength than a half- or full-storey height wall [17]. Modified specimens will be required to determine the compressive strength of masonry stressed, for example, parallel to the bed joints as may occur in reinforced or prestressed elements.

12.4.3 *Compressive tests on masonry panels and piers*

Much early work on compressive strength was carried out on piers and more recently on storey height walls. Tests on the latter, however, are expensive so that an investigation by Edgell *et al.* [17] was carried out in order to establish the relationship between the results of tests on storey and half-storey height walls. A linear relationship was found with the strength of the full-height walls being 0.875 of that of the half-storey walls. The wallette specimen, which can be accommodated in some standard testing machines, is therefore likely to be the preferred form for masonry compressive strength testing.

12.4.4 *Shear bond strength tests*

The determination of the shear bond strength of masonry has attracted considerable attention in recent years and the many different tests which have been proposed have been reviewed by Jukes and Riddington [18]. The simplest tests have employed a couplet specimen consisting of a pair of bricks joined together by a single mortar joint. Such couplet specimens give rise to the problem of trying to ensure that the resultant shear force acts in the plane of the joint, necessitating the use of rather complicated fixtures to bring this about. A triplet specimen of the type shown in figure 12.4, on the other hand, overcomes this disadvantage and is easy to prepare. It is necessary, however, to ensure that bending effects are minimised.

As shear strength is dependent on the level of normal stress across the joint, a modification of the triplet test is to apply such a stress to the triplet specimen so that this relationship can be determined. As described in section 4.3, this takes the form of the Mohr–Coulomb equation:

$$\tau = \tau_0 + \mu f_n$$

where τ_0 is the shear bond strength with zero precompression and μ is a quasi-internal friction factor. Evaluation of the relationship requires meas-

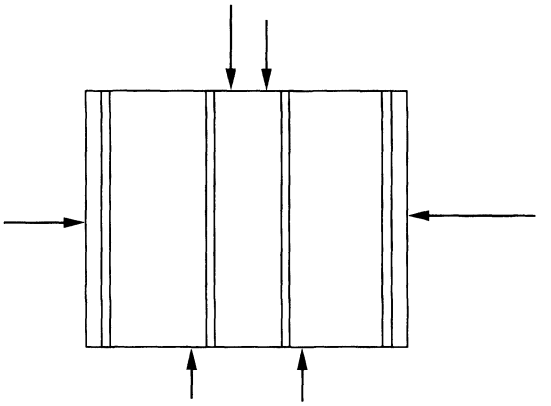

Figure 12.4 Triplet shear strength test arrangement

urement of the shear strength at various levels of precompression. In an alternative procedure, proposed by Riddington and Jukes [19], a triplet is first tested without precompression and the failed specimen is then placed on an inclined plane apparatus to determine the coefficient of friction. This method appears to give results in good agreement with the method requiring tests at various levels of precompression and has the advantages of being simpler to carry out and of not requiring expensive special equipment.

12.4.5 *Tests on shear panels*

Many investigations have been carried out on the shear strength of masonry panels. The size of the specimens and the loading conditions have varied considerably, resulting sometimes in apparently conflicting results. Leaving aside tests on full-scale shear walls, figure 12.5 illustrates diagrammatically some of the test arrangements which have been used. The effects of geometry and loading-of-specimen conditions have been examined by Samarasinghe *et al.* [20].

Some investigators have aimed to produce uniform or, at least, predictable stress fields within the test panels while others have sought to reproduce conditions likely to exist in actual shear walls. The results are, therefore, in general not strictly comparable. It would appear better to devise a test method in which the stress field is well defined and uniform so that the material strength is obtained rather than the shear strength of a particular wall. This would lead to the adoption of biaxial stress testing of masonry specimens, as has been done extensively for clay brickwork by Page [21] and on concrete blockwork by Hegemeir *et al.* [22]. However, as shown by Bernardini *et al.* [23], it is possible to derive biaxial failure criteria

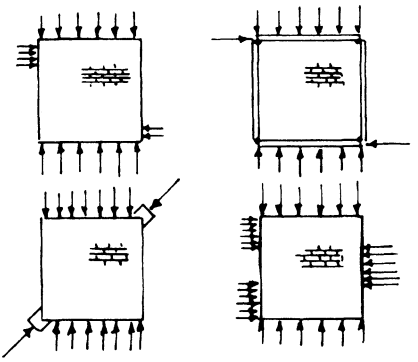

Figure 12.5 Various loading arrangements used in shear panel tests

for the compression–tension case from a combination of compression tests on simple specimens, loaded normal and parallel to the bed joints, together with tensile splitting tests in which the load axis is varied relative to the plane of the bed joints. As these tests can be carried out with standard equipment, it would seem promising to develop this approach to shear strength determination.

12.4.6 *Tensile bond tests*

Although most codes of practice either discourage or prohibit reliance on tensile bond strength, the development of adhesion between mortar and masonry unit is important. In the USA, ASTM prescribes a tensile bond test [24], but the need for a tensile bond test is more likely to relate to the adhesion of renderings rather than to structural design.

12.4.7 *Indirect tensile strength tests*

The use of tensile splitting tests has already been mentioned in the context of the derivation of biaxial stress failure criteria. Such tests may also be used simply as a means of finding the tensile strength of masonry in various directions relative to the plane of the bed joints. This information may be required in relation to masonry strength in the vicinity of prestressing cable anchorages. It would, therefore, be advantageous to standardise this test in terms of specimen form and loaded area.

12.4.8 *Flexural tensile strength tests*

This is again a type of test which has attracted considerable attention in recent years in relation to the strength of non-loadbearing, laterally loaded masonry panels. Most of the relevant research has been carried out in

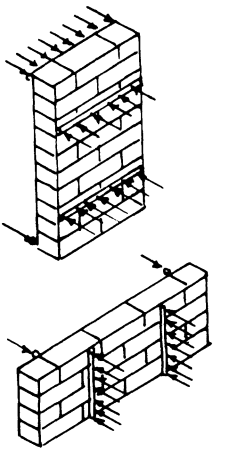

Figure 12.6 Test for flexural strength of masonry according to BS 5628

Britain [11] and in Australia [25, 26]. In the former country, tests have been evolved and included in the Code of Practice BS 5628 for the determination of flexural tensile strength for bending in planes normal to and parallel to the bed joint. The form of specimens and loading conditions adopted in these tests are shown in figure 12.6. The result is given in terms of a modulus of rupture, calculated on the assumption of linear elastic behaviour. The British Code requires ten specimens of each type to be tested and the mean, standard deviation and characteristic strength are calculated on the basis of a lognormal distribution.

It is evident that the form of specimen used in this type of test, in terms of the number of units in its width and the number of courses in its height, will have a bearing on the result obtained. In the case of the vertically spanning specimen, failure will take place at the weakest horizontal joint in the constant moment zone. The strength of horizontally spanning specimens is dependent on the strength of the perpend joints, the bed-joint strength in torsion and the unit strength. The effects of specimen size have been investigated by Lovegrove and de Vekey [27] for vertically spanning specimens and by Lawrence [28] for both types. Lawrence has developed modelling and statistical techniques which would permit the calculation of joint strength from the results of tests on specimens of different forms. However, he recommends that specimens should be tested in the horizontal rather than the vertical plane as specified in BS 5628, in order to avoid errors from dead load effects. Fried *et al.* have given conversion factors relating various types of test results, as quoted in table 4.2 (page 79).

A form of test proposed by Baker [25] in which each joint in a stack-bonded prism is tested in turn is described in section 4.2. This permits the testing of a fairly large number of individual joints with reasonable

economy and thus leads to the definition of a statistically significant estimate of the characteristic strength. Also shown in section 4.2 is the bond wrench test which can be used in the same way as a site test.

It has to be noted that the method of testing for flexural strength is closely tied to the use which is to be made of the data derived from it. Thus, the test prescribed in the British Code of Practice is related to a particular method of calculating the lateral resistance of certain types of wall panels by an empirical method. The approach developed by Baker and by Lawrence, on the other hand, is intended to provide the data necessary for an analytical solution which takes into account the effect of variability of joint strength.

12.5 **Tests on complete masonry elements**

12.5.1 ***Wall compressive strength tests***

Although a certain amount of testing of complete masonry elements or even sections of structure is essential for the verification of analytical methods and strength criteria based on small specimen tests, there has been little attempt to standardise procedures, with the possible exception of compressive tests on short lengths of wall.

12.5.2 ***Tests on shear walls***

A considerable amount of research work has been carried out on the strength of shear walls, usually on panels of approximately equal height and length. Loading arrangements have been widely variable, ranging from simple diagonal compression to rather elaborate combinations of horizontal and vertical loads. In nearly all cases, a reinforced concrete beam or slab has been placed on top of the shear wall to distribute the applied forces.

The results of shear wall tests have generally been interpreted in terms of a design shear strength, but as a rule too few specimens are tested to give a statistically valid result and it would seem that a more promising approach is likely to be through study of basic materials properties and the development of mathematical models through which these can be applied to specific cases. The need remains, of course, for full-scale testing to validate these procedures, but the standardisation of the full-scale tests is perhaps not essential provided that there is no ambiguity as to the correct representation of the conditions assumed in the model.

12.5.3 ***Tests on laterally loaded walls***

A large number of tests on storey-height wall panels under lateral loading have been carried out over the years. This form of test has proved extraordinarily sensitive to a range of test conditions, some of which are not

immediately apparent but have a considerable bearing on the result obtained. These factors have been reviewed by Baker [25] and by Lawrence [28] and include the following:

Scale
Method of loading
Self-weight
Arching
Rotational restraint at supports
Translational yielding of supports.

Since tests of this type are less expensive and more frequently undertaken than compression or shear tests, there is perhaps greater justification for standardising the procedure, or at any rate for defining test conditions which will make it possible to compare results from various sources. Lawrence [28] has, in fact, designed a test rig which would appear to overcome most of the difficulties experienced by earlier workers and which could provide a basis for a standard test method.

12.6 **Non-destructive testing of masonry**

In assessing the condition of masonry buildings and structures it is frequently necessary to determine the properties of the units and mortar from which they are built. In some cases it is feasible to remove sample units or to take cores from them but this procedure has considerable limitations, especially where the structure concerned is of historic or architectural importance. There are problems in relating the compressive strength of the specimens to that of the units [29] and it will rarely be possible to obtain a sufficient number of cores to be representative of the whole structure. Non-destructive test (NDT) methods have been used to deal with this problem. Some are well established for concrete and other materials and have been developed to a more limited extent for masonry [30, 31]. It is likely that in any particular investigation a combination of NDT methods will have to be employed. The following sections give an outline of the more widely used techniques.

12.6.1 ***Sonic echo method***

In this method sonic waves are generated in the structure by a hammer blow, the response being monitored by a sensitive accelerometer and recorded on a computer for subsequent analysis. The measurements so obtained are capable of detecting internal cracks or cavities in the masonry and of giving an indication of its strength and uniformity. The recorded signals are complex, requiring considerable expertise in their interpretation, and the necessary equipment is expensive. However, the site proce-

dures are relatively easy to carry out and a comprehensive evaluation of a structure is possible.

Examples of the successful use of the method include assessment of the condition of a masonry arch bridge [32], of stonework in the Washington Memorial in Washington D.C. [33] and of canal lock walls [34].

12.6.2 *Ultrasonic techniques*

Ultrasonic methods have been in use for many years on concrete structures and their application to masonry has been investigated by Noland *et al.* [30] and by Hobbs and Wright [35]. Ultrasonic waves are generated in the masonry by a piezoelectric transmitter and picked up by a receiver transducer which may either be on the opposite side of the wall or at some distance along the face. The essential measurement is the pulse velocity through the masonry which can be related to its strength. By taking readings at several distances along the face of the wall from the transmitter, it is possible to detect flaws. Hobbs has also suggested the use of the method for site control purposes [36]. The equipment required for ultrasonic testing is readily available, robust and comparatively inexpensive. The site procedure and interpretation of readings are straightforward, making this a useful and economical method of investigation.

12.6.3 *Acoustic emission measurements*

When micro-cracks develop in a body, small amounts of energy are released giving rise to audio-frequency waves which can be detected by suitable instrumentation. A technique has been developed whereby these waves, which are rapidly damped in the material, can be recorded as the component or structure is subjected to increasing load. The signals so recorded are referred to as acoustic emissions (AE). Thus if load application results in internal cracking a series of AE signals is recorded. The instrumentation is devised to respond only to signals exceeding a selected level of background noise which can be assumed to have been generated by cracking. Usually a series of signals will be picked up from a particular location and these together are defined as an 'event'. The location, severity and to some extent the nature of internal damage as the load is increased can be deduced from analysis of the AE data.

The method has not often been applied to masonry structures but was used to study the behaviour of a masonry arch bridge tested to failure [37]. In this case the plot of total AE events against the applied load closely reflected the load–deflection curve. This led to the suggestion that the method would provide a useful monitoring procedure in a non-destructive load test on a structure: a linear relationship between the AE count and the applied load would indicate that no irreversible damage to the material was occurring as the load was applied.

The advantage of the method lies in the fact that transducers can be easily attached to the masonry and readings quickly recorded. However, the field equipment is expensive and the data have to be processed by specialised equipment, making the operation suitable only for use in particularly important investigations. No doubt for this reason it has not been more widely used on masonry structures.

12.6.4 *Surface penetrating radar*

In this method pulses of electromagnetic energy are generated and by suitable antenna are caused to penetrate the surface of the element under examination. Pulses are of about 1 nanosecond duration and are transmitted at a rate of 0.5 to 1 GHz. These waves are reflected by any discontinuity in the material through which they travel so that, by moving the radar over the surface and recording the echoes received, it is possible to build up an image of the internal structure. The recorded echo pattern is complex, giving a rather distorted image of even simple internal features and therefore requiring skilled interpretation [38, 39].

Surface penetrating radar permits the detection of hidden defects in masonry and the possibility of identifying section characteristics of a wall, such as thickness and multi-leaf construction. Binda *et al.* [38] have reported the results of a number of investigations on old buildings using the technique.

This application of radar has considerable potential but also certain limitations in addition to those posed by interpretation of the images obtained. The equipment is moderately expensive and there may be problems in applying it to a wall, requiring extensive scaffolding to permit the scanner to be moved over the surace as the method requires.

12.6.5 *Flat jack tests*

Flat jack tests on masonry structures involve the insertion of a hydraulic jack made from thin sheet metal or rubber in one of the mortar joints with the object of determining the compressive stress in the material. This is achieved by taking deformation measurements across the joint before cutting out the mortar to enable the jack to be inserted. When the joint material is removed, the gauge points will move together and hydraulic pressure is applied to the jack until the original reading is restored. With suitable adjustment, the hydraulic pressure recorded gives the stress in the masonry.

Accurate results are dependent on calibration which has been examined by de Vekey and Skandamoorthy [40] as affected by the type of masonry. Hughes and Pritchard [41] have compared the performance of flat jacks made of stainless steel sheet and of nitrile rubber and reached the conclusion that the flexible rubber jacks allow lower stresses to be measured and require less stringent preparation of the slot in the mortar joint.

An extension of the flat jack method is to install two jacks in bed joints some distance apart vertically so that the material between them can be compressed by loading the jacks simultaneously. This permits measurement of the elastic modulus of the masonry and, if taken to failure, the compressive strength. In the latter case, however, the test ceases to be strictly non-destructive as some damage is caused to the masonry.

The flat jack method is well established and has been applied for example to historic buildings [42, 43] and masonry arch bridges [44]. The equipment required is not expensive but site work is quite lengthy. Considerable skill is needed to ensure reliable results, and measurements can be taken only at a limited number of locations.

12.6.6 **In-situ *tests for mortar strength***

Assessment of *in-situ* mortar strength presents considerable difficulties and it is not usually possible to obtain sufficiently large and undamaged specimens on which to carry out tests. Henzel and Karl [45] have developed a test in which a core is extracted from the masonry which includes the mortar joint. The pieces of the unit material which are included in the core are then carefully sawn off to give a flat mortar specimen. This is then capped with a thin gypsum layer and tested in compression between 20 mm diameter platens. This test has been calibrated against mortar prism strengths for a variety of materials and appears to give consistent results over a wide range of mortar strengths. The procedure is undoubtedly delicate and expensive to carry out but would be justified in an important investigation.

A test, described as a 'screw pull-out test', has been proposed by Ferguson and Skandamoorthy [46] in which a 6 mm diameter stainless steel helical wall tie is driven into the mortar joint. The force necessary to extract it, using a hydraulic jack, is measured which with suitable calibration gives an indication of the mortar strength, at least for weaker materials. Another simple technique which has been suggested [47] is that of measuring the energy absorbed as a 6–8 mm diameter hole is drilled in the mortar using an adapted electric drill. This appears to give a reasonable measure of mortar strength. Tassios *et al.* [48] have described a test in which a scratch is made on the surface of the mortar under controlled conditions, the width of which is related to the compressive strength. All of these simpler tests, however, require further development.

References

1. J. R. Harding, R. T. Laird and D. G. Beech, 'Effect of Rate of Loading and Type of Packing on Measured Strength of Bricks', *Proc. Br. Ceram. Soc.*, **21** (1973) 7–24.
2. N. W. Kelch and F. E. Emme, 'Effects of Type, Thickness and Age of Capping Compounds on the Apparent Compressive Strength of Brick', *ASTM Bulletin TP. 116* (1958), pp. 38–41.

3. F. M. Khalaf and A. W. Hendry, 'Effect of Bed-face Preparation in Compression Testing of Masonry Units', *Proc. Br. Masonry Soc.*, **4** (1990) 129–30.
4. W. Templeton and G. J. Edgell, 'The Compressive Strength of Clay Bricks Ground or Mortar Capped', *Masonry International*, **4** (2) (1990) 66–7.
5. D. G. Beech, J. B. Everill and H. W. H. West, 'Effect of Size of Packing Material on Brick Crushing Strength', *Proc. Br. Ceramic Soc.*, **21** (1973) 1–6.
6. A. W. Page and P. W. Kleeman, 'The Influence of Capping Material and Platen Restraint on the Failure of Hollow Masonry Units and Prisms', *Proceedings of the Ninth International Brick/Block Masonry Conference* (Berlin) 1991, pp. 662–70.
7. H. K. Hilsdorf, 'Investigation into the Failure Mechanism of Brick Masonry Loaded in Axial Compression', in *Designing, Engineering and Constructing with Masonry Products*, ed. F. B. Johnson (Gulf, Houston, Tex., 1969), pp. 34–41.
8. W. Ridinger, J. L. Noland and C. C. Feng, 'On the Effect of Interface Condition and Capping Configuration on the Results of Hollow Clay Masonry Unit Compressive Tests', *Proceedings of the Second Canadian Masonry Symposium* (Ottawa) 1980, pp. 25–38.
9. A. W. Hendry, 'Developments in Structural Masonry', in *Progress in Construction Science and Technology*, No. 2, eds R. A. Burgess *et al.* (M.T.P., Lancaster, 1973), pp. 23–55.
10. E. H. Morsy, 'An Investigation of Mortar Properties Influencing Brickwork Strength', PhD Thesis (University of Edinburgh, 1968).
11. H. W. H. West, 'The Flexural Strength of Clay Masonry determined from Wallette Specimens', *Proceedings of the Fourth International Brick Masonry Conference* (Brugge) 1976, Paper 4.a.6.
12. P. Haller, 'Load Capacity of Brick Masonry', in *Designing, Engineering and Constructing with Masonry Products*, ed. F. B. Johnson (Gulf, Houston, Tex., 1969), pp. 129–49.
13. A. H. P. Maurenbrecher, 'The Effect of Test Procedures on Compressive Strength of Masonry Prisms', *Proceedings of the Second Canadian Masonry Symposium* (Ottawa) 1980, pp. 119–132.
14. G. W. Anderson, 'Stack Bonded Small Specimens as Design and Construction Criteria', *Proceedings of the Second International Brick Masonry Conference* (Stoke-on-Trent) 1971, eds H. W. H. West and K. H. Speed (British Ceramic Research Association, Stoke-on-Trent, 1971), pp. 38–43.
15. N. G. Shrive, 'The Prism Test as a Measure of Masonry Strength', *Proceedings of the Eighth International Symposium on Loadbearing Brickwork* (British Ceramic Society, London, 1983).
16. P. K. Foster, 'Prism Tests for the Design and Control of Brick Masonry', *Tech. Report No. 22* (New Zealand Pottery and Ceramics Research Association, Lower Hutt, New Zealand, 1973).
17. G. J. Edgell, R. C. de Vekey and R. Dukes, 'The Compressive Strength of Masonry Specimens', *Proc. Br. Masonry Soc.*, **4** (1990) 131–5.
18. P. Jukes and J. R. Riddington, 'A Review of Masonry Joint Shear Strength Test Methods', *Masonry International*, **11** (2) (1997) 37–43.
19. J. R. Riddington and P. Jukes, 'A Masonry Joint Shear Strength Test Method', *Proc. Inst. Civ. Engrs Structs Buildings*, **104** (1994) 267–74.

20. S. Samarasinghe, A. W. Page and A. W. Hendry, 'Behaviour of Brick Masonry Shear Walls', *Struct. Eng.*, **59B** (1981) 42–8.
21. A. W. Page, 'An Experimental Investigation of the Bi-axial Strength of Brick Masonry', *Proceedings of the Sixth International Brick Masonry Conference* (Rome) 1982, pp. 3–15.
22. G. A. Hegemeir, R. O. Nunn and S. K. Arya, 'Behaviour of Concrete Masonry under Biaxial Stresses', *Proceedings of the North American Masonry Conference* (Boulder, Co.) 1978, pp. 1.1–1.28.
23. A. Bernardini, A. Modena and U. Vescovi, 'An Isotropic Biaxial Failure Criterion for Hollow Clay Brick Masonry', *Int. J. Masonry Construct.*, **2** (4) (1982) 165–71.
24. *Standard Test Method for Bond Strength of Mortar to Masonry Units, ASTM Designation: C-952-76* (American Society for Testing and Materials, Philadelphia, 1981).
25. L. R. Baker, 'Variability Aspects of the Flexural Strength of Brickwork', *Proceedings of the Fourth International Brick Masonry Conference* (Brugge) 1976, Paper 2.b.4.
26. L. R. Baker, 'The Lateral Strength of Brickwork – An Overview', *Proc. Br. Ceram. Soc.*, **27** (1978) 169–87.
27. R. Lovegrove and R. C. de Vekey, 'The Effects of Specimen Format on the Flexural Strength of Wallettes', *Proc. Br. Masonry Soc.*, **1** (1986) 7–9.
28. S. J. Lawrence, 'Behaviour of Brick Masonry Walls under Lateral Loading', PhD Thesis (University of New South Wales, 1983).
29. A. W. Hendry, 'Masonry Properties for Assessing Arch Bridges', *Contractor Report 244* (Transport and Road Research Laboratory, Dept. of Transport, 1990).
30. J. L. Noland, R. H. Atkinson and G. R. Kingsley, 'Non-destructive Methods for Evaluating Masonry Structures', *Proceedings of the International Conference on Structural Faults and Repairs* (Eng. Technics Press, Edinburgh, 1987), pp. 175–82.
31. R. C. de Vekey, 'Non-destructive Test Methods for Masonry Structures', *Proceedings of the Eighth International Brick/Block Masonry Conference* (Dublin) 1988, pp. 1673–81.
32. A. W. Hendry, S. R. Davies, R. Royles, D. A. Ponniah, M. C. Forde and F. Kamelyi Birjandi, 'Load Test to Collapse of a Masonry Arch Bridge at Bargower, Strathclyde', *Contractor Report 26* (Transport and Road Research Laboratory, Dept. of Transport, 1986).
33. D. A. Sack, L. D. Olson and D. Fidelman, 'Comparison of the Performance of Several Impact Echo Transducers & Application of Impact Echo NDT to the Lincoln Memorial in Washington DC', *Proceedings of the Seventh International Conference on Structural Faults and Repair* (Eng. Technics Press, Edinburgh, 1997), pp. 417–24.
34. D. C. Smale, 'NDT Investigations of Canal Lock Walls: A Geophysicist's Perspective', *Proceedings of the Seventh International Conference on Structural Faults and Repair* (Eng. Technics Press, Edinburgh, 1997), pp. 175–82.
35. B. Hobbs and S. J. Wright, 'An Assessment of Ultrasonic Testing for Structural Masonry', *Proc. Br. Masonry Soc.*, **2** (1988) 42–5.
36. B. Hobbs, 'Development of a Construction Quality Control Procedure Using

Ultrasonic Testing', *Proceedings of the Ninth International Brick/Block Masonry Conference* (Berlin) 1991, pp. 636–44.

37. A. W. Hendry, S. R. Davies and R. Royles, 'Test on a Stone Masonry Arch Bridge at Bridgemill Girvan', *Contractor Report 7* (Transport and Road Research Laboratory, Dept. of Transport, 1985).
38. L. Binda, G. Lenzi and A. Saisi, 'NDE of Masonry Structures: Use of Radar Test for the Characterisation of Stone Masonries', *Proceedings of the Seventh International Conference on Structural Faults and Repair* (Eng. Technics Press, Edinburgh, 1997), pp. 505–14.
39. G. Colla, C. B. Burnside and M. C. Forde, 'Comparison of Laboratory and Simulated Data for Radar Image Interpretation', *Proceedings of the Seventh International Conference on Structural Faults and Repair* (Eng. Technics Press, Edinburgh, 1997), pp. 523–8.
40. R. C. de Vekey and J. S. Skandamoorthy, 'Measurement of Stress in Ashlar Masonry using Flat Jacks', *Masonry International*, **11** (2) (1997) 56–9.
41. T. G. Hughes and R. Pritchard, 'An Investigation of the Significance of Flat Jack Flexibility on the Determination of In-situ Stresses', *Proceedings of the Tenth International Brick/Block Masonry Conference* (Calgary) 1994, pp. 569–78.
42. C. Blasi, Conforto and P. P. Rossi, 'Analysis of the Statical Behaviour of the Arch of Constantine in Rome', *Structural Conservation of Stone Masonry* (ICCROM Rome, 1990), pp. 467–74.
43. C. Modena, L. Binda and A. Anzani, 'Investigation for the Design and Control of the Repair Intervention on a Historic Stone Masonry Wall', *Proceedings of the Seventh International Conference on Structural Faults and Repair* (Eng. Technics Press, Edinburgh, 1997), pp. 233–42.
44. C. Abdunur, 'Direct Assessment and Mechanical Monitoring of Stresses and Mechanical Properties in Masonry Arch Bridges', *Proceedings of the First International Conference on Arch Bridges*, ed. C. Melbourne (Thomas Telford, London, 1995), pp. 327–36.
45. J. Henzel and S. Karl, 'Determination of Strength of Mortar in the Joints of Masonry by Compression on Small Specimens', *Darmstadt Concrete*, **2** (1987) 123–136.
46. W. A. Ferguson and J. Skandamoorthy, 'The Screw Pull-out Test for the In-situ Measurement of the Strength of Masonry Materials', *Proceedings of the Tenth International Brick/Block Masonry Conference* (Calgary) 1992, pp. 1257–66.
47. R. C. de Vekey, 'In-situ Tests for Masonry', *Proceedings of the Ninth International Brick/Block Masonry Conference* (Berlin) 1991, pp. 620–7.
48. T. P. Tassios, C. Vachliotis and C. Spanos, 'In-situ Strength Measurements of Masonry Mortars', *Structural Conservation of Stone Masonry* (ICCROM, Rome, 1990), pp. 53–61.

AUTHOR INDEX

SUBJECT INDEX